THE HONG KONG
POLYTECHNIC UNIVERSITY
香港理工大學
Pao Yue-kong Library
包玉剛圖書館

Copyright Undertaking

This thesis is protected by copyright, with all rights reserved.

By reading and using the thesis, the reader understands and agrees to the following terms:

1. The reader will abide by the rules and legal ordinances governing copyright regarding the use of the thesis.
2. The reader will use the thesis for the purpose of research or private study only and not for distribution or further reproduction or any other purpose.
3. The reader agrees to indemnify and hold the University harmless from and against any loss, damage, cost, liability or expenses arising from copyright infringement or unauthorized usage.

If you have reasons to believe that any materials in this thesis are deemed not suitable to be distributed in this form, or a copyright owner having difficulty with the material being included in our database, please contact lbsys@polyu.edu.hk providing details. The Library will look into your claim and consider taking remedial action upon receipt of the written requests.

Pao Yue-kong Library, The Hong Kong Polytechnic University, Hung Hom, Kowloon, Hong Kong

http://www.lib.polyu.edu.hk

RESPONSE OF TRANSFER PLATE WHEN SUBJECTED TO EARTHQUAKE

A THESIS SUBMITTED IN PARTIAL FULFILMENT OF THE

REQUIREMENTS FOR THE DOCTOR OF PHILOSOPHY

BY

LI CHI SHING

B.Eng

DEPARTMENT OF CIVIL & STRUCTURAL ENGINEERING

THE HONG KONG POLYTECHNIC UNIVERSITY

February, 2005

Pao Yue-kong Library
PolyU · Hong Kong

CERTIFICATE OF ORIGINALITY

I hereby declare that this thesis is my own work and that, to the best of my knowledge and belief, it reproduces no material previously published or written, nor material that has been accepted for the award of any other degree or diploma, except where due acknowledgement has been made in the text.

________________________(Signed)

Li Chi Shing (Name of student)

ABSTRACT

Hong Kong is a region of moderate seismic risk. However, buildings in Hong Kong are traditionally designed without seismic resistance provisions. It is well known that the use of the transfer plate system in a high-rise building structure causes an abrupt change in the lateral stiffness. If that building is under seismic attack, a “soft-storey” mechanism may be formed. Since transfer plate systems are often used in reinforced concrete high-rise buildings in Hong Kong, there are potential risks in the above circumstances. In this study, simple analytical models and analysis procedures for engineering application purposes are developed to assess the seismic performance of a high-rise building with a transfer plate, designed to non-seismic resistance requirements. It was considered in this study, based on (1) the seismic responses of transfer plates, (2) the level of seismic resistance of high-rise buildings with transfer plates, (3) the formation of possible “soft storey” mechanism in a storey below the transfer plate, and (4) the mode of failure through cycles of linear time-history analyses. Experimental results of a shaking table test, conducted by the Institute of Engineering Mechanics in Harbin, on a 1:20 scale high-rise building with a transfer plate model, were used to verify the numerical simulations conducted in this study. Pseudo-dynamic tests on a 1:4 scale transfer plate model were also carried out in this

study to assess the seismic resistance of a transfer plate. From these numerical and experimental results, some findings were obtained and used in the development of two new analytical approaches. They are as follows:

When compared the numerical results using the conventional elastic ETABS program with the rigorous finite element analyses and experimental data obtained through this study, it indicated that numerical analyses were carried out on high-rise building structures using the conventional elastic ETABS program with a rigid floor diaphragm assumption were underestimated. In order to correctly evaluate the responses of high-rise buildings using the ETABS program, a new approach, namely advanced simplified un-coupled approach, based on alternative modelling method was developed and used in this study. It was found that storey stiffness is significantly enhanced by the coupling of all the vertical structural elements (shear walls, core walls and columns) with the slabs/transfer plate. In addition, stiffness factors should be applied to account for the coupling effect of structural elements with the slabs/transfer plate. The stiffness factors are 1.2 for low-rise beam and column frame buildings, 2.0 for low-rise core wall and column frame buildings and 1.7 for high-rise wall-frame buildings.

Using the above new approach, this study also contends that it is possible to predict the inelastic behaviour of buildings structures through cycles of linear elastic time-history analyses by reducing the stiffness of the damaged structural members, determined from the previous time-history analyses. Based on the comparison of the experimental data and numerical results, displacement factors should be applied to the numerical results for estimating the actual storey drifts under a severe earthquake attack.

The experimental and numerical results have indicated that typical local high-rise buildings with transfer plates may have sufficient strength to resist an earthquake action up to the seismic intensity of VIIth degree. There is indication that main structural failures may occur immediately above the transfer plate. Notwithstanding the presence of a transfer plate, stiffness below the transfer plate is significantly improved by the coupling of the columns, core walls, with the transfer plate. This important finding indicates that current methods, such as SEAOC, UBC and the Chinese seismic design code, used in the classification of a "soft-storey" are not appropate for this type of high-rise building. Therefore, a second new analytical approach, namely ratios of deflection (R_u) and inter-storey drift ($R_{\Delta u}$), were introduced and used in this study, to predict the presence of a soft storey in a high-rise building with due allowance for the change in flexural and shear stiffness. The ratios have proved to be more satisfactory in the classification of a “soft storey”.

Based on the numerical results obtained from the rigorous finite element analysis, it has been demonstrated that rigid diaphragm behavior can be assumed for the transfer plate system in a high-rise building structure.

This study has provided new means to accurately predict the seismic responses of reinforced concrete high-rise building structures by using the advanced simplified un-coupled approach. The presence of a soft-storey can be more accurately assessed, using the two new ratios (R_u and $R_{\Delta u}$) developed in this study.

PUBLICATIONS ARISING FROM THE THESIS

LIST OF MAIN PUBLICATION:

JOURNAL PAPERS

Li, C. S., Lam, S. S. E., Zhang, M. Z. and Wong, Y. L. (2003). "Shaking Table Test of a 1:20 Scale High-rise Building with Transfer Plate System." *J of StructuralEngineering*, ASCE accepted for publication.

Li, C. S., Lam, S. S. E., Chen, A. and Wong, Y. L. (2003). "Performance of a Transfer Plate Structure." *J of Structural Engineering*, ASCE reviewed for publication.

CONFERENCE PAPERS

Lam, S. S. E., Zhang, M. Z., Wong, Y. L. and **Li, C. S.** (2002). "Shaking table tests of a 1:20 scale high-rise residential building." *International Conference on Advances and New Challengers in Earthquake Engineering Research*, Harbin conference, Aug 15-17, 2002, Harbin, China.

<u>Li, C. S.</u>, Lam, S. S. E. and Wong, Y. L. (2002). "Response of a reinforced concrete high-rise building with transfer plate system under seismic actions." *Structural Engineering World Congress (SEWC 2002)*, Oct 9-12, 2002, Yokohama, Japan.

Chen, A., **<u>Li, C. S.</u>**, Lam, S. S. E. and Wong, Y. L. (2002). "Testing of a transfer plate by pseudo-dynamic test method with substructure technique." *International Conference on Advances in Building Technology*, Dec 4-6, 2002, HKSAR, China.

<u>Li, C. S.</u>, and Lam, S. S. E. (2003). "Seismic performance of high-rise building with transfer plate", 第三屆兩岸結構與大地工程研討會, Oct 23-25, 2003, Taiwan.

RESEARCH REPORT

Lam, S. S. E., **<u>Li, C. S.</u>**, Zhang, M. Z., Wong, Y. L. and Chau, K. T. (2002). "Seismic Study of Hong Kong: Shaking Table Tests of a Typical High-rise Building in Hong Kong." *CIDARC, Hong Kong Polytechnic University*.

LIST OF MINOR PUBLICATION:

JOURNAL PAPERS

Lam. S. S. E., Wu B., Wong Y. L., Wang Z. Y., Liu Z. Q. and **Li C. S.** (2002). "Drift capacity of rectangular reinforced concrete columns with low lateral confinement", *ASCE, J of Structural Engineering*.

RESEARCH REPORT

Lam. S. S. E., Wu B., Wong Y. L. Chau K. T., Chen A and **Li C. S.** (2000). "Seismic Study for Hong Kong: Ultimate Drift Ratio of Rectangular Reinforced Concrete Columns in Hong Kong when subjected to Earthquake Action", *CIDRAC, Hong Kong Polytechnic University*.

ACKNOWLEDGMENT

I would like to acknowledge Dr. S.S. Lam, Eddie, my chief supervisor, for his guidance, advice and comment on my PhD study. Grateful thanks go to Professor J.M. Ko and Dr. Y.L. Wong, my co-supervisors for advice given regarding the study. I am indebted to all the laboratory staff in the Department of Civil & Structural Engineering. All provided technical assistance and support during my experimental work. Special thanks go to Mrs. E. Anson for proof reading this thesis.

Finally, I would like to acknowledge the support of the Research Committee of the Hong Kong Polytechnic University who is funded this study.

TABLE OF CONTENT

LIST OF FIGURES

LIST OF TABLES

NOTATIONS

The following notations are used in Chapters 3 to 9.

A_i	Cross-section area of wall i
a_r	Acceleration ratio
b	Clear span of a beam
E	Modulus of Elasticity
E_r	Modulus Ratios
EI	Flexural rigidity of the wall
EI_b	Flexural rigidity of the coupling beam
F	Horizontal force of magnitude applied at the storey level “n”
GA	Shear rigidity of the wall
GA_b	Shear rigidity of the coupling beam
H	Total height of a structure
h	Storey height of a structure
I_i	Moment of inertia of wall i
K_n	Estimated lateral stiffness at the storey level “n”
K_{n+1}	Estimated lateral stiffness at the storey level “n+1”

K_t	Estimated lateral stiffness at the level of transfer plate
L_r	Length ratio
$(m_m)_{approx}$	Total mass of the model, including self-weight and 15 tons artificial mass
$(m_p)_{approx}$	Total mass of the prototype building, including dead load, finishes and imposed load
$(m_m)_{total}$	Total mass of the model, including self-weight and artificial mass
$(m_p)_{total}$	Total mass of the prototype building, including dead load, finishes and imposed load
p_1	Neighboring maximum responses at point 1
p_2	Neighboring maximum responses at point 2
t_r	Time ratio
R	Compressive stress ratio
R_s	The codified lateral stiffness ratio
R_u	Displacement ratio
$R_{\Delta u}$	Drift ratio
u	Displacement in the original model
u^*	Displacement in the reference model
w	Lateral uniformly distributed load

y_{max}	Maximum deflection at the top of a structure
Δu	Inter-storey drift in the original model
Δu^*	Inter-storey drift in the reference model
δ	Lateral drift of the n^{th} storey
μ	Modification factor
ρ_r	Equivalent mass density ratio
ω_r	Frequency ratio
ξ	Damping ratio

FEA	FINITE ELEMENT APPROACH
FFT	FAST FOURIER TRANSFORM METHOD
SUCA	SIMPLIFIED UN-COUPLED APPROACH

1 INTRODUCTION

A brief introduction to this research study is presented. Included in this Chapter are the problem statement, aims and scope of the research study and the structure of thesis.

1.1 PROBLEM STATEMENT

Hong Kong is now a major financial centre and one of the most densely populated cities in the world. It is located on the South China Sea Plate. The active tectonic plate boundary is also relatively far from Hong Kong. Up to now Hong Kong has not been affected by earthquakes to any significant extent. Since many major cities around the world have suffered earthquake disasters during the past 20 years, local engineers and the public at large are becoming increasingly concerned about the possibility of a moderate seismic attack in Hong Kong.

Since the seismic hazard in Hong Kong is considered to be low risk, reinforced concrete structures in Hong Kong have always been designed without seismic resistance provisions. Reinforced concrete buildings in Hong Kong are designed according to either the Code of Practice for Structural Use of Concrete 1987 or BS8110:1985. As these design codes only emphasise the provision of adequate strength, prediction of the response of local buildings when subjected to moderate seismic action is not required. This is especially true for low-rise buildings where the seismic action is significantly higher than the design wind force, and for those high-rise buildings incorporating considerable transfer, e.g. a transfer plate.

There are over 22,000 residents of Telford Garden living in 21 towers above the Kowloon Bay Mass Transit Depot. Each of the 20 to 25 storey shear-wall structures sits on a 2 m thick transfer plate, which transfers the loads to primary columns passing through the depot. Transfer plates are also commonly used in commercial buildings. For example, Pacific Place consists of four towers over a large podium area. The towers sit on a 3.5 m transfer plate, which carries the loads from closely spaced shear walls above to widely spaced large columns at the podium area. Thus, at the podium area, the plaza can provide a large open area for the shopping mall. In both cases, understanding the seismic capacity of a high-rise building with a transfer plate is essential.

The main drawback of using a transfer plate system in a high-rise building is the abrupt change in lateral stiffness at transfer, e.g. from a stiffer shear wall system above to a relatively flexible column-girder system below. This creates a soft (or weak) storey and violates the seismic design concept of "strong column weak beam" (Aoyama 2001) or alternatively the capacity design concept (Paulay & Priestley 1992). Therefore, a high-rise building with a transfer plate system could be vulnerable to possible earthquake attacks. This is well demonstrated by the collapse of a reinforced concrete 7-storey apartment house with a soft first storey during the 1995 Hyogoken-Nanbu Earthquake. Yoshimura (1997) conducted numerical studies to simulate the apartment house and concluded that "if first storey mechanism might occur, the collapse could be unavoidable even for buildings with base shear strength of as much as 60% of the total weight". In particular, the so-called "piloti-type buildings" (in which strength and stiffness of the first storey are considerably smaller than in the upper storeys) are extremely vulnerable to earthquakes (Sanada *et al* 2000).

To check the existence of a transfer or soft storey, design codes use the ratio of lateral stiffness at transfer to lateral stiffness of the storey immediately above, e.g. in the United States seismic design codes - SEAOC (1999) and UBC (1997), Chinese seismic design code GB50011-2001, etc. In general, a soft storey can be defined as a storey which has a 30% reduction in the lateral stiffness. Owing to the irregularity in elevation, non-uniform and concentrated storey drift may occur at floors in the vicinity of the transfer. Design codes generally require structural members at the transfer to be designed with enhanced ductility and strength. Other requirements include the need to carry out sophisticated analyses as well as experimental verifications.

In general, transfer plate structures have the ability to redistribute the loads from the superstructure above to widely-spaced columns and core walls below. They can be easily incorporated into the architectural layout to provide column-free open space area at the lower stories. Because of such advantages, there is extensive use of transfer systems in high-rise buildings in areas where seismic hazards are not considered. However, there is no local code of practice or detailed guidelines on the design of transfer plates. Structural behaviour of a transfer plate and stress distribution of the system are not fully understood. In this study, a rational and efficient structural model is developed to predict the behaviour, load transfer and the force distribution in the transfer plate. The interaction between the transfer plate system, upper floors and supporting structures is also investigated.

1.2 AIM AND SCOPE OF THE RESEARCH STUDY

The principal objective of this research study is to quantify the seismic performance of a high-rise building with a transfer plate designed to non-seismic resistance requirements. Various numerical models are developed and adjusted to provide reasonable prediction on the location of cracks and failure of members at various stages of the seismic load. Specific means to enhance the accuracy of the analysis are highlighted. Recommendations and comments are given on the appropriate analysis procedure (including respective merits and accuracy) for the related local analysis practice.

The seismic performance of a high-rise building with a transfer plate designed to non-seismic resistance requirements is quantified based on the following:

1. A quantification of the seismic responses of a transfer plate,
2. A quantification of the level of seismic resistance of a high-rise building with a transfer plate,
3. A quantification of the soft storey mechanism in a high-rise building with a transfer plate,

4. A predication of the damage and the mode of failure in high-rise buildings with a transfer plates through a series of linear time-history analyses.

Finite elements programs, namely “ABAQUS” and “ETABS”, are used to carry out the three-dimensional numerical analyses of a high-rise building with a transfer plate. Experimental results obtained from the “shaking table test” and “pseudo dynamic tests” were used in this study. The shaking table tests were conducted by the Institute of Engineering Machanics, Harbin, in January, 2001. With the assistance of the technical staff in the Department of Civil and Structural Engineering of The Hong Kong Polytechnic University, pseudo dynamic tests were conducted in 2002. In line with the recent extensive research studies, all the buildings, upon which this study is based, are assumed to be located in a region with the basic seismic intensity categorized as VIIth degree

1.3 RESEARCH SIGNIFICANCE

Nowadays, a transfer plate is commonly used in a reinforced concrete residential high-rise building. It is generally located at a low-level in a high-rise building. Using the transfer plate system is that it leads to an abrupt change in the lateral stiffness at the transfer, e.g. from a stiffer shear wall system above to a relatively flexible column-girder system below. This creates a soft (or weak) story and violates the seismic design concept of “strong column weak beam” (Aoyama 2001) or alternatively the capacity design concept (Paulay & Priestley 1992). Therefore, a high-rise building with a transfer plate system could be vulnerable to possible earthquake attacks. This is well demonstrated through the collapse of a reinforced concrete 7-story apartment house with a soft first story during the 1995 Hyogoken-Nanbu Earthquake. Lately, Yoshimura (1997) conducted numerical studies to simulate the apartment house and concluded that “if first story mechanism might occur, the collapse could be unavoidable even for buildings with a base shear strength of as much as 60% of the total weight”. In particular, the so-called “*piloti*-type buildings” (in which strength and stiffness of the first story are considerably smaller than the upper stories) are extremely vulnerable to earthquakes (Sanada *et al* 2000).

Recently, local engineers and the general public have become increasingly concerned about the possibility of a moderate seismic attack in Hong Kong. It is recognized that Hong Kong’s reinforced concrete structures have always been designed without seismic resistance provisions. Transfer plates are commonly used in high-rise buildings. However, there is no local code of practice or detailed guidelines on the design of transfer plates in high-rise reinforced concrete buildings. The use of a transfer plate system could lead to an abrupt change in the lateral stiffness at the transfer and the formation of a “soft-storey”. In order to tackle these problems, simple means to assess the presence of a soft-story are developed for engineering application purposes.

1.4 STRUCTURE OF THE THESIS

The thesis is divided into nine chapters. A brief introduction of this research study is presented in Chapter 1. The current knowledge from relevant literature relating to high-rise buildings with a transfer plates is incorporated. Background information and the application of design assumption and analyses approaches on the high-rise buildings with transfer plates are described. The seismicity level of Hong Kong, the types of transfer structures used in a high-rise building, analyses, local design practice and construction methods of transfer plate in Hong Kong are presented in detail in Chapter 2. Main parts of this research study are presented in next six chapters. The cohesion between these six chapters is shown in Figures 1.1 and 1.2.

Chapter 3 describes two different types of analysis approaches for predicting the static and dynamic response of buildings with transfer plates, the simplified un-coupled approach and the finite element approach. Three commercial packages were used, including ETABS, SAP2000 and ABAQUS. Different numerical modelling techniques are used to examine the accuracy of the numerical results based on the analyses of high-rise buildings with transfer plates. Comparisons of the lateral performances of different type of structures estimated using different finite element programs with linear elastic analyses, are also made.

The previous Chapter incorporates a series of studies which are used to examine the accuracy of the finite element approach. The estimated lateral displacements of buildings are different when compared with the results obtained from the simplified un-coupled approach. The storey stiffnesses were increased owing to the floor slabs being considered in the finite elements model. However, the disadvantage in using the finite element approach is that a few days to weeks of computation time is wasted. Furthermore, the analysis results are difficult to be incorporated directly into the design. Numerical models are not easy to create owing to large numbers of nodes and elements used. As a result, a new analysis approach is used in the analyses of high-rise building or core walls-frame structures and described in Chapter 4. It uses an *advanced* simplified un-coupled approach to estimate the response of the buildings.

Chapter 5 addresses the seismic problems of a high-rise building with a transfer plate in a region of moderate seismicity. One of the aims of this study is to understand the seismic behaviour of a high-rise building with a transfer plate and to identify the performances of the transfer plate based on linear elastic time-history analyses. Distributions of shear force and bending moment along the height of the building and the load transferring behaviour are used to check the seismic responses.

Finite element analyses based on the response spectrum according to the GBJ11-89 (old seismic design code of buildings of China) or GB50011-2001 (new seismic design code of buildings of China) are used to predict the response through linear elastic time-history analysis. Figure 1.3 shows the response spectra according to GBJ11-89 and GB50011-2001. The difference between the two spectral accelerations is within 10% if the natural period of vibration is greater than 3 second. Since the natural period of vibration of a high-rise building with a transfer plate used in this study is about 2 second, numerical results using the response spectrum according to the old and new seismic design codes will match each other. Numerical analyses based on the GBJ11-89 will be equivalent to that obtained based on the GB50011-2001. Based on the results, some suggestions for modelling techniques to analyse a high-rise building with a transfer plate are recommended. The level of seismic resistance of a high-rise building with a transfer plate is also identified.

Chapter 6 presents an experimental investigation into the seismic performance of a high-rise building with a transfer plate designed to non-seismic resistance requirements. Shaking table tests of 1:20 scale typical reinforced concrete residential high-rise building with a transfer plate are used to assess the seismic resistance of reinforced concrete structures when subjected to various levels of seismic attacks. Experimental results of the shaking table tests and seismic resistance of the building model are reported in this Chapter. A series of numerical models is developed using the commercial package, ETABS version 6.22. The purposes of the numerical studies are to verify the experimental results obtained from the shaking table tests and to recommend practical means to predict possible damage.

Base on the damage and failure mechanisms observed from the shaking table tests, it is concluded that the mode of failure in a high-rise building with a transfer plate is different from the traditional failure mechanism in a low-rise building with a soft-storey. Notwithstanding the use of transfer plate, the bending stiffness at the transfer is still significant due to the coupling of the columns by relatively thick transfer plate. The use of “displacement ratio (R_u)” and “drift ratio ($R_{\Delta u}$)” to indicate the mode of failure are presented in Chapter 7. A series of case studies are used to explore a method to estimate the flexural stiffness effect of the storey below the transfer plate. The experimental results are used to initiate and to calibrate the method. A critical review of the response of a soft storey during major earthquakes leads to the conclusion that any method based on the usual first theory of failure is not adequate and can not predict the mode of failure in a high-rise building with a transfer plate.

Chapter 8 presents an experimental investigation using the pseudo-dynamic tests with sub-structure techniques. They were conducted on a 1:4 scale test specimen representing the first two storeys of a 18-storey high-rise building with a transfer plate. The building was subjected to the earthquake actions. The objective of this study is to assess the seismic performance of a transfer plate incorporated in a 18 storey high-rise building designed to non-seismic resistance requirements. Columns in the test specimen were strengthened to prevent them from failure under the pseudo-dynamic tests. Numerical models were developed using a commercial package, ABAQUS version 6.3.1 to verify the experimental results obtained from the pseudo-dynamic tests and to recommend practical means to represent possible damage. Purposes of the numerical studies are to verify the experimental results and to examine accuracy of using the ratio of deflection of transfer plate level to indicate the mode of failure, see Chapter 7. Damaged structural members of a 18-storey high-rise building with a transfer plate under earthquake attacks are quantified.

Finally, Chapter 9 draws the overall conclusions based on the key findings in Chapters 3 to 8. The limitations of this research study are summarised and the recommendations for further research are explored.

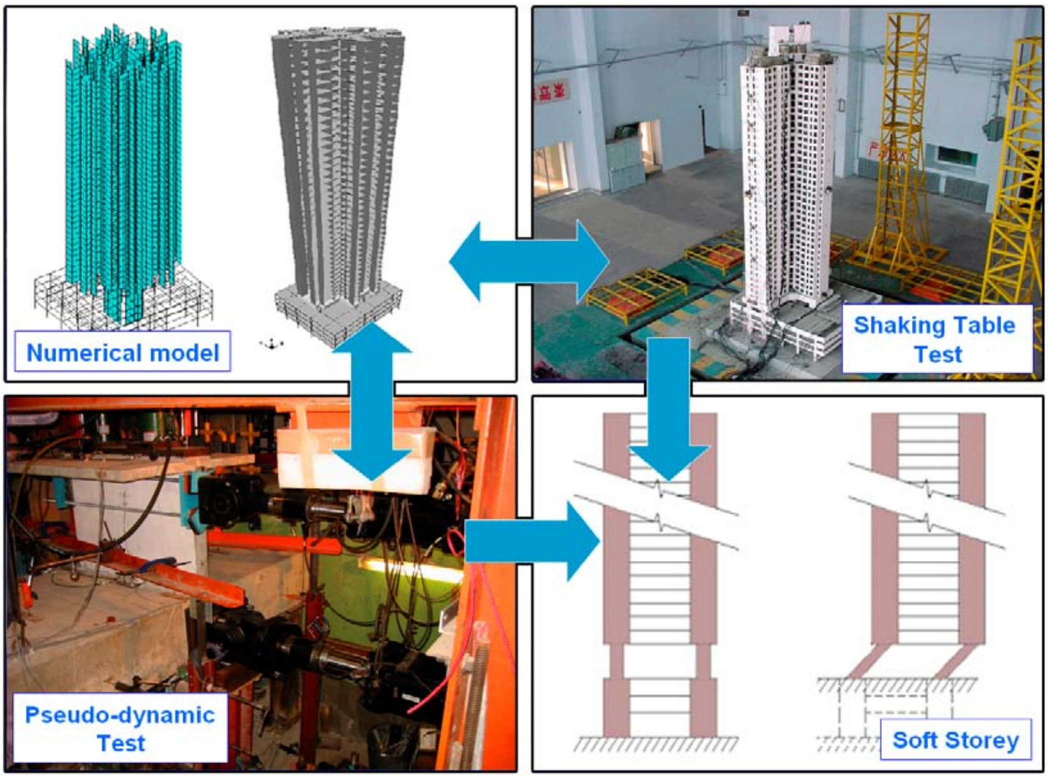

●	**Numerical model**	Develop a new simple numerical model to analyse a high-rise building with transfer plate.
●	**Shaking Table Test**	Predict the “failure mode” and “damage level” of a high-rise building with transfer plate.
●	**Pseudo-dynamic Test**	Predict the seismic resistance of a transfer plate.
●	**Soft Storey**	Develop new methods of classifying the formation of possible “soft storey” failure mechanism at a storey below the transfer plate.

Figure 1.1 General view on the main parts of thesis.

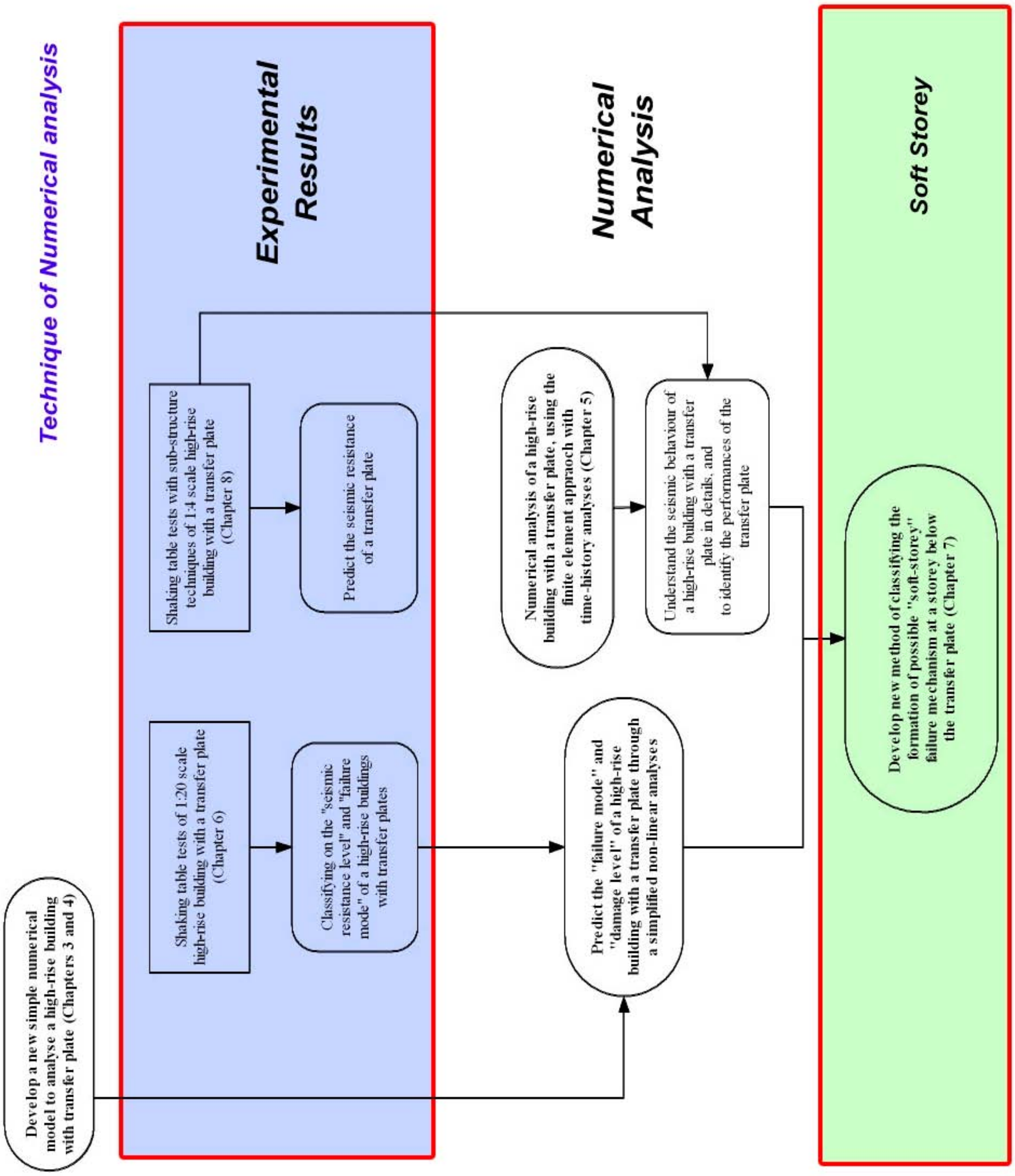

Figure 1.2 The details cohesion between the chapters in the main parts of thesis.

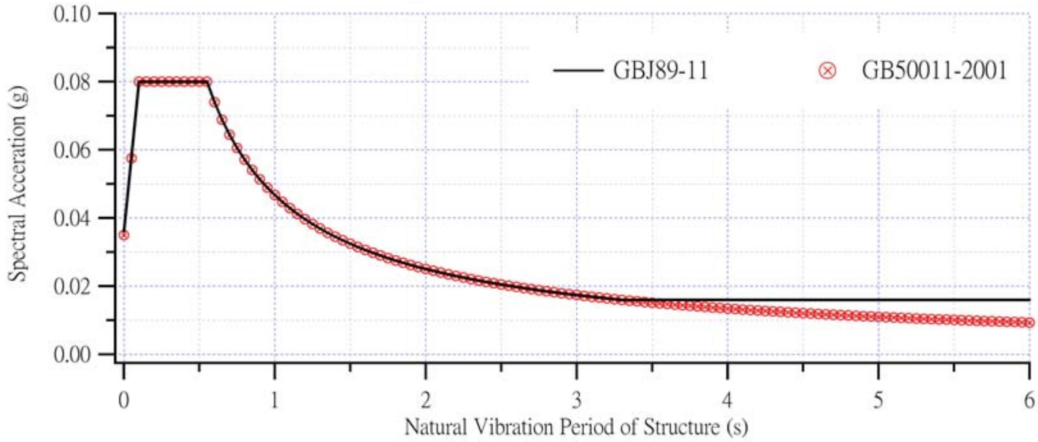

Figure 1.3 Comparison of the response spectra of GBJ89-11 and GB50011-2001.

2 LITERATURE REVIEW

Since the seismic hazard in Hong Kong has traditionally been considered low, reinforced concrete structures in Hong Kong have always been designed without seismic resistance provisions. Reinforced concrete buildings in Hong Kong are designed according to either the Code of Practice for Structural Use of Concrete 1987 or BS8110:1985. As these design codes only emphasise the provision of adequate strength, there is a need to predict the response of local buildings when subjected to moderate seismic action. This is especially true for low-rise buildings where the seismic action is significantly greater than the design wind force, and for those high-rise buildings incorporating a substantial transfer system, e.g. a transfer plate.

The structure of this chapter is as follow. A review of the seismicity level for Hong Kong is given in Section 2.1. The transfer plate systems are summarized in Section 2.2. Types of transfer structure used in high-rise buildings are reviewed in Section 2.3. Design and analyses methods for transfer plates are described in Section 2.4. Construction methods for transfer plates are discussed in Section 2.5. Summary of the literature review is given in Section 2.6.

2.1 HISTORICAL REVIEW ON SEISMICITY LEVEL OF HONG KONG

Hong Kong is located on the South China Sea Plate. The nearest active tectonic plate boundary is that of the Philippine Sea Plate and the South China Sea Plate between Taiwan and the Philippines. Although this active boundary is relatively far away from Hong Kong, destructive earthquakes have occurred in the southern part of China and the Southern China Sea with the potential of affecting Hong Kong significantly.

Considering the past 500 year earthquake records within a 300km radius of Hong Kong, Hong Kong has experienced moderate earthquakes. The largest two earthquakes were recorded when Hong Kong was a small village. The magnitude 5.7 earthquake at Danagen Island in 1984, which was 30 km away from Hong Kong, was the largest earthquake observed within 100 km of Hong Kong. The biggest earthquake of magnitude 7.4 was in the Shantou area in 1918, which was about 300 km away from Hong Kong. There was no serious damage, economic loss or loss of life in the past earthquakes. According to the results obtained from these studies, geographically Hong Kong is not an area experiencing destructive earthquake activities. Therefore seismic resistance provisions and seismic design are not provided for building structures in Hong Kong.

However, Hong Kong is now a major financial centre and one of the densely populated cities in the world. Following recent earthquake disasters in many cities around the world; for instance in San Francisco in 1989, Los Angeles in 1994, Kobe in 1995 and Taiwan in 1999, there is increasing concern by local engineers and also the public at large about the possibility of a moderate seismic attack in the vicinity of Hong Kong. The Geotechnical Control Office (1991) also published a report after reviewing the earthquake data within a region of about 350 km radius of Hong Kong including those “observed” and “felt” effects of earthquakes more than 900 years ago.

The Buildings Department of the Hong Kong Government setup a working group in 1996 to examine the effects of earthquakes on buildings in Hong Kong. Seminars and workshops on earthquake engineering were organized by the Hong Kong Institution of Engineers, Joint Structural Division and the three universities in Hong

Kong with civil engineering departments. Certainly, earthquake resistant design for structures in Hong Kong is now an important issue that needs urgent attention. In early 2002, the Buildings Department called for technical proposals bidding for a consultancy project “Seismic Effects on Buildings in Hong Kong”. More earthquake-related studies in Hong Kong are expected in the future.

In recent years, extensive research studies have been conducted to estimate the seismicity level of Hong Kong. Lee *et al.* (1996) estimated the peak acceleration at bedrock is in the range of 75-115 gal for the Hong Kong region. Pun *et al.* (1998) suggested the ground motion in Hong Kong associated with a 10% probability of being exceeded in 50 years would have a peak acceleration around 0.1g. Wong *et al.* (1998a, 1998b) concluded that the seismicity level of Hong Kong could be similar to that of New York city. The seismicity level of Hong Kong is of seismic intensity VII according to the seismic design code of building of China (GB50011-2001). The seismic zoning map, published by the Chinese Seismological Bureau, gives the seismic level of Hong Kong as seismic intensity VII.

Based on the above studies, Hong Kong should be considered of moderate seismicity level (Lam *et al.* 2002b). Appropriate seismic resistance provisions should be provided for the structures, and the inherent strength of existing structures would have to be assessed for their ability to withstand possible earthquake attacks.

2.2 TRANSFER PLATE

Hong Kong is a densely populated city. As land is at a premium, high-rise buildings are common features of the landscape. Within high-rise buildings, the disposition of columns and walls are dictated largely by functional, aesthetic and economic considerations. Transfer structures are suitable for offering large spacing and modulation of the vertical structure. This concept is commonly adopted not only for commercial buildings, but also residential buildings in Hong Kong, and transfer structures are usually incorporated as a common feature in high-rise buildings. In particular, transfer plate systems are increasingly used in Hong Kong as a structural systems in high-rise buildings. They enable large open areas for diversified commercial facilities such as car parks, swimming pools or shopping malls, lobbies and banking. Figures 2.1 to 2.3 show the use of transfer plates in high-rise buildings.

The change in function between floor levels in high-rise buildings leads to a modulation of the vertical layout of the structural plan. For residential buildings, a regular arrangement of columns or load-bearing shear walls at the higher levels sit on podiums that make provision for public and commercial facilities, shopping centre or a mass transit facility at the lower levels.

Figures 2.4 and 2.5 show a residential high-rise building with a transfer plate in Hong Kong - Tung Chung Crescent located in Tung Chung. The transfer plate has made provision for a large area of public plazas, whereas the shopping centres and car parks are provided at the lower levels of the structure. Figures 2.6 to 2.11 show other residential high-rise buildings with a transfer plates in Hong Kong.

In these buildings, the architects are faced with changing functional needs that demand responses from the engineer in the choice of the appropriate structural systems for the transfer structure. A transfer plate is commonly constructed in reinforced concrete residential buildings, as shown in Figure 2.12. It is a thick plate structure that can carry both vertical and lateral loads imposed from the superstructure above, and redistributes those gravity and lateral loads to the widely spaced columns and core walls of the base. Transfer plate systems, which can redirect loads in more than one direction, are particularly suitable for shear wall buildings, such as hotels and residential buildings. It is beyond doubt that the transfer plate system can provide large public and commercial areas. However, a major problem is the abrupt change in the lateral stiffness of a building, from a stiff shear wall system above the transfer plate to a column-girder system below. This introduces a soft or weak storey.

There is in no local code of practice or a standard for the design of transfer plate structures. The Buildings Department of the HKSAR does not provide guidelines on the design of transfer plates. The structural behaviour of a transfer plate and stress distribution within the system are not fully understood. In this study, a rational and efficient structural model has been developed to predict the behaviour, load transfer and the force distribution in the system. Furthermore, the interactions between the transfer plate system, the upper floors and the supporting structures are also investigated.

The following sections introduce other types of transfer structure used in Hong Kong. Common design practices and the construction methods for transfer plates are discussed.

2.3 TYPES OF TRANSFER STRUCTURE USED IN HIGH-RISE BUILDINGS

The use of transfer structures as part of the structural system in high-rise buildings has increased rapidly during the past two decades. Different kinds of transfer system have been introduced, such as transfer frame/truss, transfer box, transfer girder, vierendeel truss system, transfer plate, etc.

TRANSFER FRAME OR TRUSS SYSTEM

Zunz and Wise (1998) rationalized the transfer frame system. A transfer frame is generally located at a low-level in a high-rise building. Vertical and horizontal loads are transferred to the main columns by a transfer truss and frame. Ho (1999) introduced the Cheung Kong Center (completed in 1999). It is a composite steel structure with a transfer truss that collects the loads from a superstructure of over 70-storey and 289.8 m in height and transfers it to eight widely-spaced primary columns at the ground level. It reduces the number of columns at ground level in order to provide a large usable open space. Another example is the Oversea Chinese

Banking Corporation Centre (completed in 1976) in Singapore. It has 52 storeys and is 201 m in height. It uses two levels truss system to transfer the typical floor loads to the core walls.

VIERENDEEL TRUSS SYSTEMS (VTS)

With demands from developers and architects for flexible building layouts, there is increasing use of multi-storey vierendeel truss systems (VTS) as structural frames. VTS were originally developed for steel trusses. With no cross bracing, the VTS offers a transparent exterior appearance that matches favourably with the cladding. They facilitate open-plan floor layout for better interior planning and better views in all directions. From a large usable space to column free skygardens, VTS are indeed a challenge for Structural Engineers. Lam (1999) investigated the structural behaviour of VTS with elastic and inelastic analyses.

In the last two decades, several renowned high-rise buildings having multi-storey VTS have been completed. The first is the new headquarters of Commerzbank in Frankfurt, Germany. The 54 storeys steel structure comprises twelve steel vierendeel frames of 34m span, 8 storeys high to support the sky-gardens. Another example is the 33 storeys Citic Tower in Hong Kong. VTS in the form of composite structures is used to support the skygardens to provide spectacular views over the harbour. The Hong Kong Bank Headquarters (completed in Hong Kong in 1985) contains a 45 storeys, a 4 level basement and is 180 m above ground. The masts are linked at five levels by trusses creating a VTS system with superb structural stability.

TRANSFER BOX SYSTEM

Some high-rise buildings combine the use of shear wall structures at upper levels and beam-column frame structure at lower levels without changing the grid lines. For this type of a building, a transfer box structure is used. It comprises beam girders and thick slabs at top and bottom of the transfer structure and structural walls between the beam girders. It is not necessary to provide a large deep beam for transferring the loading from the upper to the lower part. A Box structure has the advantage of providing a strong stiff structure with optimal self-weight. For example, the Overseas Building in Harbin, China, contains 32 storeys and 2 level basements and is 109.7 m height above the ground. The transfer box structure is used to connect the higher levels shear wall structure to the lower level column frame structure.

TRANSFER GIRDER SYSTEM

This type of structural system is widely used in Hong Kong. Often dictated by architectural requirements, structural walls and columns are terminated at a plate or girders level before reaching the foundation. The increased column spacing at lower levels, together with the elimination of spandrel beams over the height of the tower base, results in an increased flexibility of the external frame. The Central Plaza (completed in 1992) in Hong Kong has 78 storeys, 3 levels of basement and is 314 m in height above the ground. It has large perimeter girders and transfer girders to transmit the loads from the discontinued walls to other walls and columns that continue to the foundation below. Similar transfer girder structures are commonly adopted in the public housing blocks such as the Harmony and Annex Block in the 90's and the recent Concord Block. These are 20 to 40 storeys reinforced concrete shear wall buildings with transfer girders at the first floor. The structural form allows open space at ground floor for service rooms and social functions.

Structural behaviour, analysis and design of reinforced concrete transfer girder systems in tall buildings have been studies. Kuang and Li (2001) studied the analysis and behaviour of single transfer beams that support in-plane loaded shear walls. The interaction effect causes significant stress re-distributions both in the transfer beam and in the shear wall within an interactive zone. Kuang and Puvvala (1996) and Kuang and Atanda (1998) presented an analysis of and investigation of the structural behaviour of continuous transfer girder framing into columns. The upper structural layout consists of a single shear wall systems in the high-rise buildings. The upper levels structural form has a significant effect on the failure mechanism of the transfer girders. Li *et. al.* (2002) presented the structural performance of a 7 storeys reinforced concrete frame structure with transfer beam under potential seismic actions. It was pointed out that failure mechanism of this structure takes place below the transfer beam.

2.4 DESIGN OF TRANSFER PLATE STRUCTURE

As studied above, there is no local code of practice or standards governing the design of transfer plates. Local practice only proposes design principles and analytical concepts. There are basically two approaches for the design of a transfer plate. Since depth of a transfer plate is usually over 2 m, it can not be designed like a normal floor slab. The deep beam theory and thick plate theory must be used, both of which do not assume a rigid diaphragm.

RIGID DIAPHRAGM ASSUMPTION

Floor diaphragms in the reinforced concrete buildings are typically presumed as rigid for the design purposes. In fact, the rigid diaphragm assumption is the most commonly used for the analysis of transfer plate systems. Thus, the in-plane stiffness of the plate system is infinite. Consequently, floor (horizontal) displacements may be expressed in terms of two orthogonal translations and a rotation. Usually, in-plane deformations of the diaphragm are small when compared with the lateral deformations. So, a rigid diaphragm assumption can be used to estimate the lateral response of a building.

In local design practice, engineers adopt the rigid floor assumption and the transfer plate is considered as a thick plate, rigid not only in-plane but also out-of-plane. Loading from the upper structures and the supporting frame or central core is directly applied to the plate. No interaction effect is considered between the plate and superstructure. As a result, the design of a transfer plate structure is simplified.

FLEXIBLE FLOOR ASSUMPTION

Reinhorn *et al* (1988) studied the effects of inelastic inplane flexibility of a diaphragm on the analysis of reinforced concrete building structures. A single storey 1:6 scale micro-concrete model was used in the study. Floor-slabs were incorporated into the numerical model. Numerical results were compared with shaking table test data. The results indicated that inplane floor flexibility is an important factor for predicating the seismic response of shear-wall-frame buildings. Inplane deflections of the floor diaphragms may increase strength and ductility demands on the columns of the flexible frames below. Therefore, a rigid floor diaphragms assumption is not recommended for adaption in the design of flexible frame structures.

A flexible floor assumption can be used in the numerical models whereby the floor slabs are modelled using two dimensional plate elements. Flexibility also increases the lateral load transfer to frames or walls due to the deformation in the slabs, including shear and flexible effects. The flexible floor assumption may provide more accurate estimates of the lateral deformation of the building structures. When a flexible floor assumption is incorporated, structures above the transfer plate and those below, must be modelled to include the interaction between the transfer plate and the structure.

DEEP BEAM ASSUMPTION

Transfer girders or reinforced concrete deep beams, are commonly used to carry heavy transfer loads with large spans. Deep beams with depths comparable to their spans are used in a variety of structures. Numerous experiments have been conducted. Li *et al* (1952), Sadd and Hendary (1961), Archer and Kitchen (1960), Howard (1972), Max (1937) and Ashraf (1997) investigated the distribution of bending, shear and maximum displacement in deep beams with different end conditions and different length to span ratios. Tan *et al* (1995, 1997a, 1997b and 1998), Foster and Gilbert (1996) and Hwang and Yun (2004) studied the stress and strain distributions in high-strength concrete deep beams. These studies indicate that the stresses and strains in deep beams depart completely from the simple elementary theory. Distributions of the bending stresses on vertical sections are not linear and the distributions of shear stresses are not parabolic. Consequently, a transverse section which is a plane before bending does not remain approximately plane after bending and the neutral axis does not usually lie at the mid-depth. A number of numerical analyses have been developed by Shawki and Arnold (1961), Coull (1966), Robins (1973), Goh (1995), Lin (1995), Ahmed *et al* (1995), Foster and Gilbert (1998), Averbuch and Buhan (1999), and Zhao *et al* (2004) for estimating the stress and strain at different levels within reinforced concrete deep beams.

A deep beam is in fact a vertical plate subjected to loading in its own plane. The strain or stress distribution from top to bottom is no longer a straight line, and the variation is mainly dependent on the span-to-depth ratio of the beam. Analysis of a deep beam should, therefore, be treated as a two-dimensional plane stress problem. Two-dimensional stress analysis should be used in order to obtain a realistic stress distribution in deep beams, even in the case of a linear elastic solution. In general, this class of two-dimensional stress problems can be solved by a two-dimensional displacement function approach or by Airy's stress function approach.

TRUSS AND TIE ANALOGY

Since the transfer plate is a thick structure, a truss model could also be used in the design. For instance, various deep beam and pile cap designs have been developed in the last few centuries. The truss model has high adaptability when dealing with arbitrary geometric and loading configurations. Two advantages can be observed for the truss model. Firstly, the flow of forces can be easily visualized. Secondly, the influences of both shear and moment are accounted for simultaneously and directly in the design. A three-dimensional truss model can also be generated to represent a transfer plate with irregular geometry when subjected to general form of loading.

ASCE-ACI Committee 445 (1998) presented several truss models and related theories for the design of reinforced concrete deep beam members subject to high shear loading. The approaches incorporated the so-called concrete contribution with assumptions for the angles and the spacing of the inclined cracks. Stress transfer across the cracks could then be determined. The state of stress in the web has a tensile stress perpendicular to the principal compressive stresses. Schlaich *et al* (1987) proposed to generalize the truss analogy in the form of strut ant tie models by following the path of the forces through a structure. Foster (1998) describes the mechanics of non-flexural behaviour in the concrete struts and determined the minimum reinforcement demands and minimum web reinforcement requirements. Foster and Malik (2002) determined the efficiency of the various models. They accounted for the angle of the strut and tie models based on the modified compression field theory. A summary of the several truss model approaches are described as follows:

Vecchio and Collins (1981) developed and proposed the first softened stress-strain curve for concrete under compression. The rotating-angle softened-truss model was improved and developed by Belarbi and Hsu (1994 and 1995), Pang and Hsu (1995) and Zhang and Hsu (1998). The method assumes inclination of the principal stress direction in the cracked concrete coincides with the principal strain direction. For typical elements, this angle will decrease as the shear increases. So the angle of the crack varies and rotates with increase loading. Pang and Hsu (1995) recommended that if the rotating angle does not deviate by more than 12 degrees, the use of a rotating-angle model can approximate the possibility of local yielding at the crack. Otherwise the use of a fixed angle model is recommended.

Eurocodes No.2 (1991) influences the strut and tie model. Corbels, deep beams and anchorage zones can be analysed, designed and detailed in accordance with the truss model approach. For non-prestressed or prestressed concrete members without shear reinforcement, the strut angle should be assumed as low as 18 degrees. For non-prestressed or prestressed beams with shear reinforcement, Ramirez and Breen (1991) and Eurocode No. 2 (1991) discuss the use of the modified sectional-truss model approach. Limitation of the angle of inclination for the truss diagonals is 30 degrees for non-prestressed concrete and 25 degree for prestressed beams.

Pang and Hus (1996) proposed the fixed-angle softened truss model to predict the response of membrane moments when subjected to shear and normal stress. Orientation of the initial crack direction is assumed to remain unchanged through out the cracking process. This model is capable of including the contribution of concrete.

Marti (1985a and 1985b) applied the simple strut and tie model to analyse concrete members with longitudinal and transverse reinforcements. The strut and tie model was successfully used to analyse deep members without transverse reinforcement. Siao (1993 and 1995) verified and examined the behaviour of deep beams and pile caps. Analysis results using the strut and tie approach compared well with those obtained from the experiments.

Marti (1990) studied transverse shear in thick plate design. The use of a truss model for shear design of beams was extended to transversely reinforced slabs. Application of the design procedures was illustrated with a thick transfer plate in a high-rise building. The thick plate was represented by a sandwich model to compute the normal stress. In the case of a cracked core, transverse reinforcement should not be provided. It is not necessary to allow for transverse shear by strengthening the in-plane reinforcement. For a diagonally cracked core, a truss-model based design procedure has been developed that permits the design of the necessary transverse and in-plane reinforcement.

While such methods are simple and conservative, they have at least three shortcomings. Firstly, they do not provide a basic understanding of the transverse shear forces in the interior of reinforced concrete slabs. Secondly, they do not recognize the shear force transference by twisting moments along the slab edges. Thirdly, they do not provide a consistent model for the dimensioning of transversely reinforced slabs.

2.5 CONSTRUCTION METHODS FOR TRANSFER PLATE

Many high-rise reinforced concrete residential buildings in Hong Kong have transfer plates in their structures. The transfer plate is a tool that enables the architect and developer to alter the usage of a floor by a simple change in the column layout. The complicated layout of structural walls in a residential building can be simply realigned to a constant column grid to transform the floor space for commercial usage. Based on the preliminary information obtained at the planning stage, both reinforced concrete and post-tensioned concrete transfer plate scheme have been developed for comparison on the cost and program. Their construction methods are discussed in this Chapter.

It is common in Hong Kong to design and construct a building using reinforced concrete. The function of the transfer plate is to transfer the loads between the different structural layouts above and below the transfer plate. A transfer plate has considerable depth and contains large reinforcement quantities. The depth of a transfer plate is greater than 2 m and the reinforcement is almost always greater than 5.0%. The transfer plate has a heavy self-weight, and a large amount of heat can be released during the concreting and curing process. It is common, therefore, to divide the transfer plate into two or more parts during construction using vertical construction joints or horizontal construction joints.

VERTICAL JOINT CONSTRUCTION

A vertical joint construction is now rarely used. Figure 2.13 shows the layout of a transfer plate, which is cast in 5 parts during the construction process. The four side wings, numbered (1) to (4), and the centre core, numbered (5), are separately constructed. A falsework system, or scaffolding system, is shared by the slabs below the transfer plate structure to carry the heavy gravity forces resulting from the self-weight of the four side wings.

HORIZONTAL JOINT CONSTRUCTION

The transfer plate is cast in 2 stages, as shown in Figure 2.14. 1 to 1.5 m of concrete is cast first as the 1^{st} layer. The 2^{nd} layer, the remainder part, is cast 5 days after the casting of the first layer. Cement mortar floating on top of the concrete surface of the 1^{st} layer is removed by a water jet machine. Plastic sheeting is used during curing of the concrete and water is sprayed evenly on the top of the surface twice a day for the period of 3 days after concreting. Before casting the 2^{nd} layer, a slush coat of Daraweld-C is applied over the surface of the 1^{st} layer to obtain an integral bond with the 2^{nd} layer. The 1st layer at the age of 5 days is strong enough to support the loading from the 2^{nd} layer of concrete. The scaffolding system can be removed 16 days after the casting of the 1^{st} layer.

POST-TENSIONED TRANSFER PLATE CONSTRUCTION

Post-tensioning is an extremely effective way to reduce the main reinforcement by replacing it with high strength steel strand tendons. Post-tensioning allows a combination of compression arches and struts to form in conjunction with the tension ties provided by the post-tensioning tendons. Using the "load balancing" of characteristics the post-tensioning concept, the post-tensioned transfer plate has the benefits of reduced plate thickness and reduced normal reinforcement quantities.

During the construction process, the transfer plate in general is divided into two or three horizontal layers. The first layer is designed to support the subsequent layers through partial stressing of the permanent bottom layer tendons. This reduces the cost of and time needed for falsework and reduces the concrete pours to manageable sizes. The partial prestress also provides measures against possible early age shrinkage cracking in the concrete.

2.6 CONCLUDING SUMMARY

Based on the recent research studies, Wong *et al.* (1998a, 1998b) concluded that the seismicity level of Hong Kong is of intensity VII based also on the seismic design code of China (GB50011-2001). The seismic zoning map published by the Chinese Seismological Bureau, rates Hong Kong at seismic intensity VII.

Transfer structures are commonly provided in reinforced concrete high-rise residential or commercial buildings in Hong Kong to provide large spaces and modulation of the vertical structure. In recent researches, Zunz and Wise (1998) and Ho (1999) studied the performance of transfer frame and truss systems in high-rise building structures. Lam (1999) investigated the structural behaviour of vierendeel truss systems in high-rise buildings using both elastic and inelastic analyses. Structural behaviour, analysis and design of reinforced concrete transfer girder systems in tall buildings formed a series of studies. Kuang and Li (2001), Kuang and Puvvala (1996), Kuang and Atanda (1998) and Li *et. al.* (2002) analysed and investigated the structural behaviour of transfer girder framing in low-rise buildings. However, there is a lack of research studying the lateral performance of high-rise buildings with a transfer plates in relation to the static and dynamic response of these buildings.

Since transfer plate structures are increasingly used in Hong Kong as structural systems in high-rise buildings, a major problem for study is the abrupt change in the lateral stiffness of a building, from a stiff shear wall system above the transfer plate to a column-girder system below. This introduces a soft or weak storey. There is no local code of practice or standard to design such transfer plate structures. Since there is a lack of research and design codes for transfer plate structures in the high-rise buildings, the structural behaviour of transfer plate and the stress distribution within the system is yet to be fully understood.

Local practice only proposes design principles and analytical concepts. A transfer plate is also designed using deep beam theory (or transfer girder approach) and thick plate theory, both of which do not assume a rigid diaphragm. Since the transfer plate is a thick structure, engineers accept the truss model for use in the design.

Using deep beam theory or the transfer girder approach in the design of transfer plates makes use of the fully developed knowledge and behaviour of deep beam and transfer girder structures. Transfer girders and reinforced concrete deep beams research starting with Max (1937) to Zhao *et al* (2004) in studying the stress and strain distributions in different types of reinforced concrete deep beam. ASCE-ACI Committee 445 (1998) and Eurocode No. 2 (1991) present several truss models and related theories for the design of reinforced concrete deep beam members subjected to high shear loading. These approaches incorporate the past research results from Vecchio and Collins (1981) to Foster and Malik (2002), to enable engineers to use the truss and tie analogy in simple and conservative ways.

Since there is a lack of research and design codes for transfer plate structure in high-rise buildings, the structural behaviour of transfer plate and stress distribution of the system is not fully understood as stated above. In this study, a rational and efficient structural model has been developed to predict the behaviour, load transfer and the force distribution in the system. Furthermore, the interaction between the transfer plate system, upper floors and supporting structures has also been investigated.

Figure 2.1 Transfer plate for a single high-rise building – Royal Reninsula.

Figure 2.2 High-rise building with a transfer plate system – Royal Reninsula.

Figure 2.3 Transfer plate structures for a building estate – Park Avenue in Tai Kok Tsui.

Figure 2.4 Connection between a single transfer plate and continuous transfer plate in high-rise buildings system – Tung Chung Crescent in Tung Chung.

Figure 2.5 High-rise building with a transfer plate system –Tung Chung Crescent in Tung Chung.

Figure 2.6 High-rise building with a transfer plate system – Sham Wan Towers in Aberdeen**.**

Figure 2.7 High-rise building with a transfer plate system – The Belcher's in Pokfulam.

Figure 2.8 High-rise building with a transfer plate system – Island Resort in Siu Sai Wan.

Figure 2.9 High-rise building with a transfer plate system – Sky Garden in Kowloon City.

Figure 2.10 High-rise building with a transfer plate system completed in Tseung Kwan O.

Figure 2.11 High-rise building with a transfer plate system – King Ming Court in Tseung Kwan O.

Figure 2.12 Structural layout of a high-rise building with a transfer plate.

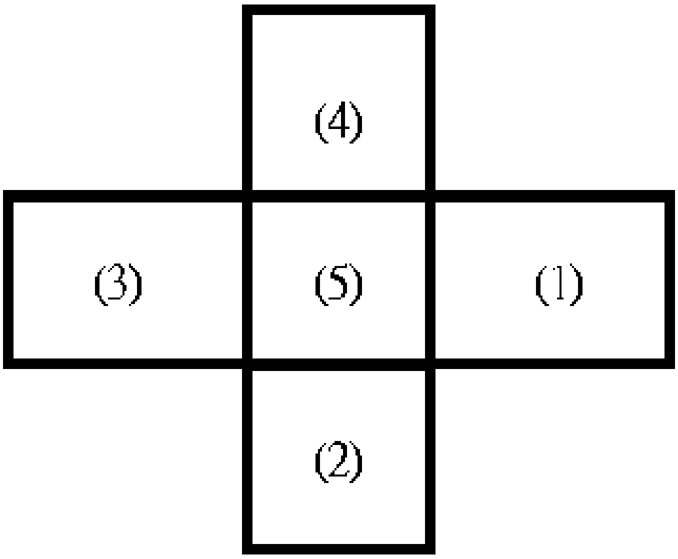

Figure 2.13 Construction layout of the Vertical Joints Method.

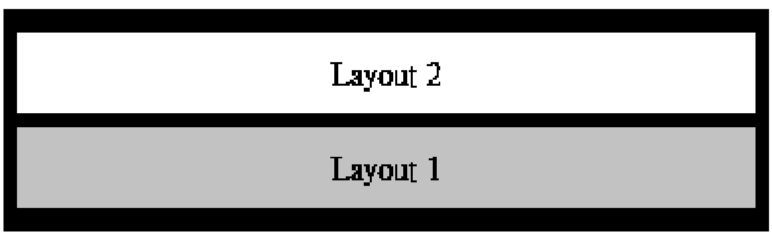

Figure 2.14 Construction layout of the Horizontal Joints Method.

3 ANALYSIS OF A HIGH-RISE BUILDING WITH A TRANSFER PLATE

Based on the review of local design practice and construction practice for transfer plates in Hong Kong in Chapter 2, two different types of numerical analysis to predict the static and dynamic response of the buildings with a transfer plates are discussed in this chapter. These two methods consist of a simplified un-coupled approach and a finite element approach. The three commercial packages ETABS, SAP2000 and ABAQUS were used. Numerical models of the transfer plate required different modelling techniques for the different programs. ETABS and SAP2000 provide lists of examples to help check accuracy of analyses. However, the accuracy of the ABAQUS results needed careful examination and a series of reinforced concrete structures or buildings examples were considered.

In this study, a simplified un-coupled approach and a finite element approach were used to evaluate the structural characteristics of a typical residential building with a transfer plate structure. The modelling techniques for a high-rise building with a transfer plate using different approaches are described. The prototype building used in this study is a high-rise residential building representative of considerable fraction of the building stock in Hong Kong. Detailed information on this high-rise building is described in Section 3.1.

3.1 CHARACTERISTICS OF THE PROTOTYPE BUILDING

The prototype building, in common with many high-rise buildings in Hong Kong has a transfer plate and a podium, and there is no seismic resistance provision in the design. It is a reinforced concrete structure with 39 typical floors supported by a transfer plate and a 4 level podium below the transfer plate. Typical floor area is 613 m^2 and total building area is 29987 m^2. The building is relatively regular in plan and elevation. A typical storey height is 3 m, storey heights at the podium are 4.0 m from level 1 to level 3, and storey height at podium level 4 is 6.15 m. The total height of the building is 141.65 m.

Figure 3.1 shows the structural form of the prototype building. The transfer plate is 2.5 m thick. The typical floor plan consists of shear walls and a central core. The central core is continuous to the foundation, and its walls thickness below the transfer plate is 1 m. This is reduced to 475 mm from 5th to 17th floor, 350 mm from 18th to 30th floor and 250 mm from 31st to 43rd floor. The shear walls are 200 to 250 mm thick. Below the transfer plate, 8 columns are used to support all the shear walls above the transfer plate. The columns are circular section of 2.2 m diameter. A wall-frame dual system is provided at the podium levels. Typical floor slabs are 150 mm thick and the podium floor slabs are 250 mm thick.

The characteristic strength of concrete for structural members is 40 MPa for the 1st to 17th floors (including structural walls, central core walls, transfer plate, beams and columns). For the 18th to 30th floors, the characteristic strength of concrete is 30 MPa for structural walls, beams and columns, and 40 MPa for central core walls. The characteristic strength of concrete for all structural members from 31st to 43rd floors is 30 MPa. Loading on the prototype building is given in Table 3.1. According to the Code of Practice for the Structural Use of Concrete-1987, the modulus of elasticity was assumed to be 21.7 MPa for the Grade 30 concrete and 24.0 MPa for the Grade 40 concrete. Imposed loads acting on the prototype building are based on the Hong Kong Building (Construction) Regulations S17. The unfactored dead and live loads acting on the typical floor slab is 6 kN/m^2 and on the podium slab is 9 kN/m^2.

3.2 COMPUTER MODELLING OF A HIGH-RISE BUILDING WITH A TRANSFER PLATE STRUCUTRE

To predict the static and dynamic response of a building with a transfer plate, a three-dimensional building model was constructed. Two different modelling approaches were introduced in this study, namely the simplified un-coupled approach and the finite element approach.

The simplified un-coupled approach is a standard, simple and commonly used design approach accepted in Hong Kong. Commercial packages provide the ability to use the simplified un-coupled approach to analyse the behaviour of the buildings for shorter computational duration.

In this approach, a rigid diaphragm assumption is applied in the building model. Loadings from the upper structures and the supporting frame and central core are directly applied to the plate. No interaction effect is considered between the slab and the vertical elements. The building sections are fixed in the horizontal plane due to the horizontal rigidity of the floor slabs. Warping behaviour of all vertical walls and core walls is not considered. Therefore, it is not necessary to consider slabs. Flexural and in-plane responses are uncoupled in the numerical models. The behaviour of the building structure can be represented by only three degrees of freedom per floor. These three degrees of freedom are the rigid body translations and rotations, as shown in Figure 3.2. Relative displacements of all the vertical elements can be readily derived. Thus the computational effort for the dynamic analysis of structures can be greatly reduced.

As a result, the transfer plate model can only provide an estimate based on the deep beam theory or thick plate theory. Basically, engineers in Hong Kong adopt the “simplified un-coupled approach” design concept to analyse high-rise building using a standard structural analysis computer program such as ETABS and SAP2000. Since floor slabs are not considered in the model and the transfer plate is assumed to be acting as a rigid diaphragm, loading behaviour on the transfer plate caused by the transfer of loads from the structure above the transfer plate to the structure below the transfer is not considered. It is desirable, therefore, to use a three-dimensional finite element model to carry out an accurate analysis of a building structure with the in-plane deformation of floor slabs also allowed for. However, there are shortcomings caused by very tedious input preparation and longer computation time.

A finite element model was, therefore, developed to represent only the transfer plate for a high-rise building structure. Vertical loads and moments acting on the finite element model are derived from the results obtained from the previous analysis, i.e. the high-rise building model. Using the finite element method, stresses and deformations of the transfer plate can be predicted in sufficient detail for the design of the transfer plate. In this study, the numerical models estimated by the finite element approach are based on ABAQUS version 5.8.14.

3.3 ANALYTICAL COMPUTER MODELLING TECHNIQUES

In this study, the simplified un-coupled approach and the finite element approach have been applied to evaluate the structural characteristics of a typical residential building with a transfer plate structure. The advantages and disadvantages of these modelling approaches are discussed in Table 3.2. Numerical models have been generated using the analysis program ETABS version 6.22 for the simplified un-coupled approach and modified simplified un-coupled approach. Numerical models for the finite element approach were generated using the finite element program, ABAQUS version 5.8.14. Parametric studies with respect to the numerical models were conducted and are discussed below.

3.3.1 FINITE ELEMENT MODELS

Three dimensional finite element building models were constructed using ABAQUS version 5.8.14. Modelling techniques implemented in the ABAQUS models and the underlying assumptions are as follows:

1. Geometries were defined at the element's centrelines. Dimensions of walls were defined by the geometric centre of columns or by exterior borders if columns were not present.
2. Beams and columns are modelled using three dimensional beam elements.
3. Shear walls, core walls and slabs are modelled by first order rectangular shell elements.
4. Floor slabs were considered to be rigid in plan and rigid diaphragm action was assumed.
5. Transfer plate was modelled using eight nodes solid elements.
6. All the elements were considered to be elastic.
7. Boundaries at the foundation level were assumed to be in a fixed condition.

As the whole of the high-rise building structure was modelled in the finite element model, thousands of nodes and elements were used to create a fine mesh. Because of the limitation of the computational source, substructures or super elements were used. A distinction can be made between substructures and super-elements. The response within a substructure can be recovered from the response of its retained degrees of freedom. The equations that relate the linear response of the eliminated (internal) degrees of freedom to that of the retained degrees of freedom are retained as part of the substructure's definition. These internal equations are not retained in a super-element, thus saving a large amount of storage space in the substructure or super-element library file for large models at the expense of not being able to recover the solution within the super-element. Figures 3.3 to 3.5 show the super-element model of transfer plate and typical floor of the high-rise building. Figure 3.6 shows part of the combined super-element model. The complete finite element model is shown in Figure 3.7.

3.3.2 SIMPLIFIED UN-COUPLED MODELS IN ETABS PROGRAM

The simplified un-coupled building models were constructed using a commercial package, ETABS version 6.22. Modelling techniques implemented in the ETABS models and the underlying assumptions were as follows.

1. Geometries are defined at the centrelines of the elements. Dimensions of walls are defined at the geometric centres or the exterior borders.
2. All beams and columns are modelled by “BEAM” and “COLUMN” elements respectively.
3. All shear walls and core walls are modelled by “PANEL” elements.
4. The transfer plate is assumed to be a rigid diaphragm and is modelled by using “BEAM” elements to connect all the walls above and columns below the transfer structure.
5. Walls modelled with a few small panels have membrane properties if the height / length ratio is not greater than 1.5. When the height / length ratio is greater than 1.5, the panels are modelled by “COLUMN” elements.
6. All the members are assumed to be elastic.
7. Boundaries at the foundation level are assumed to be in a fixed condition.
8. Floor slabs are considered to be rigid in-plane, and displacement compatibility is applied to all the joints at the same level.
9. Loadings are assumed to be acting on each floor.

Here, the “BEAM”, COLUMN” and “PANEL” are the specific names of the elements defined in ETABS. The characteristic of these elements are described below:

A “BEAM” element generally exists horizontally at any level in a predefined bay. “BEAM” connections are assumed to be fixed and rigid at the two ends.

A “COLUMN” element exists vertically at any level. Length of the “COLUMN” element is the storey height. End conditions of “COLUMN” element are assumed to be continuous and rigid.

A “PANEL” element exists vertically at any level and between any two consecutive levels. The bottom of the “PANEL” is assumed to be fixed. “PANEL” elements are assumed to incorporate both bending and shear stiffnesses.

Parts of the ETABS model are shown in Figure 3.8. Figure 3.9 shows the complete model of the high-rise building structure.

Since the transfer plate is assumed to be acting as a rigid diaphragm, loading effect above and below the transfer plate are not considered in the model. As a result, the response of the transfer plate has to be estimated using thick plate theory. A commercial package SAP2000 version 7.12 was used to estimate the responses of the transfer plate, as shown in Figure 3.10. The modelling techniques implemented in the SAP2000 model and the underlying assumptions are as follows.

1. The transfer plate is generated by 4-nodes thick shell elements.
2. The boundary conditions at supporting points from the structure below are assumed to be fixed.
3. Loadings applied to the transfer plate are estimated using the ETABS model.

3.4 SIMPLIFIED UN-COUPLED APPROACH AND FINITE ELEMENT APPROACH

In all the studies, lateral responses of the building structures were estimated using linear elastic analyses. The high-rise building models are subjected to static lateral loads. In the first six cases, the structures carry static lateral uniformly distributed loads that represent the wind loadings applied at the horizontal direction along the height of a building. In the next four cases, wind loads are considered based on the Code of Practice on Wind Effect Hong Kong 1983.

In particular, the first three cases were also used to verify the rate of convergence and accuracy achieved by the 4-nodes shell elements and the three dimensional beam elements of ABAQUS. The next five cases were also used to verify the coupling effect of floor slabs. The last case was also used to verify the techniques in the modelling of the transfer plate.

Characteristic strength of concrete used in all the models is Grade 40 concrete and the respective Modulus of Elasticity, according to Table 2.1 in the Code of Practice for the Structural Use of Concrete (1987), was assumed to be 2.4×10^7 kN/m^2.

3.4.1 TWO-DIMENSIONAL SINGLE SHEAR WALL STRUCTURE

This problem was used to evaluate the behaviour of the ABAQUS 4-nodes shell elements by means of structural wall configurations.

The basic structural layout is shown in Figure 3.11(a). The two-dimensional reinforced concrete single shear wall has 40 floors supported on the ground floor. It carries a lateral uniformly distributed load of 5.55 kN/m and the lateral loads are applied at the floor levels. In order to consider a reasonable range of wall dimensions, aspect ratios of 13.33, 17.39, 40 and 80 are considered. Aspect ratios of the walls are determined using “total height of wall” divided by “width of wall” In each case, the wall has a 3 m floor to floor height and the thickness of the wall is 0.5 m. In the finite element approach, the element size used for generating the structures is 0.3 m × 0.3 m and uses 4-nodes shell elements.

In accordance with fundamental theory, the flexural and shear rigidity of the wall are taken into account. Maximum deflection of a single shear wall with equivalent uniformly distributed lateral load is

$$y_{\max} = \frac{wH^4}{8EI} + \frac{wH^2}{2GA} \tag{3.1}$$

where

H is the height of the single shear wall

w is the lateral uniformly distributed load

EI is the flexural rigidity of the wall

GA is the shear rigidity of the wall

Figure 3.11(b) shows the deflected shape of the single wall structure. Both the finite element approach and the simplified un-coupled approach provide accurate predictions for this type of structure. Results of the deflection at the top of the walls are summarized in Table 3.3.

3.4.2 TWO-DIMENSIONAL COUPLED SHEAR WALL STRUCTURE

To further explore the accuracy of the finite element approach, the deformation of the coupled shear wall structure was predicted.

Figure 3.12(a) shows a coupled shear wall subjected to static lateral uniformly distributed loads of 5.55 kN/m. In each case, buildings of 10 and 40 storeys were considered. Aspect ratios for the walls of the 40-storey building include 30, 40, 60 and 120. Aspect ratios for the walls of the 10-storey building include 7.5, 10, 15 and 30. The aspect ratio is defined as “total height of wall” divided by “width of wall”. The floor to floor height is 3 m and the thicknesses of walls are 3 m for the 40-storey building and 0.2 m for the 10-storey building. The depth of the coupling beam is

0.55 m and 0.9 m span. Detailed information of the coupled shear wall structures is summarized in Tables 3.4 and 3.5.

In the finite element approach, the element size used for creating the structures is 0.25 m × 0.25 m and 4-nodes shell elements are used. The coupling beams are modelled by using 3D beam elements.

In accordance with the fundamental theory, the maximum flexural deflection of coupled shear wall with equivalent uniformly distributed lateral loads is

$$y_{\max} = \frac{wH^4}{8EI}\left\langle 1 - \frac{1}{k^2}\left[1 - \frac{4}{(k\alpha H)^2} + \frac{8}{(k\alpha H)^4 \cosh(k\alpha H)}(1 + k\alpha H \sinh(k\alpha H) - \cosh(k\alpha H)\right]\right\rangle \tag{3.2}$$

and

$$k^2 = 1 + \frac{(A_1 + A_{2)}(I_1 + I_2)}{A_1 A_2 l^2} \quad , \tag{3.3}$$

$$\alpha^2 = \frac{12 I_c l^2}{b^3 h (I_1 + I_2)} \quad , \tag{3.4}$$

$$I_c = \frac{I_b}{1 + (\frac{14.4 E I_b}{b^2 G A_b})} \tag{3.5}$$

where

EI_b is the flexural rigidity of the coupling beam

GA_b is the shear rigidity of the coupling beam

b is the clear span of a beam

h is the storey height

I_i and A_i are the moment of inertia and the cross-section area of wall i

H is the total height

Deflected shapes of the coupled shear wall structures are plotted in Figure 3.12(b). Numerical results obtained from the finite element approach and the simplified un-coupled approach are in close. Results of the deflection at the top of the coupled shear wall structures are shown in Tables 3.6 and 3.7. Since the finite element approach considers both flexural and shear rigidities of coupled shear wall, deflections obtained from the finite element approach show a slight different to those obtained using fundamental theory, by about 0.5% in 40-storey coupled shear wall structures. For the case of the 10-storey coupled shear wall structure, the estimated maximum deflections at the top of the structures are smaller than or equal to about 0.06 m. Deflections at the top of the structures obtained using the finite element approach are about 30% greater than those obtained from fundamental theory.

3.4.3 THREE-DIMENSIONAL SINGLE SHEAR WALL STRUCTURE

The two reinforced concrete single shear walls have 40 floors supported on the ground floor, as shown in Figure 3.13. Static lateral uniformly distributed loads of 22.2 kN/m are applied along the height of the structure and these lateral loads are applied at the floor levels. The floor-to-floor height of the structure and the clear span of the slab between two walls are 3 m and 6 m respectively. The wall aspect ratio is 17.39 and the thickness of wall is 0.25 m. In the finite element models, walls and the slabs are represented by 0.3 m × 0.3 m 4-nodes shell elements.

The accuracy of using the finite element approach in a three-dimensional single shear wall structure was illustrated in this example.

Results of the deflection at the top of the walls are summarized in Table 3.8. The three-dimensional results are in excellent agreement with the two dimensional finite element analysis results for this type of structure.

3.4.4 THREE-DIMENSIONAL COUPLED SHEAR WALL STRUCTURE

This problem is similar to the case studies in section 5.3. The structure is shown in Figure 3.14. Two sets of reinforced concrete coupled shear walls have 40 floors supported on the ground floor and carry static lateral uniformly distributed loads of 22.2 kN/m along the height of the structure. The lateral loads are applied at the floor levels. The clear span of the slabs between two walls is 6.0 m. The storey height is 3.0 m. The wall aspect ratio is 40 and the thickness of wall is 0.25 m. In the finite element approach, walls and the slabs are created by using 0.25 m × 0.25 m 4-nodes shell elements.

Table 3.9 summarized the results of the deflection at the top of the walls The three-dimensional results are in excellent agreement with the two dimensional finite element analysis results for this type of structure.

3.4.5 THREE-DIMENSIONAL U-SHAPED WALL STRUCTURE

An un-symmetrical wall configuration subjected to a static load was considered in this example to evaluate the slab behaviour.

A reinforced concrete U-shaped wall structure with 40 floors supported on the ground floor is illustrated in Figure 3.15. The structural layout is symmetrical in the x-direction and un-symmetrical in the y-direction. Two static lateral load cases are considered to evaluate the slab effect in a high-rise structure with un-symmetrical layout. Uniformly distributed loads of 22.2 kN/m are considered in both directions separately. The lateral loads are applied at the floor levels. The storey height is 3.0 m and the thickness of walls is 0.25 m. In the finite element approach, the walls and the slabs are generated by using 0.3 m × 0.3 m 4-nodes shell elements.

Brief descriptions of the various models are as follows:

Model "FEA-R" represents a 40-storey U-shaped wall structure. The model is created using finite elements and the slab is modelled using 4-nodes shell finite elements. Rigid floor diaphragm assumption is applied to the slab.

Model "FEA-nR" is similar to Model "FEA-R", except that rigid floor diaphragm assumption is not applied to the floor slab.

<u>Model "SUA-0"</u> represents a 40-storey U-shaped wall structure. The model is created by using simplified un-coupling approach with rigid floor diaphragm assumption, and slabs are not modeled.

<u>Model "SUA-S"</u> is similar to Model "SUA-0", except that slabs are modelled using "FLOOR" elements.

<u>Model "SUA-B"</u> is similar to Model "SUA-0", except that slabs are modelled using "BEAM" elements.

A "FLOOR" element generally exists horizontally at any level in a predefined bay. The "FLOOR" element stiffness is only activated if all floor joints of an element are not connected to the same diaphragm.

Figure 3.16 shows the deformation of the building subjected to lateral load and the results are compiled in Table 3.10 for the lateral displacement of the high-rise U-shaped wall structure. The difference between the two finite element models, that with/without rigid floor diaphragm assumption, in the maximum deflection at the top of the structure in the both directions is about 1%. Based on the results estimated using simplified un-coupling approach with rigid floor diaphragm assumption, the difference between these three models in the maximum deflection at the top of the structure in the x-direction is about 0.5%. When subjected to a lateral load in the y-direction, the maximum deflection at the top of the structure is about 50% less when the slab is modelled using “BEAM” element.

The difference between the two approaches in the maximum deflection at the top of the structure in the x-direction is about 10%. When subjected to a lateral load in the y-direction, a large difference is obtained when the slab is modelled by finite elements. Floor slabs are considered in the models and are assumed to be flexible. The maximum deflection estimated by the finite element approach is about 75% less than that of the simplified un-coupled approach. The slabs provide connections between the two separated side walls and act as coupling beams, as shown in Figure 3.17. Both ends of the slabs are allowed to rotate and to displace vertically and floor slabs bend in double curvature and thus resist free bending of the walls. Therefore, storey stiffness of the structure increases due to the coupling effect of the slabs.

3.4.6 THREE-DIMENSIONAL LOW-RISE BUILDING STRUCTURE – TYPE 1

The eight-storey reinforced concrete building was completed probably in the seventies. The building is 20 m in height with a reasonably regular vertical configuration. The structural layout consists of reinforced concrete frames and traditional beam and slab floors. The characteristic strengths of concrete used for the columns and other members respectively are Grade C30 and C20 concrete. The framing plan is shown in Figure 3.18(a). A three-dimensional finite element model was constructed as shown in Figure 3.18(b). Wind loads were considered at the floor levels and are determined by the Code of Practice on Wind Effect Hong Kong 1983.

The purpose of this analysis is to examine the accuracy of finite element analysis in predicting deformation, a low-rise frame structure was considered.

The results are compiled in Table 3.11 for the lateral displacement of low-rise frame building. Figure 3.19 shows the deformation of the building subjected to wind load. Since the slabs were considered in the finite element model, the storey stiffness of the low-rise building increases due to the coupling effect of the slabs. Therefore, the displacement of the low-rise building in the finite element approach is about 15% less than that obtained by the simplified un-coupled approach.

3.4.7 THREE-DIMENSIONAL LOW-RISE BUILDING STRUCTURE – TYPE 2

This problem is presented to explore the accuracy of finite element analysis in predicting the deformed shape of a low-rise core walls and column frame structure.

The 4-storey core walls-frame building represents the “podium” of a high-rise building with a transfer plate. The building is 16 m in height with reasonably regular vertical configuration. The structural system consists of reinforced concrete frames, central core walls and traditional beam and slab floors. The strength of concrete used for the columns and other members is Grade C40. The framing plan is shown in Figure 3.20(a). The three-dimensional finite element model is constructed as shown in Figure 3.20(b). Detailed information about the structure is given in Section 3.1. In accordance with the Code of Practice on Wind Effect Hong Kong 1983, static lateral loads are applied at the floor levels.

The results are compiled in Table 3.12 for lateral displacements of the low-rise building with a transfer plate. Figure 3.21 shows the deformed shape of the building when subjected to lateral wind load.

Slabs are considered in the finite element model and storey stiffness of the low-rise core walls-frame structure increases. Since the structural layout of the low-rise building is formed by the core walls, beams, columns and frames, height is a major factor in determining the lateral stiffness of the wall-frames. The core walls behave as flexural cantilevers and the frames behave as shear cantilever. As a result, the displacements at the 1st and the 2nd floor levels estimated by the finite element approach are about 25% difference from those of the simplified un-coupled approach. At the 3rd and 4th floor levels, the estimated displacements in the finite element model are about 55% less than those of the simplified un-coupled approach.

3.4.8 THREE-DIMENSIONAL HIGH-RISE BUILDING STRUCTURE

To further explore accuracy of the finite element analysis in predicting the deformation, a 39-storey reinforced concrete building, representing the upper part of a high-rise building with a transfer plate was examined. The building is 117 m in height with reasonably regular vertical configuration. The structural system consists of reinforced concrete walls, beam and slab floors. The characteristic strengths of concrete used for the walls and other members respectively are Grade C40 and C30. The framing plan is shown in Figure 3.22(a). A finite element model was constructed as shown in Figure 3.22(b). A description of the structure being modelled is given in Section 3.1. The high-rise building structure is subjected to the lateral wind load, are considered. The lateral wind loadings are applied at the floor levels and are determined by the Code of Practice on Wind Effect Hong Kong 1983.

Figure 3.23 shows deformations of the building subjected to lateral load and the results are compiled in Table 3.13 for the lateral displacement of the high-rise wall-frame building. The difference between the two approaches in the maximum deflection at the top of the structure in the x-direction is about 25%. When subjected to a lateral load in the y-direction, a large difference is obtained if the slab is represented by finite elements. The maximum deflection estimated by the finite element approach is about 40% less than that of the simplified un-coupled approach. Floor slabs are considered in the models and are assumed to be flexible and provide connection between the two separated side walls. Acting as coupling beams, both ends of the slabs are allowed to rotate and to displace vertically and the bend in double curvature and thus resist free bending of the walls. Therefore, storey stiffness of the structure increases due to the coupling effect of the slabs.

3.4.9 THREE-DIMENSIONAL LOW-RISE BUILDING STRUCTURE WITH A TRANSFER PLATE

This problem is an example of a static lateral load analysis of core wall column and frame structural configurations to evaluate accuracy of the three different modeling techniques used for the transfer plate, including bending modelled as beams, thick plate elements and three-dimensional solid elements. The model used in this analysis is a low-rise building structure with a transfer plate. The accuracy of using the finite element approach to predict deformation was explored.

The 4-storey wall-frame building with a transfer plate structure represents the lower part of a high-rise building with a transfer plate. The building is 24.65 m in height with reasonably regular vertical configuration. The structural system consists of reinforced concrete frames, central core wall and traditional beam and slab floors. The strength of concrete used for the columns and other members was Grade C40. The framing plan is shown in Figure 3.24. Detailed information about the structure is given in Section 3.1. In accordance with the Code of Practice on Wind Effect Hong Kong 1983, static lateral load is applied at the floor levels. Two different modelling techniques for transfer plate structures are used in the finite element models to explore the implications of using the plate element in the analyses. There are “FEA-SOLID” and “FEA-SHELL”. In addition, a “SUCA” model is used and is a simplified un-coupled model. These three types of models are shown in Figure 3.25. Brief descriptions of the various models are as follows:

Model “FEA-SOLID” represents a 4-storey wall-frame building with a transfer plate structure. The model is created using finite elements and the transfer plate is modelled using 8-nodes solid finite elements.

Model “FEA-SHELL” is similar to Model “FEA-SOLID”, except that the transfer plate is modelled using 4-nodes shell elements.

Model “SUCA” represents a 4-storey wall-frame building with a transfer plate structure. The model is created by using simplified un-coupling approach and the transfer plate is modelled using “BEAM” elements.

The results are compiled in Tables 3.14 and 3.15 giving lateral displacements of the low-rise building with a transfer plate. Figure 3.26 shows the deformed shape of the building when subjected to lateral wind load.

On including the slabs in the finite element approach, storey stiffness of the low-rise building increases. Therefore, the estimated displacement at the podium levels of the low-rise building using the finite element approach is about half of the results predicted by the simplified un-coupled approach.

Since the transfer plate is supported by the central core walls and the columns, the storey stiffness not only includes the shear stiffness of the core walls and columns but also includes the coupling effect on the core walls and columns providing by the transfer plate. Therefore, the modelling technique for a transfer plate becomes a major factor in accurately for estimating the lateral response of a structure. The deformed shape of building estimated by the “FEA-SHELL” model is close to the analysis results obtained from the “FEA-SOLID” model. As the transfer plate is modelled using “BEAM” elements, the estimated storey stiffness of the structure is reduced to half of the results predicted by 8-nodes solid finite elements model.

3.4.10 THREE-DIMENSIONAL HIGH-RISE BUILDING STRUCTURE WITH A TRANSFER PLATE

To further explore accuracy of the finite element analysis in predicting the dynamic response of a reinforced concrete structure, a high-rise building with a transfer plate was examined through time-history analysis. The building is 141.65 m in height with reasonably regular vertical configuration. A description of the structure being modelled is given in Section 3.1. The high-rise building with transfer plate, is subjected to seismic intensity VII and is estimated using the response spectrum analyses. The seismic response spectrum is determined by the Code for Seismic Design of Buildings, GB50011-2001.

Brief descriptions of the various models are as follows:

Model "FEA-R2" represents a high-rise building with a transfer plate. The model is created using finite elements. Floor slab is modelled using 4-nodes shell finite elements, and the transfer plate is modelled using 8-nodes solid finite elements. Rigid floor diaphragm assumption is applied to the floor slabs.

<u>Model “FEA-nR2”</u> is similar to Model “FEA-R2”, except that rigid floor diaphragm assumption is not considered in the floor slabs.

<u>Model “UCSA”</u> represents a high-rise building with a transfer plate. The model is created by using simplified un-coupling approach with rigid floor diaphragm assumption, and the transfer plate is modelled using “BEAM” elements.

Table3.16 and 3.17 summarise the fundamental frequencies of a high-rise building with a transfer plate in the x-direction and that in the y-direction. The difference between the finite element approach and simplified un-coupled approach, in the fundamental frequencies of the structure in the both directions is about 25%. It indicates that storey stiffness is significantly enhanced by the coupling all vertical structural element, such as shear walls, core walls and columns, with the transfer plate or floor slab. The storey stiffnesses of a high-rise building with a transfer plate are underestimated using the simplified un-coupled approach.

3.5 CONCLUDING SUMMARY

In all of the studies, the responses of building structures when subjected to a lateral load were estimated by linear elastic analysis. The use of 4-nodes shell elements and three dimensional beam elements in the finite element models are able to achieve accurate results. There is no significant difference when using the finite element approach and the simplified un-coupled approach in the prediction of the lateral response for single shear wall and a coupled shear wall structure.

The following six cases were used to verify the coupling effect of floor slabs in different types of structures, including high-rise wall-frame structures and low-rise beams and columns frame structures. Deflections of the structures estimated by the finite element approach are different from those of the simplified un-coupled approach, because the effect of the floor slabs are considered in the finite element models. In the finite elements approach, floor slabs are important parameters for predicting the lateral response of the high-rise wall-frame structures, because the slabs acting as coupling beams provide connection between the two separated side walls.

Lateral responses estimated by using the 8 nodes solid finite elements and the thick plate method to model the transfer plate agree well. If the transfer plate is modelled using “BEAM” elements, the estimated lateral deformations of the structure are twice the estimation using 8 node solid finite elements.

The simplified un-coupled approach has over-estimated the lateral responses of the high-rise wall-frame structure. A modified analysis approach is recommended in Chapter 4 to predict the lateral deflections of a high-rise building with a transfer plate structure.

Table 3.1 Characteristic loads of the prototype building.

Type of loading	Characteristic Loads (kPa)
Finishes, screeding and ceiling	0.5 (for typical floors) 2.0 (for the podium levels)
Imposed load on the typical floors	3.0
Imposed load on the podium levels	5.0
Imposed load acting on the transfer plate	3.0

Table 3.2 Advantages and disadvantages of the simplified un-coupled approach and the finite element approach.

SIMPLIFIED UN-COUPLED APPROACH	FINITE ELEMENT APPROACH
Easy to construct the numerical model	Very difficult to generate the mesh.
	Large amount of elements
The computation time is from a few minutes to hours.	The computation time is from a few days to weeks.
The required computer storage is small.	The required computer capacity is large.
Three degrees of freedom per floor, only is required due to the floor diaphragms	The models are large and complex.
Results obtained from the analysis can be used directly.	Substructure or super-element technique is needed to construct the model.
	All six degrees of freedom are considered.
	Difficult to apply the results of the analysis to design directly.

Table 3.3 Comparison of the maximum deflection on the top of 40 storey single shear wall structure.

Aspect ratio for the wall	DEFLECTION (m)			RATIO	
	THEORY	SUA[1]	FEA[2]	SUA[1] / THEORY	FEA[2] / THEORY
13.33	0.071	0.071	0.071	1.00	1.00
17.39	0.158	0.158	0.158	1.00	1.00
40	1.920	1.920	1.920	1.00	1.00
80	15.360	15.360	15.360	1.00	1.00

Table 3.4 Detail information of 40 storey coupled shear wall structures.

Aspect ratio for the wall	Width of Both Walls (m)	Size of connecting beam (m)			A	k	kαH
		width	depth	span			
30	4.0	3.00	0.55	0.90	0.287	1.105	38.104
40	3.0	3.00	0.55	0.90	0.352	1.094	46.215
60	2.0	3.00	0.55	0.90	0.481	1.076	62.104
120	1.0	3.00	0.55	0.90	0.891	1.045	111.748

Table 3.5 Detail information of 10 storey coupled shear wall structures.

Aspect ratio for the wall	Width of Both Walls (m)	Size of connecting beam (m)			A	K	kαH
		width	depth	span			
7.5	4.0	0.25	0.55	0.90	0.287	1.105	9.526
10	3.0	0.25	0.55	0.90	0.352	1.094	11.554
15	2.0	0.25	0.55	0.90	0.481	1.076	15.526
30	1.0	0.25	0.55	0.90	0.891	1.045	27.937

[1] SUA – Simplified un-coupled approach
[2] FEA – Finite element approach

Table 3.6 Comparison of the maximum deflection on the top of 40 storey coupled shear wall structures.

Aspect ratio for the wall	DEFLECTION (m)			RATIO	
	THEORY	SUA[3]	FEA[4]	SUA[3] / THEORY	FEA[4] / THEORY
30	0.069	0.069	0.073	1.00	1.06
40	0.148	0.148	0.155	1.00	1.05
60	0.413	0.409	0.425	0.99	1.03
120	2.034	1.993	2.034	0.98	1.00

Table 3.7 Comparison of the maximum deflection on the top of 10 storey coupled shear wall structures.

Aspect ratio for the wall	DEFLECTION (m)			RATIO	
	THEORY	SUCA[3]	FEA[4]	SUA[3] / THEORY	FEA[4] / THEORY
7.5	0.002	0.002	0.004	0.93	1.62
10	0.005	0.004	0.005	0.95	1.05
15	0.013	0.013	0.018	0.97	1.41
30	0.062	0.060	0.079	0.97	1.27

Table 3.8 Comparison of the maximum deflection on the top of single shear wall structure.

Aspect ratio for the wall	Deflection (m)			Ratio	
	THEORY	2D- Model	3D- Model	2D- Model / THEORY	3D- Model / THEORY
17.39	1.75	1.76	1.81	1.02	1.03

[3] SUA – Simplified un-coupled approach
[4] FEA – Finite element approach

Table 3.9 Comparison of the maximum deflection on the top of coupled shear wall structure.

Aspect ratio for the wall	Deflection (m)			Ratio	
	THEORY	2D- Model	3D- Model	$\frac{\text{2D- Model}}{\text{THEORY}}$	$\frac{\text{3D- Model}}{\text{THEORY}}$
40	1.77	1.86	1.80	1.05	1.02

Table 3.10 Comparison of the maximum deflection on the top of U-shaped wall structure.

MODEL	Deflection (m)		Ratio	
	In the x-direction	In the y-direction	In the x-direction	In the y-direction
SUA-0	0.918	9.380	0.91	4.09
SUA-S	0.918	9.380	0.91	4.09
SUA-B	0.915	6.177	0.91	2.70
FEA-R	1.011	2.291	1.00	1.00
FEA-nR	1.020	2.316	1.01	1.01

Table 3.11 Comparison of the deflection of low-rise building – Type 1.

STOREY	Wind Load at X-direction			Wind Load at Y-direction		
	FEA[5] ($\times 10^{-3}$ m)	SUA[6] ($\times 10^{-3}$ m)	Ratio: $\frac{\text{SUA}^6}{\text{FEA}^5}$	FEA[5] ($\times 10^{-3}$ m)	SUA[6] ($\times 10^{-3}$ m)	Ratio: $\frac{\text{SUA}^6}{\text{FEA}^5}$
ROOF	15.6	17.1	1.10	17.2	20.6	1.20
5/F	14.2	15.5	1.09	15.6	18.7	1.20
4/F	12.4	13.8	1.11	13.9	16.6	1.19
3/F	10.0	11.1	1.11	11.2	13.4	1.20
2/F	7.4	8.3	1.12	8.4	10.1	1.20
1/F	4.7	5.3	1.13	5.3	6.4	1.21
MEZ	2.4	2.9	1.21	2.9	3.5	1.21
G/F	0.3	0.4	1.33	0.4	0.5	1.25

[5] FEA – Finite element

[6] SUA –Simplified un-coupled

Table 3.12 Comparison of the deflection of low-rise building – Type 2.

STOREY	Wind Load at X-direction			Wind Load at Y-direction		
	FEA[7]* ($\times 10^{-3}$ m)	SUA[8]* ($\times 10^{-3}$ m)	Ratio: $\frac{SUA^8}{FEA^7}$	FEA[7] ($\times 10^{-3}$ m)	SUA[8] ($\times 10^{-3}$ m)	Ratio: $\frac{SUA^8}{FEA^7}$
4/F	0.243	0.114	2.128	0.146	0.056	2.600
3/F	0.182	0.095	1.916	0.110	0.042	2.619
2/F	0.112	0.095	1.183	0.069	0.042	1.643
1/F	0.043	0.051	0.845	0.028	0.021	1.324

Table 3.13 Summary of the deflection results of a high-rise building.

STOREY	Wind Load at X-direction			Wind Load at Y-direction		
	FEA[7] ($\times 10^{-3}$ m)	SUA[8] ($\times 10^{-3}$ m)	Ratio: $\frac{SUA^8}{FEA^7}$	FEA[7] ($\times 10^{-3}$ m)	SUA[8] ($\times 10^{-3}$ m)	Ratio: $\frac{SUA^8}{FEA^7}$
43/F	69.4	91.6	1.32	56.6	96	1.70
39/F	64.1	84.4	1.32	51	85.2	1.67
35/F	58.1	76.2	1.31	44.9	73.9	1.64
31/F	51	66.8	1.31	38.4	62.2	1.62
27/F	43.2	56.4	1.31	31.6	50.3	1.59
23/F	34.8	45.3	1.30	24.7	38.5	1.56
19/F	26.1	33.8	1.30	17.8	27.1	1.52
15/F	17.5	22.6	1.29	11.4	16.9	1.48
11/F	9.5	12.2	1.29	5.8	8.4	1.43
10/F	7.6	9.8	1.29	4.6	6.5	1.42
9/F	5.8	7.5	1.28	3.5	4.9	1.40
8/F	4.2	5.4	1.28	2.5	3.4	1.38
7/F	2.7	3.5	1.28	1.6	2.1	1.37
6/F	1.5	1.9	1.28	0.8	1.1	1.35
5/F	0.5	0.6	1.31	0.3	0.4	1.36

[7] FEA – Finite element
[8] SUA – Simplified un-coupled

Table 3.14 Summary of the deflection results of low-rise building with a transfer plate in the x-direction.

STOREY	Model			Ratio	
	SUCA ($\times10^{-3}$ m)	FEA-SOLID ($\times10^{-3}$ m)	FEA-SHELL ($\times10^{-3}$ m)	$\frac{\text{SUCA}}{\text{FEA-SOLID}}$	$\frac{\text{FEA-SHEL}}{\text{FEA-SOLID}}$
TRANSFER	0.45	0.22	0.22	2.01	0.99
4/F	0.32	0.16	0.16	2.00	0.99
3/F	0.24	0.13	0.13	1.87	0.99
2/F	0.14	0.13	0.13	1.14	0.99
1/F	0.05	0.07	0.07	0.82	1.00

Table 3.15 Summary of the deflection results of low-rise building with a transfer plate in the y-direction.

STOREY	Model			Ratio	
	SUCA ($\times10^{-3}$ m)	FEA-SOLID ($\times10^{-3}$ m)	FEA-SHELL ($\times10^{-3}$ m)	$\frac{\text{SUCA}}{\text{FEA-SOLID}}$	$\frac{\text{FEA-SHEL}}{\text{FEA-SOLID}}$
TRANSFER	0.33	0.13	0.13	2.46	0.98
4/F	0.22	0.09	0.09	2.55	0.99
3/F	0.16	0.06	0.06	2.66	1.00
2/F	0.10	0.06	0.06	1.61	1.00
1/F	0.04	0.03	0.03	1.31	0.97

Table 3.16 Summary of the first three fundamental frequencies of high-rise building with a transfer plate in the x-direction.

MODEL	FUNDAMENTAL FREQUENCIES (Hz)		
	1st mode	2^{nd} mode	3rd mode
FEA-D2	0.506	1.779	2.877
FEA-nD2	0.504	1.764	2.854
UCSA	0.399	1.587	3.094

Table 3.17 Summary of the first three fundamental frequencies of high-rise building with a transfer plate in the y-direction.

MODEL	FUNDAMENTAL FREQUENCIES (Hz)		
	1st mode	2^{nd} mode	3rd mode
FEA-R2	0.511	2.051	3.526
FEA-nR2	0.508	2.026	3.477
UCSA	0.373	1.721	3.756

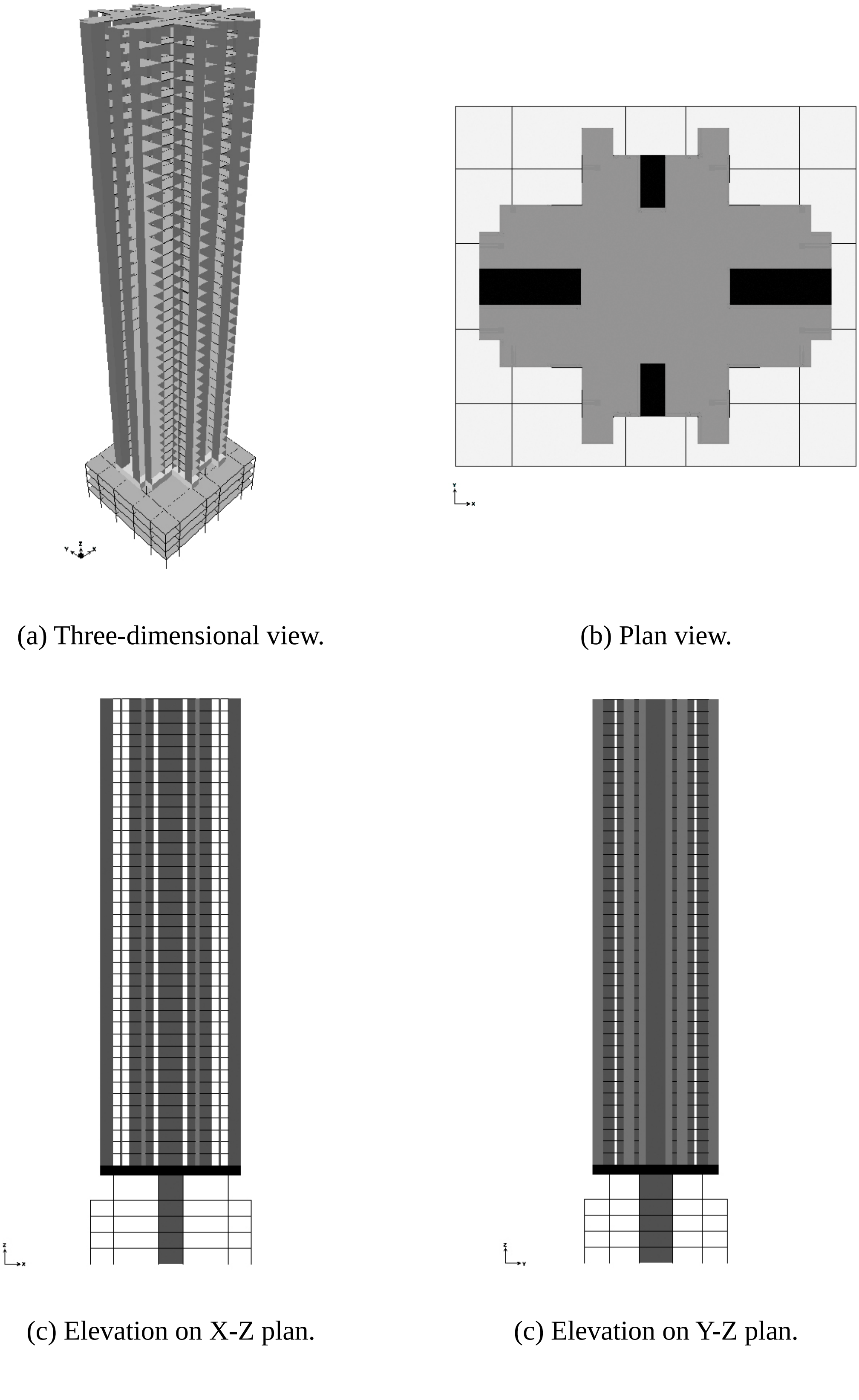

(a) Three-dimensional view.

(b) Plan view.

(c) Elevation on X-Z plan.

(c) Elevation on Y-Z plan.

Figure 3.1 Structural form of a high-rise building.

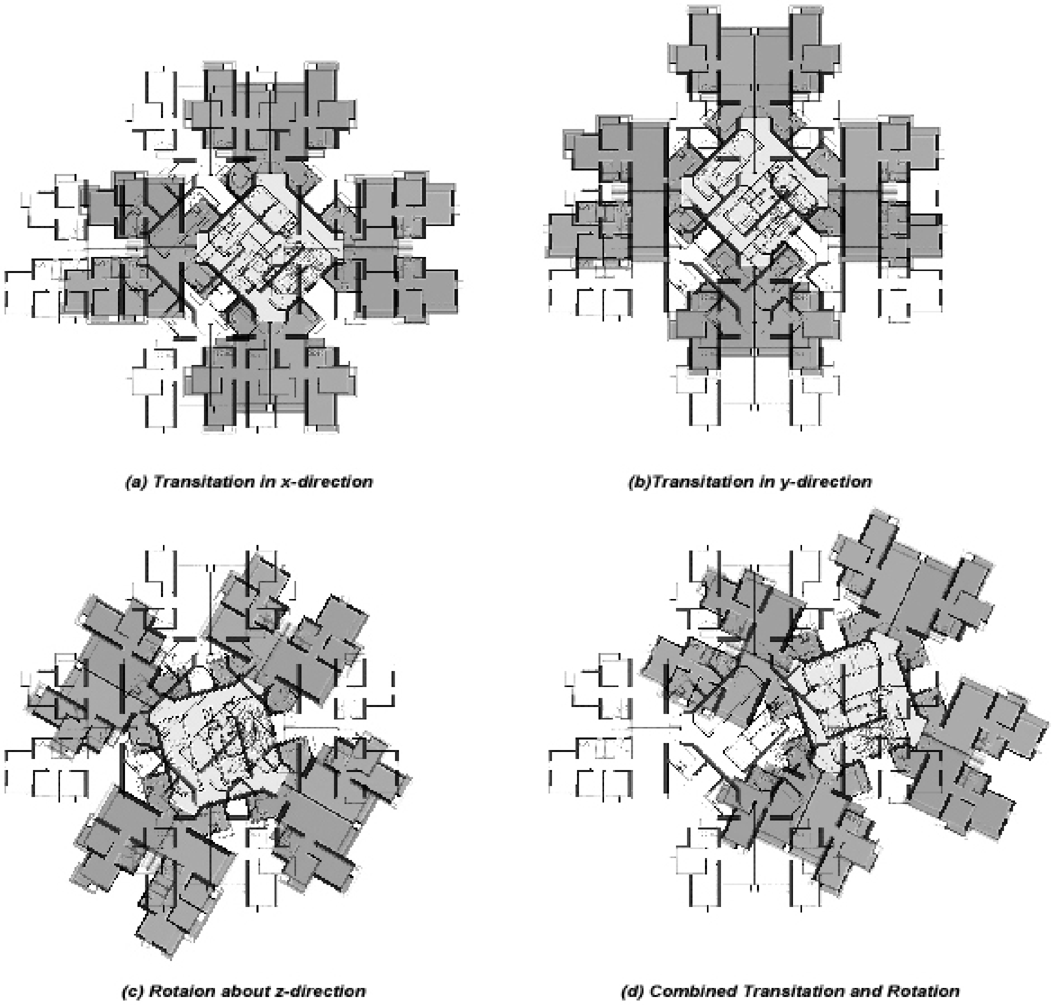

Figure 3.2 Relative floor displacements.

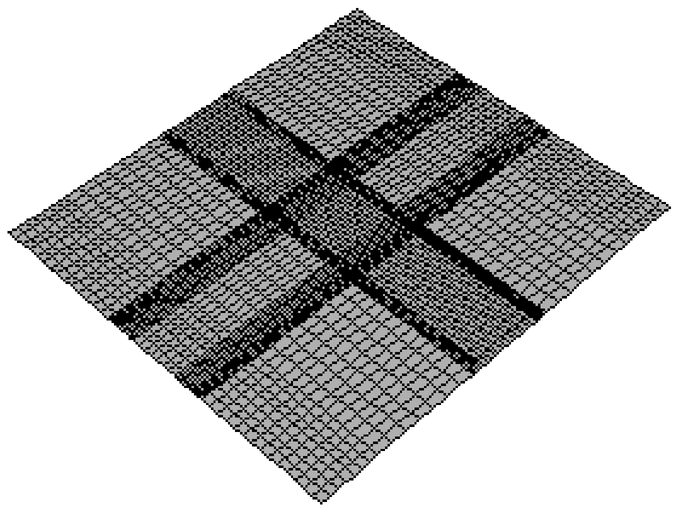

(a) Podium Slab.

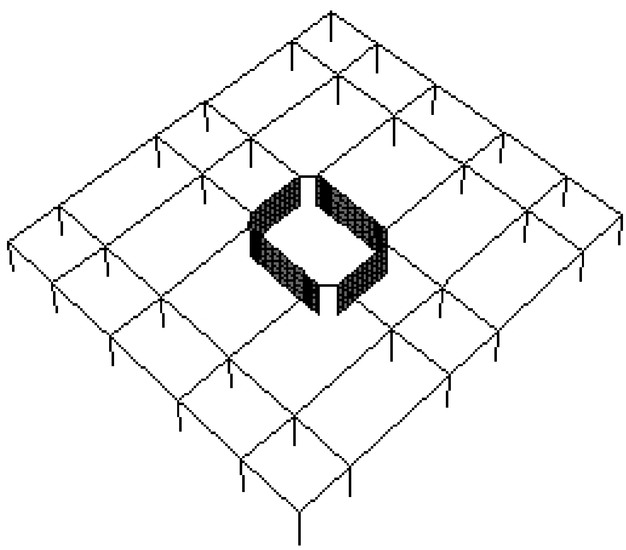

(b) Podium structure – beams and columns frame and central core-walls.

Figure 3.3 Finite element model of podium structure.

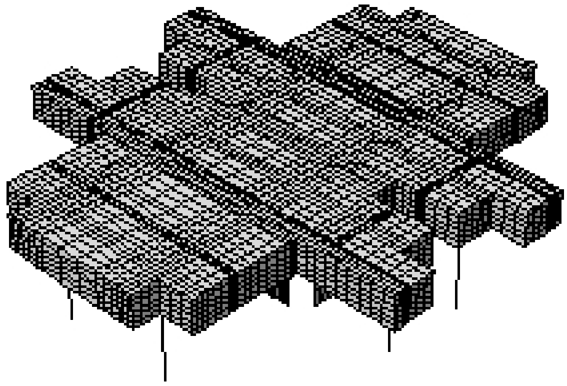

Figure 3.4 Finite element model of transfer plate structure.

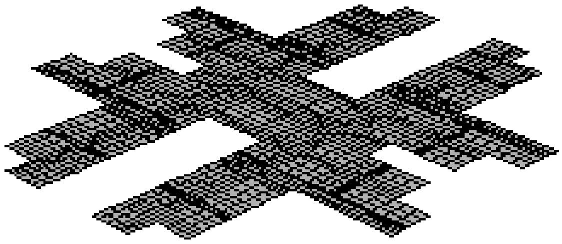

(a) Typical floor slabs.

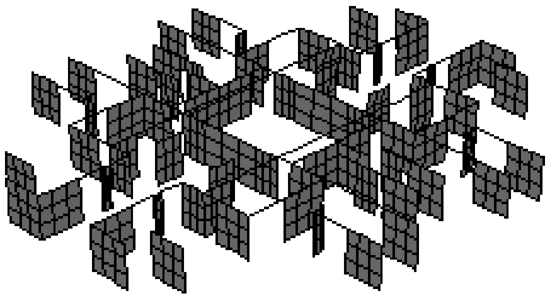

(b) Typical floor – walls and beams.

Figure 3.5 Finite element model of typical floor structure.

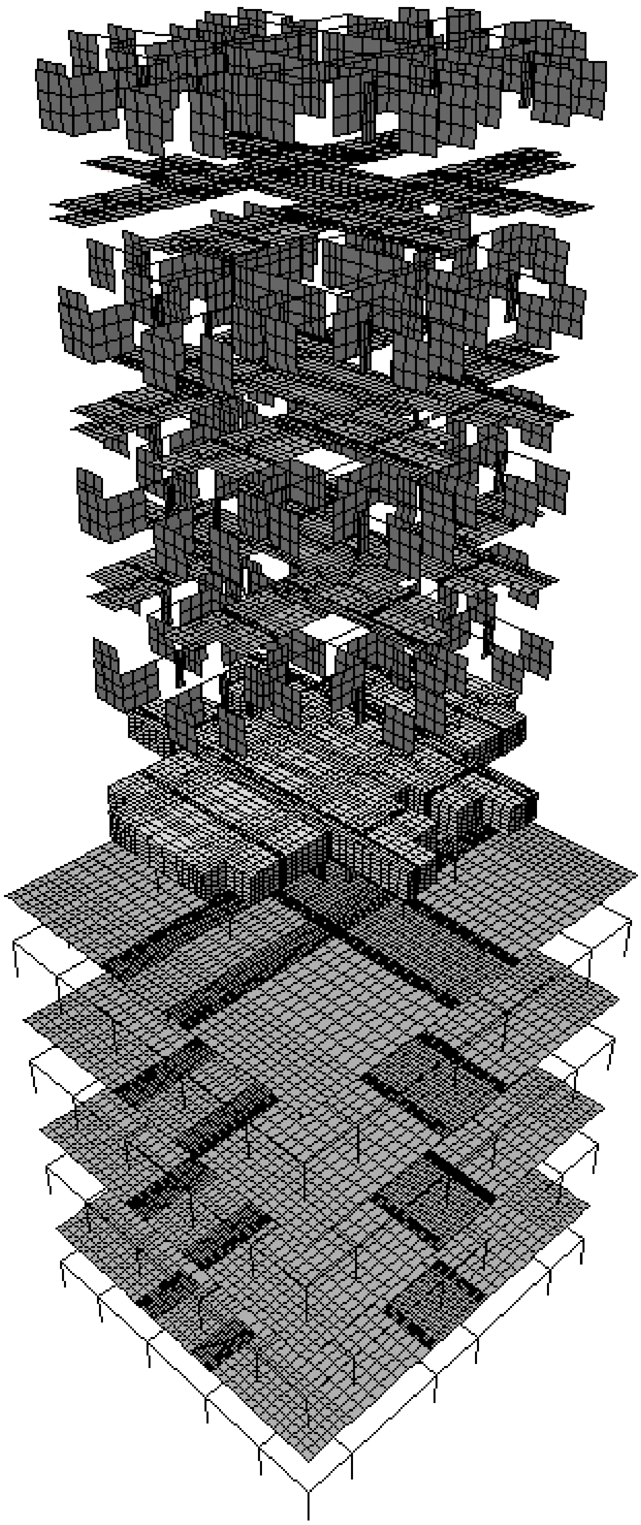

Figure 3.6 Part of the finite element model using super-elements.

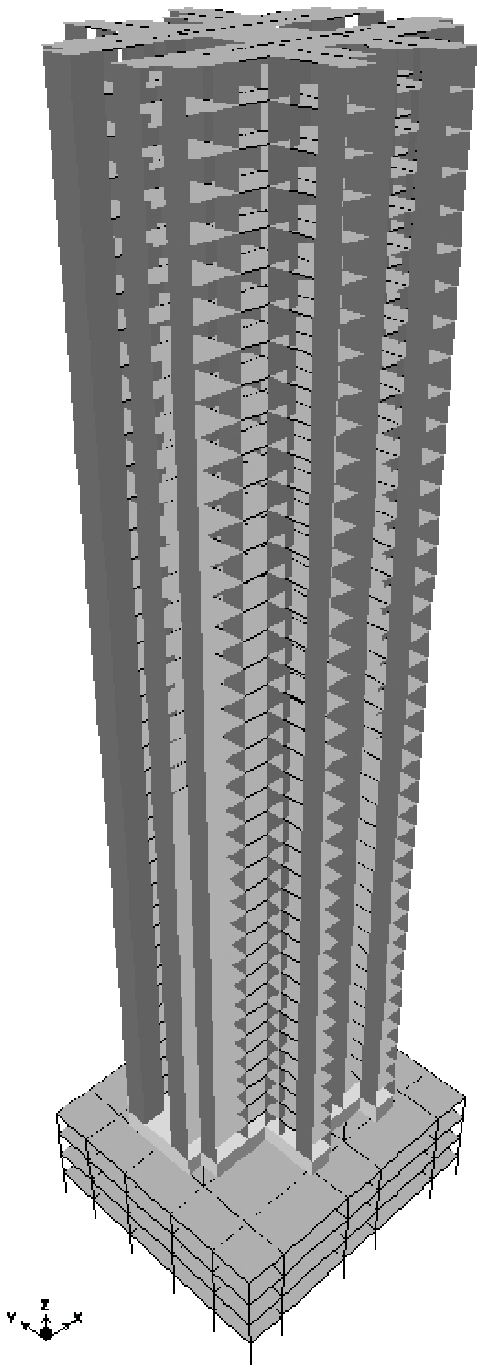

Figure 3.7 Complete finite element model.

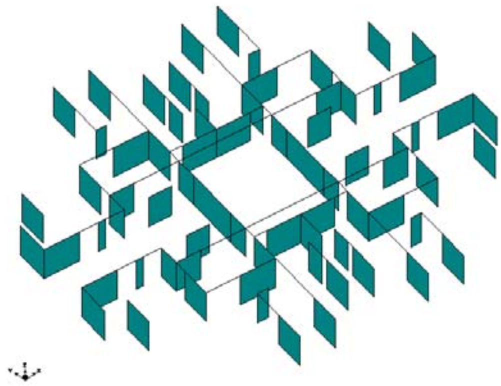

(a) Typical floor structure.

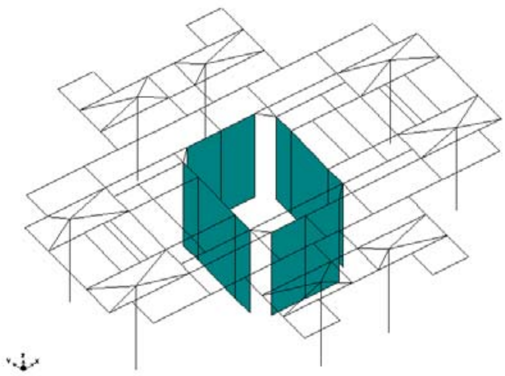

(b) Transfer plate structure.

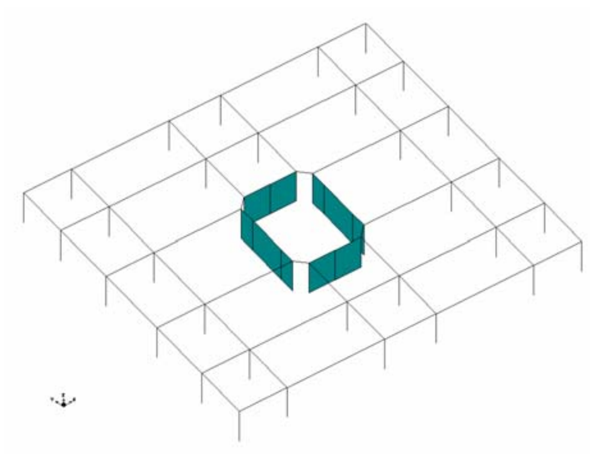

(c) Podium structure.

Figure 3.8 ETABS model of the high-rise building in parts.

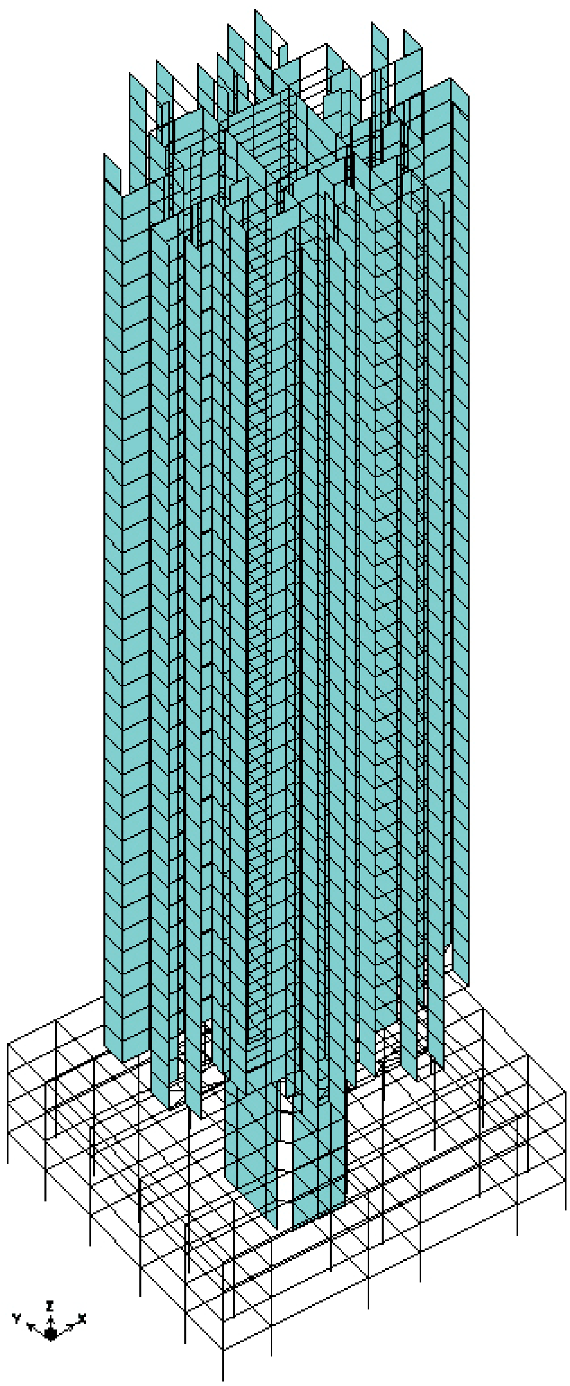

Figure 3.9 Complete numerical model of the high-rise building using ETABS.

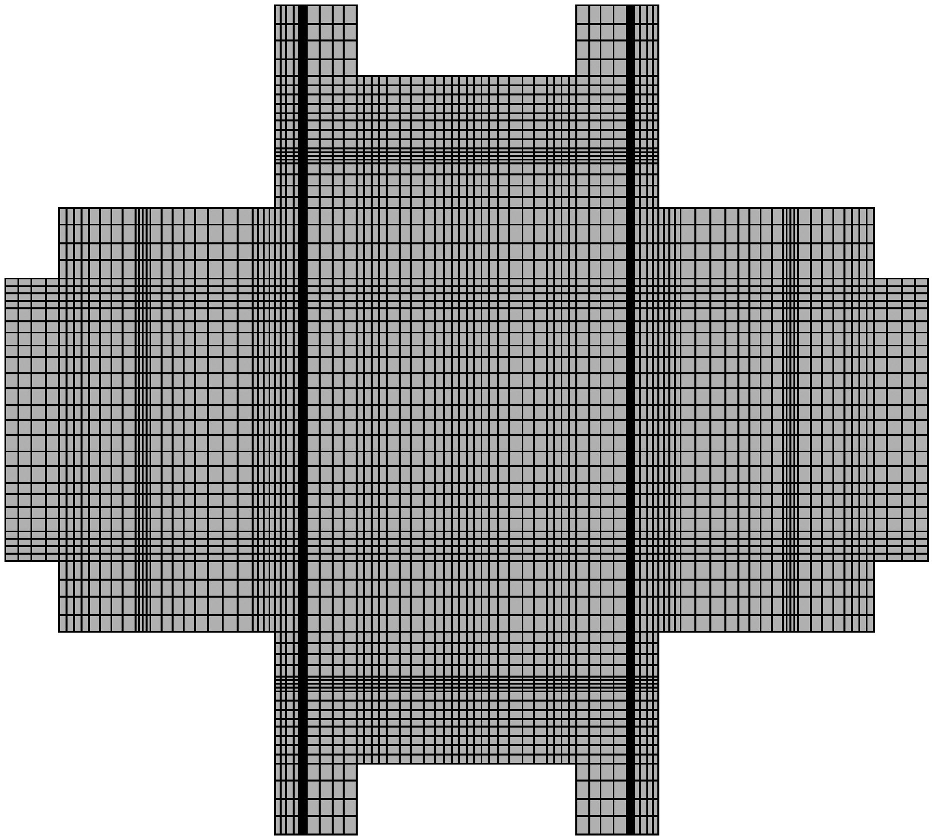

Figure 3.10 Numerical model of the transfer plate using SAP2000.

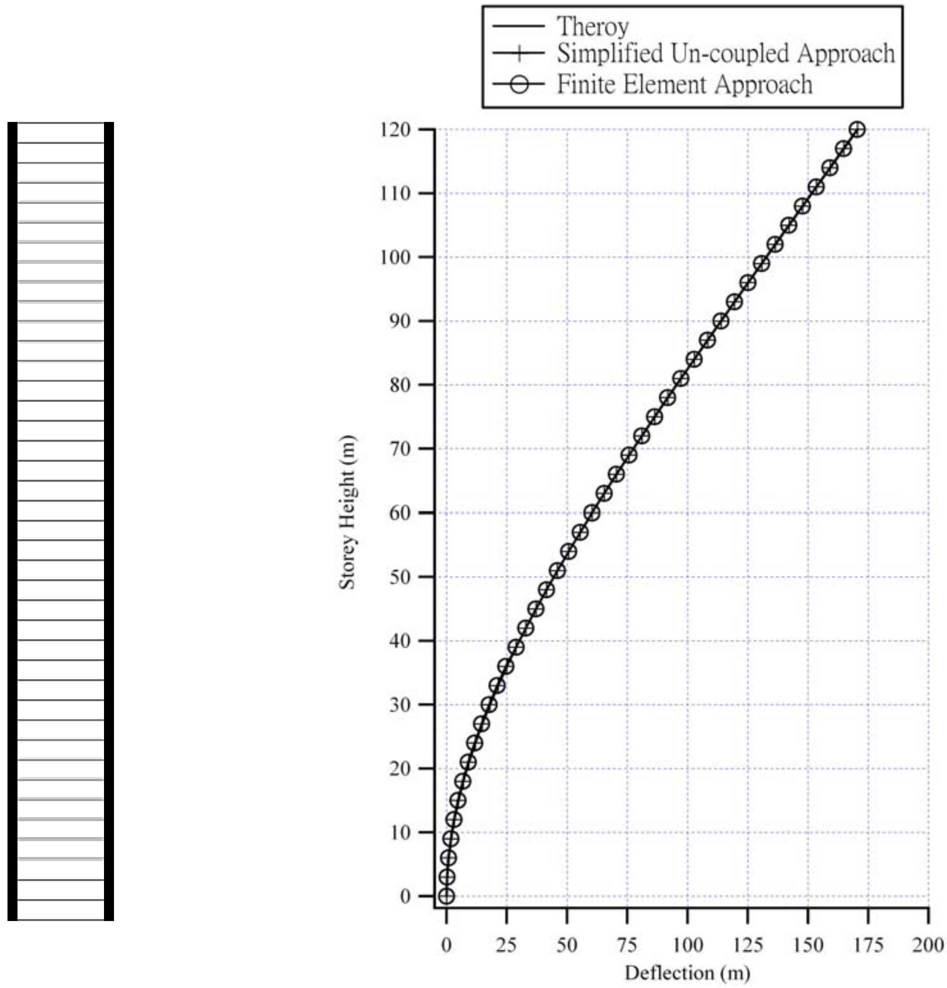

(a) Single Shear Wall Structure.

(b) Deflection Shape.

Figure 3.11 Single shear wall structure.

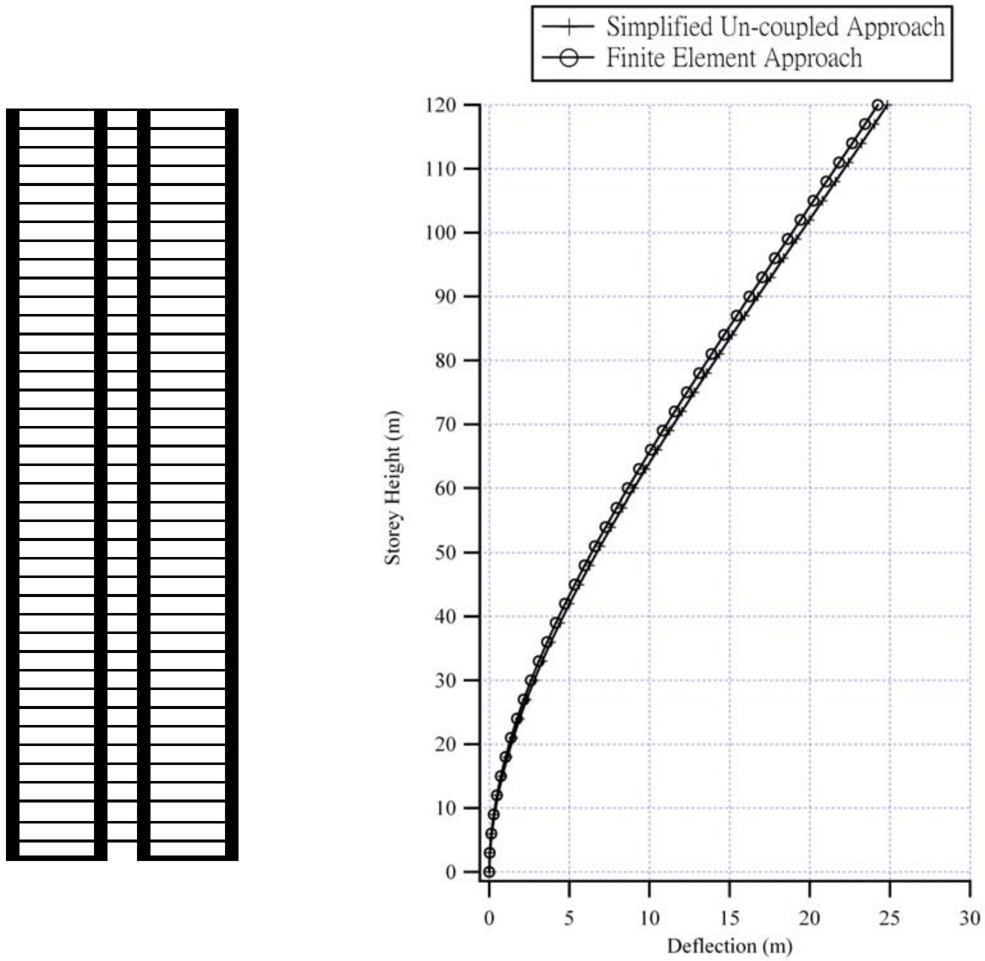

(a) Coupled Shear Wall Structure.

(b) Deflection Shape.

Figure 3.12 Coupled shear wall structure.

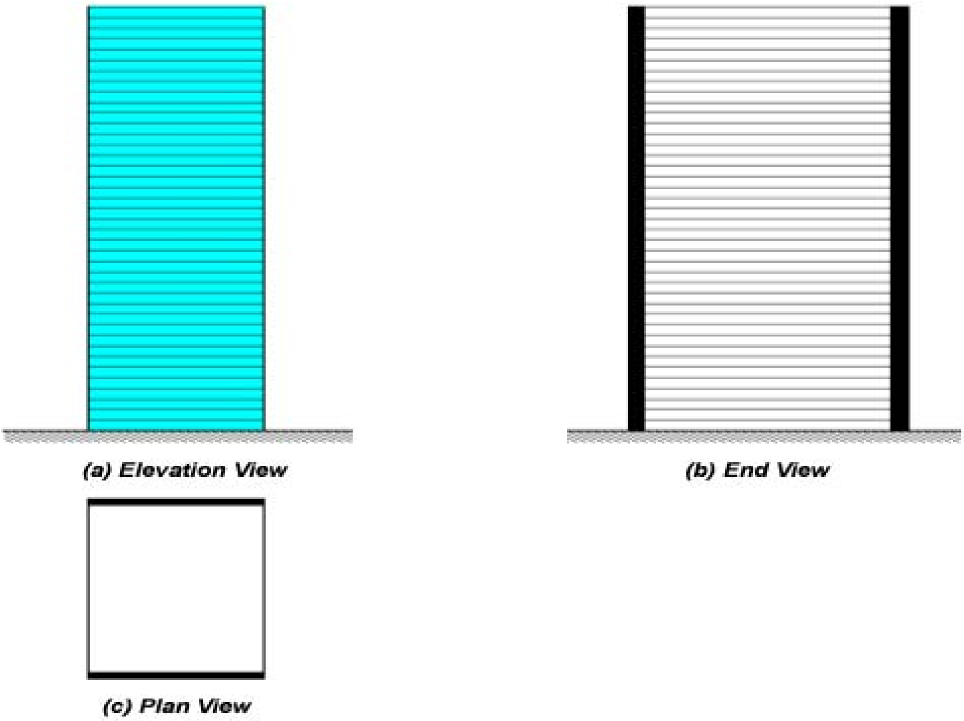

Figure 3.13 Three-dimensional single shear wall structure.

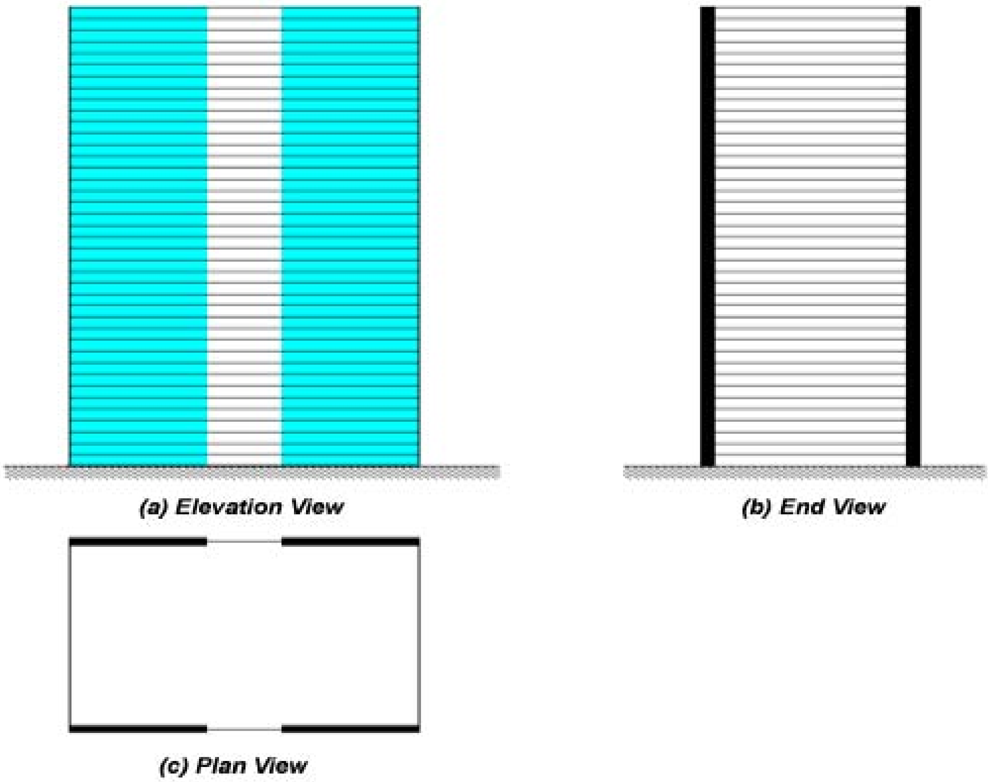

Figure 3.14 Three-dimensional coupled shear wall structure.

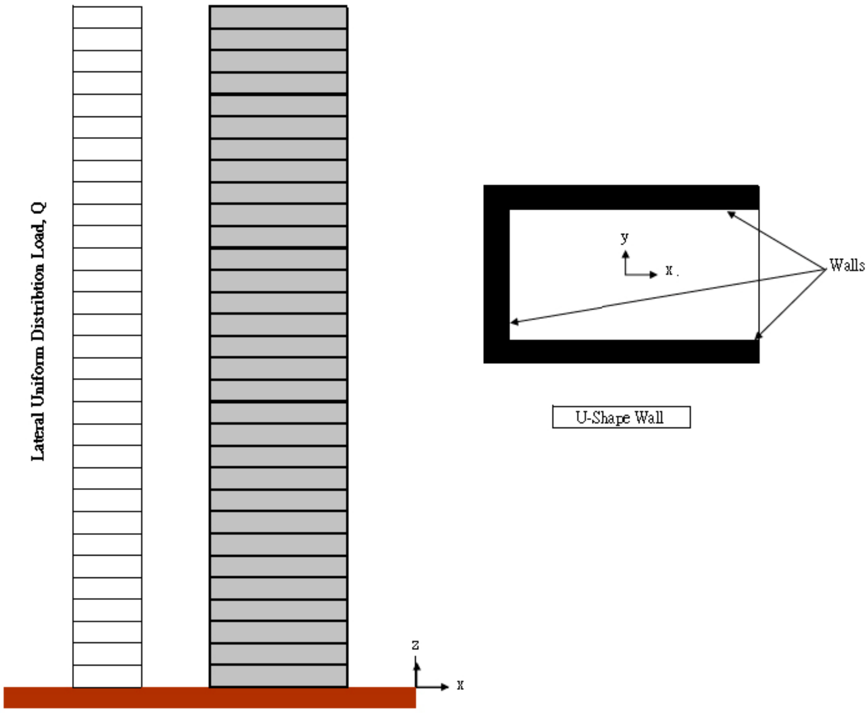

Figure 3.15 Three-dimensional U-shaped wall structure.

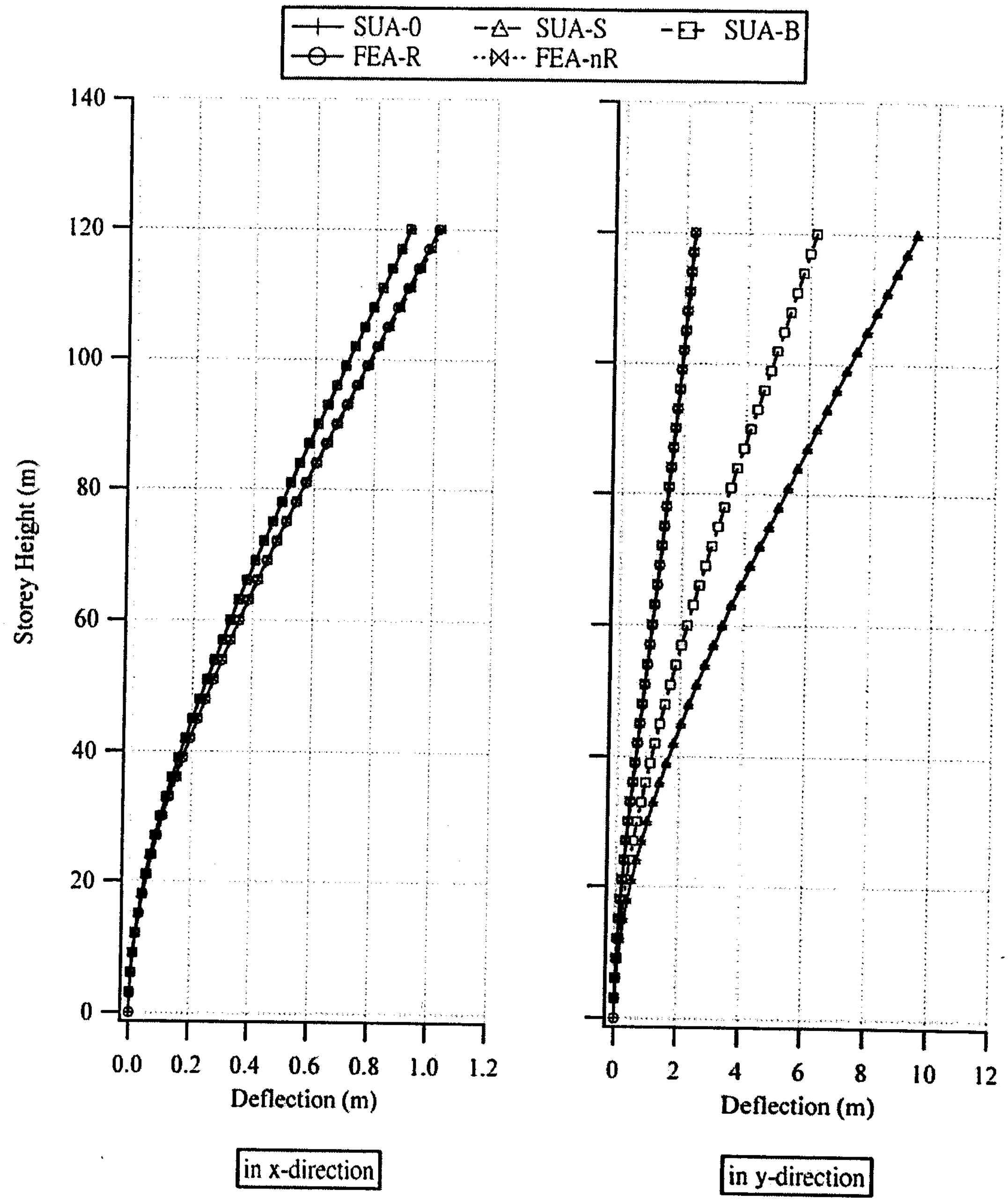

Figure 3.16 Comparison of the lateral displacement of U-shaped wall structure.

Pao Yue-kong Library
PolyU • Hong Kong

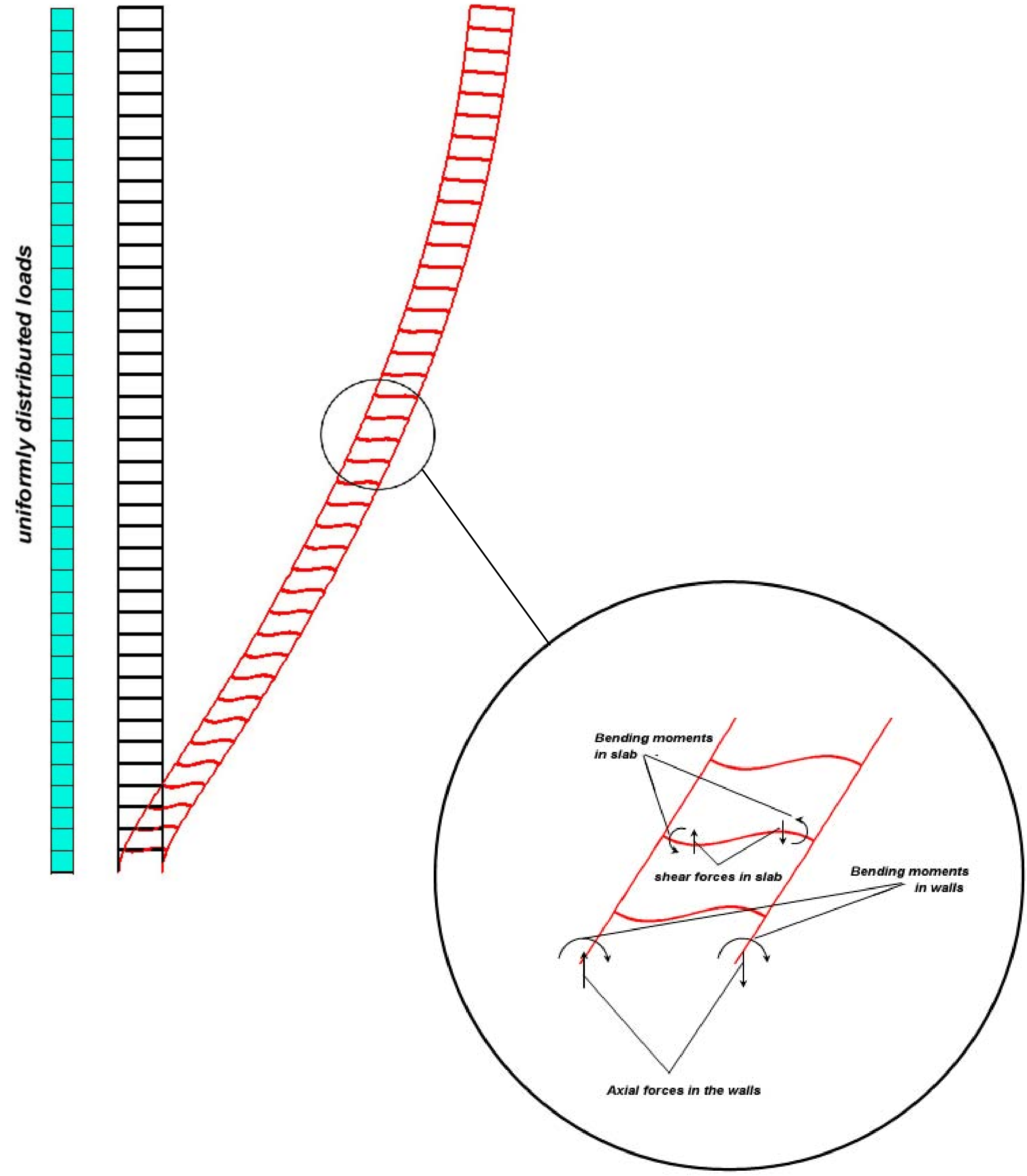

Figure 3.17 Internal forces in U-shaped wall structure in the y-direction.

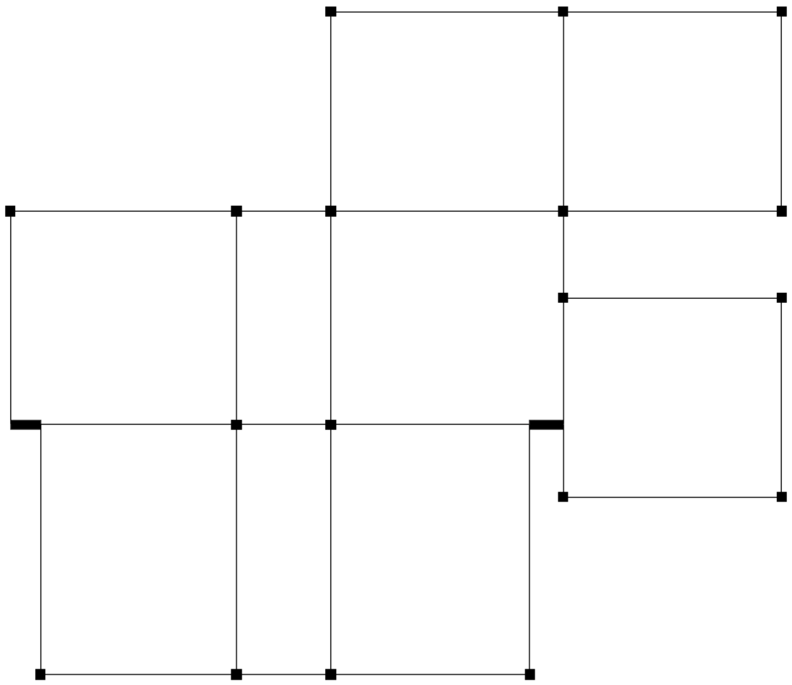

(a) Framing plan.

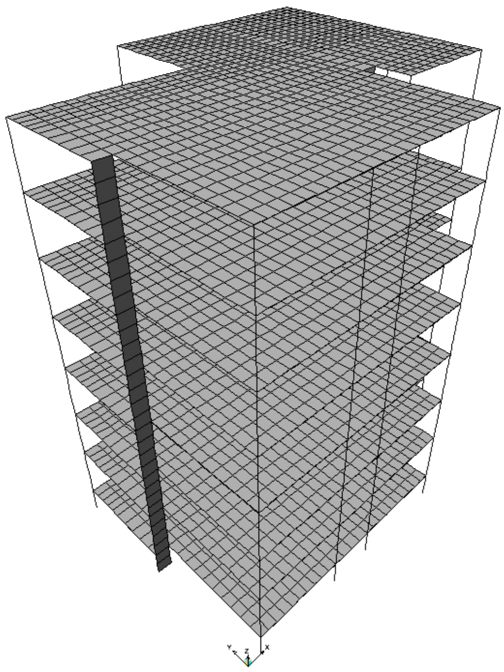

(b) Three dimensional view.

Figure 3.18 Low-rise building – Type 1.

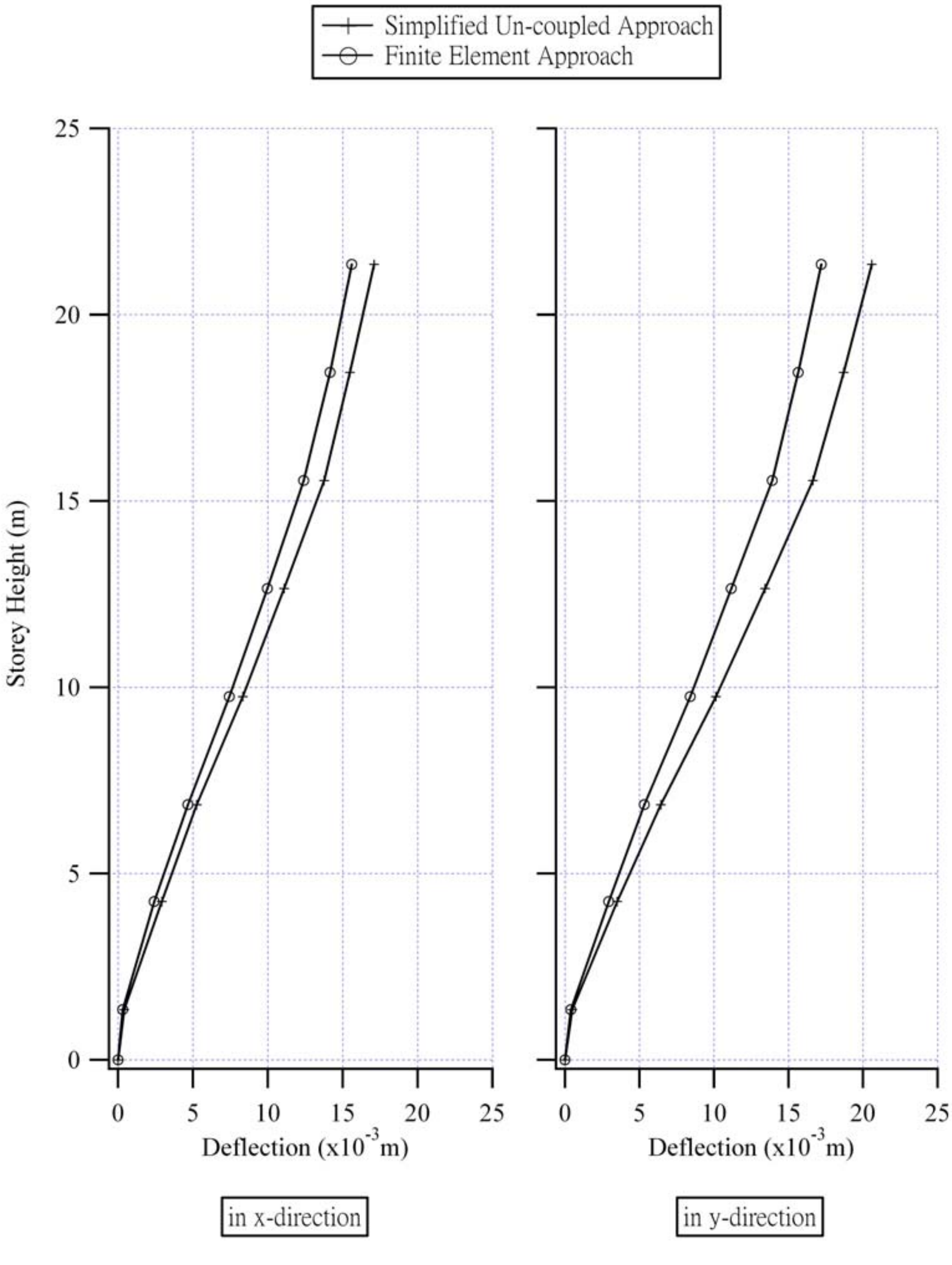

Figure 3.19 Comparison of the lateral displacement at each floor of low-rise building – Type 1.

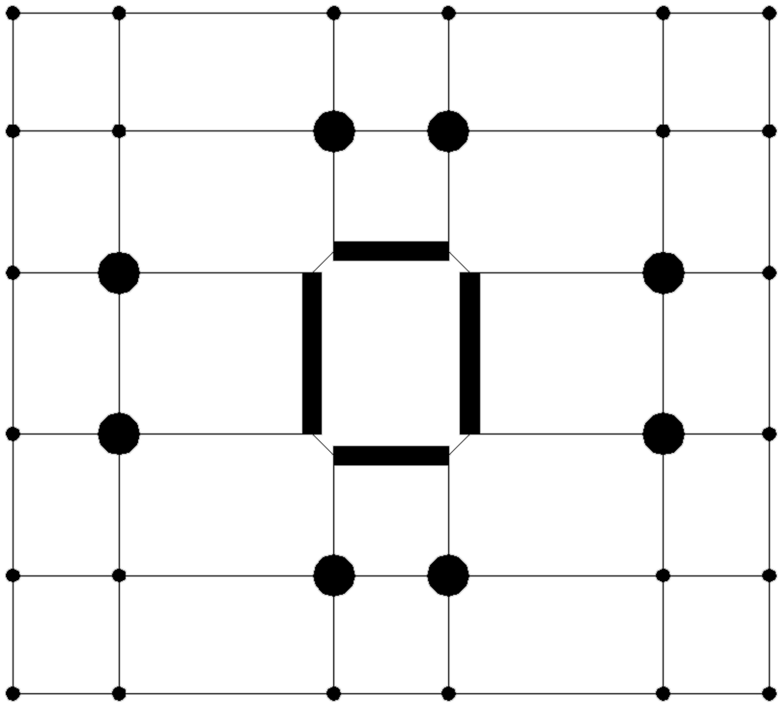

(a) Framing plan.

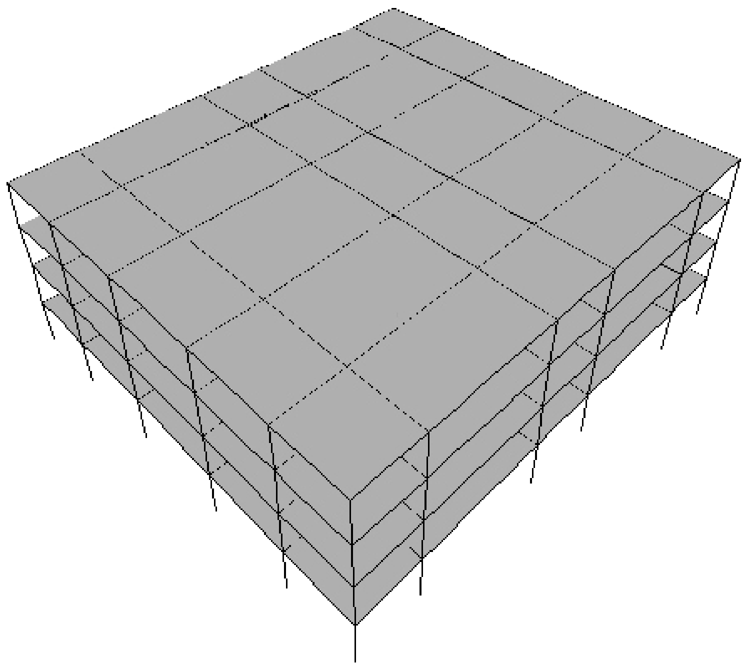

(b) Three dimensional view.

Figure 3.20 Low-rise building – Type 2.

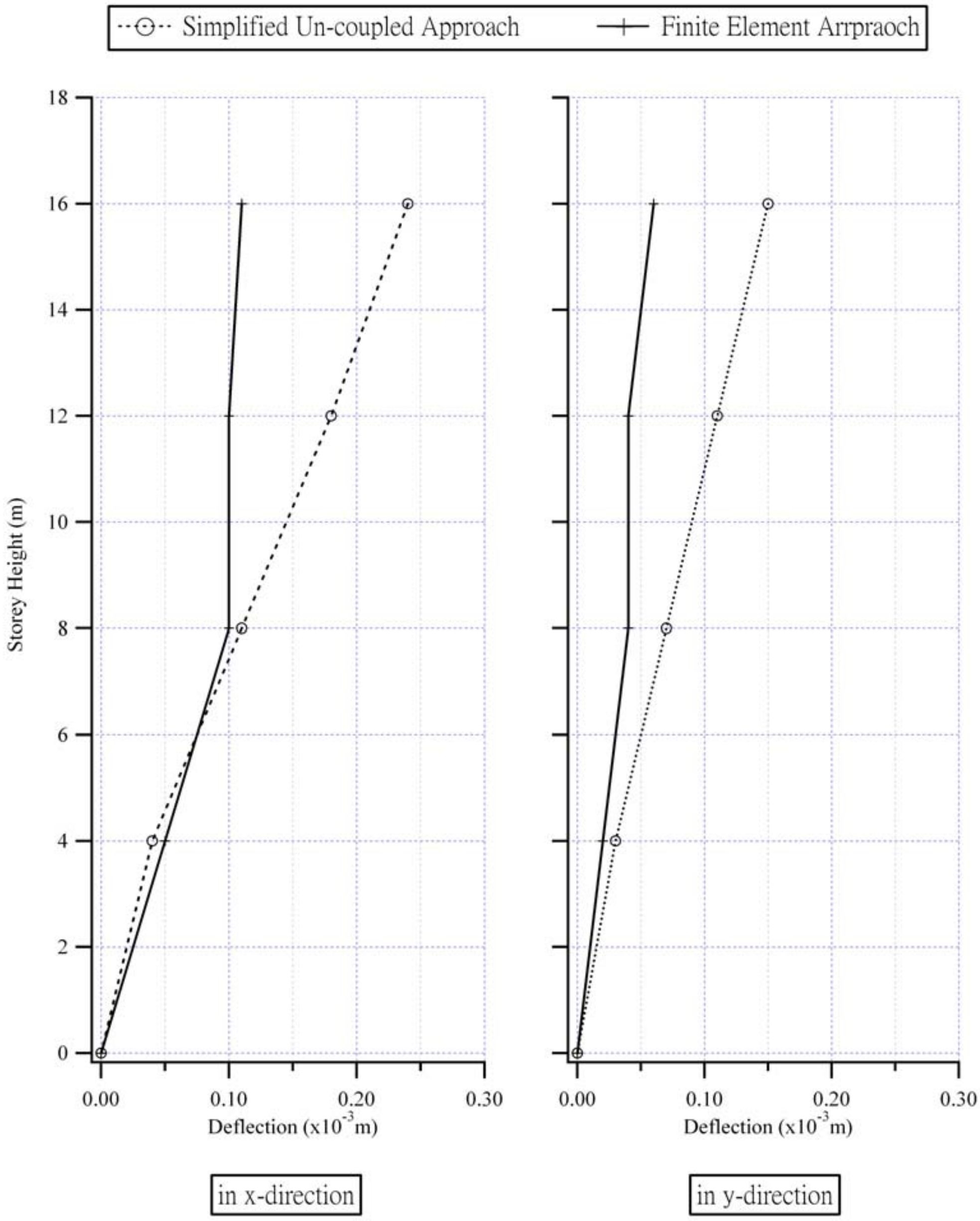

Figure 3.21 Comparison of the lateral displacement at each floor of low-rise building – Type 2.

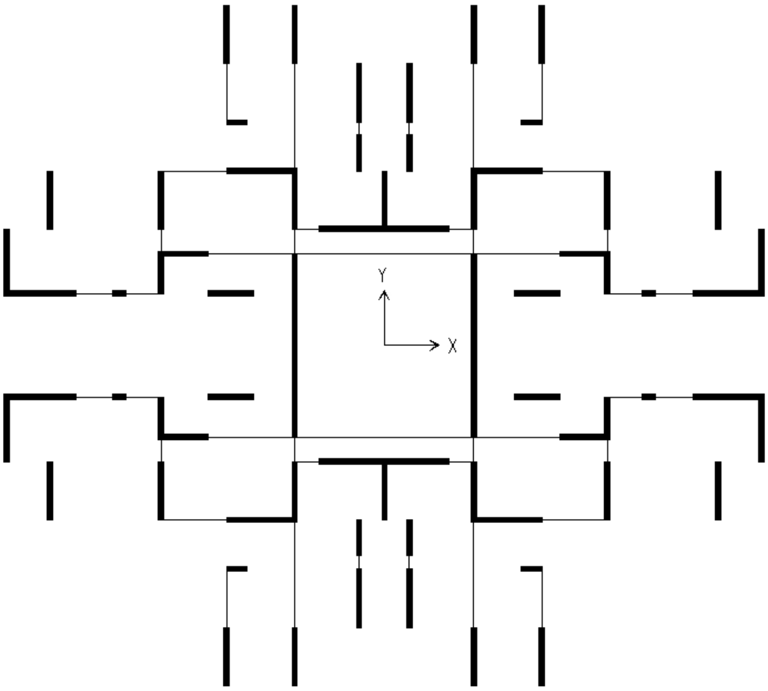

(a) Framing plan.

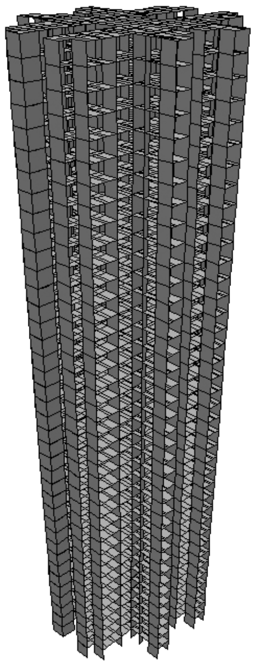

(b) Three-dimensional view.

Figure 3.22 High-rise building.

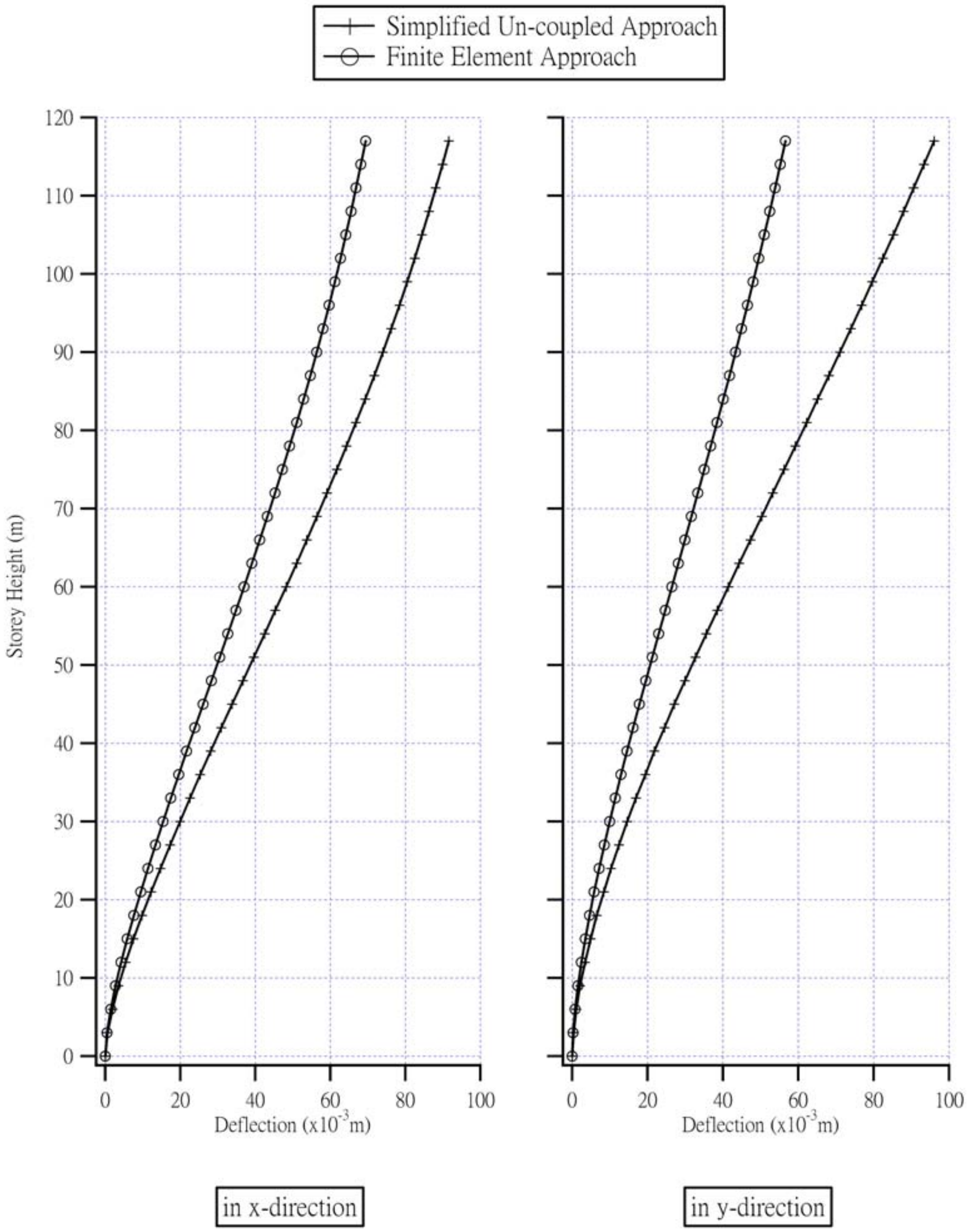

Figure 3.23 Comparison of the lateral displacement at each floor of a high-rise building.

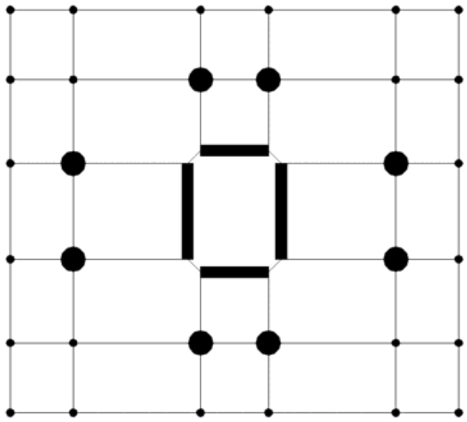

(a) Framing plan of “Podium” structure.

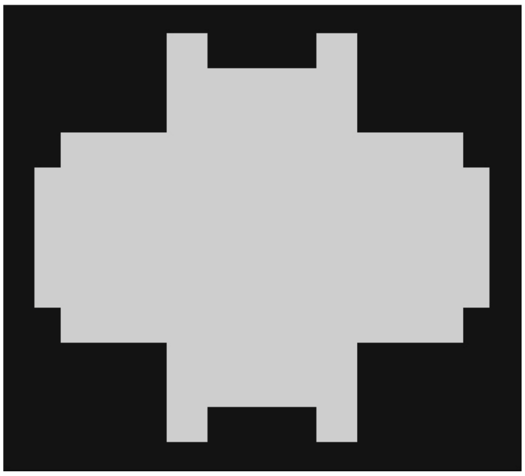

(b) Top view.

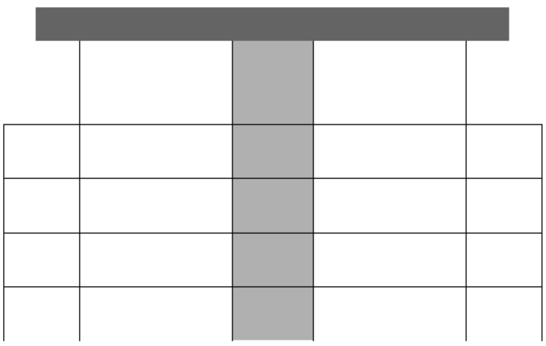

(c) Elevation view.

Figure 3.24 Low-rise building with a transfer plate.

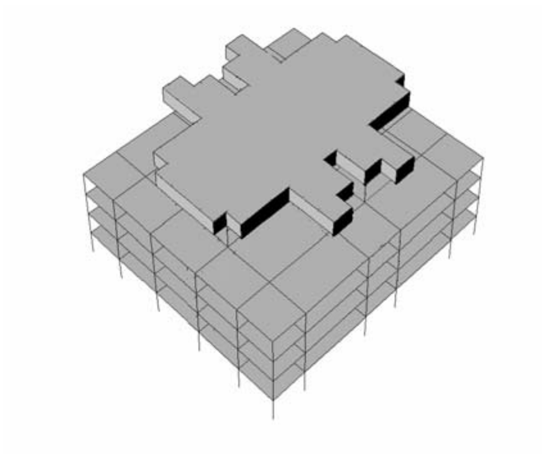

(a) FEA – SOLID.

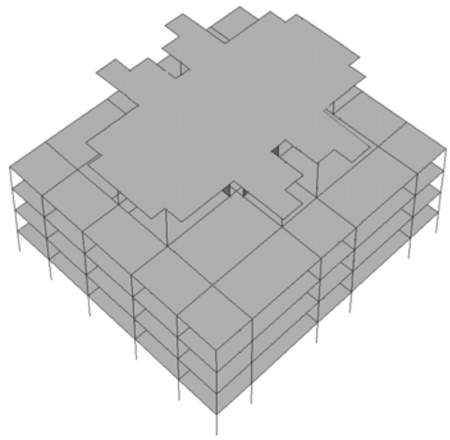

(b) FEA – SHELL.

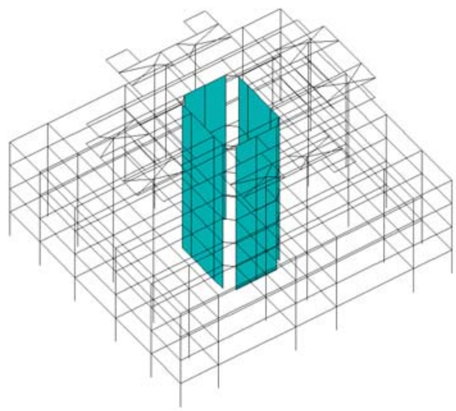

(c) SUCA.

Figure 3.25 Finite element models.

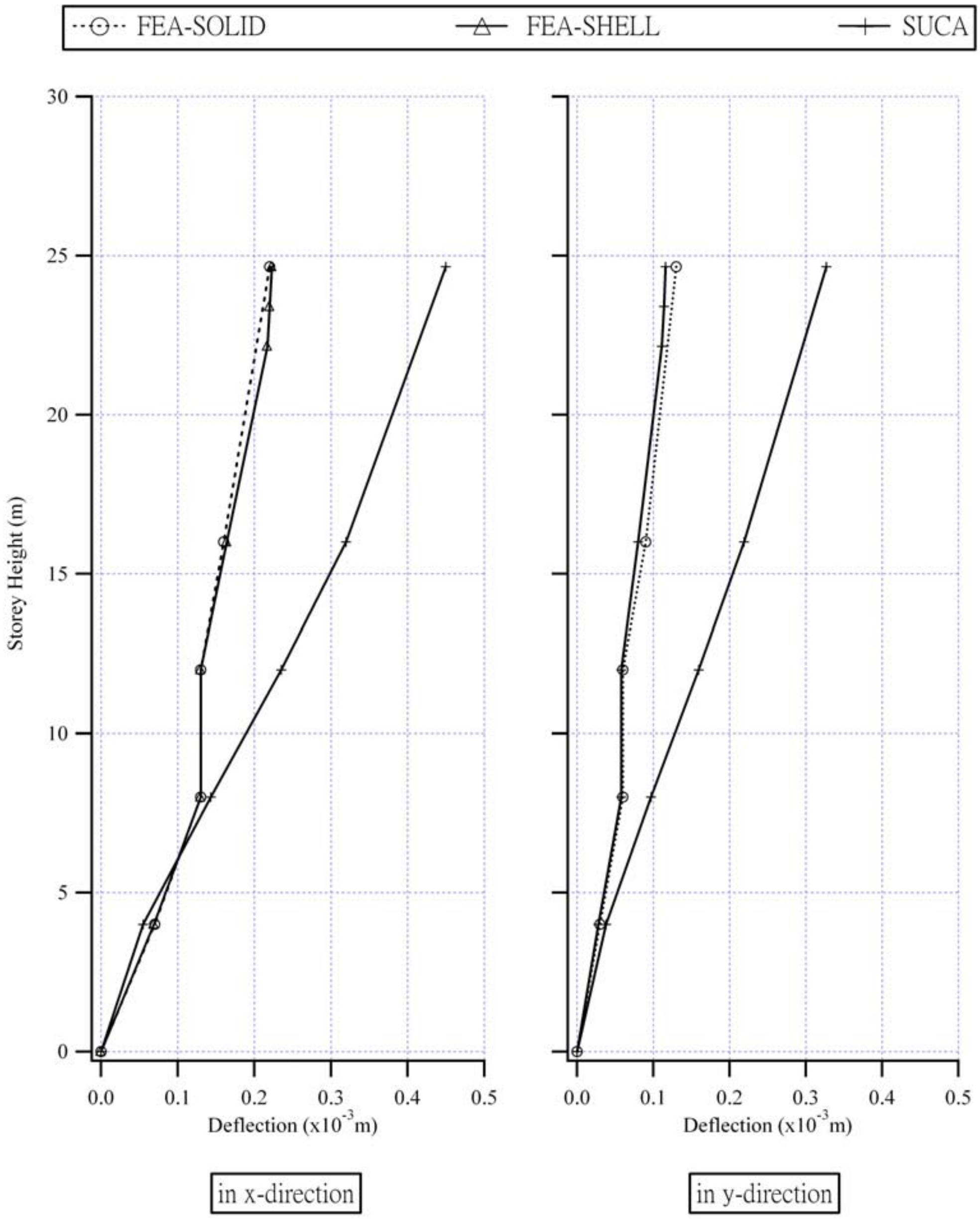

Figure 3.26 Comparison of the lateral displacement at each floor of low-rise building with a transfer plate.

4 NUMERICAL MODELLING OF A HIGH-RISE BUILDING WITH A TRANSFER PLATE

Nowadays, the power of the modern computer and the development of the finite element method have made it possible to perform rational analyses of the behaviour of large and complex reinforced concrete structures. The combination of increased computing power and the development of modern analytical tools provide us with enough predictive capacity in high-rise buildings analyses. The disadvantage of using the finite element approach is the need of a few days to weeks of computation time. Furthermore, the analysis results are difficult to use in the design directly. Numerical models are also not easy to create due to the large number of nodes and elements in the models. Therefore, engineers prefer to use the simplified un-coupled approach to analyse a high-rise building.

In Chapter 3, a series of studies are designed to examine the accuracy of the finite element approach. The increase in the storey stiffness due to the coupled floor slabs are incorporated in the finite elements model. The calculated displacements are different from those obtained from the simplified un-coupled approach. As a result, a new analysis approach is recommended for used in the analyses of high-rise building or core walls-frame structures. In this Chapter, an *advanced* simplified un-coupled approach is introduced.

To explore the implications of using an *advanced sim*plified un-coupled approach to estimate the response of the buildings, a prototype high-rise building with a transfer plate is utilised.

4.1 THE PROTOTYPE BUILDING

As shown in Figure 4.4, the prototype building is a high-rise residential building, and representative of much of the building stock in Hong Kong. It is a reinforced concrete structure designed to BS8110:1985 and has 39 typical floors supported by a transfer plate and a 4-level podium. Loadings on the prototype building follow the Hong Kong Building (Construction) Regulations. Structural details and characteristic loads are given in Table 4.1. The typical floor slabs are 150 mm thick and the podium floor slabs are 250 mm thick. Characteristic strength of concrete for structural members is 40 MPa for 1st to 17th floors. For 18th to 30th floors, the characteristic strength of concrete is 30 MPa for structural walls, beam and columns, and 40 MPa for central core wall. Lastly, the characteristic strength of concrete for all structural members at 31st to 43rd floors is 30 MPa.

4.2 MODELLING TECHNIQUES

In Hong Kong, the high-rise buildings with transfer plates are usually analysed by computer programs, such as ETABS and SAFE or SAP2000. Owing to the complexity in creating a numerical model for a high-rise building with a transfer plate, as shown in Figure 4.1, it is common to simplify the analysis into two separate analyses. The structures above the transfer plate are modelled and analysed using the ETABS, as shown in Figure 4.1. The structure below the transfer plate is computed using SAP2000, as shown in Figure 4.2. Alternatively, engineers may use SAFE to analyses the transfer plate, as shown in Figure 4.3. The transfer plate is modelled using “PLATE” elements in both SAFE and SAP2000. As far as static lateral load and gravity loads are considered, a transfer plate is assumed to behave as a rigid diaphragm. The above modelling technique is very general and can be applied to analyse high-rise buildings with transfer plates. For gravity loads, the above approach is inconsistent if a high concentration load is applied to the transfer plate with high stress redistribution through the thickness of the transfer plate.

In this Chapter, a complete finite element model of the high-rise building with a transfer plate, including the superstructure above the transfer plate and wall-frame structure below it, is created. The transfer plate is modelled using "SOLID" elements to estimate the behaviour accurately. The whole numerical model of a high-rise reinforced concrete building with a transfer plate is created using ABAQUS, a finite element program, as shown in Figure 4.4.

Engineers however, as stated above, tend to use a simplified un-coupled approach in building analyses, since it provides a simple design method and shorter computational analysis time. As demonstrated in Chapter 3, the simplified un-coupled approach over-estimates the lateral deflections of the buildings when compared with the finite element approach. Therefore, an *advanced* simplified un-coupled approach has been developed and used in the analyses of the static and dynamic responses of high-rise building with a transfer plate structure. The computational analysis time is shorten by comparing with the finite element method. Lam *et al* (2002) used this approach to estimate the dynamic characteristics of 1:20

scaled high-rise building with a transfer plate structure.

Since the coupling effects of floor slabs in different types of structures will differ, it is controlled by some parameters, such as the height of the structure and the structural form used in the storey. It is difficult to provide a guideline for estimating the coupling effect in structures by using the simplified un-coupled approach. However, the advantages of using the simplified un-coupled approach provide a simple design method and shorter computational time. As a result, an *advanced* simplified un-coupled approach is developed based on the modelling techniques of the simplified un-coupled approach. A step by step procedure to describe the advanced simplified un-coupled approach is shown in Figure 4.5. The advanced numerical model is the same as the simplified un-coupling model, as shown in Figure 4.6. Slabs are not considered. Storey stiffness of the structure, however, are adjusted by changing the values of the elasticity of the material for considering the coupling effects of floor slabs in the structures. Based on the numerical results estimated using a linear elastic static analysis in Chapter 3, the adjusting factors for the Young's Modulus of the materials are 1.2 for the low-rise beam and column frames structure, 1.7 for the high-rise wall-frame structure and 2.0 for the low-rise core walls-frame structure.

4.3 NUMERICAL MODELS

The transfer plate can be modelled using either “SOLID” elements, “SHELL” elements or “BEAM” elements. Furthermore, using the “BEAM” elements, the beams can be modelled as situated at the top, the middle or the bottom of the transfer plate. To explore the accuracy of the modelling technique for the transfer plate, a high-rise building with a transfer plate is utilised.

Five numerical models were developed using the commercial packages, ETABS version 6.22 and ABAQUS version 5.8.14. The purposes of the numerical studies are to compare the accuracy of the numerical results obtained when the whole structures are modelled. Characteristics of the models are summarized in Table 4.2 and brief descriptions are as follows.

Model A-SOLID (FULL Model) represents a prototype building with a transfer plate. The model is created using finite elements and the transfer plate is modelled using 8 nodes “SOLID” elements, as shown in Figure 4.4.

Model A-SHELL is similar to Model A-SOLID, except that the transfer plate is modelled by using 4 nodes “SHELL” elements.

Model E-TBT represents a prototype building with a transfer plate. The model is created by using the advanced simplified un-coupled approach and the transfer plate is modelled by using “BEAM” elements. The location of the transfer plate is assumed at the top of its thickness, as shown in Figure 4.6.

Model E-TBM is similar to Model E-TBT, except that the transfer plate is modelled at the middle position of its thickness.

Model E-TBL is similar to Model E-TBT, except that the transfer plate is modelled at the bottom position of its thickness.

Models “A-SOLID” and “A-SHELL” are analysed using the finite element approach. Models “E-TBT”, “E-TBM” and “E-TBL” are analysed using advanced simplified un-coupled approach.

The Modulus of Elasticity used in the model varies according to the material data and the analysis approaches, as shown in Table 4.2.

4.4 NUMERICAL ANALYSIS

4.4.1 RESULTS OF STATIC LATERAL DISPLACMENT

Figure 4.7 compares the static lateral displacements estimated by advanced simplified un-coupled approaches with those obtained from the finite element approaches. The numerical results of the advanced simplified un-coupled approach models and “A-SHELL” generally agree with the “FULL Model” (A-SOLID). In the x-direction, the lateral deflections above the transfer plate are the same as those obtained from the “FULL Model”. Relatively larger discrepancies between the advanced simplified un-coupled approaches and finite element approaches are observed at and below the transfer plate. Similar conclusions are obtained when comparing the results in the y-direction. Deflections obtained at the top of a high-rise building with a transfer plate from the finite element approach are about 15% different to those of the advanced simplified un-coupled approach.

Tables 4.3 and 4.4 compare the lateral deflection estimated by the advanced simplified un-coupled approach and the finite element approach. All the numerical results using the advanced simplified un-coupled approach models are very close to each other within 5%, the difference caused by the change in the position of the transfer plate.

4.4.2 RESULTS OF FUNDAMENTAL FREQUENCIES

Figures 4.8 to 4.13 compare the first three mode shapes estimated by advanced simplified un-coupled approaches with those obtained from the finite element approaches. Numerical results for the advanced simplified un-coupled approach models and “A-SHELL” models generally agree with the “FULL Model” (A-SOLID). In the x-direction, the first three mode shapes are the same as those obtained from the “FULL Model”. With the exception, relatively larger discrepancies are observed at the third mode between the “A-SHEL” model and the “FULL Model”. Similar conclusions are obtained when comparing the results in the y-direction. Larger errors occur above the transfer plate. This difference between the results from the models “A-SOLID” and “A-SHELL” can be attributed to the element type used in modeling the transfer plate.

Tables 4.5 and 4.6 compare the fundamental frequencies estimated by the advanced simplified un-coupled approach and finite element approach. Numerical results obtained from the advanced simplified un-coupled approach are very close to each other to within 5%.

4.5 CONCLUDING SUMMARY

The main objective of this study is to compare the accuracies achieved by the various numerical techniques when predicting the static lateral performance and the dynamic behaviour of a high-rise building with a transfer plate. In the case of the structural response of a high-rise building with a transfer plate, the estimated deflections and fundamental frequencies of the building are close to the results from the "FULL Model" when the transfer plate is modelled by the "SHELL" elements. Based on these results, the transfer plate may be analysed as a thick plate.

The advanced simplified un-coupled approach provides accurate results when compared with the finite element approach. The advanced simplified un-coupled approach is recommended for use to predict the lateral response and the dynamic characteristics of a high-rise building with a transfer plate. The appropriate position to model the transfer plate in the advanced simplified un-coupled approach is recommended to be at the top of the transfer plate.

Table 4.1 Structural detail and characteristic loads of the prototype building.

Floor level	Structural system	Structural detail	Characteristic loads	
			Imposed load (kPa)	Finishes, screeding and ceiling (kPa)
Typical (5/F-17/F)	Shear wall	200-250mm	3.0	0.5
	Core wall	475mm		
Typical (18/F-30/F)	Shear wall	200-250mm	3.0	0.5
	Core wall	350mm		
Typical (30/F-43/F)	Shear wall	200-250mm	3.0	0.5
	Core wall	250mm		
Transfer Plate		2500mm	3.0	2.0
Podium (G/F-4/F)	Column	8@2200 mm diameter 28@700mm diameter	4.0	2.0
	Core wall	1000mm		

Table 4.2 Modulus of Elasticity (kN/m^2) used in models.

FLOOR	CONCRETE GRADE	MODELS	
		Finite Element Approach (A-SOLID & A-SHELL)	Advanced simplified un-coupled approach (E-TBT, E-TBM & E-TBL)
5/F – 43/F	C30	2.17×10^7	3.43×10^7
	C40	2.40×10^7	3.79×10^7
TRANSFER PLATE	C30	2.17×10^7	3.27×10^7
	C40	2.40×10^7	3.62×10^7
4/F	C30	2.17×10^7	2.89×10^7
	C40	2.40×10^7	3.19×10^7
3/F	C30	2.17×10^7	2.82×10^7
	C40	2.40×10^7	3.12×10^7
2/F	C30	2.17×10^7	2.78×10^7
	C40	2.40×10^7	3.07×10^7
1/F	C30	2.17×10^7	3.09×10^7
	C40	2.40×10^7	3.42×10^7

Table 4.3 Static lateral displacement (m) in the x-direction.

LEVEL	MODEL					RATIO		
	E-TBT	E-TBM	E-TBL	A-SOLID	A-SHELL	E-TBT / A-SOLID	E-TBM / A-SOLID	E-TBL / A-SOLID
43/F	0.1106	0.1109	0.1114	0.1125	0.1115	0.98	0.99	0.99
39/F	0.1019	0.1022	0.1027	0.1039	0.1031	0.98	0.98	0.99
35/F	0.0925	0.0928	0.0933	0.0945	0.0938	0.98	0.98	0.99
31/F	0.0824	0.0827	0.0831	0.0842	0.0836	0.98	0.98	0.99
27/F	0.0716	0.0719	0.0723	0.0731	0.0726	0.98	0.98	0.99
23/F	0.0604	0.0606	0.0610	0.0613	0.0609	0.98	0.99	0.99
19/F	0.0488	0.0489	0.0493	0.0492	0.0489	0.99	0.99	1.00
15/F	0.0373	0.0374	0.0378	0.0372	0.0370	1.00	1.01	1.02
11/F	0.0262	0.0263	0.0266	0.0257	0.0257	1.02	1.02	1.03
10/F	0.0236	0.0236	0.0238	0.0229	0.0230	1.03	1.03	1.04
9/F	0.0209	0.0210	0.0212	0.0203	0.0204	1.03	1.03	1.04
8/F	0.0184	0.0184	0.0186	0.0177	0.0179	1.04	1.04	1.05
7/F	0.0160	0.0159	0.0161	0.0153	0.0155	1.05	1.04	1.05
6/F	0.0137	0.0136	0.0137	0.0131	0.0133	1.05	1.04	1.04
5/F	0.0117	0.0114	0.0114	0.0111	0.0114	1.05	1.03	1.03
TRANSFER	0.0035	0.0034	0.0033	0.0096	0.0100	0.36	0.35	0.35
4/F	0.0007	0.0007	0.0007	0.0055	0.0058	0.13	0.12	0.12
3/F	0.0002	0.0002	0.0002	0.0036	0.0037	0.07	0.07	0.07
2/F	0.0002	0.0002	0.0002	0.0019	0.0020	0.12	0.12	0.12
1/F	0.0002	0.0002	0.0002	0.0006	0.0006	0.38	0.39	0.39

Table 4.4 Static lateral displacement (m) in the y-direction.

LEVEL	MODEL					RATIO		
	E-TBT	E-TBM	E-TBL	A-SOLID	A-SHELL	E-TBT / A-SOLID	E-TBM / A-SOLID	E-TBL / A-SOLID
43/F	0.1120	0.1132	0.1146	0.1003	0.0989	1.12	1.13	1.14
39/F	0.1005	0.1016	0.1028	0.0909	0.0897	1.10	1.12	1.13
35/F	0.0886	0.0896	0.0907	0.0812	0.0801	1.09	1.10	1.12
31/F	0.0764	0.0773	0.0783	0.0710	0.0700	1.08	1.09	1.10
27/F	0.0642	0.0649	0.0658	0.0605	0.0597	1.06	1.07	1.09
23/F	0.0520	0.0526	0.0534	0.0499	0.0492	1.04	1.06	1.07
19/F	0.0402	0.0407	0.0414	0.0393	0.0388	1.02	1.04	1.05
15/F	0.0292	0.0296	0.0301	0.0291	0.0288	1.00	1.02	1.03
11/F	0.0193	0.0195	0.0198	0.0198	0.0195	0.98	0.99	1.00
10/F	0.0170	0.0172	0.0175	0.0176	0.0174	0.97	0.98	0.99
9/F	0.0148	0.0150	0.0152	0.0155	0.0153	0.96	0.97	0.98
8/F	0.0128	0.0129	0.0131	0.0135	0.0134	0.95	0.96	0.97
7/F	0.0110	0.0110	0.0111	0.0116	0.0116	0.94	0.94	0.95
6/F	0.0090	0.0090	0.0090	0.0099	0.0099	0.91	0.91	0.91
5/F	0.0025	0.0025	0.0025	0.0084	0.0084	0.29	0.30	0.29
TRANSFER	0.0002	0.0005	0.0005	0.0071	0.0072	0.03	0.07	0.07
4/F	0.0000	0.0005	0.0005	0.0038	0.0039	0.00	0.13	0.13
3/F	0.0071	0.0005	0.0005	0.0024	0.0025	2.92	0.20	0.20
2/F	0.0079	0.0005	0.0005	0.0013	0.0013	6.24	0.38	0.38
1/F	0.0079	0.0005	0.0005	0.0004	0.0004	19.21	1.14	1.13

Table 4.5 First three fundamental frequencies in the x-direction.

Model no	Model name	Fundamental Frequencies (Hz)		
		1st mode	2nd model	3rd mode
1	A-SOLID	0.506	1.911	3.582
2	A-SHELL	0.508	1.794	2.900
3	E-TBT	0.513	2.068	4.045
4	E-TBM	0.512	2.068	4.063
5	E-TBL	0.510	2.071	4.070

Table 4.6 First three fundamental frequencies in the y-direction.

Model no	Model name	Fundamental Frequencies (Hz)		
		1st mode	2nd model	3rd mode
1	A-SOLID	0.511	2.196	4.422
2	A-SHELL	0.514	2.076	3.576
3	E-TBT	0.481	2.239	4.901
4	E-TBM	0.479	2.244	4.932
5	E-TBL	0.476	2.243	4.947

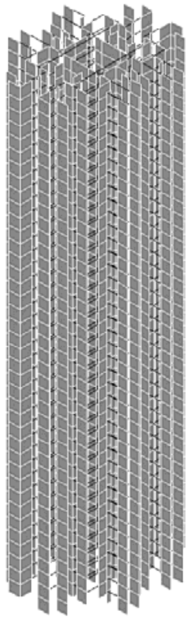

Figure 4.1 Numerical model of superstructure using ETABS.

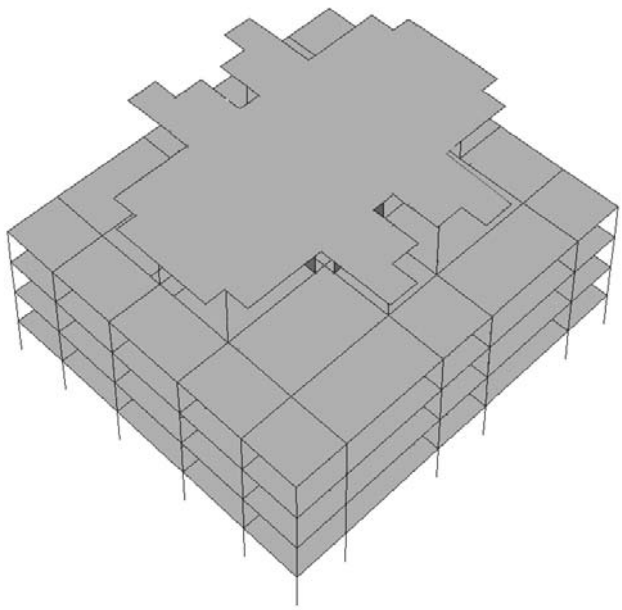

Figure 4.2 Numerical model of structure below transfer using SAP2000.

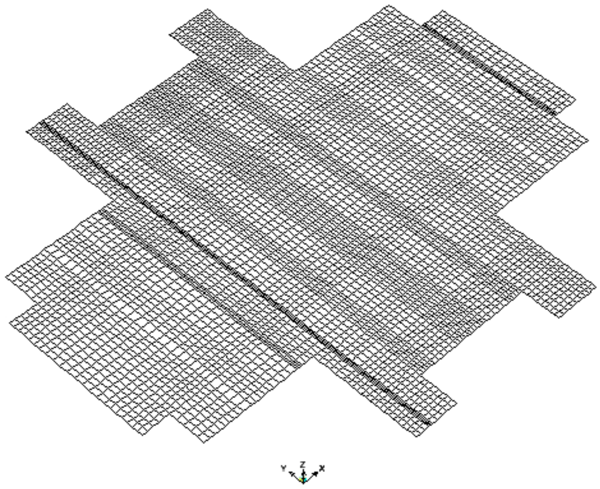

Figure 4.3 Numerical model of transfer plate using SAFE.

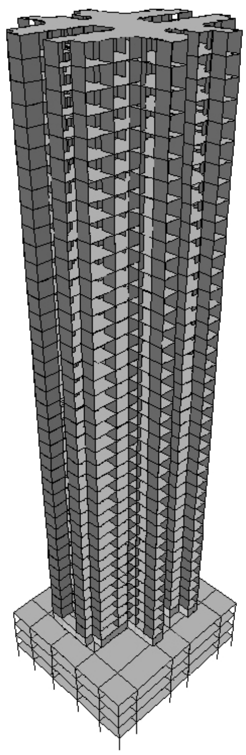

Figure 4.4 Numerical model of whole high-rise building with a transfer plate using finite elements.

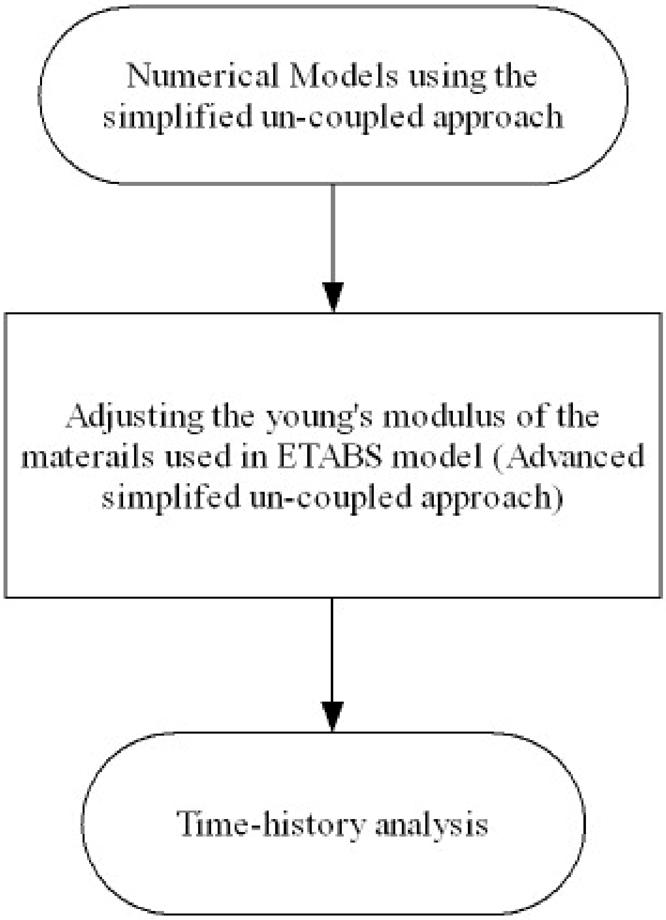

Figure 4.5 A step by step procedure of advanced simplified un-coupling approach.

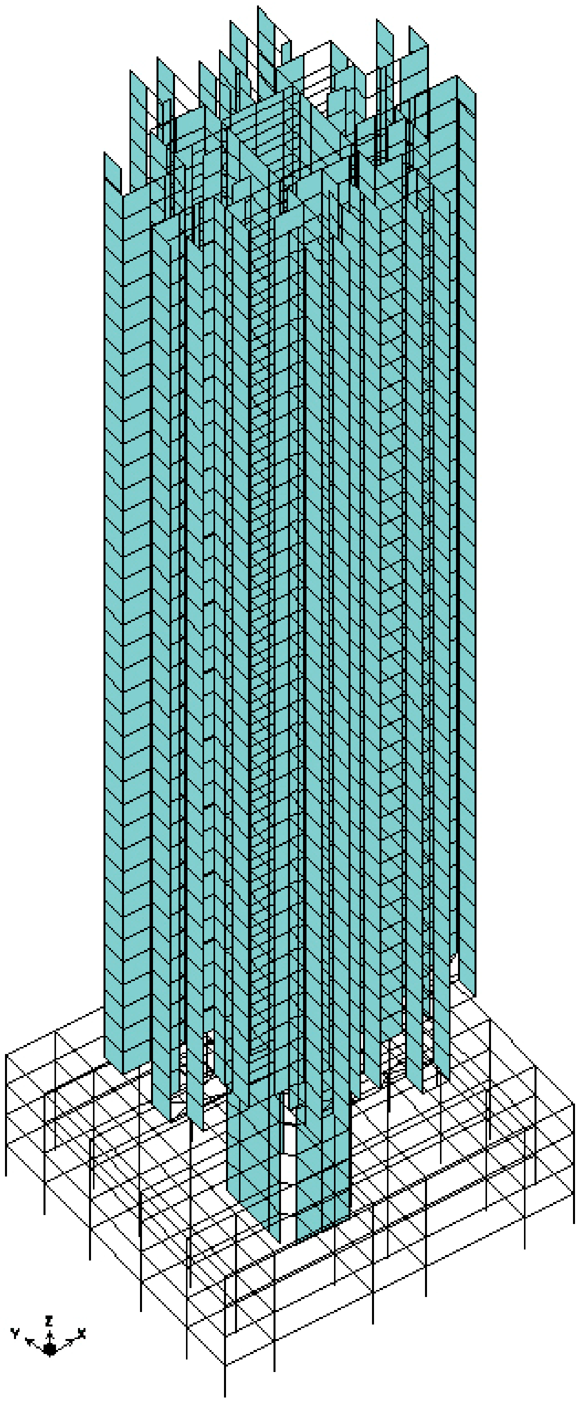

Figure 4.6 Advanced simplified un-coupling model using ETABS.

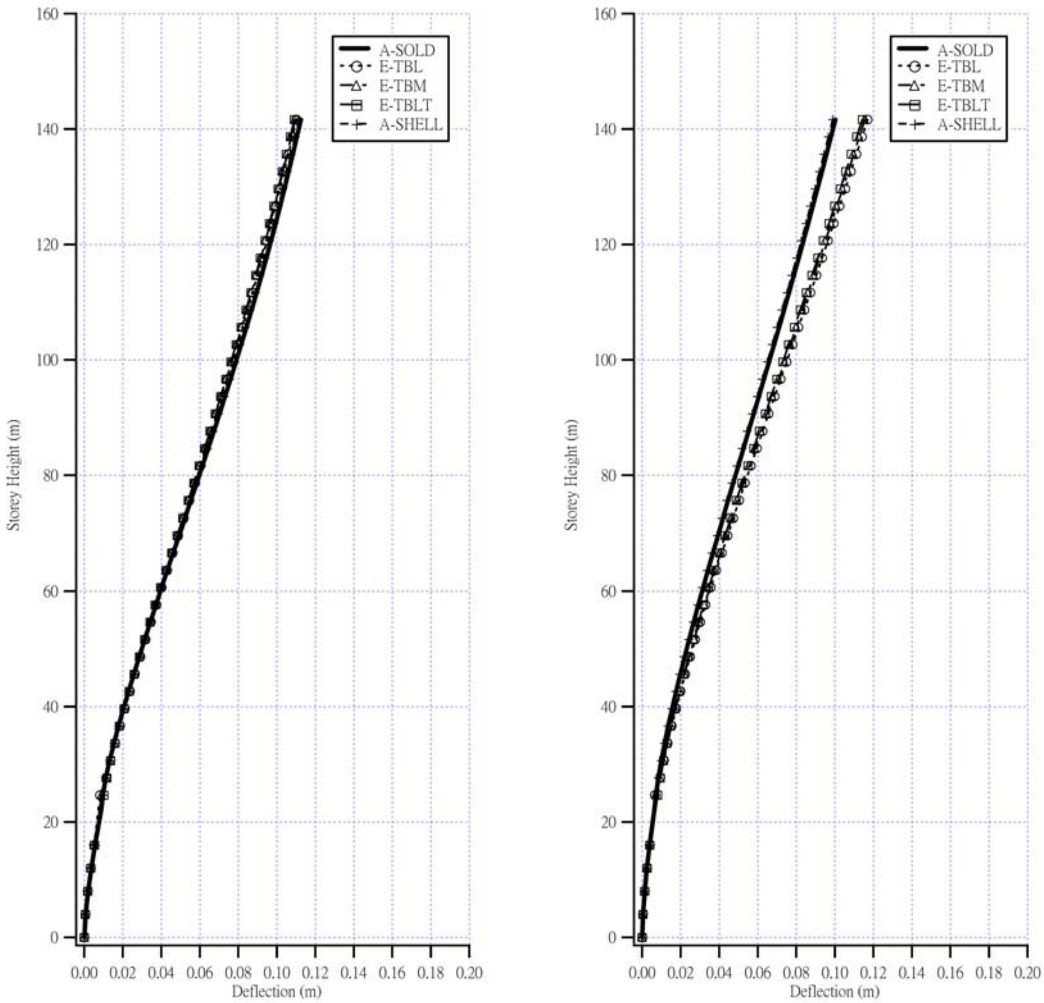

(a) in the x-direction (b) in the y-direction

Figure 4.7 Comparison of static lateral deflections.

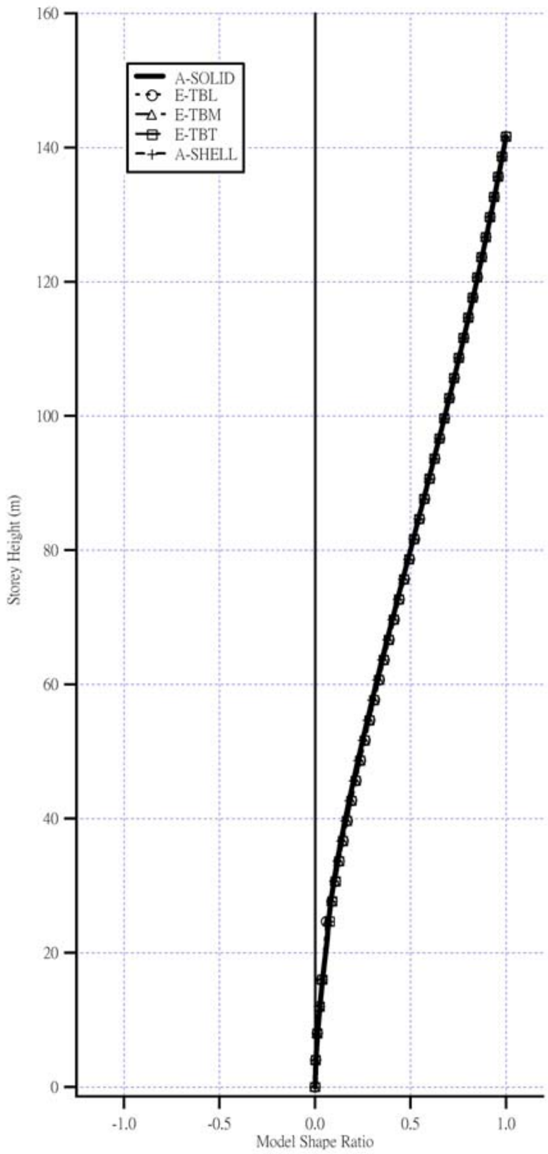

Figure 4.8 Comparison of the 1st mode shapes in the x-direction.

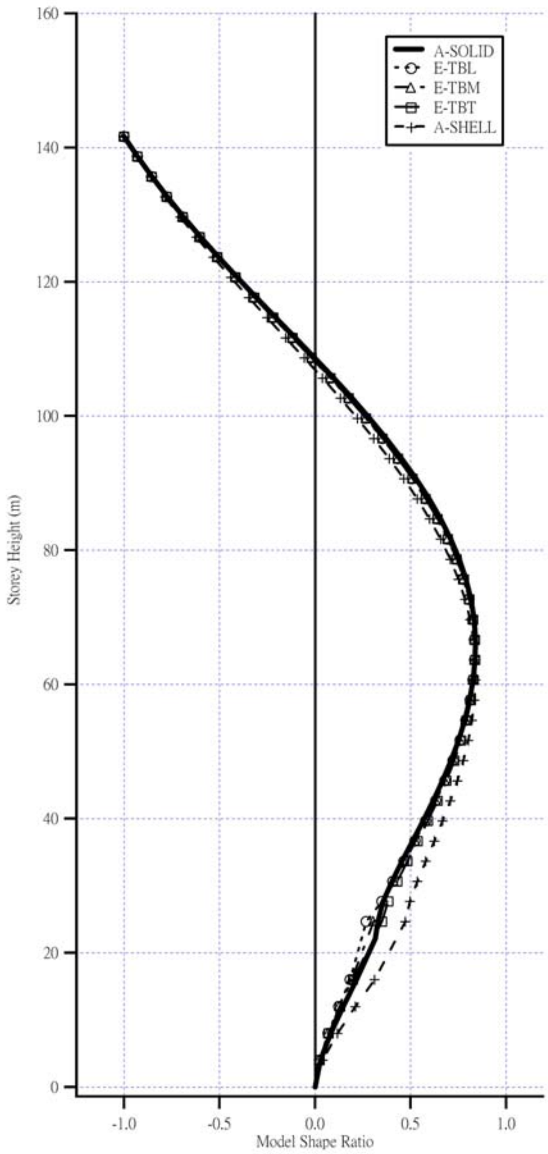

Figure 4.9 Comparison of the 2nd mode shapes in the x-direction.

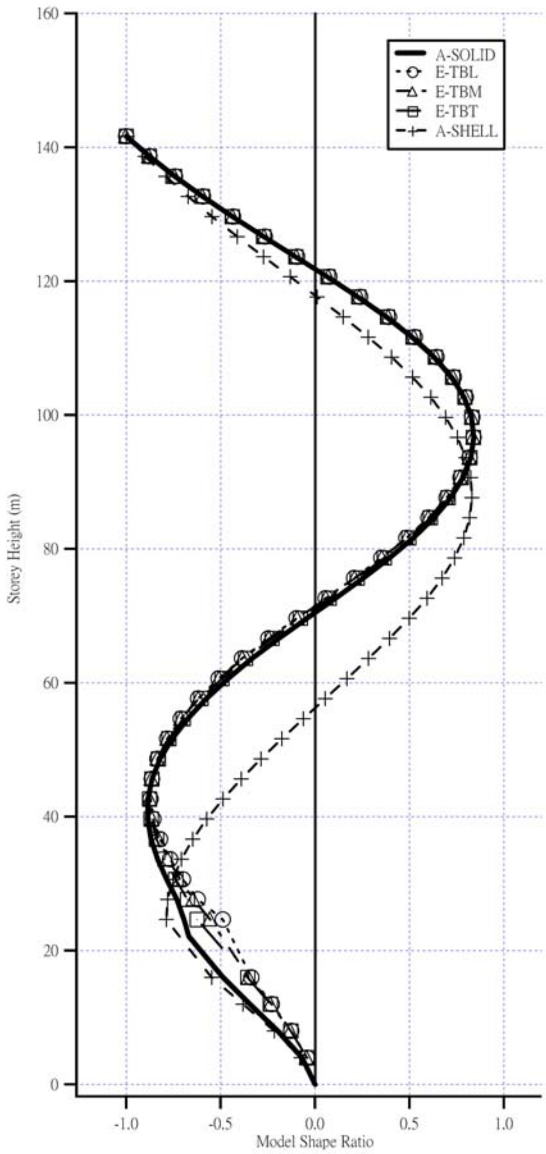

Figure 4.10 Comparison of the 3rd mode shapes in the x-direction.

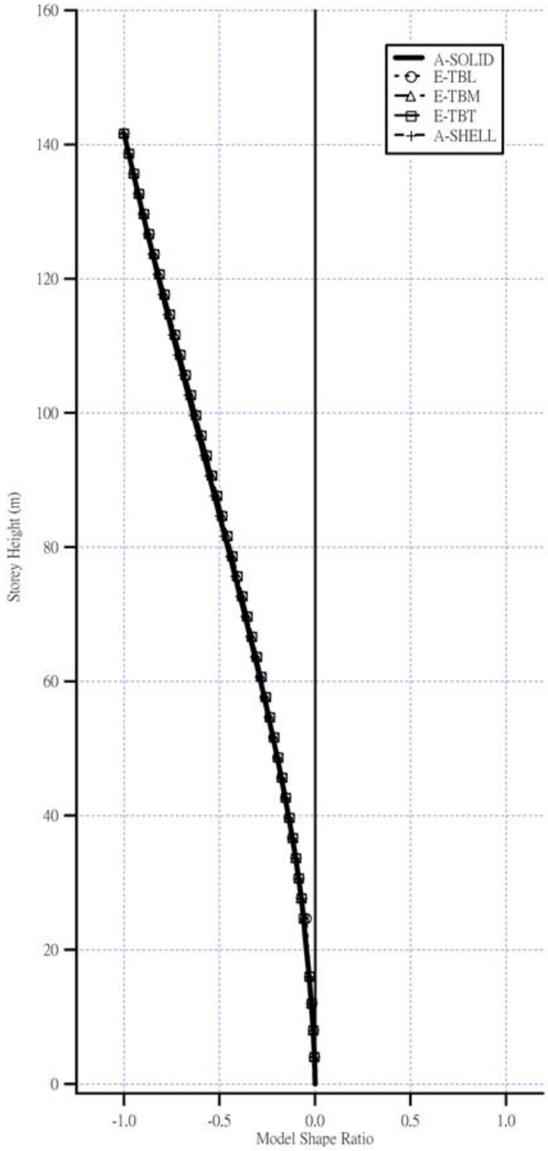

Figure 4.11 Comparison of the 1st mode shapes in the y-direction.

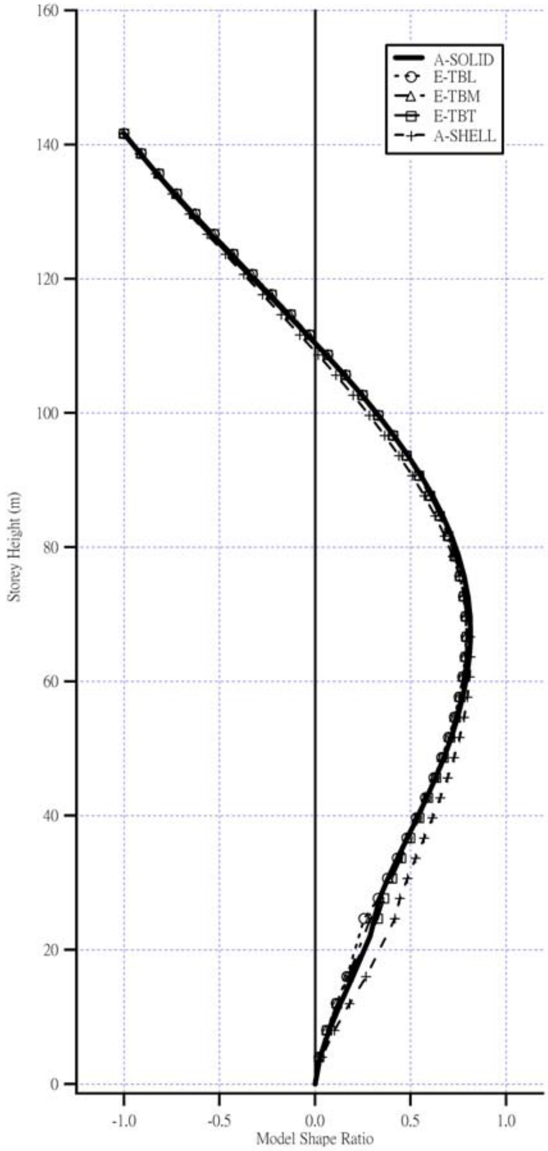

Figure 4.12 Comparison of the 2nd mode shapes in the y-direction.

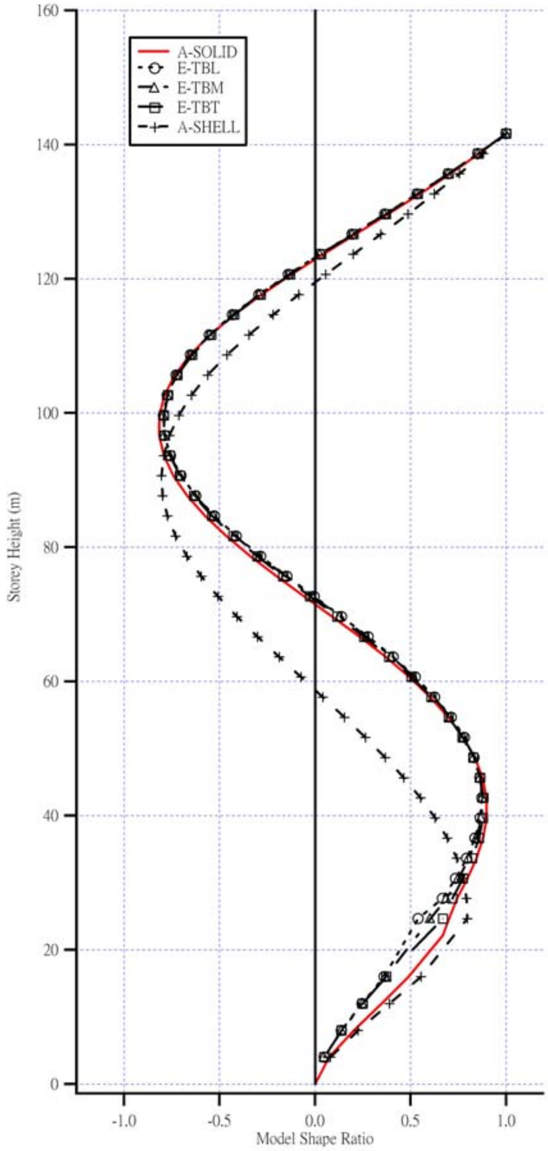

Figure 4.13 Comparison of the 3rd mode shapes in the y-direction.

5 SEISMIC RESPONSE OF A HIGH-RISE BUILDING WITH A TRANSFER PLATE

Different types of analysis have been developed to predict the seismic performance of a structure, such as time-history analysis, response spectrum analysis and the simplified equivalent static lateral force procedure … etc. High-rise reinforced concrete buildings are formed by core walls-frames and the dynamic response is more significant than static behaviour. Many design codes specify the elastic response spectrum method in the analysis and design, such as GB50011-2001, UBC and European Codes. In this study, finite element models using linear time-history analysis are used to predict the response of a high-rise building with a transfer plate in details. The finite element models are created using the commercial package, ABAQUS program. Based on the numerical results, performances of the transfer plate is investigated to identify response of a high-rise building with a transfer plate.

5.1 NUMERICAL MODELS

The prototype building considered in this section is a high-rise residential building with a transfer plate as shown in Figure 5.1. Detailed description of the prototype building is given in Chapter 4.1. The purposes of the numerical studies are to compare and verify the seismic performances obtained from seismic response spectra with different intensities. The seismic responses of the building structures were estimated using linear elastic time-history analyses.

According to the numerical results in Chapter 4.4.2, the natural period of vibration of a high-rise building with a transfer plate is about 2 second. Numerical results using the response spectrum analysis according to the old and new codes for seismic design of buildings of China, GBJ11-89 and GB50011-2001, match each other. Numerical analyses based on GBJ11-89 will be equivalent to that obtained based on GB50011-2001. Response spectrum analyses have been performed. The seismic response spectrum is based on the Code for Seismic Design of Buildings of China, GBJ11-89, as shown in Figure 5.2. Characteristic period of site is 0.55. Maximum values of the horizontal seismic effect coefficient in different seismic intensity levels are summarized in Table 5.1.

Models were developed using the commercial package, ABAQUS version 5.8.14. The four numerical models used in this study were generated based on the "A-SOLID" model, see Chapter 5. Characteristics of the finite element models are summarized in Tables 5.2 and 5.3. Brief descriptions of the various models are as follows.

Model MWD is used to explore the lateral response of a high-rise building subjected to lateral wind loads. The wind profiles are calculated based on the Code of Practice on Wind Effects of Hong Kong 1983.

Model MSA7 is used to explore the seismic response of a high-rise building when subjected to seismic intensity VII.

Model MSA8 is similar to model "MSA7", except that the seismicity level is the VIIIth degree.

Model MSA9 is similar to model "MSA7", except that the seismicity level is the IXth degree.

Lateral stiffness at the transfer plate level of transfer (K_t) and that at the 5^{th} floor level (K_5) are estimated. The ratio in lateral stiffness is simply K_t/K_5. Lateral stiffness at the level of transfer is estimated as follows. Translational and rotational degrees-of-freedom for all the vertical members are restrained at the 4^{th} floor level. A horizontal force of magnitude F is then applied to the transfer plate. If the corresponding lateral displacement is δ, then lateral stiffness at the transfer will be F/δ. The ratios of lateral stiffness are compiled in Table 5.4. Here, ratio of lateral stiffnesses, defined as the ratio of lateral stiffness of the floor to the lateral stiffness of the floor above. The reduction in lateral stiffness due to the transfer plate is substantial, and the transfer level is generally classified as a soft-story level.

5.2 NUMERICAL ANALYSIS

5.2.1 FUNDAMENTAL FREQUENCIES

The high-rise building under consideration is symmetric on plan. Except the first few modes of vibration, higher order modes of vibration consist of a combination of translational and rotational displacements. Therefore, not less than 20 modes of vibration have been estimated in each of the numerical analyses to determine the first three fundamental frequencies. Table 5.5 summarises the fundamental frequencies of the finite element model

5.2.2 LATERAL DEFORMATION OF A HIGH-RISE BUILDING WITH TRANSFER PLATE

Figure 5.3 compares the lateral displacements of the numerical models. The lateral deflections estimated by the finite element analyses are listed in Tables 5.6 and 5.7. Since the building has no seismic resistance provisions and is designed for lateral resistance to the lateral wind loads, seismic resistance provision on the high-rise building is taken as equal to the lateral resistance to static wind loads. In the x-direction, the lateral deflections below the transfer plate are closed to those obtained from the results of the response spectrum analyses. Large discrepancies are observed at and above the transfer plate. Similar conclusions are obtained when comparing the results in the y-direction. The lateral resistance due to the lateral wind load can provide enough seismic resistance when the site is rated at or below seismic intensity VIII. The building could collapse when the seismic intensity level is at the IXth degree.

5.2.3 STOREY FORCES OF A HIGH-RISE BUILDING WITH A TRANSFER PLATE

Figures 5.4 and 5.5 compare the storey shear force of the numerical models in the case of static lateral wind loads and at different seismic intensities. It shows the interaction of storey shear force distribution between the transfer plate system, upper floors and supporting structures. In all loading cases, the shear forces transmitted from above the transfer to the support structures are over 80% of total storey shear force distributed in core walls and about 20% of that in columns system. Shear resistance under the wind load cases could be sufficient to withstand seismic intensity VII attacks in the x-direction. When the site condition is rated at seismic intensity VIII level, the shear force increases from the bottom to the top of the structure. Seismic shear forces are greater than the lateral resistance of building at or above the 31st floor. Cracks and damage can be obtained in the walls and core walls in the high-rise building with a transfer plate. The building will collapse when the site condition is rated as seismic intensity IX. Similar conclusions are obtained when comparing the results in the y-direction.

Figures 5.6 and 5.7 compare the moment resultants. Over 70% of total moment is carried from above the transfer plate and transmitted as axial forces in the column system by transfer through the transfer plate. Core walls carry about 30% of total moment from above the transfer plate into foundation. In the x-direction, the moment resultants under the wind load cases are greater than those obtained under seismic intensity VII. When the site condition is rated as seismic intensity VIII, the moment resultants are greater than the moment of resistance at or above the 22nd floor. Cracks and damage can be obtained in the walls and core walls in the high-rise building with a transfer plate. The building will collapse when the site condition is rated as seismic intensity IX. Similar conclusions are obtained when comparing the results in the y-direction.

Considering the storey shear and moment resultants overall, the high-rise building with a transfer plate satisfies the seismic resistance provision when subjected to seismic intensity VII attacks. If the site is rated at seismic intensity VIII or above, the building will collapse.

5.2.4 RESPONSES OF THE TRANSFER PLATE STRUCTURE

Table 5.9 summarises the shear force and moment resultants of the transfer plate element in the numerical models, in the case of static lateral wind loads and at different seismic intensities. It indicates that vertical shear force resistance in the transfer plate system under the wind load cases could be sufficient to withstand seismic intensity VII attacks. Seismic shear forces in the vertical direction are greater than the shear resistance of transfer plate, when the site condition is rated at seismic intensity VIII level. Cracks and damage can be obtained in transfer plate. Seismic shear forces in the vertical direction and seismic moment resultants are about twice times the force resistances of transfer plate, when the site condition is rated as seismic intensity IX. Similar conclusions are obtained when comparing the results in the y-direction.

Figures 5.8 to 5.12 show the deformation of the transfer plate under different loading conditions, such as a gravity load and lateral load cases. And the stress distribution on the transfer plate at the top and bottom levels are shown in Figures 5.13 to 5.22. The observation of stress distribution on the transfer plate was investigated by comparing the analysis results from the high-rise building with a transfer plate carrying different types of loadings conditions, such as a gravity load, lateral load and seismic load cases. For all cases, these figures clearly indicate the shear and moment resultants distribution pattern in the transfer plate structures and is match in the deflection shape of the transfer plate.

Based on these results, the structural behaviour of the transfer plate can be classified by observation of the local deformation. The maximum and minimum vertical deformations at the top and bottom of transfer plate are summarized in Table 5.9. In the table, “ratio of curvature” is defined as the difference between two vertical deformations divided by 2 times the horizontal distance between these two points. The “deflection / depth” ratio is defined as the maximum deflection divided by the thickness of the transfer plate. The limited design values of “deflection /depth” ratio and “ratio of curvature” are determined by the BS8110:1985. The maximum “deflection / depth” ratio and “ratio of curvature” of the transfer plate is much less than limited design values. It means that the transfer plate becomes effectively a rigid plate and the rigid diaphragm assumption could be adopted in the analyses of transfer plate.

5.3 CONCLUDING SUMMARY

Using the response spectrum analyses, seismic responses of a prototype high-rise building with a transfer plate were explored and estimated using the finite element approach. Since the prototype building has no seismic resistance provisions, the high-rise building with a transfer plate is only designed to resist the lateral wind loads. The building provides sufficient seismic resistance when subjected to seismic intensity VII level. Reduction in the lateral stiffness at the transfer plate is up to 63%, and damage occurs at the storey above the transfer plate when the site condition is rated as seismic intensity VIII. The use of the ratio of lateral stiffnesses to check the existence of a soft storey may not be appropriate for the high-rise buildings. From the analyses results, the structural response of the transfer plate can be classified as rigid. In this case, a rigid floor assumption is recommended for use in the analysis of a transfer plate.

Table 5.1 Maximum value of horizontal seismic effect coefficient.

Seismic Intensity	VII	VIII	IX
Maximum value	0.08	0.16	0.32

Table 5.2 Structural detail and characteristic loads of the prototype building.

<table>
<tr><th rowspan="2">Floor level</th><th rowspan="2">Structural system</th><th rowspan="2">Structural detail</th><th colspan="2">Characteristic loads</th></tr>
<tr><th>Imposed load (kPa)</th><th>Finishes, screeding and ceiling (kPa)</th></tr>
<tr><td rowspan="2">Typical (5/F-17/F)</td><td>Shear wall</td><td>200-250mm</td><td rowspan="2">3.0</td><td rowspan="2">0.5</td></tr>
<tr><td>Core wall</td><td>475mm</td></tr>
<tr><td rowspan="2">Typical (18/F-30/F)</td><td>Shear wall</td><td>200-250mm</td><td rowspan="2">3.0</td><td rowspan="2">0.5</td></tr>
<tr><td>Core wall</td><td>350mm</td></tr>
<tr><td rowspan="2">Typical (30/F-43/F)</td><td>Shear wall</td><td>200-250mm</td><td rowspan="2">3.0</td><td rowspan="2">0.5</td></tr>
<tr><td>Core wall</td><td>250mm</td></tr>
<tr><td colspan="2">Transfer Plate</td><td>2500mm</td><td>3.0</td><td>2.0</td></tr>
<tr><td rowspan="2">Podium (G/F-4/F)</td><td>Column</td><td>8@2200 mm diameter
28@700mm diameter</td><td rowspan="2">4.0</td><td rowspan="2">2.0</td></tr>
<tr><td>Core wall</td><td>1000mm</td></tr>
</table>

Table 5.3 Modulus of Elasticity (kN/m^2) used in models.

Floor	Concrete Grade	Modulus of Elasticity ($\times 10^7$ kN/m^2)
5/F - 43/F	C30	2.17
	C40	2.40
TRANSFER PLATE	C30	2.17
	C40	2.40
4/F	C30	2.17
	C40	2.40
3/F	C30	2.17
	C40	2.40
2/F	C30	2.17
	C40	2.40
1/F	C30	2.17
	C40	2.40

Table 5.4 Lateral stiffness ($\times 10^7$ kN/m) at and above the transfer.

	Floor level	x-direction	y-direction
Lateral stiffness (kN/m)	5/F	3.528	6.154
	Transfer	1.620	2.267
Ratio of lateral stiffness K_t/K_5		0.459	0.368

Table 5.5 First three fundamental frequencies.

	Fundamental frequencies (Hz)		
	1st mode	2^{nd} mode	3rd mode
In the x-direction	0.506	1.911	3.582
In the y-direction	0.511	2.196	4.422

Table 5.6 Lateral displacements in the x-direction.

Storey level	Deflection (m)			
	MWD	MSA7	MSA8	MSA9
43/F	0.1125	0.0362	0.0723	0.1447
39/F	0.1039	0.0331	0.0662	0.1324
35/F	0.0945	0.0298	0.0595	0.1191
31/F	0.0842	0.0262	0.0524	0.1048
27/F	0.0731	0.0225	0.0450	0.0900
23/F	0.0613	0.0187	0.0374	0.0749
19/F	0.0492	0.0149	0.0298	0.0597
15/F	0.0372	0.0112	0.0225	0.0449
11/F	0.0257	0.0077	0.0155	0.0310
10/F	0.0229	0.0069	0.0138	0.0277
9/F	0.0203	0.0061	0.0122	0.0245
8/F	0.0177	0.0053	0.0107	0.0214
7/F	0.0153	0.0046	0.0092	0.0184
6/F	0.0131	0.0039	0.0079	0.0158
5/F	0.0111	0.0033	0.0067	0.0134
TRANSFER	0.0096	0.0029	0.0058	0.0116
4/F	0.0055	0.0017	0.0034	0.0068
3/F	0.0036	0.0011	0.0022	0.0045
2/F	0.0019	0.0006	0.0012	0.0024
1/F	0.0006	0.0002	0.0004	0.0008
GROUND	0.0000	0.0000	0.0000	0.0000

Table 5.7 Lateral displacements in the y-direction.

Storey level	Deflection (m)			
	MWD	MSA7	MSA8	MSA9
43/F	0.1003	0.0365	0.0731	0.1461
39/F	0.0909	0.0329	0.0657	0.1315
35/F	0.0812	0.0291	0.0581	0.1162
31/F	0.0710	0.0251	0.0503	0.1006
27/F	0.0605	0.0212	0.0425	0.0849
23/F	0.0499	0.0173	0.0347	0.0694
19/F	0.0393	0.0136	0.0271	0.0543
15/F	0.0291	0.0100	0.0200	0.0400
11/F	0.0198	0.0068	0.0135	0.0270
10/F	0.0176	0.0060	0.0120	0.0240
9/F	0.0155	0.0053	0.0106	0.0212
8/F	0.0135	0.0046	0.0092	0.0184
7/F	0.0116	0.0040	0.0079	0.0159
6/F	0.0099	0.0034	0.0068	0.0135
5/F	0.0084	0.0029	0.0057	0.0114
TRANSFER	0.0071	0.0024	0.0049	0.0097
4/F	0.0038	0.0013	0.0026	0.0053
3/F	0.0024	0.0008	0.0017	0.0034
2/F	0.0013	0.0004	0.0009	0.0018
1/F	0.0004	0.0001	0.0003	0.0006
GROUND	0.0000	0.0000	0.0000	0.0000

Table 5.8 Comparison of shear forces and bending moment resultants in the transfer plate system.

Direction	Horizontal force (KN/m)			Moment (KNm/m)			Vertical shear force (KN/m)	
	in the x-direction	in the y-direction	in the x-y plan	about x-direction	about y-direction	about x-y plan	In the x-z plan	In the y-z plan
Gravity Loadings Case								
	6.3	7.5	3.1	5608.6	5029.7	1442.5	8543.8	5772.7
Wind Loadings Cases								
In the x-direction	42.4	22	16.5	5177.3	4262.5	1870.1	5929.9	4254.4
In the y-direction	11.6	30.9	12.8	4626	3886.6	1185.7	6020.1	6665.4
Seismic Loadings Cases at the seismicity intensity VIIth degree								
In the x-direction	10.3	5.9	4.7	2326.4	1408.8	597.9	4027.6	2535.6
In the y-direction	3.8	10.8	3.9	1709.1	1912.8	443.7	2744.7	3721.8
Seismic Loadings Cases at the seismicity intensity VIIIth degree								
In the x-direction	20.5	11.8	9.4	4654.8	2818.2	1196.0	8059.6	5073.1
In the y-direction	7.6	21.6	7.8	3418.4	3825.7	887.6	5489.7	7443.8
Seismic Loadings Cases at the seismicity intensity IXth degree								
In the x-direction	41.1	23.6	18.8	9309.5	5636.3	2392.1	16119.3	10146.1
In the y-direction	15.2	43.1	15.7	6836.8	7651.3	1775.1	10979.4	14887.7

Table 5.9 Comparison of vertical displacements of transfer plate.

Load Case	Loading Direction	Displacements (m)				Ratio	
		TOP		BOTTOM		Ratio of curvature	Deflection / depth
		MAX	MIN	MAX	MIN		
Gravity Load	Z	-0.00208	-0.00343	-0.00208	-0.00344	1 / 26144	0.00054
MWD	X	0.00382	0.003378	0.003818	0.003394	1 / 34662	0.00018
	Y	0.002823	0.002182	0.002808	0.00259	1 / 144928	0.00026
MSA7	X	0.000866	0.000663	0.000861	0.000665	1 / 161290	0.00008
	Y	0.001334	0.001176	0.001334	0.001182	1 / 96618	0.00006
MSA8	X	0.001732	0.001327	0.001723	0.001331	1 / 80646	0.00016
	Y	0.002669	0.002353	0.002668	0.002364	1 / 48310	0.00013
MSA9	X	0.003463	0.002654	0.003445	0.002662	1 / 40404	0.00032
	Y	0.005337	0.004706	0.005335	0.004728	1 / 24214	0.00025
Limited design value	-	-	-	-	-	1/250	0.1

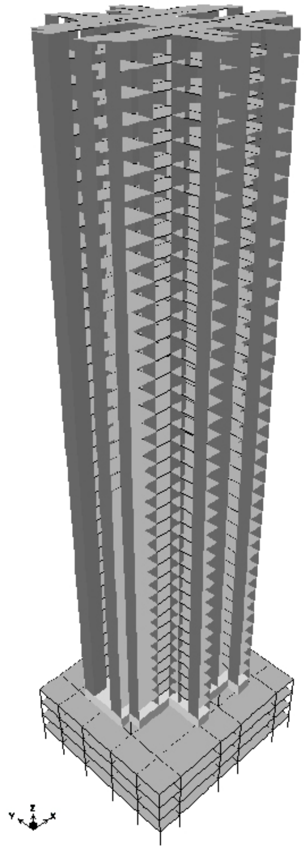

Figure 5.1 Finite element model of a high-rise building with a transfer plate.

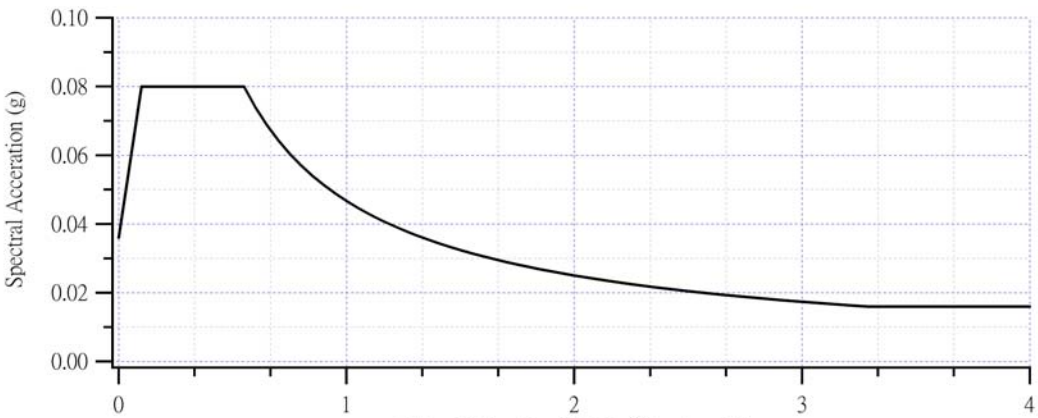

Figure 5.2 Response spectra curve.

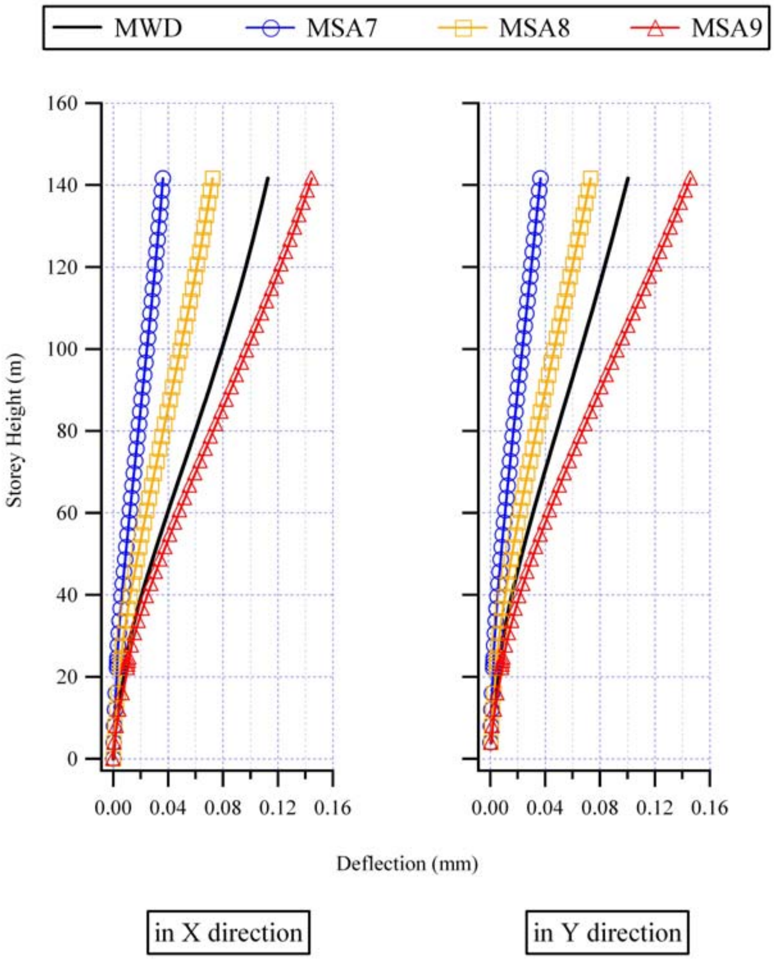

Figure 5.3 Comparison of static lateral deflection of numerical models.

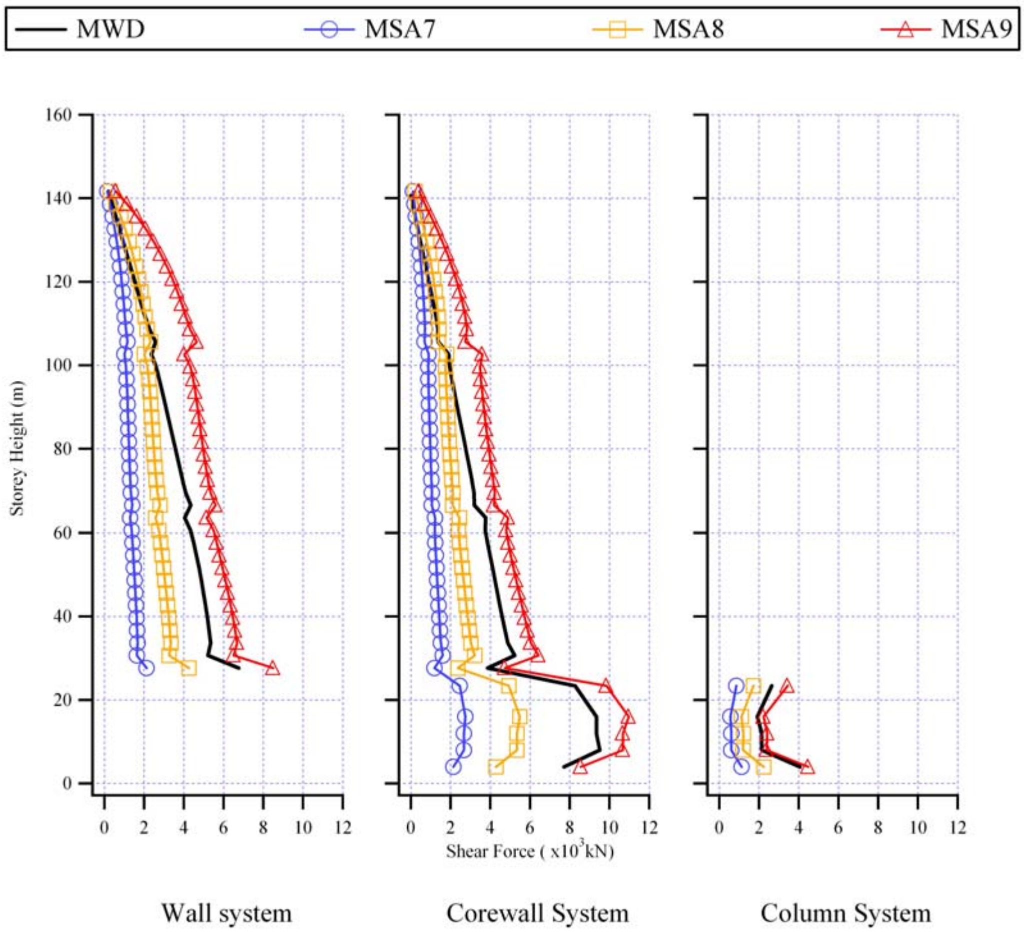

Figure 5.4 Comparison of storey shear force of numerical models in the x-direction.

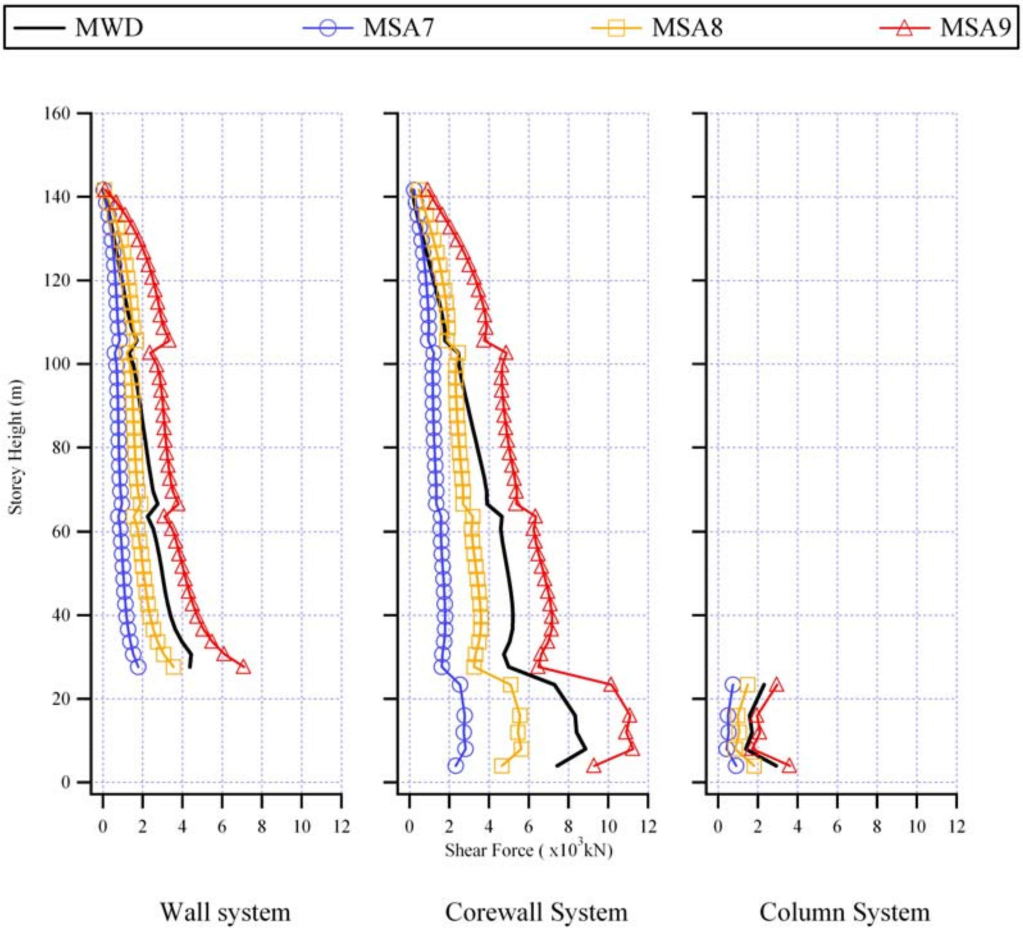

Figure 5.5 Comparison of storey shear force of numerical models in the y-direction.

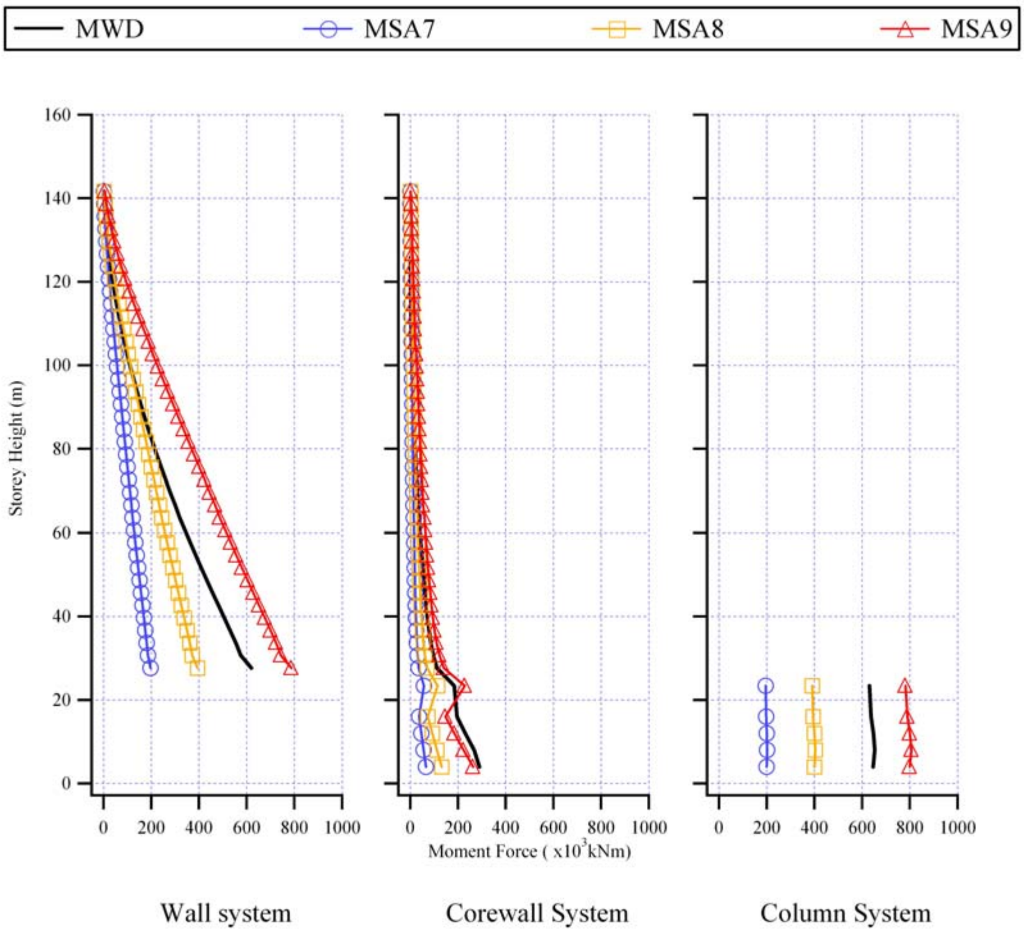

Figure 5.6 Comparison of storey moment force of numerical models in the x-direction.

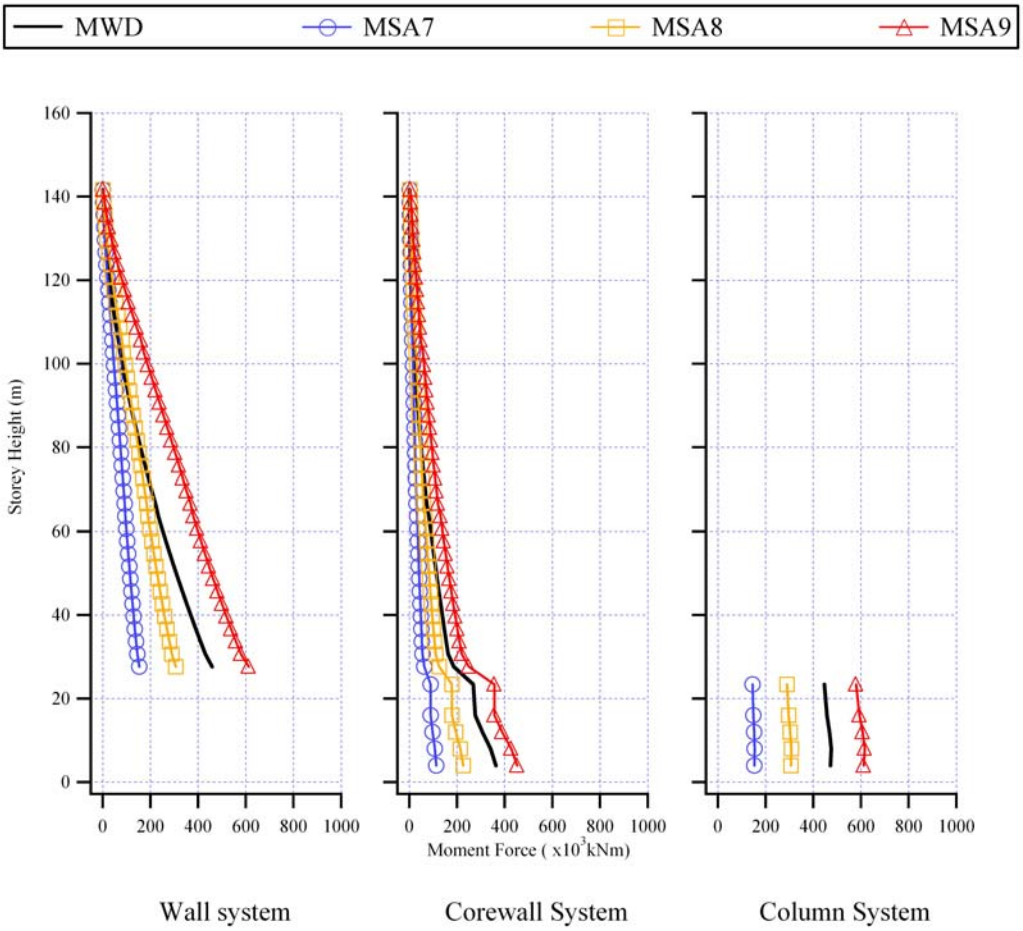

Figure 5.7 Comparison of storey moment force of numerical models in the y-direction.

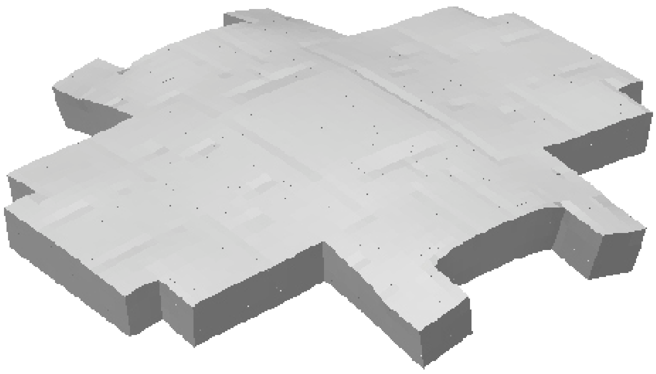

Figure 5.8 Deformed shape of transfer plate when the high-rise building with a transfer plate subjected to a gravity load.

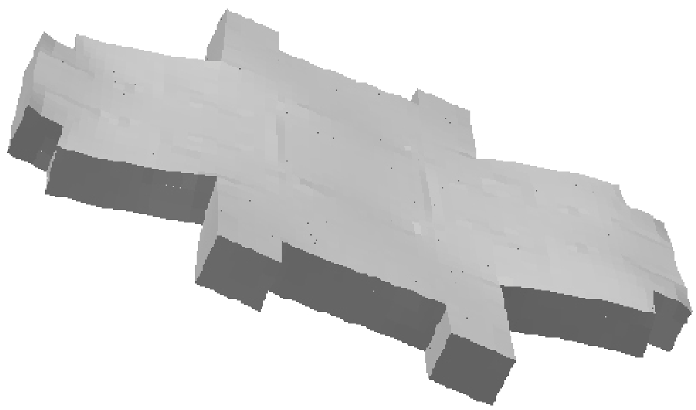

Figure 5.9 Deformed shape of transfer plate when the high-rise building with a transfer plate subjected to a wind load in x-direction.

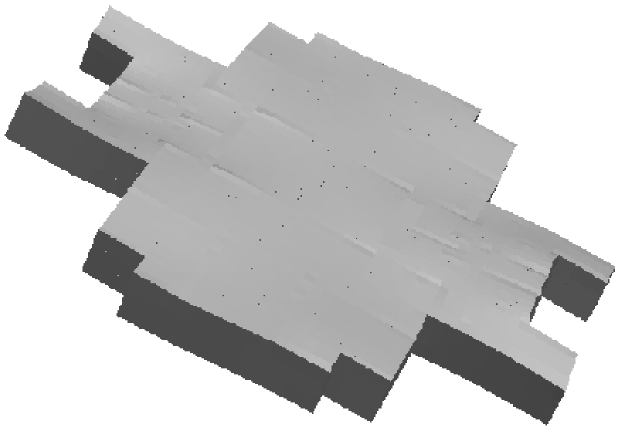

Figure 5.10 Deformed shape of transfer plate when the high-rise building with a transfer plate subjected to a wind load in y-direction.

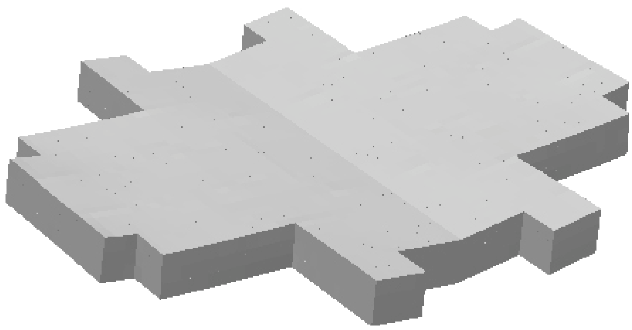

Figure 5.11 Deformed shape of transfer plate when the high-rise building with a transfer plate subjected to an earthquake attacks in the x-direction.

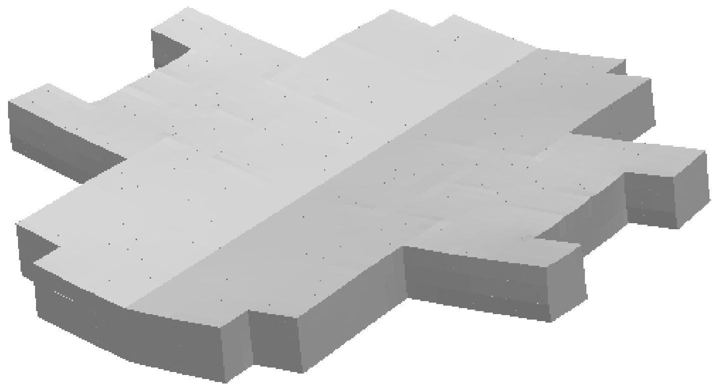

Figure 5.12 Deformed shape of transfer plate when the high-rise building with a transfer plate subjected to an earthquake attacks at the y-direction.

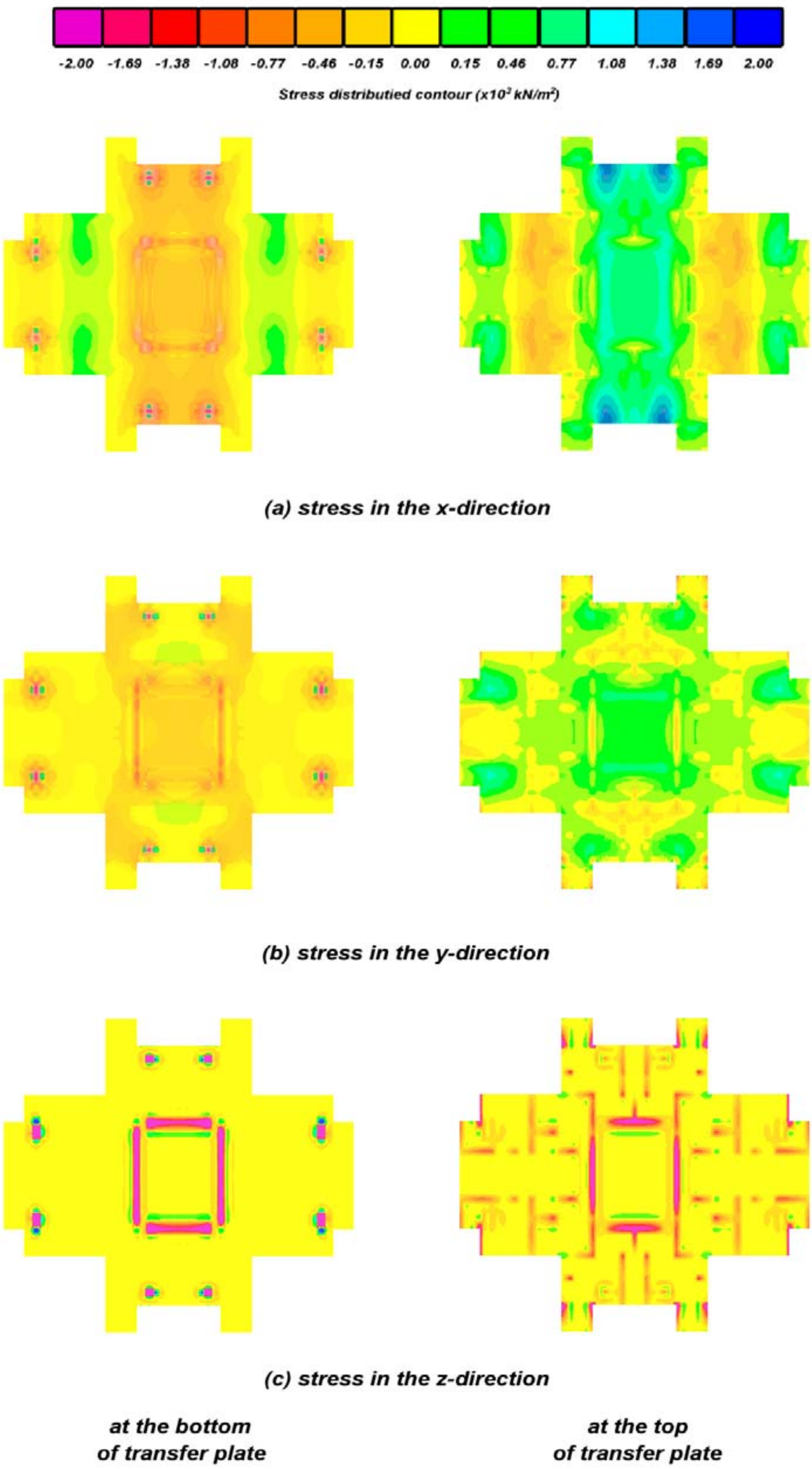

Figure 5.13 Stress distribution of the transfer plate when the high-rise building with a transfer plate subjected to a gravity loads.

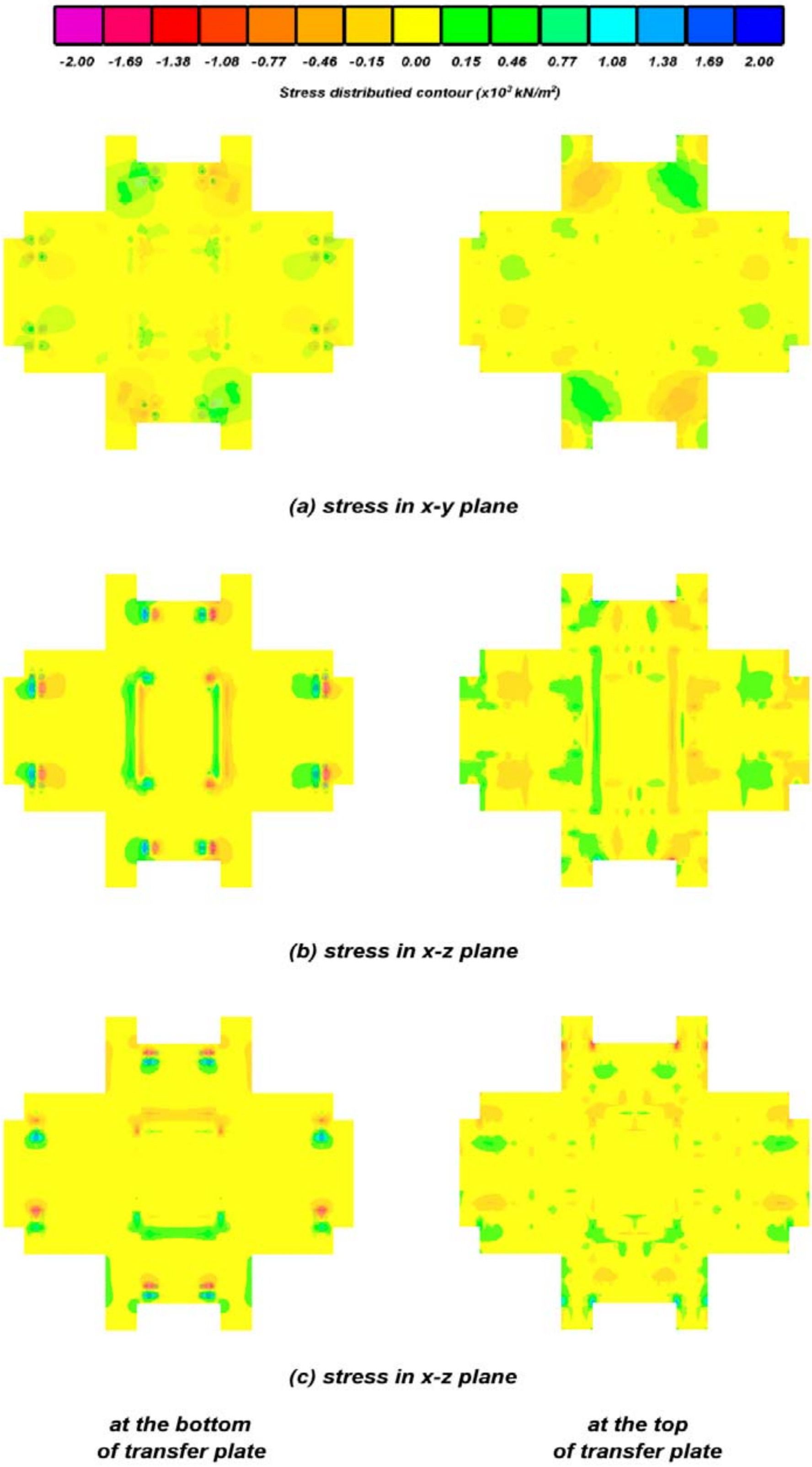

Figure 5.14 Shear stress distribution on the transfer plate when the high-rise building with a transfer plate subjected to a gravity loads.

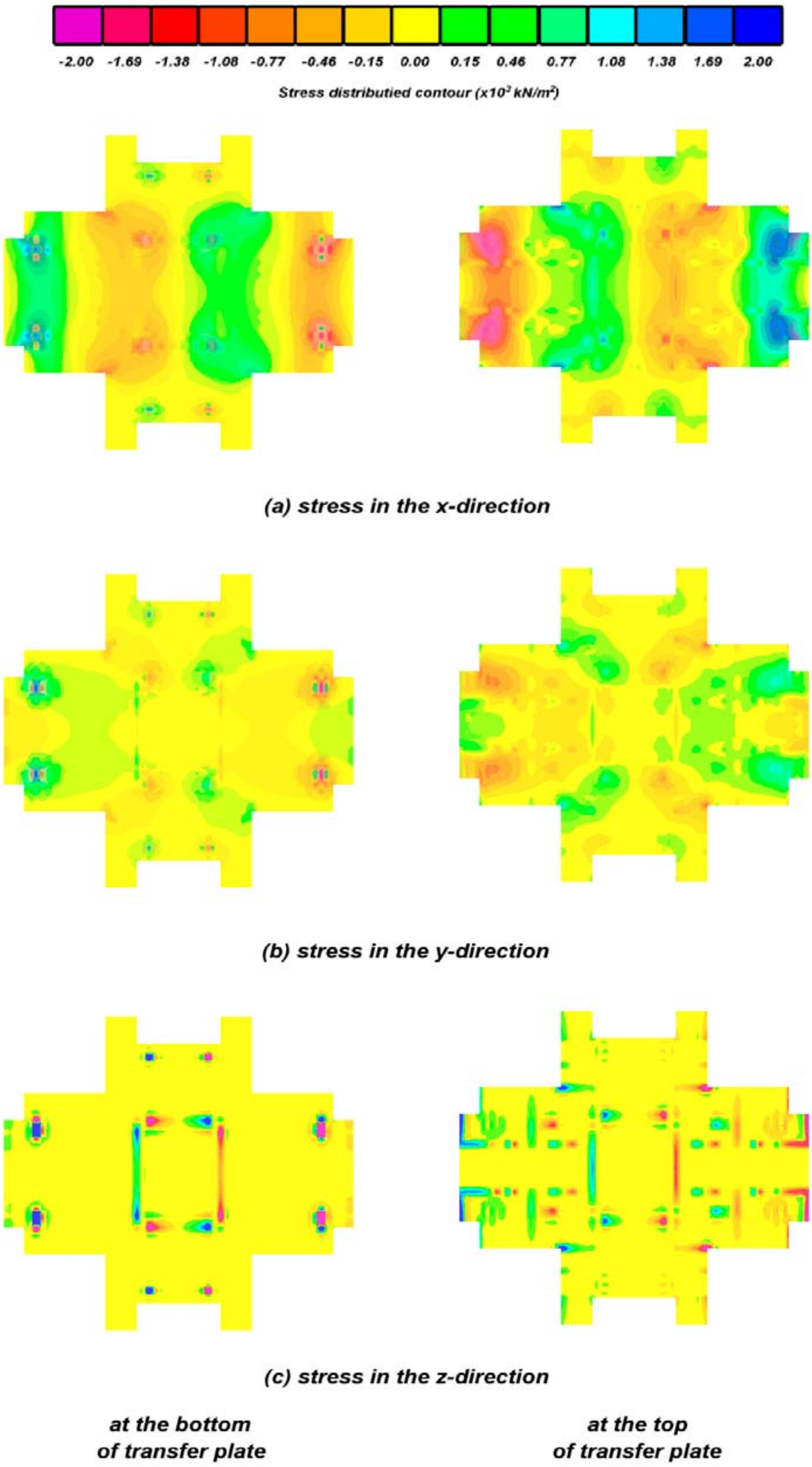

Figure 5.15 Stress distribution transfer plate when the high-rise building with a transfer plate subjected to a wind load in the x-direction.

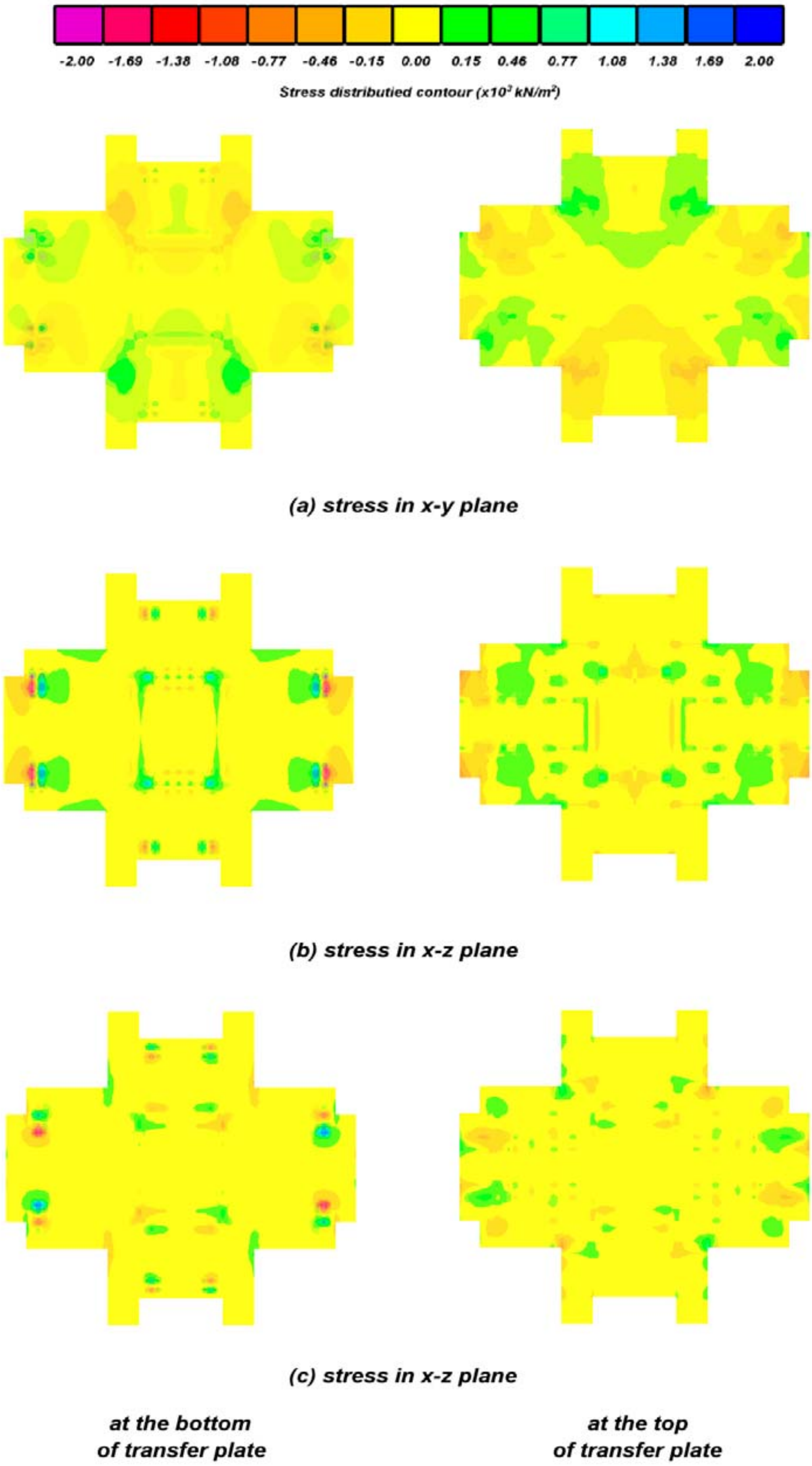

Figure 5.16 Shear stress distribution transfer plate when the high-rise building with a transfer plate subjected to a wind load in the x-direction.

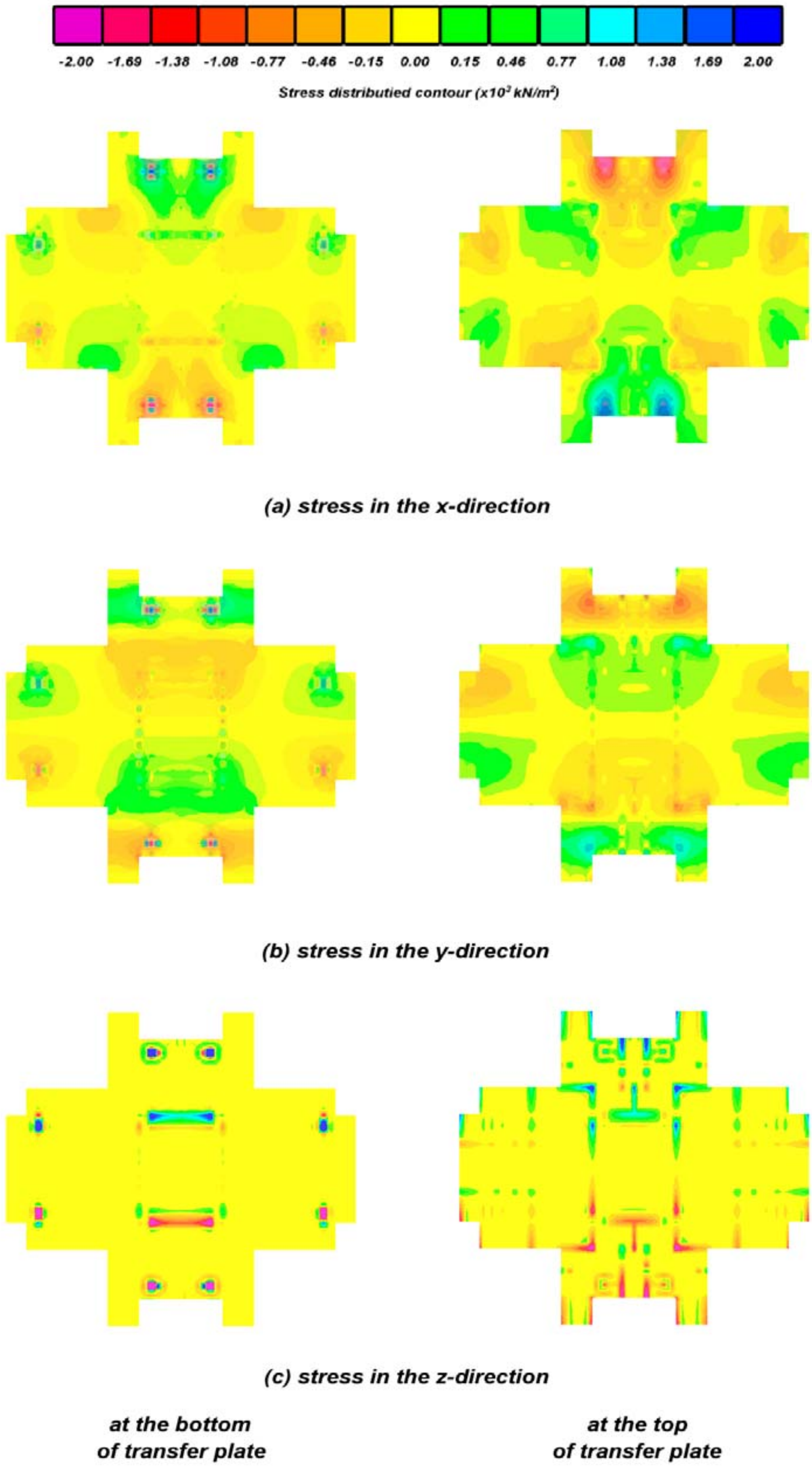

Figure 5.17 Stress distribution transfer plate when the high-rise building with a transfer plate subjected to a wind load in the y-direction.

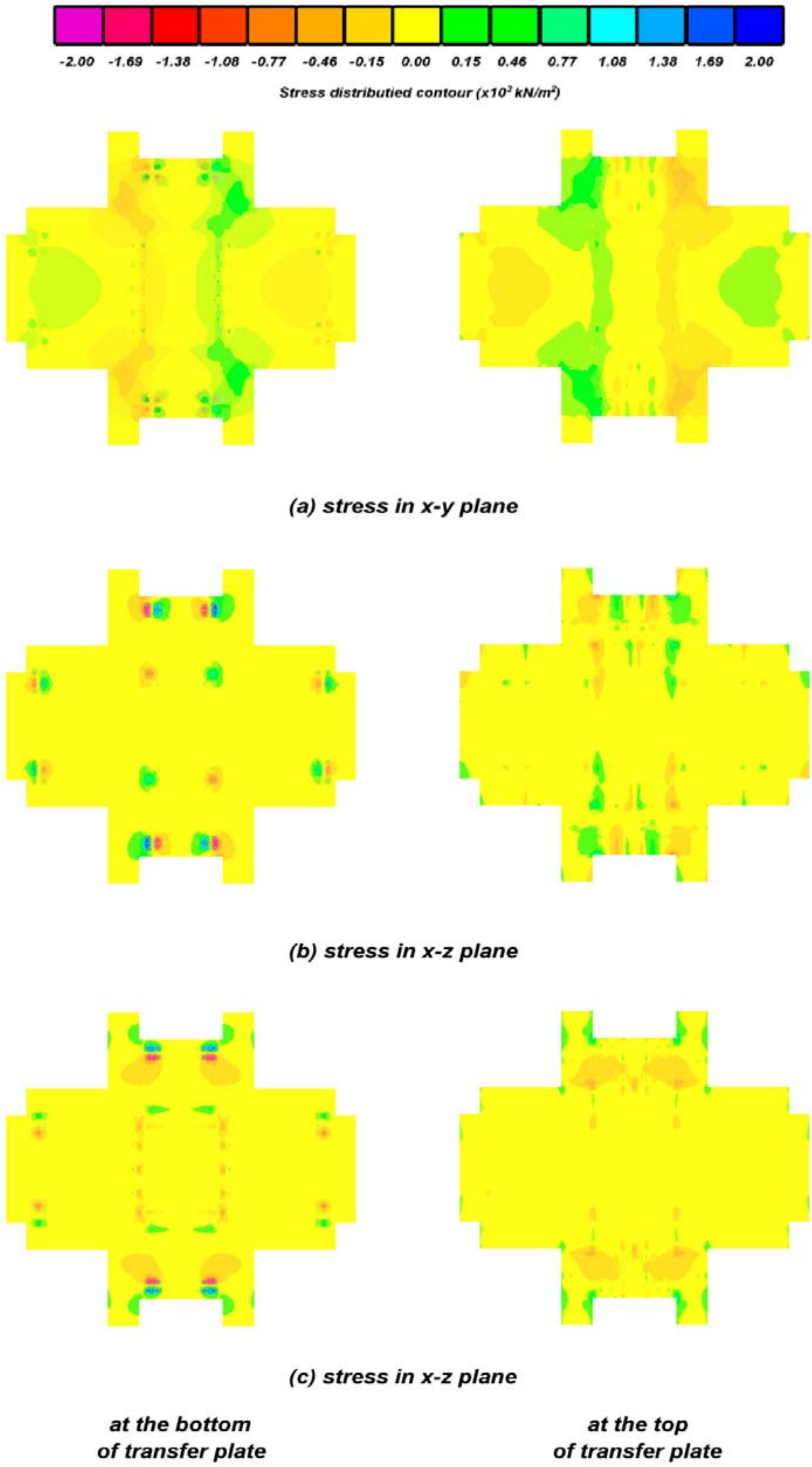

Figure 5.18 Shear stress distribution transfer plate when the high-rise building with a transfer plate subjected to a wind load in the y-direction.

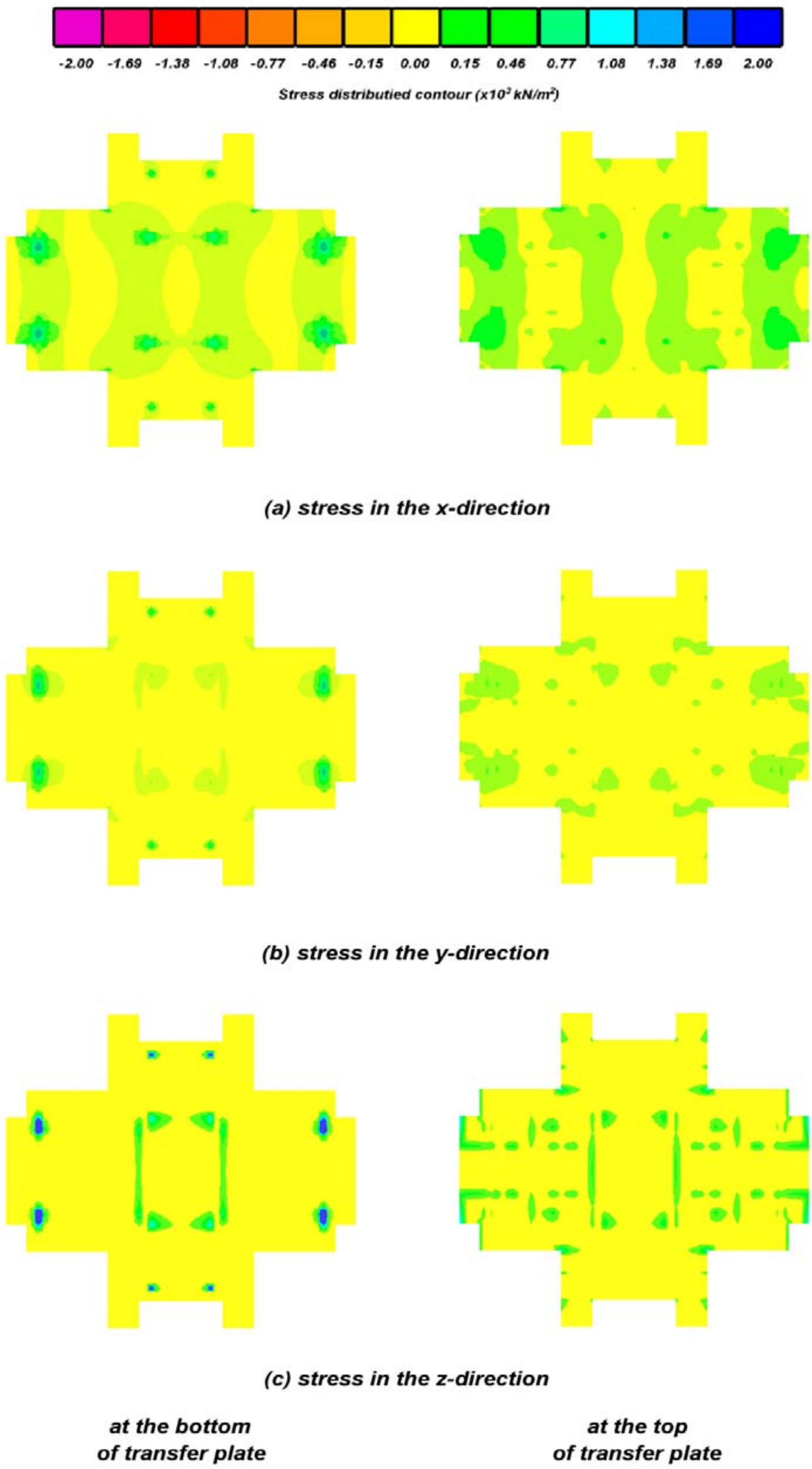

Figure 5.19 Stress distribution on the transfer plate when the high-rise building with a transfer plate subjected to an earthquake attacks in the x-direction.

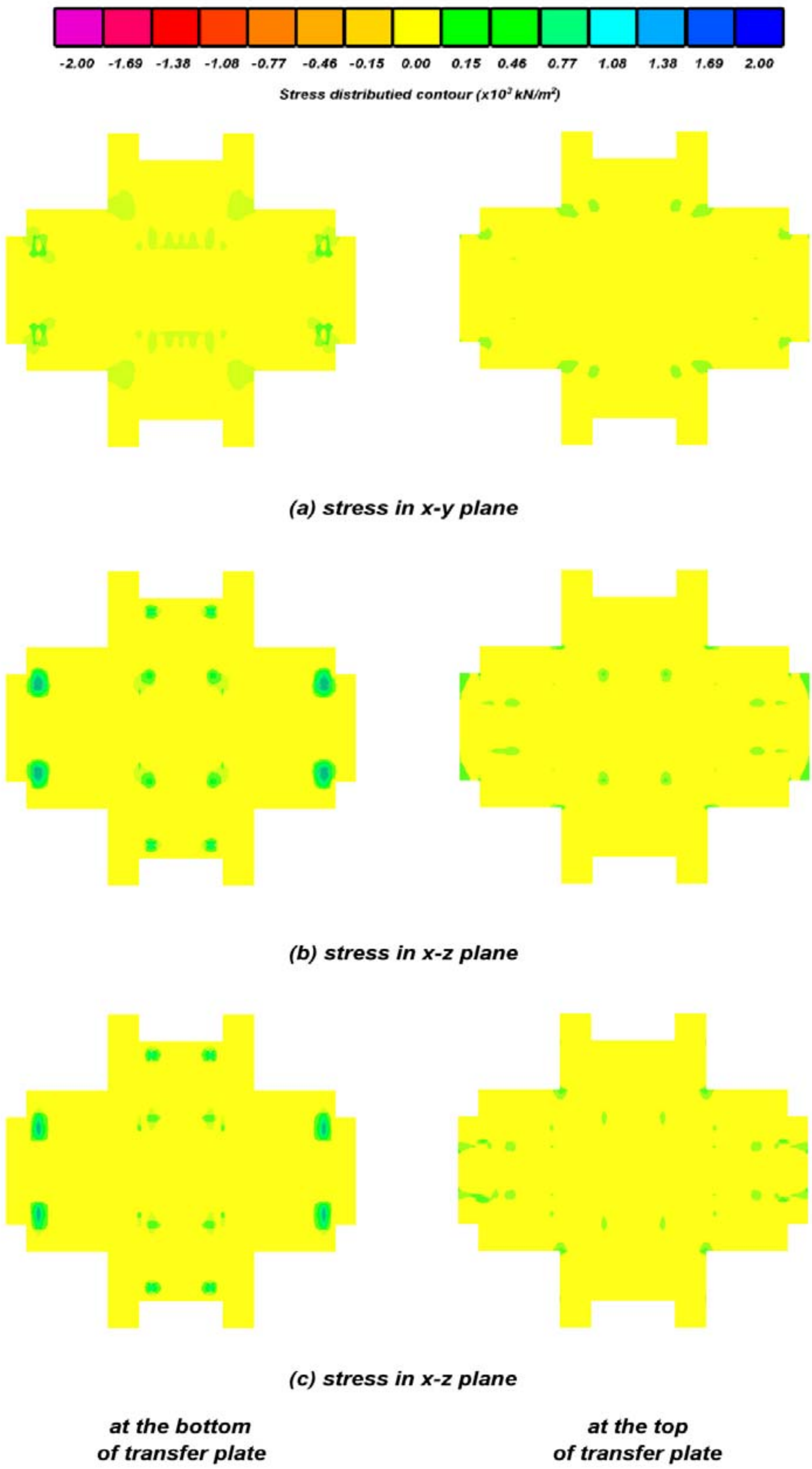

Figure 5.20 Shear stress distribution on the transfer plate when the high-rise building with a transfer plate subjected to an earthquake attacks in the x-direction.

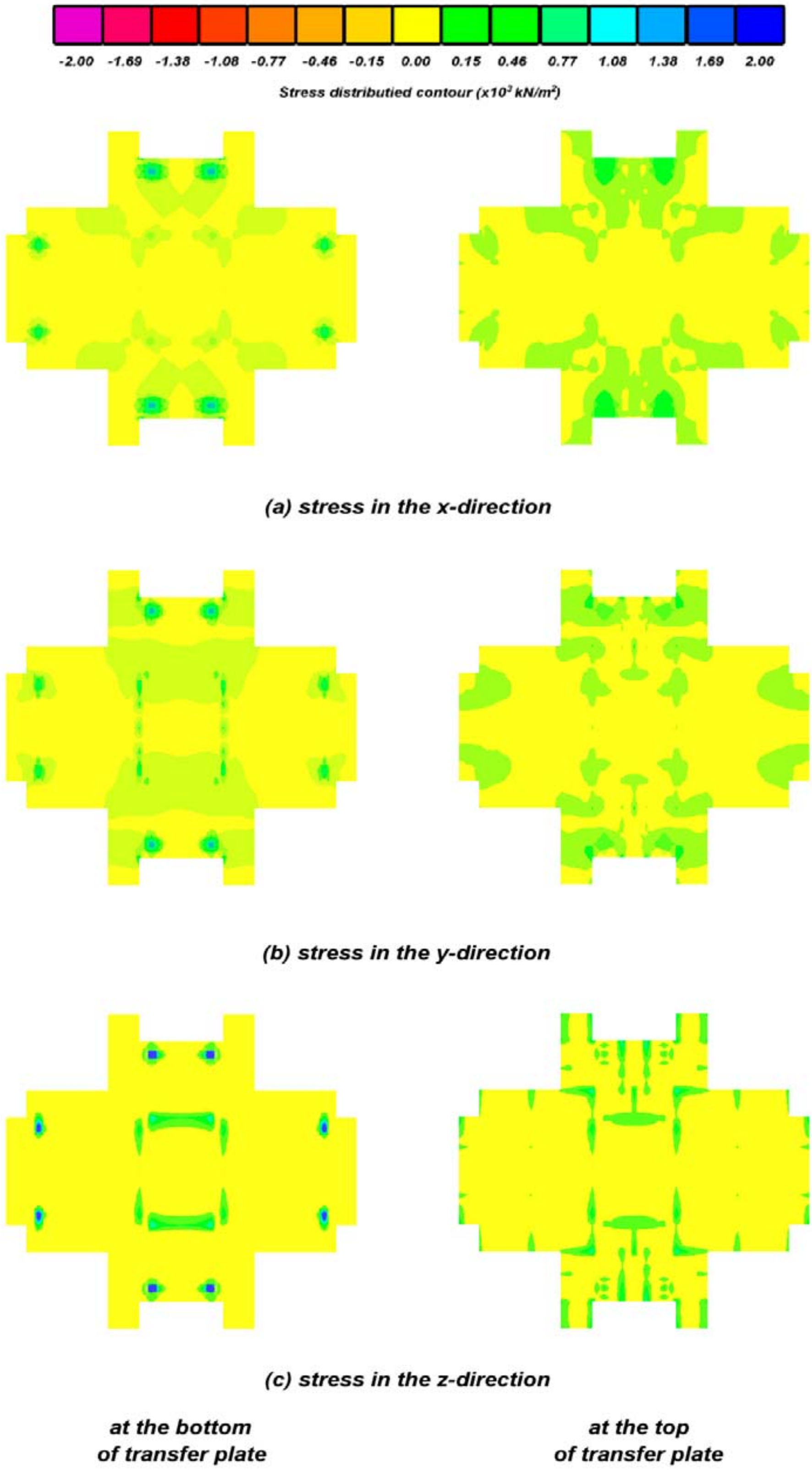

Figure 5.21 Stress distribution on the transfer plate when the high-rise building with a transfer plate subjected to an earthquake attacks in the y-direction.

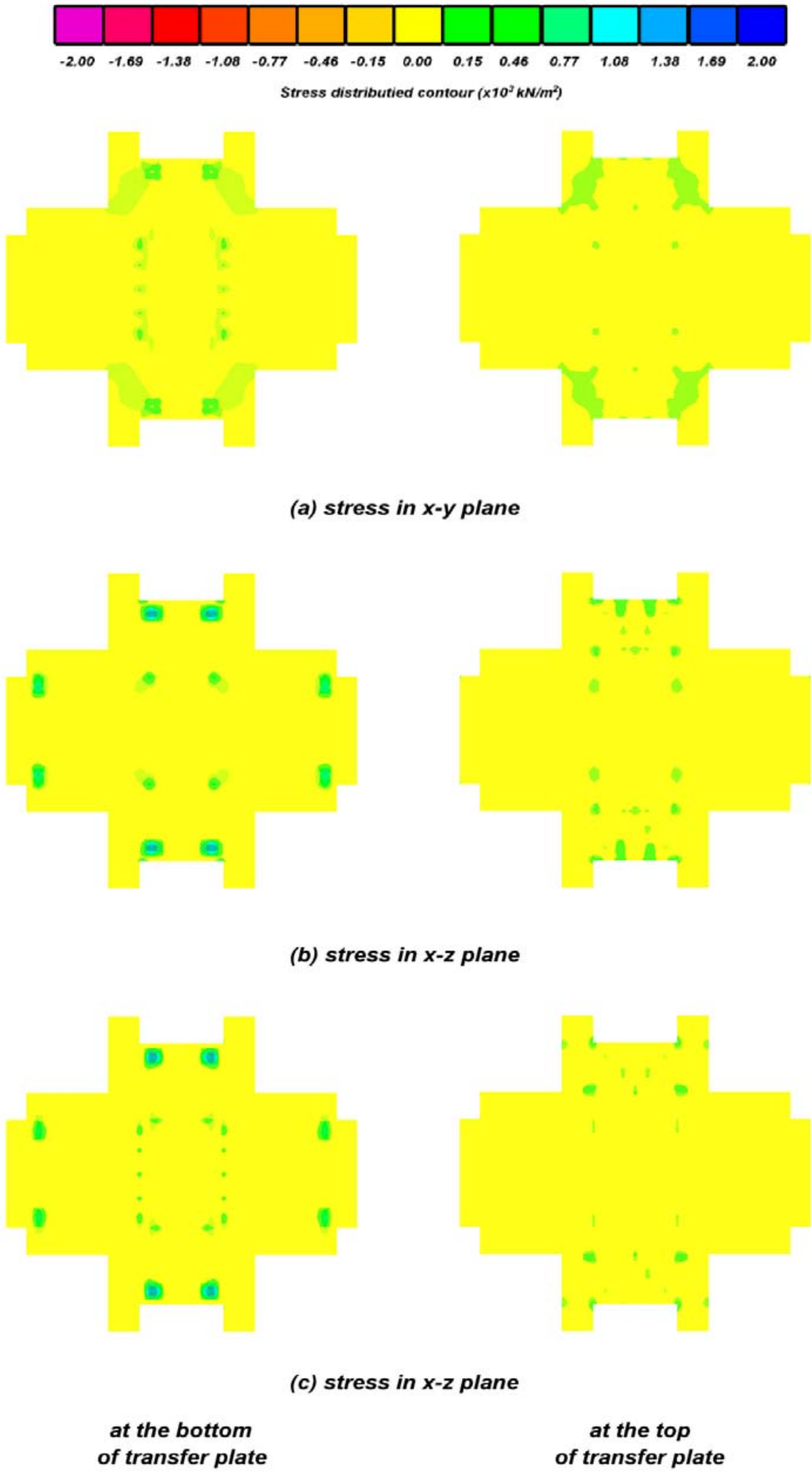

Figure 5.22 Shear stress distribution on the transfer plate when the high-rise building with a transfer plate subjected to an earthquake attacks in the y-direction.

6 SHAKING TABLE TEST OF A HIGH-RISE BUILDING WITH TRANSFER

Numerical analysis and experimental studies are the two main approaches used to predict and understand the behaviour of structures. Both approaches have been developed rapidly through advances in computer technology and modern test equipment. Numerical methods, especially the finite element method, have been successfully used with a supercomputer to solve engineering problems. For highly complex structures, it is impossible to accurately reflect the behaviour by accurately modelling all factors which have an influence. In those situations, experimental studies are often used to simulate the behaviour and to test analytical predictions.

Shaking table tests are one of the most commonly used approaches to assess the seismic resistance of reinforced concrete structures. Lu (1995) and Elwood (2001) carried out shaking table tests on large-scale reinforced concrete column specimens. Blondet *et al* (1980) and Lee and Woo (2002) applied the technique to examine the response of reinforced concrete frames. Lu *et al* (1998) fabricated a 1:25 scale high-rise building model for the Guangzhou Tianwang Building with 49 floors and 3 basements. The building model was tested on a shaking table. Similar studies have also been carried out on a 1:32 scale model of a 54-storey super high-rise tube-in-tube structure with a transfer storey (Huang *et al* 2002).

It is the objective of this study to assess the seismic performance of a high-rise building with a transfer plate designed to non-seismic resistance requirements (Lam *et al* 2002). With the support of the Hong Kong Housing Authority, one of its typical residential blocks has been selected and fabricated at 1:20 scale. Experimental shaking table tests were conducted in January 2001 using the 25 tons, 5 m by 5 m and 6 degrees-of-freedom shaking table installed in the Laboratory of Earthquake and Engineering Vibration of the Institute of Engineering Mechanics, China Seismology Bureau in Harbin. This chapter reports results of the shaking table tests and seismic resistance of the building model when subjected to various levels of seismic attacks.

Six numerical models were developed using the commercial package, ETABS version 6.22. The purposes of the numerical studies are to verify the experimental results obtained from the shaking table tests and to recommend a practical means to represent possible damage in model form.

6.1 THE PROTOTYPE BUILDING

As shown in Figure 6.1, the prototype building for this study is a high-rise residential building, and representative of much of the building stock in Hong Kong. It is a reinforced concrete structure designed to BS8110:1985 and has 34 typical floors supported by a transfer plate and a 3-level podium. Loadings of the prototype building follow the Hong Kong Building (Construction) Regulations. Structural details and characteristic loads are given in Table 6.1. Characteristic strength of concrete for structural members is 35 MPa. The total dead load and total imposed load (including finishes) of the prototype building are 449,330 kN and 127,934 kN respectively.

A numerical model was developed using the commercial package, ETABS version 6.22, to estimate the change in stiffness due to the transfer plate. The ETABS model was constructed based on 1:20 scale as shown in Figure 6.5. Firstly, lateral stiffness at the level of transfer (K_t) and that at the 4^{th} floor level (K_4) were estimated. The change in lateral stiffness is simply K_t/K_4. Lateral stiffness at the level of transfer is estimated and described in Section 5.1. Table 6.2 is a compilation of the ratios of lateral stiffness. Here, ratio of lateral stiffness is defined as the ratio of lateral stiffness of the floor to the lateral stiffness of the floor above. The reduction in lateral stiffness at the transfer plate is substantial, and the transfer level is generally classified as a soft-storey level.

6.2 SIMILITUDE LAW

Because of limited headroom in the Laboratory, the model was designed to 1:20 scale, i.e. a length ratio (L_r) of 0.05. Plan and elevation of the 1:20 scale model are shown in Figure 6.2. Total height of the model is 6.515m excluding the base plate. The definition of x- and y- directions of the model are shown in Figure 6.4. Figure 6.3 shows the reinforcement details of the model.

The 1:20 scale model was fabricated using micro-concrete. The characteristic strength of the micro-concrete used in this study is 2.5 MPa. Thus, the Modulus of Elasticity of the model is different from that of the prototype building. Table 6.3 provides the modulus ratios (E_r) at different levels of compressive stress (Zhang, 1997). Since the majority of the members in the model will be subjected to moderate levels of compressive stress. The modulus ratio is assumed to be 0.177 at all levels of stress.

Another important parameter needed in defining the similitude law is the amount of artificial mass to be added to the model. The mass scale factor obtained from an ideal Similitude Law is in the form of (Mirza *et al* 1979)

$$\frac{(m_m)_{total}}{(m_p)_{total}} = E_r l_r^2 \tag{6.1}$$

$(m_m)_{total}$ is the total mass of the model (including self-weight and artificial mass) and $(m_p)_{total}$ is the total mass of the prototype building (including dead load, finishes and imposed load). Using equation (6.1), the artificial mass to be added to the model is 20.65 tons. In considering the limited free-space at each and every floor of the model, the maximum amount of steel bars and steel plates that could be inserted in all the floors was only 15 tons. Therefore, the mass simulation law was only approximately satisfied based on the following equation.

$$\frac{(m_m)_{approx}}{(m_p)_{approx}} = \rho_r l_r^3 \tag{6.2}$$

$(m_m)_{approx}$ is the total mass of the model (including self-weight and 15 tons artificial mass), $(m_p)_{approx}$ is the total mass of the prototype building (including dead load, finishes and imposed load) and ρ_r is the equivalent mass density ratio. Since, the equivalent mass density ratio (ρ_r) is not equal to E_r/l_r, scale factors for time (t_r), acceleration (a_r) and frequency (ω_r) were adjusted to take into account the effect of the equivalent mass density ratio.

Time: $$t_r = l_r\sqrt{\frac{\rho_r}{E_r}} \tag{6.3}$$

Frequency: $$\omega_r = \left(\sqrt{\frac{E_r}{\rho_r}}\right)/l_r \tag{6.4}$$

Acceleration: $$a_r = \frac{E_r}{l_r\rho_r} \tag{6.5}$$

The main parameters used in defining the Similitude Law for all the shaking table tests conducted in this study are summarized in Table 6.4. Note that the artificial mass used in all the shaking table tests was 14.56 tons.

6.3 TESTING PROCEDURE OF THE SHAKING TABLE TEST

Shaking table tests were conducted in 5 consecutive stages with increasing magnitudes of earthquake excitation. Four levels of earthquake were considered including minor, moderate, strong and super-strong earthquakes. In each level of earthquake, there is a set of three earthquake records representing (a) rock site; (b) medium soil site; and (c) soft soil site. Maximum accelerations of the various seismic records were appropriately magnified to reflect different levels of earthquake attack.

Earthquake records to be generated by the shaking table were based on existing acceleration records. For instance the NS component of the 1940 El Centro earthquake, with the peak accelerations appropriately reduced/increased. The Similitude Law (Table 6.4) was used to scale the acceleration and time. Peak accelerations of the earthquake excitations generated by the shaking table are listed in Table 6.5. In particular, strong earthquake excitations are targeted for a VIIth degree earthquake with a 2~3% probability of occurrence over a 50 years return period. Predominant periods of the three types of earthquake records are shown in Table 6.7. Figure 6.7 shows the respective earthquake records and response spectra for strong earthquake excitations. It is worth noting that as far as the frequency content is concerned, the shaking table can reproduce the dynamic characteristics of medium soil site earthquake and soft soil site earthquake with reasonable accuracy, but not for rock site earthquake.

The sequence of the shaking table tests is summarized in Table 6.7. Stage 0 is the control test with the objective of quantifying the dynamic characteristic of the model. Stages 1 to 4 are the respective tests for four different levels of earthquake excitations including minor, moderate, strong and super-strong earthquakes. There are altogether 29 different tests involving 18 shaking table tests, 6 modal tests to estimate the fundamental frequencies and mode shapes of the model, and 5 tests for damage detection.

Measurements obtained from the shaking table tests include accelerations, displacements and strains. 49 accelerometers (14 SLJ strong motion accelerometers and 35 SLJ - 200 micro - vibration accelerometers), 18 displacement transducers (8 transducers for absolute displacement, 4 transducers for relative displacement and 6 laser transducers) and 76 strain gauges were installed. The accelerometers were accurately orientated to record the accelerations in the x- or y-direction. Modal tests were carried out by applying white noise excitation to the test model.

6.4 EXPERIMENTAL RESULTS

6.4.1 OBSERVATIONS

Table 6.8 summarizes the structural damage observed from the model at various levels of earthquake excitations.

When subjected to minor earthquakes, there was no noticeable shaking and no structural damage was observed. Based on the responses of the model, it is predicted that the prototype building will remain in serviceable condition after minor earthquake attacks and there will not be any need for structural repair.

When subjected to moderate earthquakes, the model responded with small amount of vibrations. Cracks were found on the end walls between the 4th and 8th floor. It is predicted that the prototype building will still be in serviceable condition. Although it is not necessary to strengthen the prototype building, some of the structural members will have to be repaired.

In the case of strong earthquake excitations, the model vibrated significantly. A large number of cracks was observed at the middle and upper storeys (i.e. at storeys above the transfer plate). Diagonal cracks appeared at the periphery openings of the central core at the middle storeys. Notwithstanding that there was no spalling of concrete, the model was severely damaged and the responses involved considerable inelastic behaviour. It is predicted that the prototype building will not collapse after strong earthquake attacks, but will lose most of its load-carrying capacity. It will be in need of substantial retrofitting work.

When subjected to a soft soil site super-strong earthquake, the structural integrity of the model was destroyed with the upper part of the model broken off and separated from the podium at the transfer level. The main cause is a tensile failure of the south-end shear walls at the vicinity just above the transfer plate. Many structural members were severely damaged. A horizontal crack was found cutting the shear walls into two-halves at the 4th and the 10th floor (see Figure 6.7). There was substantial spalling of concrete and buckling of main reinforcement. Shear failures were also observed at the interior walls with spalling of concrete. Horizontal cracks appeared on the surfaces of the floor slabs at all storeys. In general, the model was severely damaged, beyond repair, and on the verge of collapsing.

6.4.2 FUNDAMENTAL FREQUENCIES

After each series of earthquake excitations, modal tests were carried out. Ambient vibrations in the form of sine-wave type excitation and white noise excitation were generated through a small electromagnetic exciter. Signals were recorded by micro-vibration accelerometers installed on the model at two mutually perpendicular directions. In Table 6.9 are compiled the natural frequencies estimated subsequently by spectral analysis. The first three mode shapes of the model at the initial state ("perfect model") and after super-strong earthquake attack are shown in Figure 6.8 for x- and y-directions.

As an alternative, Fast Fourier Transform (FFT) analysis has been carried out on the data obtained from the accelerometers to determine the fundamental frequencies. The results are compiled in Table 6.10. Using the time-history data, the dynamic characteristics so obtained will include the inelastic behaviour of the damaged model. As shown in Tables 6.10 and 6.11, frequencies estimated based on ambient vibration are different from that obtained from the time-history data. Since the modal tests were based on ambient vibration, the frequencies only reflect the dynamic characteristics of the model under an elastic response. However, it is still possible to identify structural damage by carrying out the modal tests.

From Table 6.10, under minor earthquake excitations, the model remained elastic when subject to rock or medium soil site earthquake attacks. In the case of a soft soil site earthquake, the first frequency was reduced from 4.4 Hz to 4.2 Hz. Since the frequency returned to 4.4 Hz in subsequent moderate earthquake excitation, the model was only slightly damaged. Under moderate earthquake excitations, the fundamental frequency of the model after soft soil site earthquake attack was reduced from 4.2 Hz to 3.8 Hz and it did not return to 4.4 Hz in subsequent tests. Some of the structural members were damaged and the model started to respond in-elastically. Under strong earthquake excitations, the reduction in frequency for the soft soil site case was greater that those for the rock and medium soil site cases. This confirms that most of the damage was caused by the soft soil site earthquake action.

6.4.3 ACCELERATION RESPONSES

Figure 6.9 plots the accelerations against time at various floors for different levels of soft soil site earthquake excitations. Characteristics of the accelerations at the floors are basically the same as for the respective earthquake excitation. As shown in Table 6.11, spectra frequencies (estimated based on carrying out FFT on acceleration data) of the model were reduced in subsequent earthquake excitations. After minor and moderate earthquake excitations, spectra frequencies were reduced by about 10%. This indicates that some of the structural members were damaged, but the model was still in serviceable condition. Under strong earthquake excitations, spectra frequencies were reduced by about 25% at the typical floors and 35% at and below the podium. More structural members were damaged. After super-strong excitations, spectra frequencies were reduced by about 60% in the x-direction and 45% in the y-direction. Spectra frequencies at transfer were reduced by about 40% in the x-direction and 30% in the y-direction. The significant reduction in the spectra frequencies indicates that structural integrity was seriously impaired at the level above the transfer plate. This agrees well with the experimental observations in that the main damage occurred at the level above the transfer plate.

6.4.4 STOREY DRIFTS

As shown in Figure 6.10, storey drift is defined as the storey deflection divided by the storey height. In this study, displacement transducers were installed at some of the floors. Therefore, storey drifts were estimated based on the average drift angle of several consecutive floors (i.e. by taking the difference between the two lateral displacements and divided by the vertical distance between the two measurement points). Table 6.12 shows the maximum storey drifts when the model was subjected to soft soil site earthquakes. Largest storey drifts occurred at the storeys above the transfer and at the upper storeys. Figure 6.11 shows the response of the model against time at the transfer plate level (i.e. 4th floor level) and at the roof for various types of earthquake attacks. There is a relatively small increase in the storey drift with progressive increase in the magnitude of the earthquake excitation at the floors below the transfer plate (i.e. Ground floor level to 4th floor level) as compared with the upper storeys. This indicates that the damage is concentrated at the upper floors. The model was severely damaged when subjected to super-strong earthquake excitations. As shown, failure occurred in the x-direction and at the level above the transfer plate.

The correlations between the observed damage at various levels of earthquake excitations and storey drifts estimated from the displacement measurements are compiled in Table 6.13. It clearly indicates that there is a strong connection between the deformation in terms of storey drift and the extent of structural damage, and that the storey drift is a useful indicator to provide some insight on the location of structural damage.

6.4.5 STIFFNESS

Consider the equation of motion of a single degree-of-freedom system in the form of

$$M\ddot{u} + Ku = 0 \tag{6.6}$$

The incremental form of equation (6.6) can be expressed as

$$M\Delta\ddot{u} + K\Delta u = 0 \tag{6.7}$$

or

$$K = \frac{M\Delta\ddot{u}}{\Delta u} \qquad (6.8)$$

Therefore, plots of acceleration against displacement can be a good indicator of possible changes in stiffness of the model and hence inelastic behaviour or damage. These are now shown in Figure 6.12 at the 4th floor level, 21st floor level and Roof. There is relatively no change in stiffness at the floors below the transfer plate (i.e. Ground floor level to 4th floor level) when subjected to the minor, moderate, strong and super-strong earthquakes. However, under super-strong earthquakes, there are considerable changes in the stiffness at the 21st floor level and the roof. This indicates that structural damage was mainly concentrated at the upper floors and collapse occurred above the transfer plate. Furthermore, the reduction in stiffness at the level above the transfer plate is more serious in the x-direction than in the y-direction.

6.5 NUMERICAL MODELS

The various ETABS models using the advanced simplified un-coupled approach were constructed based on the prototype building, i.e. in full scale. Figure 6.13

shows the ETABS model on plan at a typical floor, and Figure 6.14 shows an elevation of the ETABS model (with external façade included). The modelling techniques implemented in the ETABS models and the underlying assumptions are as follows.

1. Dimensions were defined along centrelines of the elements.
2. Boundary conditions at foundation level were assumed to have a fixed condition.
3. Floor slabs were considered to be rigid in their plane, and rigid diaphragm action was assumed.
4. All the shear walls and core walls were modelled by “PANEL” elements or “COLUMN” elements. If the height/length ratio of a wall is less than 1.5, it was represented by a “PANEL”. Vice versa, it was modelled by a “COLUMN”.
5. The transfer plate was assumed to be a rigid diaphragm. Nodal points of the columns below and walls above the transfer plate were connected by “artificial beams” of apparent stiffness, see Figure 6.15. In this study, the “artificial beams” were assumed to be 2750 mm deep by 1000 mm in width.

6. Lintel beams were modelled using “BEAM” elements, and columns by “COLUMN” elements.
7. Distributed loadings were assumed concentrated and acting on each floor.

In total, six different ETABS models were developed. Characteristics of the ETABS models are summarized in Table 6.14.

Brief descriptions of the various models are as follows.

<u>Model E-C</u> represents a prototype building without external façade. The Modulus of Elasticity was assumed to be uniform throughout the building height, and $E = 1.50 \times 10^7$ kN/m^2.

<u>Model E-C-P</u> is similar to Model E-C, except that the external façades were modelled using panel elements without any opening. The Modulus of Elasticity was assumed to be uniform throughout the building height, and $E = 1.50 \times 10^7$ kN/m^2. The purpose of the model is to estimate the increase in stiffness due to the incorporation of the external façades.

Model E-V-B is similar to model E-C-B, except that Modulus of Elasticity used in the model varies according to the material data as shown in Table 6.15. The E-values used in Model E-V-B are compiled in Table 6.15.

Unlike Models E-C-B and E-C-P, external façades were modelled using “PANEL” elements and “BEAM” elements. Furthermore, window openings were allowed in the model.

6.6 STIFFNESS REDUCTION AT TRANSFER LEVEL

One of the ETABS models, Model E-C, has also been used to estimate the ratio in lateral stiffness at the transfer plate level. Firstly, lateral stiffness at the level of transfer (K_t) and that at the 4/F (K_4) were estimated. The ratio in lateral stiffness is simply K_t/K_4. Lateral stiffness at the level of transfer is estimated and the detailed information is given in Section 5.1. Results of the estimation of lateral stiffness are shown in Table 6.16. Two conditions are considered, namely excluding and including the stiffness of the external façade in the estimations.

In Table 6.17 are compiled the various ratios of lateral stiffness based on the estimations. Here, ratio of lateral stiffness is defined as the ratio of lateral stiffness of the floor to the lateral stiffness of the floor above. The reduction in stiffness due to the transfer is substantial. Since the ratio of lateral stiffness at the transfer plate level is less than 70%, the transfer level is generally classified as a soft-storey level.

The increase in stiffness due to the incorporation of the stiffness of the external façade into the model is insignificant. There is only about 7% and 3% increase in stiffness in the x- and y-direction respectively.

6.7 RESULTS OF LINEAR ANALYSES

6.7.1 FUNDAMENTAL FREQUENCIES AND MODE SHAPES

The high-rise building under consideration is asymmetric on plan. Except for the first few modes of vibration, higher order modes of vibration consist of a combination of translational and rotational displacements. Therefore, not less than 30 modes of vibration have been estimated in each of the numerical analyses to determine the first three fundamental frequencies.

Tables 6.18 to 6.21 compare the fundamental frequencies of the test model before the shaking table tests. Based on the comparison, the Modulus of Elasticity of the numerical model was appropriately adjusted to 17 kN/mm^2, and was assumed to be uniform throughout the height of the model. Maximum errors are within 15% for a building model with artificial mass and 30% for a building model without artificial mass. Firstly, errors are deduced from Model E-C-P, E-C-B and EV-B in that order. Secondly, fundamental frequencies estimated by Model E-C-B and E-V-B errors are within 3% difference. It is not necessary to vary the Modulus of Elasticity from floor to floor. Therefore, Model E-C-B will be used in the time-history analysis.

Figures 6.16 and 6.17 compare the first three mode shapes of the building estimated by Model E-C-P, E-C-B and EV-B with those obtained from the shaking table tests. The numerical results generally agree with the experimental data. In the x-direction, the first two mode shapes are the same as those obtained from the shaking table tests. Relatively larger discrepancies between the numerical and experimental data are observed at the third mode. Similar conclusions are obtained when comparing the results in the y-direction. Notice that larger errors occur above the transfer plate.

This is probably due to structural damage leading to substantial change in the material property used in the experimental model.

6.8 RESULTS OF NONLINEAR LINEAR ANALYSES

6.8.1 NONLINEAR ANALYSIS

Accurate and realistic prediction of nonlinear behaviour of the building may be achieved by performing a complete nonlinear analysis, for instance using DRAIN (Prakash 1992) and RUAUMOKO (Carr 1998). This is impractical as far as high-rise buildings are concerned. As an alternative, a simplified method of analysis was adopted following the principle recommended by Paulay and Priestley (1992). Nonlinear behaviour can be approximated through a series of linear time-history analyses. A step by step procedures of simplified non-linear analysis is shown in Figure 6.18. On completion of a linear time-history analysis, applied moments of all the structural members (including beams, columns and shear walls) were compared with the respective moment capacities. Member capacities were calculated according to BS8110:1985. Flexural stiffness of a damaged member was reduced according to the values as shown in Table 6.22.

Here, EI is the estimated flexural stiffness based on the gross sectional area of the member. After adjusting all the stiffnesses, another time-history analysis was conducted. The process of checking the member moment capacities was repeated. The linear time-history analyses continued until no new damage was found in the structural members.

In this study, two series of linear time-history analyses were performed to estimate the damage under strong and super-strong earthquake attacks. Soft-soil site earthquake data generated from the shaking table was used in the analyses. In simulating the response when subject to strong earthquake attacks, the analysis was completed after 7 consecutive time-history analyses. In the case of super-strong earthquake attacks, 14 time-history analyses were required.

Table 6.23 compares the first three fundamental frequencies estimated numerically with those obtained from the shaking table tests. In the case of strong earthquake attack, the frequencies are in good agreement. In the case of super-strong earthquake attack, frequencies of the higher order modes are in good agreement. However, there is about 30% difference at the first mode of vibration. The discrepancy is due to some degree of inability of the numerical model to represent a structural form in the vicinity of collapsing.

6.8.2 STRUCTURAL DAMAGE

Figures 6.19 to 6.22 show the damage estimated by the Model E-C-B-S representing the condition after strong earthquake attacks. Figures 6.23 to 6.26 show the extent of damage predicted numerically with those obtained from the shaking table tests after super-strong earthquake attacks. Below the transfer plate, columns and beams were not damaged when the building was under going either the strong or super strong earthquake actions. The core-wall was damaged due to shear. Nevertheless, damage occurred in walls and core-wall systems at the typical floor levels. Most beams were damaged due to bending.

Structural damage observed from the testing model at various levels of earthquake excitations are represented through changing the material behaviour. Detailed description is given in section 6.4.1. The non-linear behaviour of the testing model is approximated through a series of linear time-history analyses. Structural damage predicted from the numerical models is compared with the observation from tests. The numerical model using the simplified non-linear analysis can predict the first occurrence of damage on a high-rise building with a transfer plate.

The numerical model has successfully indicated that most of the damage occurs at the storey above the transfer plate. This is also the principal mode of failure observed from the shaking table tests as shown in Figure 6.27. The numerical model also provides reasonable predictions on the locations that are particularly vulnerable to earthquake attack.

Table 6.24 summarised the numerical analysis results of the lateral stiffness of the storeys which were used to estimate the lateral stiffness ratio at the transfer plate. After the actions of the strong and super-strong earthquake records were considered in the high-rise building with a transfer plate, the lateral stiffnesses of the storeys were reduced because of the damage to the structural elements in the building. Because of the damage at the end walls at the south of the model, the large reduction of the lateral stiffness at the 4/F in the x-direction is considerable. The ratio in lateral stiffness ratio at the transfer plate is less significant as an indication of the damage level of the building.

6.8.3 STOREY DRIFTS

In the shaking table tests, displacement transducers were installed at some of the floors. Therefore, storey drifts are estimated based on the average drift angle of several consecutive floors (i.e. by taking the difference between the two lateral displacements divided by the vertical distance between the two measurement points). Table 6.25 compares the storey drifts estimated from the numerical analysis with the test data. "Error ratio" is defined as the storey drift obtained from the shaking table test divided by the corresponding numerical estimation.

Better agreements are obtained at the storeys above the transfer. The numerical model has underestimated the damage below the transfer plate. Due to the inherent limitations of the simplified method of analysis, the analysis has neglected any plastic deformation accumulated during the hysteresis behaviour. As a result, the predicted values are smaller than the actual displacements. A modification factor μ is introduced, such that the actual storey drift will be the storey drift predicted by the numerical model multiplied by the modification factor μ. Typical values of μ are given in Table 6.26.

To determine whether the structure is in the vicinity of collapsing, the members are considered as severely damaged. Modification factor μ=2 is assumed to estimate the "actual" storey drifts. If the "actual" storey drift of a member is greater than the drift capacity, that member will be assumed close to failure and μ=4 is applied. If such a condition exists in a considerable proportion of the damaged members, the structure will be assumed to be close to collapse and μ=4 will be applied to all the storey drifts.

6.9 CONCLUDING SUMMARY

Based on the results obtained from the shaking table tests, it is predicted that the high-rise building will not collapse when subjected to strong earthquake action. Most of the damage is caused by ground motion with the longest predominant period of vibration, such as that corresponding to a soft soil site or from a distant earthquake event. Notwithstanding there is significant reduction in the lateral stiffness at the transfer plate (up to 76% reduction), the main damage and failure occurs at the storey above the transfer plate. The use of the ratio of lateral stiffness to check the existence of a soft storey may not be appropriate for high-rise buildings. To minimize damage, it is desirable to strengthen the walls between the 4th floor level and 15th floor level as well as reducing any change in stiffness at the transfer zone.

A good indication of the degree of damage to the building would be provided by determining the frequency of the acceleration spectra using a FFT method. In a structural system, severe damage would occur if the spectra frequency is reduced by about 40% from that frequency estimated in the un-damped model and would collapse if the spectra frequency is reduced by about 60%.

Deformation measurements are able to provide good indication of damage. In particularly, storey drift relates well with the degree of structural damage. For a structural system comprising shear walls, slight damage, moderate damage and severe damage would occur if the storey drift approaches 1/1000, in the range of 1/300-1/700, and in the range of 1/80-1/200 respectively.

Shaking table tests were conducted on a 1/20-scale model to assess the seismic performance of a typical high-rise residential building with a transfer plate. This study reports the use of simplified numerical models using advanced simplified un-coupled approach to predict the damage and seismic performance. Nonlinear behaviour is approximated through a series of linear time-history analyses. Inelastic behaviour is taken into account by reducing the stiffness of damaged members. It is possible to reasonably predict the extent and locations of damage through such a simple procedure. The estimated displacements and storey drifts were smaller than those obtained from the shaking table tests. For members that are severely damaged or in the vicinity of failure, actual storey drifts will be about 2 and 4 times the estimated values. Such modification factors should be accordingly applied to the calculated results.

Table 6.1 Structural detail and characteristic loads of the prototype building.

Floor level	Structural system	Structural detail	% reinforcement	Characteristic loads	
				Imposed load (kPa)	Finishes, screeding and ceiling (kPa)
Typical (4/F – 39/F)	Shear walls	200-250 mm thickness	1.5	3.0	0.5
	Core walls	300-350 mm thickness	2.0		
Transfer Plate		2700 mm thickness	1.2	25.8	2.0
Podium (G/F – 3/F)	Column	4 @ 1400x1300 mm 8 @ 1400x2000 mm 20 @ 600x900 mm	5.0	4.0	2.0
	Core walls	1000 mm thickness	2.0		

Table 6.2 Lateral stiffness ($\times 10^6$ kN/m) at and above the transfer.

	Floor level	x-direction	y-direction
Lateral stiffnesses (kN/m)	4/F	2.524	2.116
	Transfer	0.905	0.497
Ratio of lateral stiffness K_t/K_4		0.402	0.235

Table 6.3 Modulus ratio between micro-concrete (2.5 MPa) and prototype concrete (40 MPa).

R	0.1-0.7	0.8	0.9	1.0
Modulus ratio Er	0.177	0.176	0.175	0.169

$$E_r = \frac{\text{Elastic modulus of the micro-concrete}}{\text{Elastic modulus of prototype concrete}}$$

$$R = \frac{\text{Compressive stress in the micro-concrete}}{\text{Compressive strength of the micro-concrete}}$$

Table 6.4 Similitude Law.

Basic parameters	Ideal Similitude Law (Equation 6.1)	Approximate Similitude Law (Equation 6.2)
Length ratio L_r	0.050	0.050
Modulus ratio E_r	0.177	0.177
Equivalent density ratio ρ_r	3.540	3.541
Time ratio t_r	0.224	0.224
Frequency ratio ω_r	4.472	4.472
Acceleration ratio a_r	1.000	1.000

Table 6.5 Earthquake records.

Earthquake	Acceleration	Direction of Excitation
Minor	0.02-0.06g	Uni-directional and bi-directional
Moderate	0.08-0.14g	Bi-directional
Strong	0.15-0.20g	Bi-directional
Super-strong	0.25-0.34g	Bi-directional

Table 6.6 Predominant periods of vibration of earthquake records.

Predominant periods	Characteristic of soil sites		
	Rock site	Medium soil site	Soft soil site
Input earthquake record	0.100s	0.330s	1.430s
After compression (Table 6.4)	0.022s	0.074s	0.320s
Generated by the shaking table	0.125s	0.125s	0.301s

Table 6.7 Sequence of the shaking table tests.

Type of tests	Test no	Detail
Stage 0 – Control tests		
Model tests	1	Frequencies and mode shapes measurement without artificial mass
	2	Frequencies and mode shapes measurement with artificial mass
Damage detection	3	Excitation under white noise signals
Stage 1 – Minor earthquake excitation tests		
Shaking table tests	4-6	Bi-directional excitation for a set of 3 earthquake records
	7-8	Unidirectional excitation (rock site) in the x- and y- directions
	9-10	Unidirectional excitation (medium soil site) in the x- and y- directions
	11-12	Unidirectional excitation (soft soil site) in the x- and y- directions
Modal tests	13	Frequencies and mode shapes measurement
Damage detection	14	Excitation under white noise signals
Stage 2 – Moderate earthquake excitation tests		
Shaking table tests	15-17	Bi-directional excitation for a set of 3 earthquake records
Modal tests	18	Frequencies and mode shapes measurement
Damage detection	19	Excitation under white noise signals
Stage 3 – Strong earthquake excitation tests		
Shaking table tests	20-22	Bi-directional excitation for a set of 3 earthquake records
Modal tests	23	Frequencies and mode shapes measurement
Damage detection	24	Excitation under white noise signals
Stage 4 – Super-strong earthquake excitation tests		
Shaking table tests	25-27	Bi-directional excitation for a set of 3 earthquake records
Modal tests	28	Frequencies and mode shapes measurement
Damage detection	29	Excitation under white noise signals

Table 6.8 Observed damage.

Earthquake	Observations and types of damage	Condition
Minor	No noticeable shaking, and some small cracks barely noticeable	Serviceable condition
Moderate	Observable vibrations and 8 new cracks at storeys above the transfer	Serviceable condition
Strong	Significant vibrations and 56 new cracks at storey above the transfer and at middle and upper storeys	Moderately damaged, no collapse and requiring repair
Super-strong	Structural integrity was destroyed at level right above the transfer	Collapse

Table 6.9 Frequencies estimated from ambient vibration measurements (Hz).

Earthquake action	Natural frequencies in the x-direction			Natural frequencies in the y-direction		
	1st mode	2nd mode	3rd mode	1st mode	2nd mode	3rd mode
Initial stage – control	4.40	15.04	35.60	4.72	15.80	36.00
After minor earthquakes	4.40	14.40	34.80	4.80	15.60	35.20
After moderate earthquakes	4.20	14.00	33.80	4.40	15.00	34.20
After major earthquakes	3.60	13.60	32.20	4.00	14.40	31.00
After super-major earthquakes	2.40	11.60	27.20	2.94	12.60	27.10

Table 6.10 Frequencies estimated by FFT method (Hz).

Earthquake action	1st mode of vibration in the x-direction		
	Rock site	Medium soil site	Soft soil site
Minor earthquake	4. 4	4. 4	4. 2
Moderate earthquake	4. 4	4. 4	3. 8
Strong earthquake	3. 8	3. 8	3. 1

Table 6.11 Spectra frequencies estimated by FFT method (Hz).

Direction	Earthquake	Frequency (Hz)				
		Transfer	10/F	21/F	30F	39/F
X	Minor	3.80	3.80	3.80	3.80	3.80
	Moderate	3.38	3.38	3.38	3.38	3.38
	Strong	2.41	2.82	2.82	2.82	2.82
	Super-strong	2.26	1.58	1.58	1.58	1.58
Y	Minor	3.33	3.33	4.10	4.10	4.10
	Moderate	3.40	3.40	3.79	3.40	3.79
	Strong	2.27	2.27	3.22	3.22	3.22
	Super-strong	2.24	2.24	2.25	2.25	2.25

Table 6.12 Maximum storey drifts for soft soil site earthquakes.

Drift direction	Earthquake type	G/F to 4/F	4/F to 21/F	21/F to Roof	G/F to Roof
X	Moderate	1/670	1/1100	1/980	1/1220
	Strong	1/550	1/320	1/290	1/350
	Super-strong	1/460	1/80	1/80	1/100
Y	Moderate	1/950	1/1260	1/1200	1/1540
	Strong	1/500	1/580	1/680	1/670
	Super-strong	1/320	1/190	1/250	1/250

Table 6.13 Relationship between structural damage and storey drift.

Description of structural damage	Storey drift
Small cracks on columns in frames	1/1000 - 1/1300
A few number of small cracks on shear walls	1/1100 - 1/1200
Many through-cracks on shear walls	1/300 - 1/700
Shear walls damaged with concrete crushed and reinforcement exposed	1/80- 1/200

Table 6.14 Description of the ETABS models.

<table>
<tr><th>Model no</th><th>Model name</th><th>External façade</th><th>E value at floors</th><th>Extent of damage</th></tr>
<tr><td>1</td><td>E-C</td><td>Excluded</td><td rowspan="3">Uniform</td><td rowspan="4">No damage</td></tr>
<tr><td>2</td><td>E-C-P</td><td rowspan="5">Included</td></tr>
<tr><td>3</td><td>E-C-B</td></tr>
<tr><td>4</td><td>E-V-B</td><td>Varying</td></tr>
<tr><td>5</td><td>E-C-B-S</td><td rowspan="2">Uniform</td><td>Strong damaged</td></tr>
<tr><td>6</td><td>E-C-B-SS</td><td>Super-Strong damaged</td></tr>
</table>

Table 6.15 Modulus of Elasticity (kN/m^2) used in Model E-V-B.

LEVEL	E ($\times 10^7$ kN/m2)
36/F-38/F	1.49
33/F-35/F	1.62
29/F-32/F	1.86
26/F-28/F	1.49
21/F-25/F	1.62
17/F-20/F	1.74
13/F-16/F	1.49
9/F-12/F	1.86
7/F-8/F	1.99
4/F-6/F	2.11
TRANSFER	1.86
2/F-3/F	1.86
1/F	1.74

Table 6.16 Estimation on lateral stiffness (kN/m) at and above the transfer.

External Façade	Level	Lateral stiffness($\times 10^6$ kN/m)	
		x-direction	y-direction
Excluding	6/F	2.638	2.396
	5/F	2.638	2.396
	4/F	2.638	2.396
	3/F (Transfer Plate)	0.904	0.496
Including	6/F	2.524	2.116
	5/F	2.524	2.116
	4/F	2.524	2.116
	Transfer	0.905	0.497
	2/F	3.258	2.084

Table 6.17 Ratios of lateral stiffness.

External Façade	Level	Ratio of lateral stiffness	
		x-direction	y-direction
Excluding	3/F (Transfer Plate)	0.343	0.207
Including	4/F	1.000	1.000
	3/F (Transfer Plate)	0.402	0.235
	2/F	3.599	4.197

Table 6.18 First three fundamental frequencies in the x-direction and without artificial mass.

Model no	Model name	Fundamental frequencies (Hz)		
		1^{st} mode	2^{nd} mode	3^{rd} mode
Shaking table tests		7.30	24.60	49.80
1	E-C	7.02	26.07	58.62
2	E-C-P	7.82	28.77	58.29
3	E-C-B	7.49	27.82	55.83
4	E-V-B	7.70	27.84	55.55

Table 6.19 First three fundamental frequencies in the x-direction.

Model no	Model name	Fundamental frequencies (Hz)		
		1st mode	2nd mode	3rd mode
Shaking table tests		4.40	15.04	35.60
1	E-C	3.69	14.20	32.43
2	E-C-P	4.11	15.79	34.12
3	E-C-B	3.94	15.21	33.52
4	E-V-B	4.05	15.35	33.23

Table 6.20 First three fundamental frequencies in the y-direction and without artificial mass.

Model no	Model name	Fundamental frequencies (Hz)		
		1st mode	2nd mode	3rd mode
Shaking table tests		7.80	24.90	24.90
1	E-C	8.49	30.72	42.70
2	E-C-P	9.65	33.65	44.87
3	E-C-B	8.97	32.21	44.22
4	E-V-B	9.19	32.60	43.09

Table 6.21 First three fundamental frequencies in the y-direction.

Model no	Model name	Fundamental frequencies (Hz)		
		1st mode	2nd mode	3rd mode
Shaking table tests		7.80	4.72	15.80
1	E-C	4.43	16.26	30.27
2	E-C-P	5.05	18.18	32.99
3	E-C-B	4.69	17.08	31.71
4	E-V-B	4.81	17.32	31.71

Table 6.22 Reduction on flexural stiffness for damaged members.

Structural member	Damaged stiffness
Beams	0.4EI
Columns	0.7EI
Shear walls	0.7EI

Table 6.23 Fundamental frequencies (Hz) after strong and super-strong earthquakes.

	Mode	Numerical predictions		Test data	
		x-direction	y-direction	x-direction	y-direction
Strong Earthquake	1	3.53	4.30	3.60	4.00
	2	13.75	15.42	13.60	14.40
	3	29.51	28.76	32.20	31.00
Super-Strong Earthquake	1	3.46	4.07	2.40	2.94
	2	13.46	14.72	11.60	12.60
	3	28.94	27.47	27.20	27.10

Table 6.24 Lateral stiffness ($\times 10^7$ kN/m) at and above the transfer.

Level	Undamaged Model (E-C-B)		After Strong Earthquake (E-C-B-S)		After Super-strong Earthquake (E-C-B-SS)	
	Lateral stiffness (x 10^6 kN/m)					
	x-direction	y-direction	x-direction	y-direction	x-direction	y-direction
6/F	2.254	2.116	2.04	1.938	1.924	1.805
5/F	2.254	2.116	2.013	1.936	1.859	1.797
4/F	2.254	2.116	2.011	1.897	1.752	1.73
Transfer	0.9052	0.4966	0.819	0.4467	0.8175	0.4464
P3	3.258	2.084	2.859	1.827	2.858	1.827

Level	Ratio of lateral stiffness					
Transfer	0.402	0.235	0.407	0.235	0.466	0.258

Table 6.25 Storey drifts.

Displacement	Test condition	Data type	G/F to 4/F	4/F to 21/F	21/F to 38/F	G/F to 39/F
Storey drifts in the x-direction	Strong earthquake excitation	Test data	1/550	1/320	1/290	1/350
		Numerical	1/3253	1/706	1/566	1/721
		Error ratio	5.92	2.21	1.95	2.0
	Super-strong earthquake excitation	Test data	1/460	1/80	1/80	1/100
		Numerical	1/1983	1/365	1/315	1/390
		Error ratio	4.31	4.56	3.94	3.90
Storey drifts in the y-direction	Strong earthquake excitation	Test data	1/500	1/580	1/680	1/670
		Numerical	1/2895	1/952	1/1084	1/1135
		Error ratio	5.79	1.64	1.59	1.69
	Super-strong earthquake excitation	Test data	1/320	1/190	1/250	1/250
		Numerical	1/1863	1/515	1/607	1/630
		Error ratio	5.82	2.71	2.43	2.52

Table 6.26 Recommended values for modification factor μ.

Type of damage	Modification factor μ
Severely damaged	2.0
Close to collapse	4.0

(a) High-rise residential development

(b) Transfer plate

Figure 6.1 High-rise residential development with a transfer plate system.

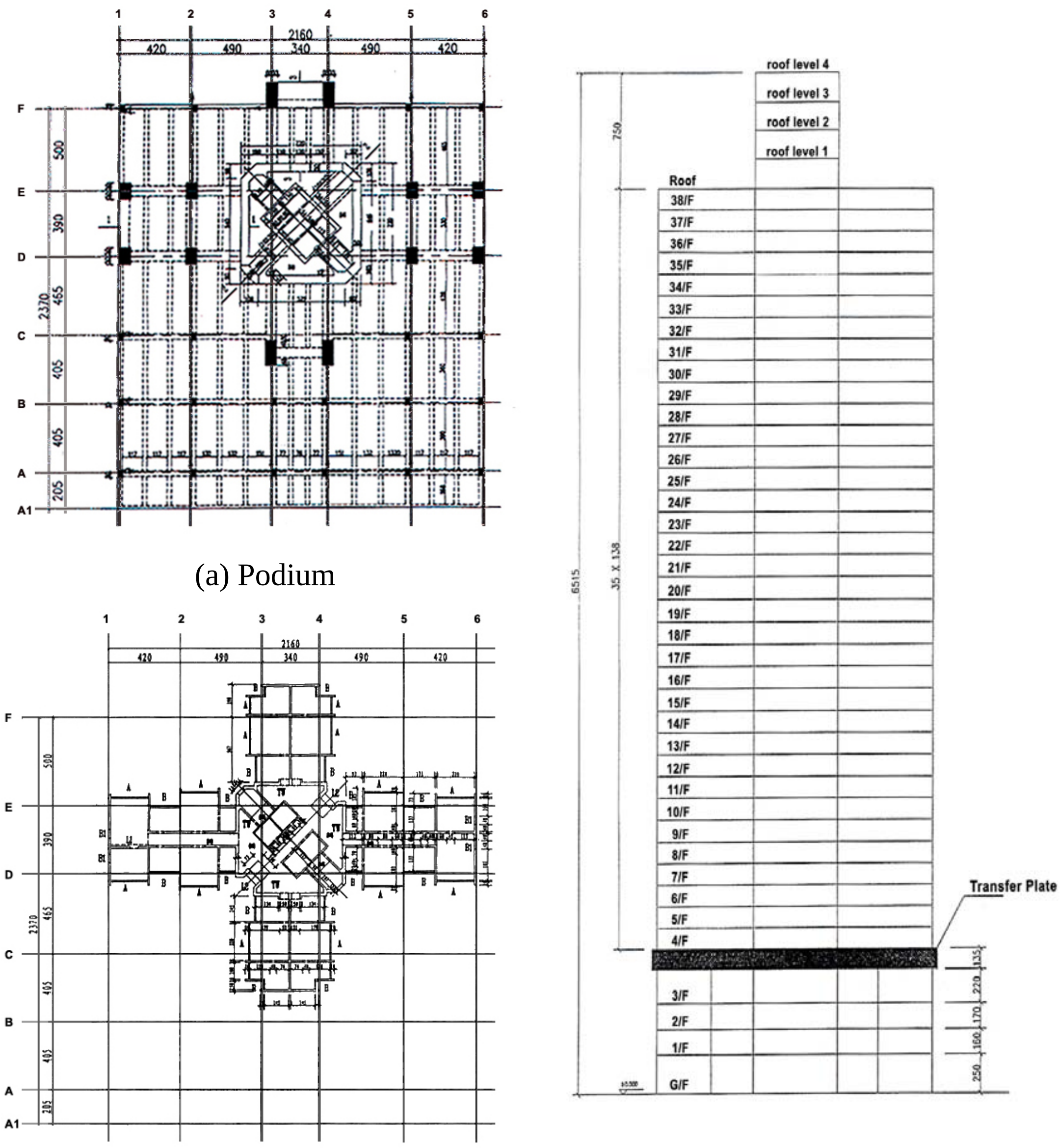

(c) Elevation

Figure 6.2 Framing plans of the 1:20 scale model.

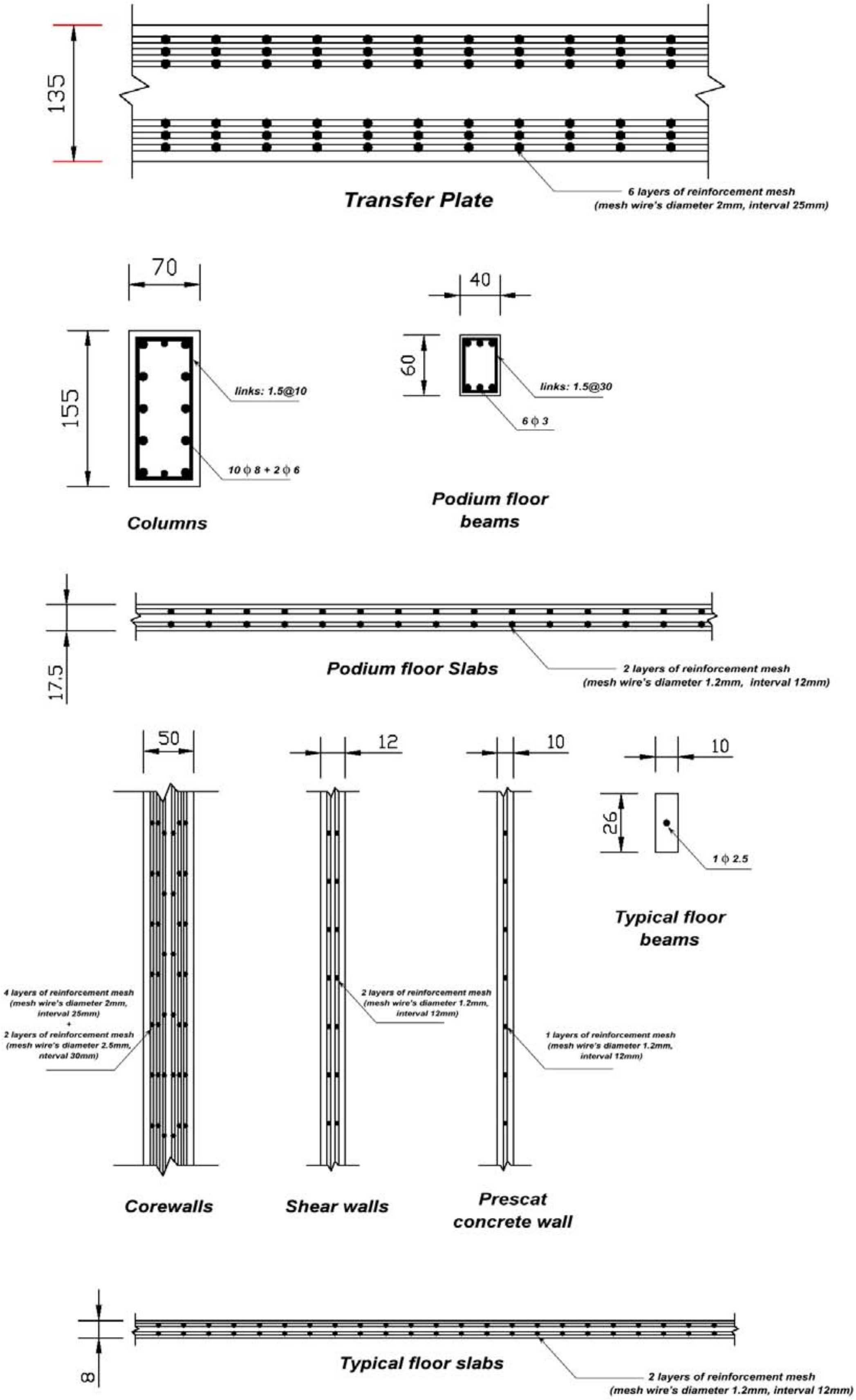

Figure 6.3 Reinforcement details of the shaking table tests model.

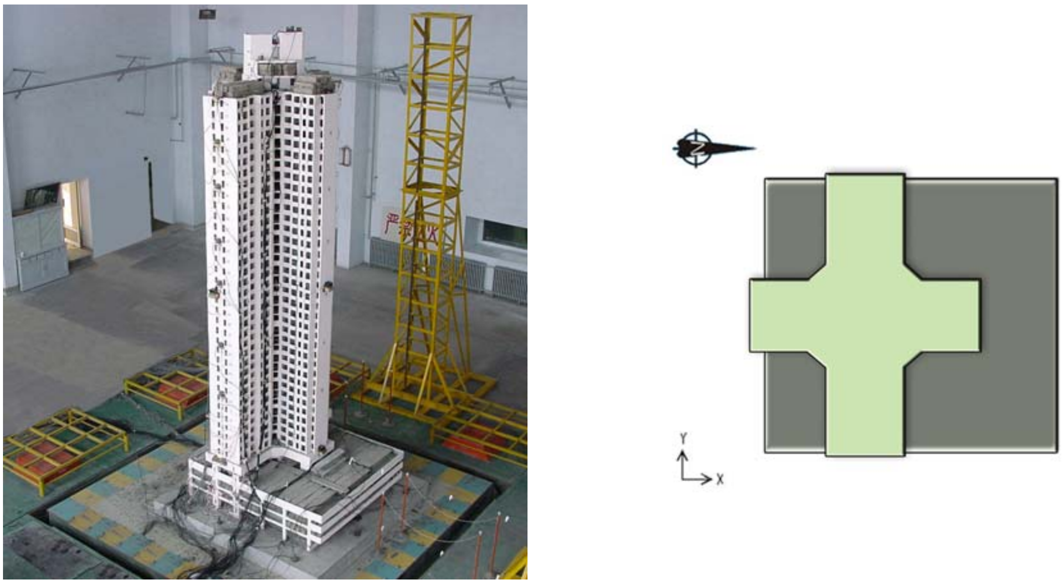

Figure 6.4 The model and definition of x- and y-direction.

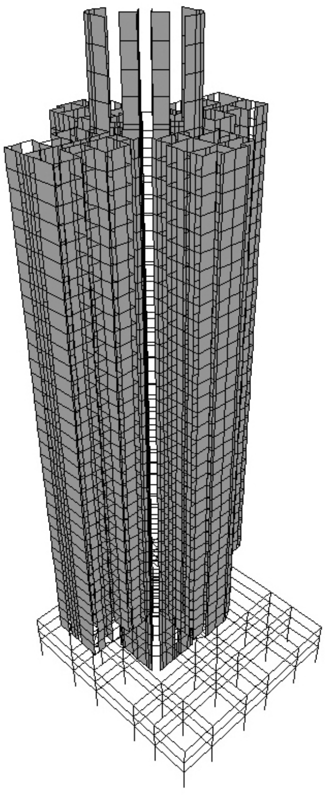

Figure 6.5 Numerical model of the building in 1:20 scale.

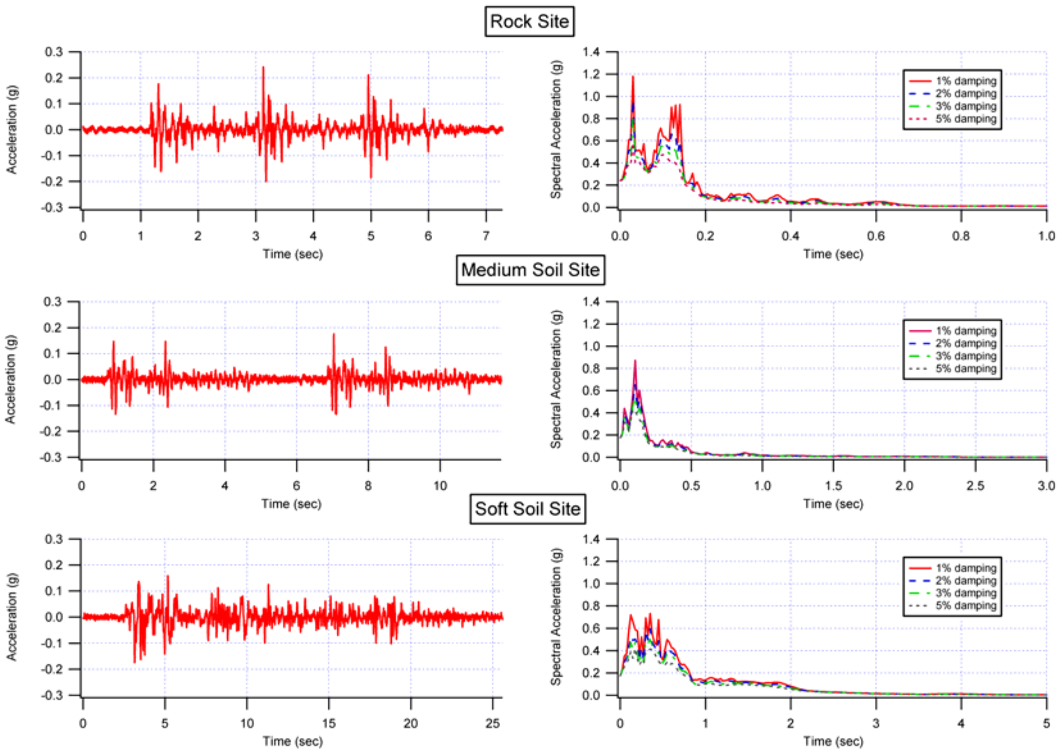

Figure 6.6 Earthquake records and response spectra for strong earthquake excitations.

(a) East Wing

(b) South Wing

(c) West Wing

(d) North Wing

Figure 6.7 Mode of failure.

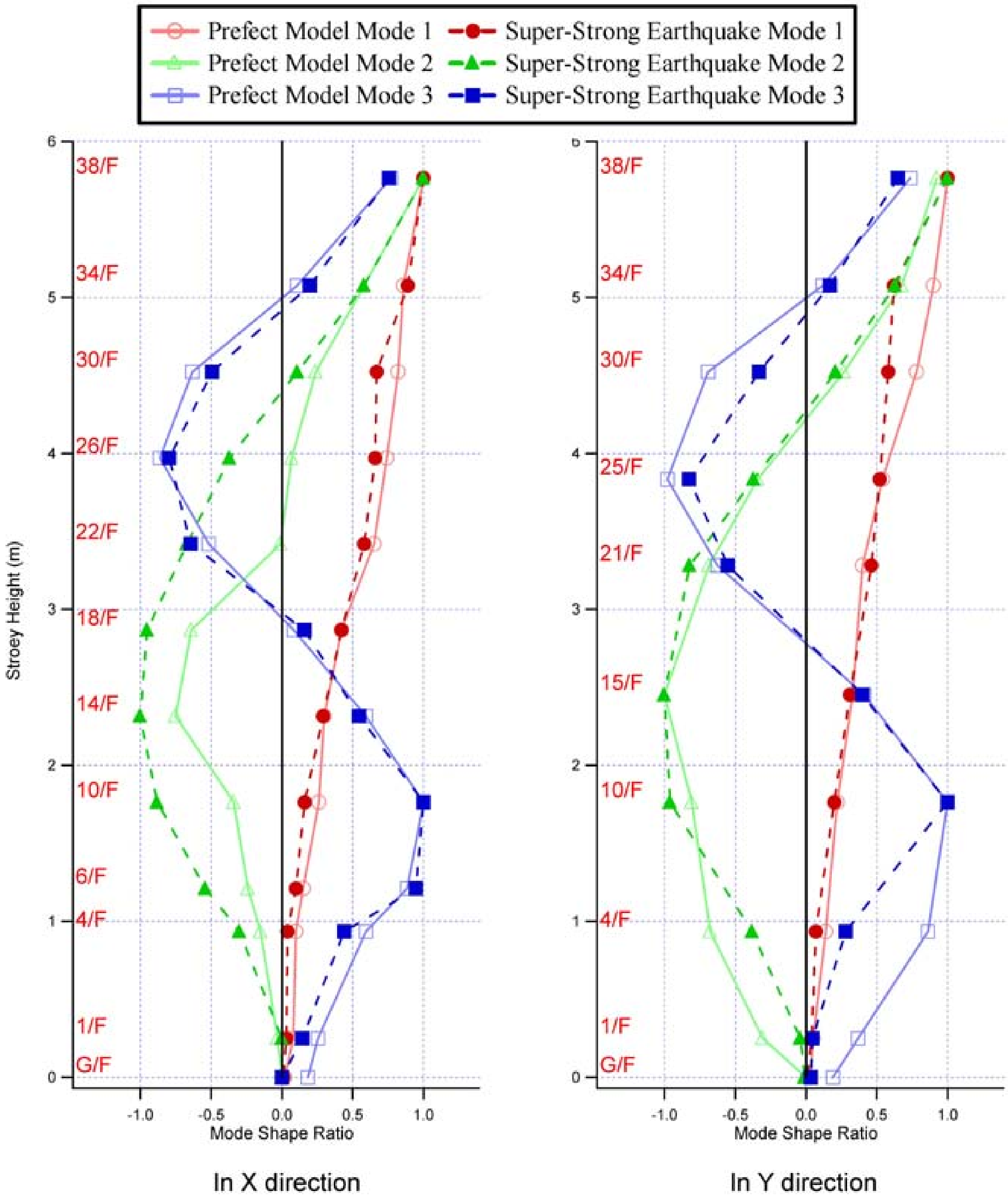

Figure 6.8 Comparisons of mode shapes of the model at the initial stage ("Perfect Model") and after super-strong earthquake attacks.

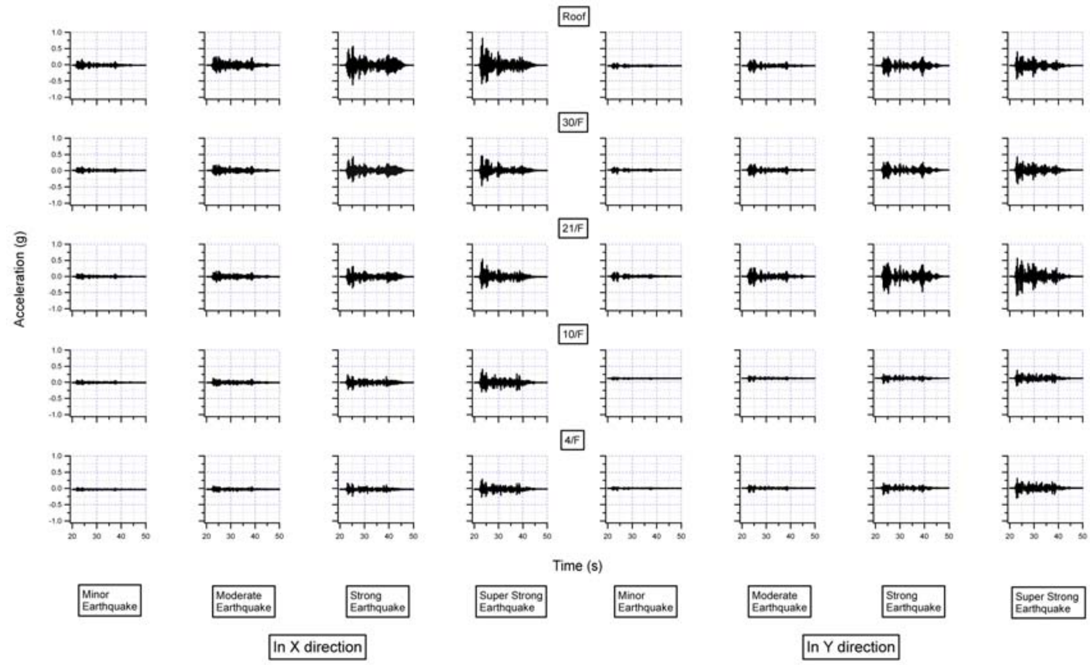

Figure 6.9 Plots of maximum acceleration against time for soft soil site earthquakes.

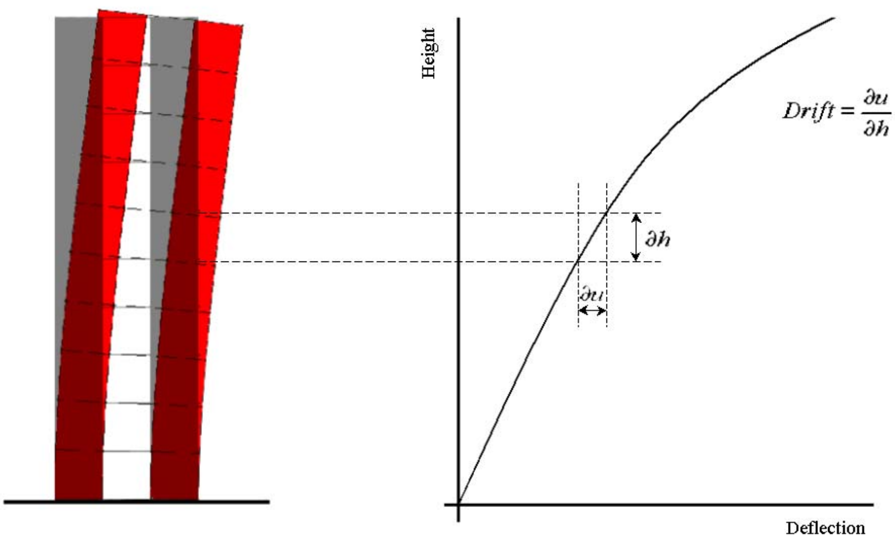

Figure 6.10 Storey drift.

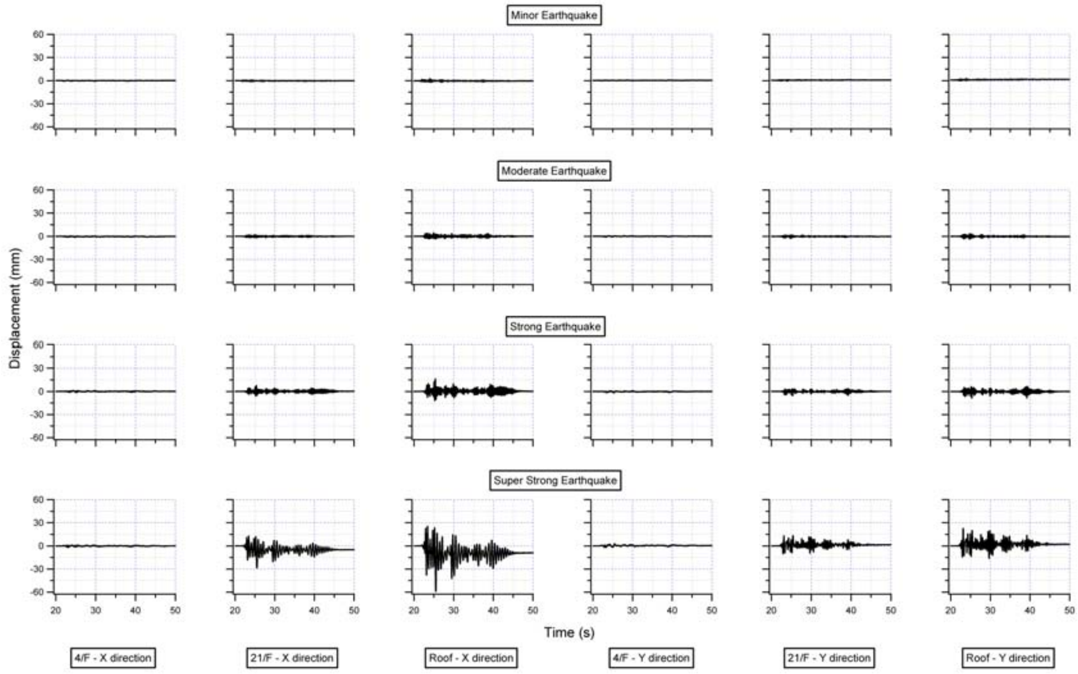

Figure 6.11 Plots of maximum storey drift against time for soft soil site earthquakes.

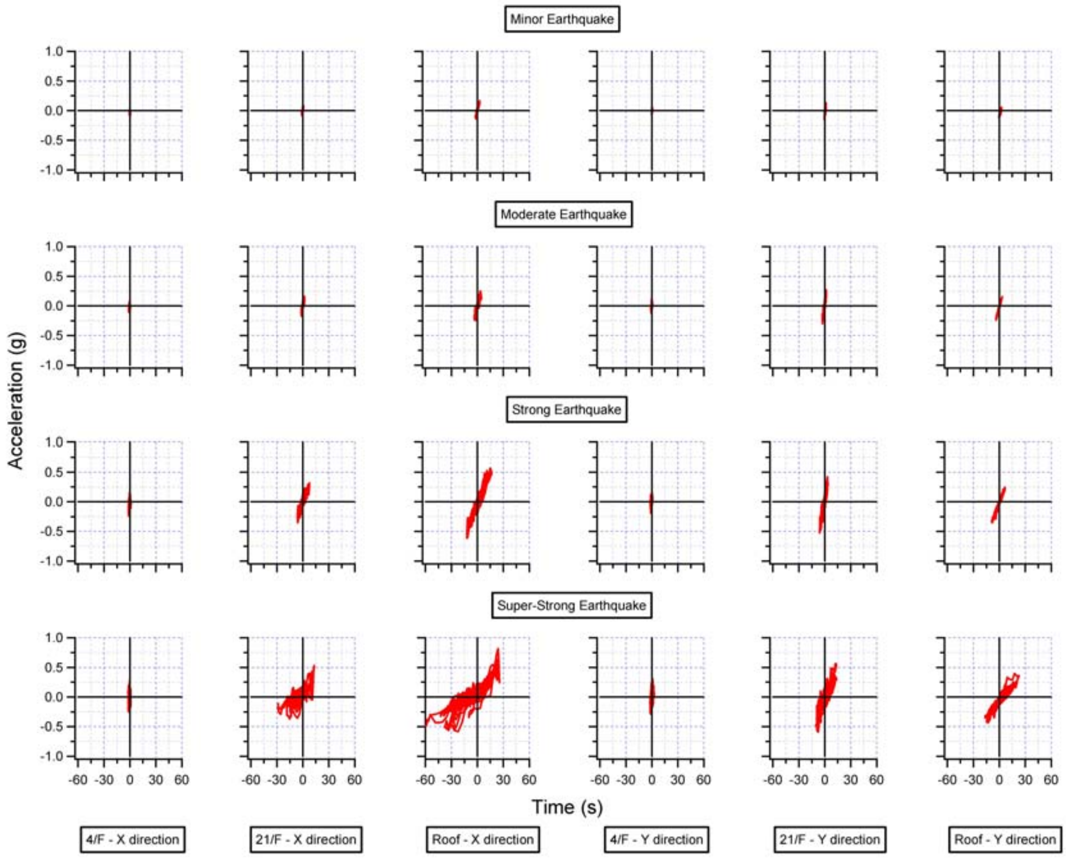

Figure 6.12 Plots of acceleration against maximum displacement for soft soil site earthquakes.

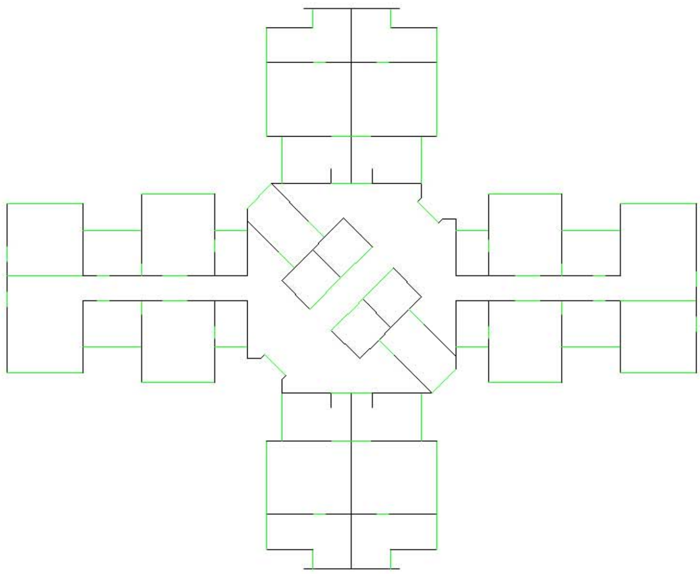

(a)

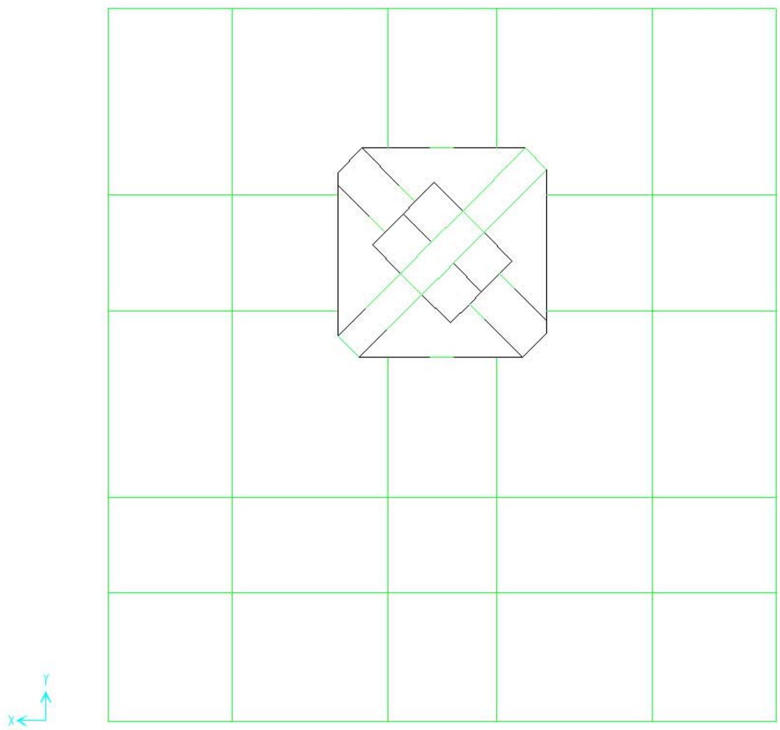

(b)

Figure 6.13 Plan view of ETABS model for Typical Floor (4/F - 38/F) and 3/F Podium Floor.

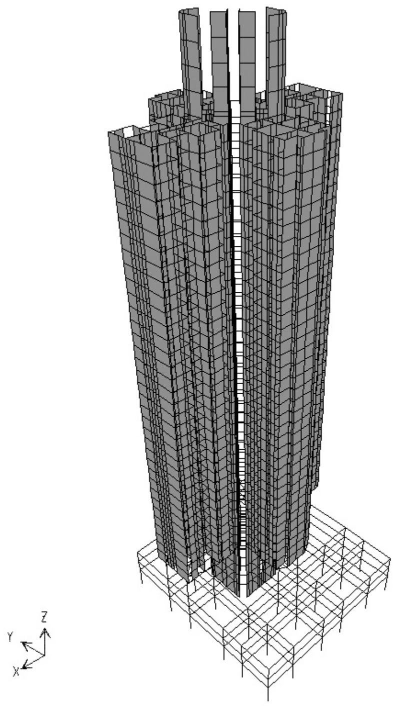

Figure 6.14 3D elevation view of ETABS model.

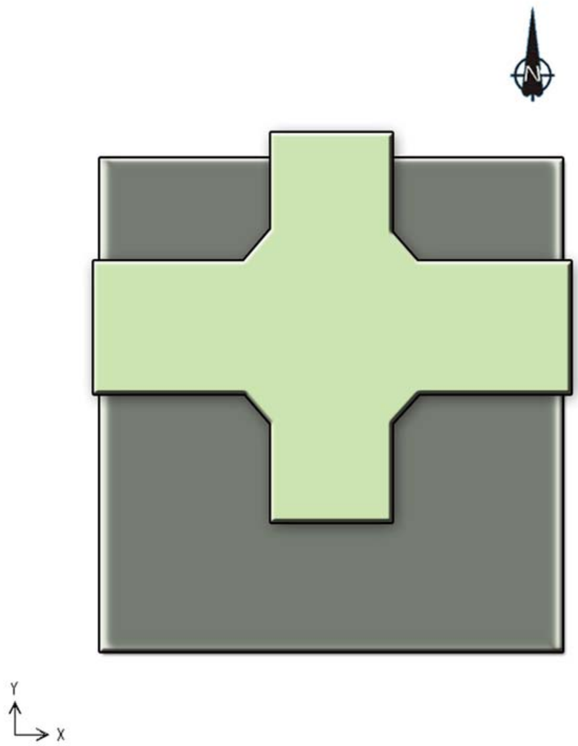

Figure 6.15 Direction layout plan of building.

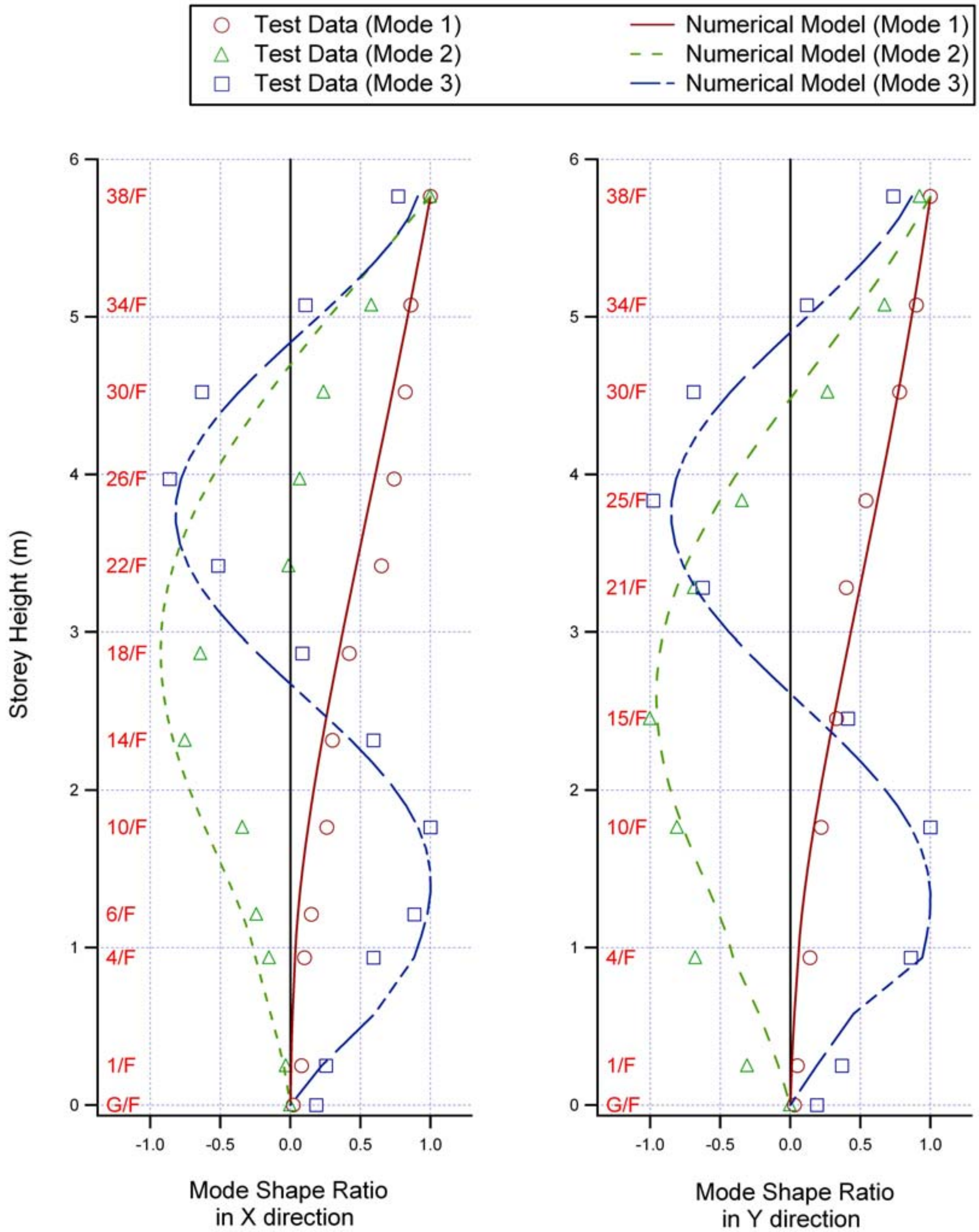

Figure 6.16 Compare with the prefect mode shapes of ETABS and IEM models.

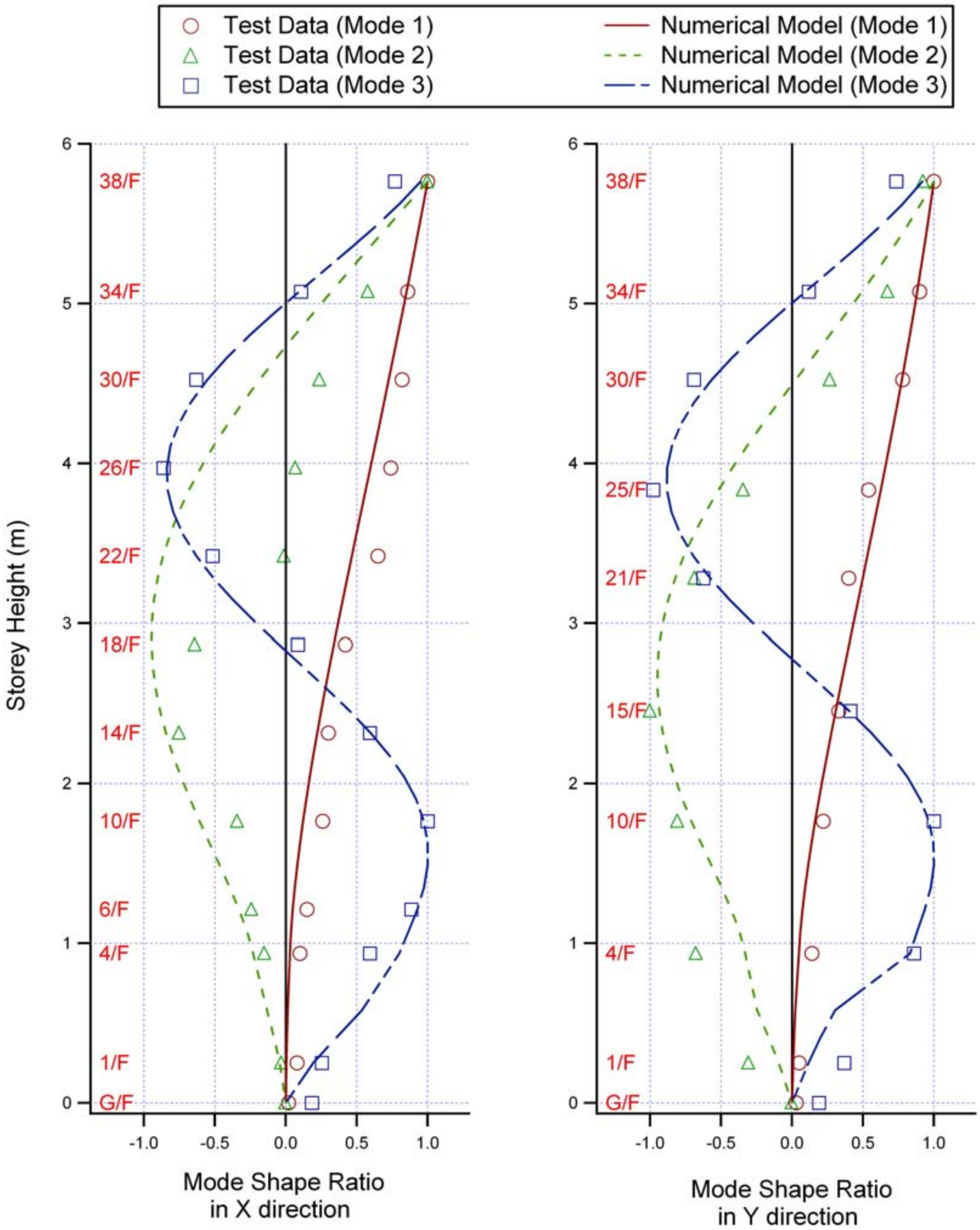

Figure 6.17 Compare with the mode shapes of ETABS and IEM models when the building subjected to a super-strong earthquake motion.

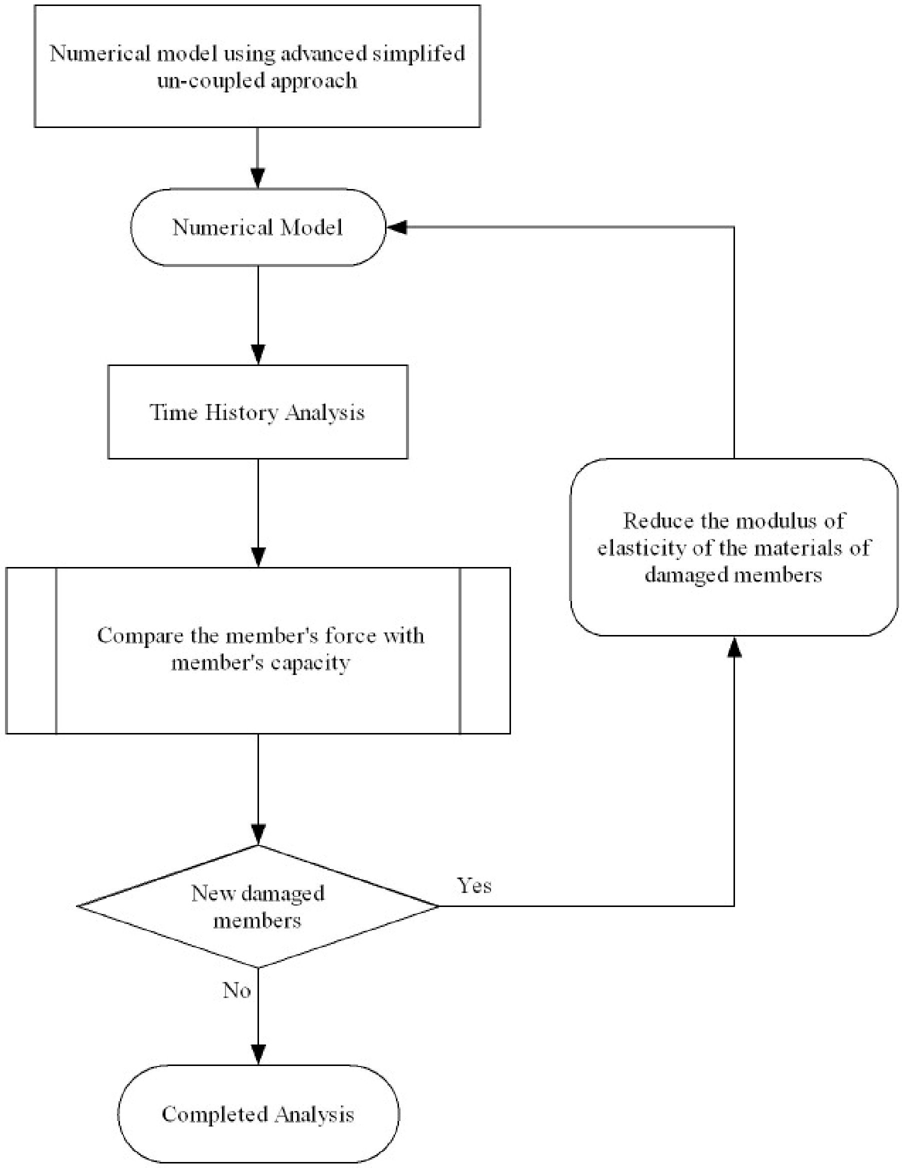

Figure 6.18 Simplified non-linear analysis procedures.

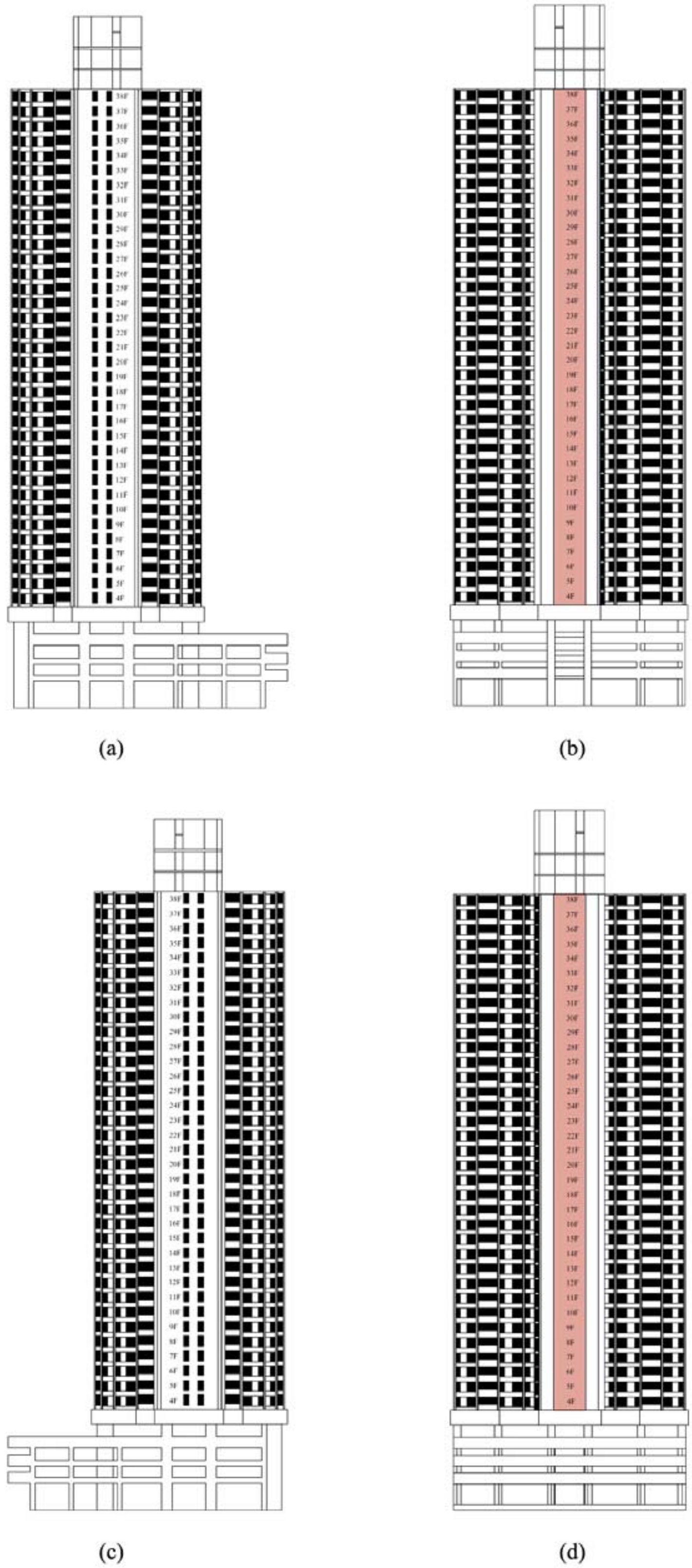

Figure 6.19 Location of cracking elements (in red) under strong earthquake motion.

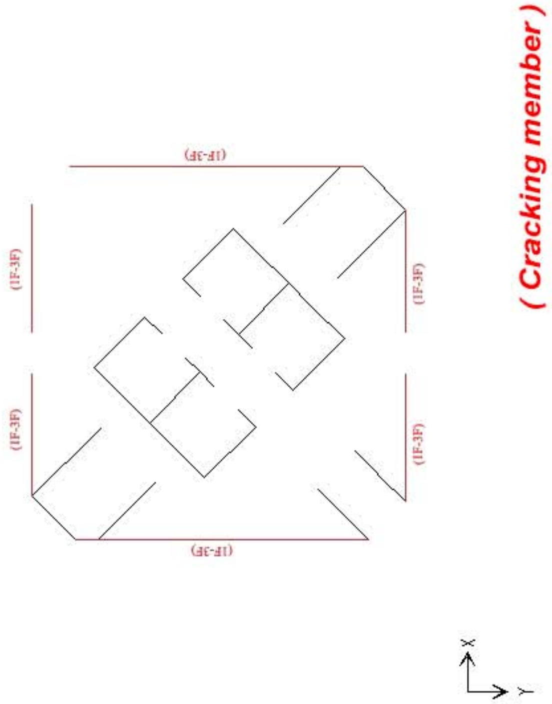

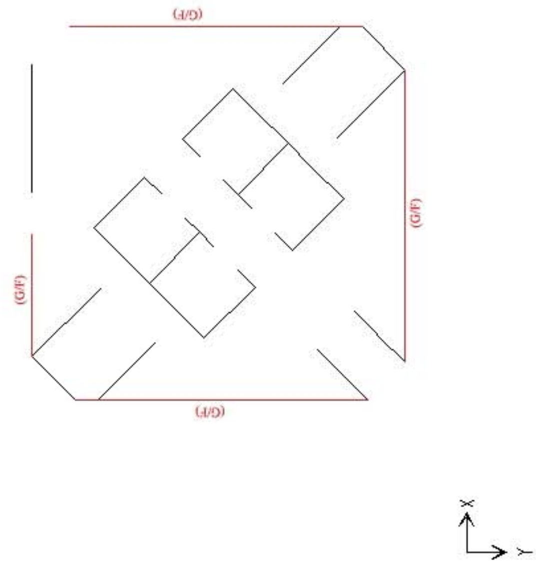

Figure 6.20 Location of cracks on central core at or below transfer plate under strong earthquake motion.

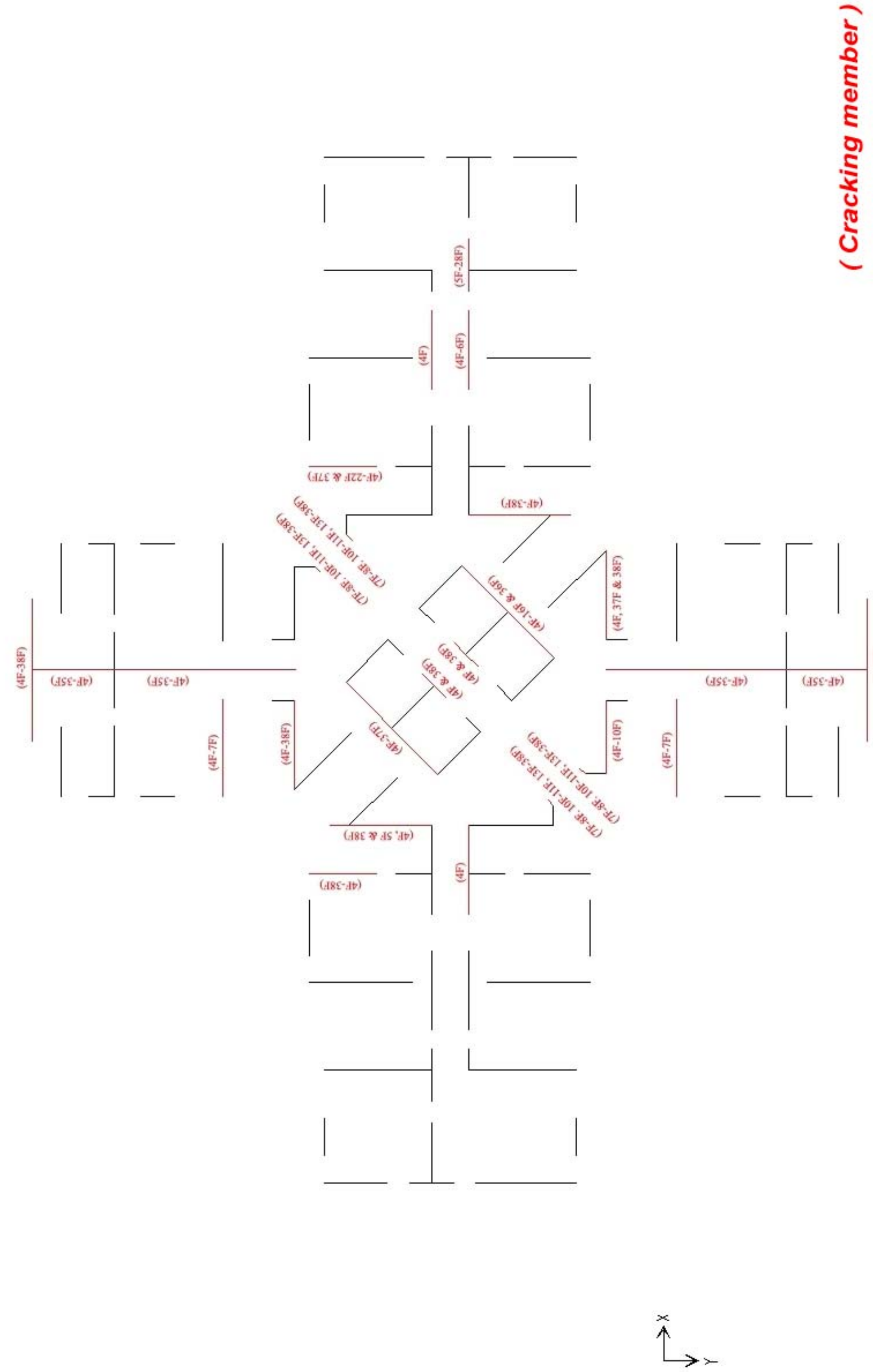

Figure 6.21 Location of cracking walls at the typical floor (4/F – 38/F) under strong earthquake motion.

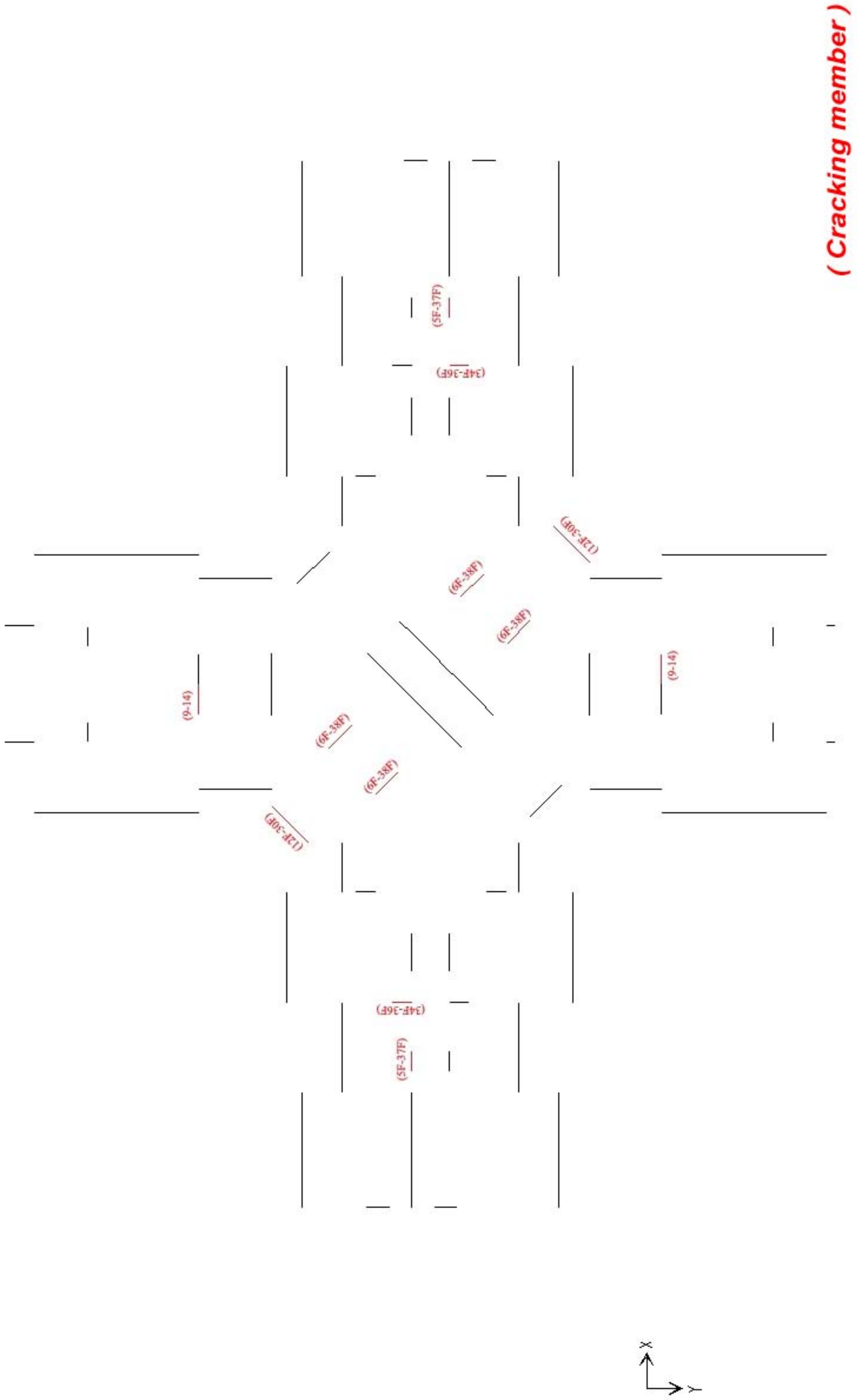

Figure 6.22 Location of cracking beams at the typical floor (4/F – 38/F) under strong earthquake motion.

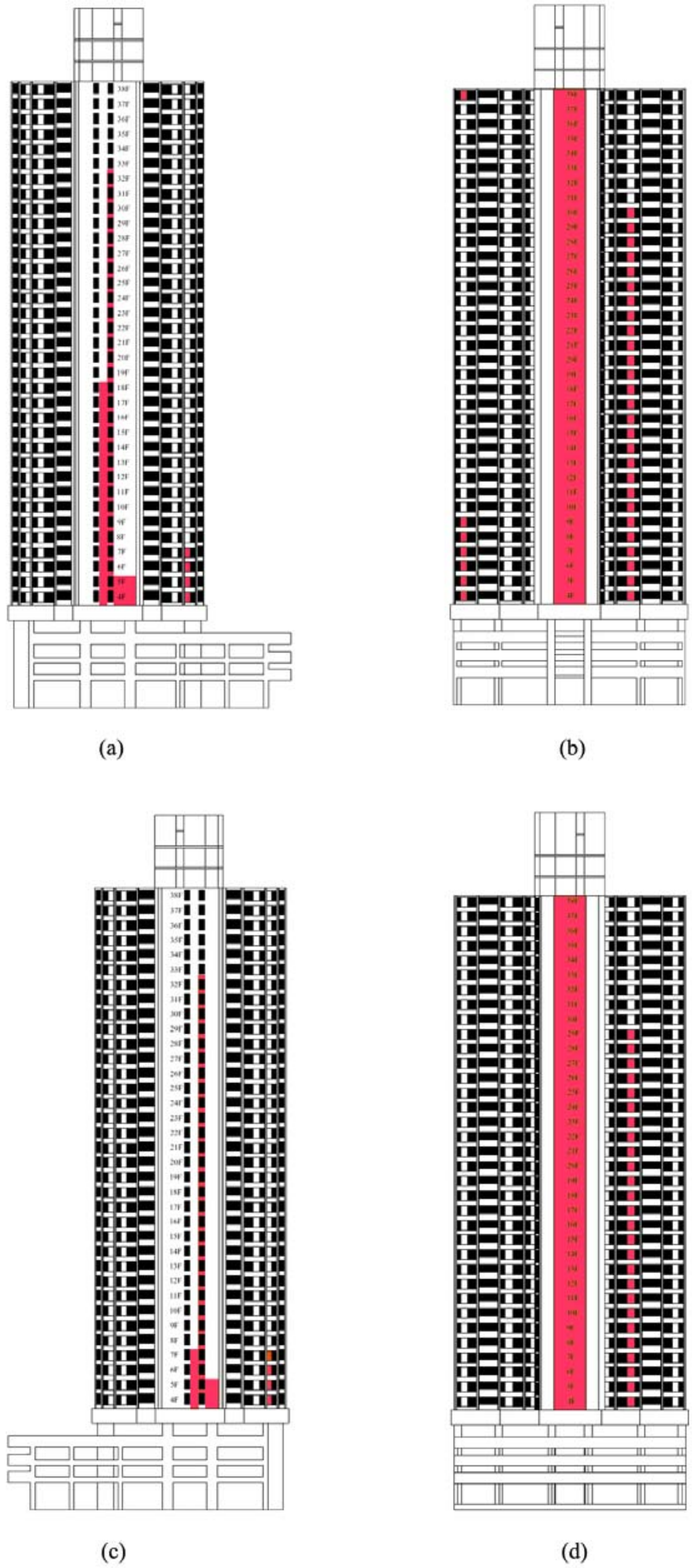

Figure 6.23 Location of cracking elements (in red) under super-strong earthquake motion.

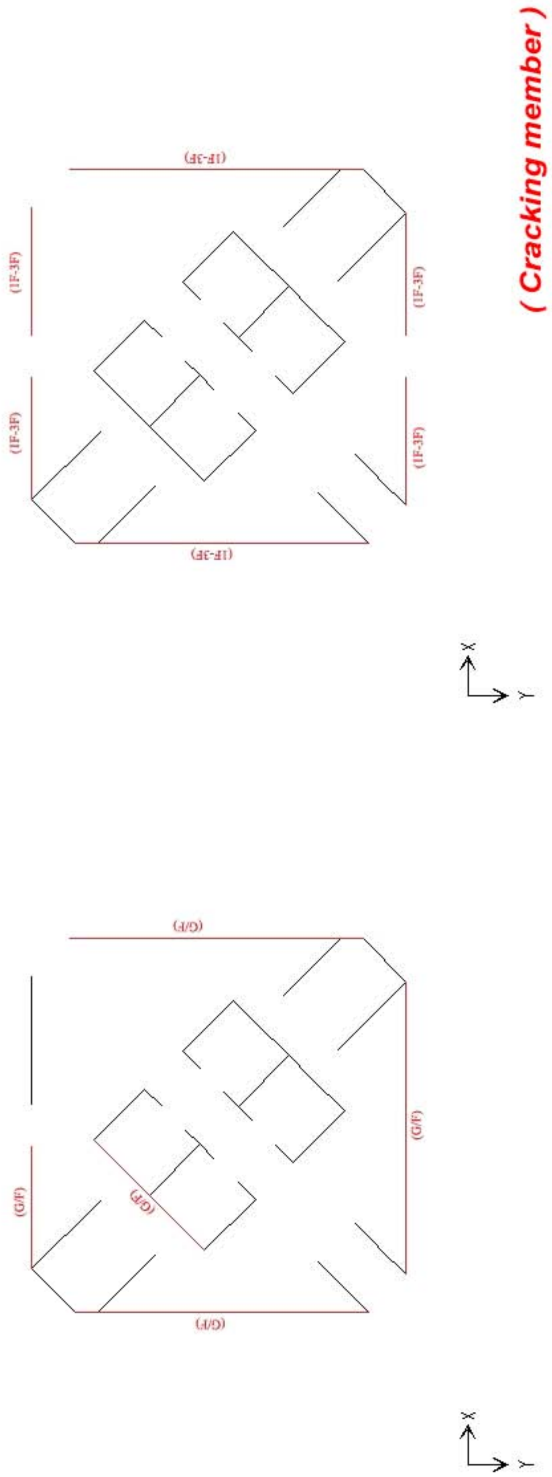

Figure 6.24 Location of cracks on central core at or below transfer plate under super strong earthquake motion.

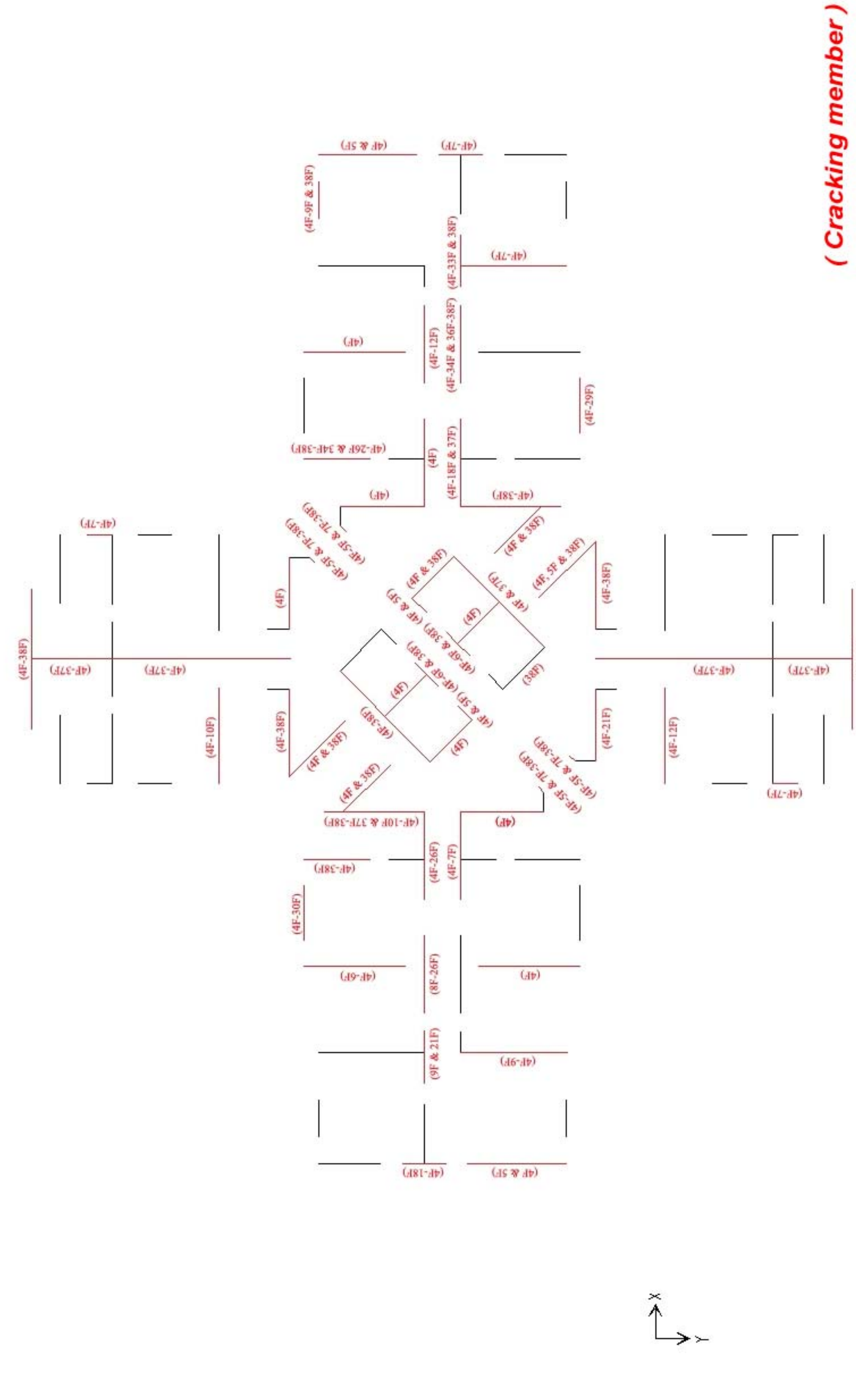

Figure 6.25 Location of cracking walls at the typical floor (4/F – 38/F) under super strong earthquake motion.

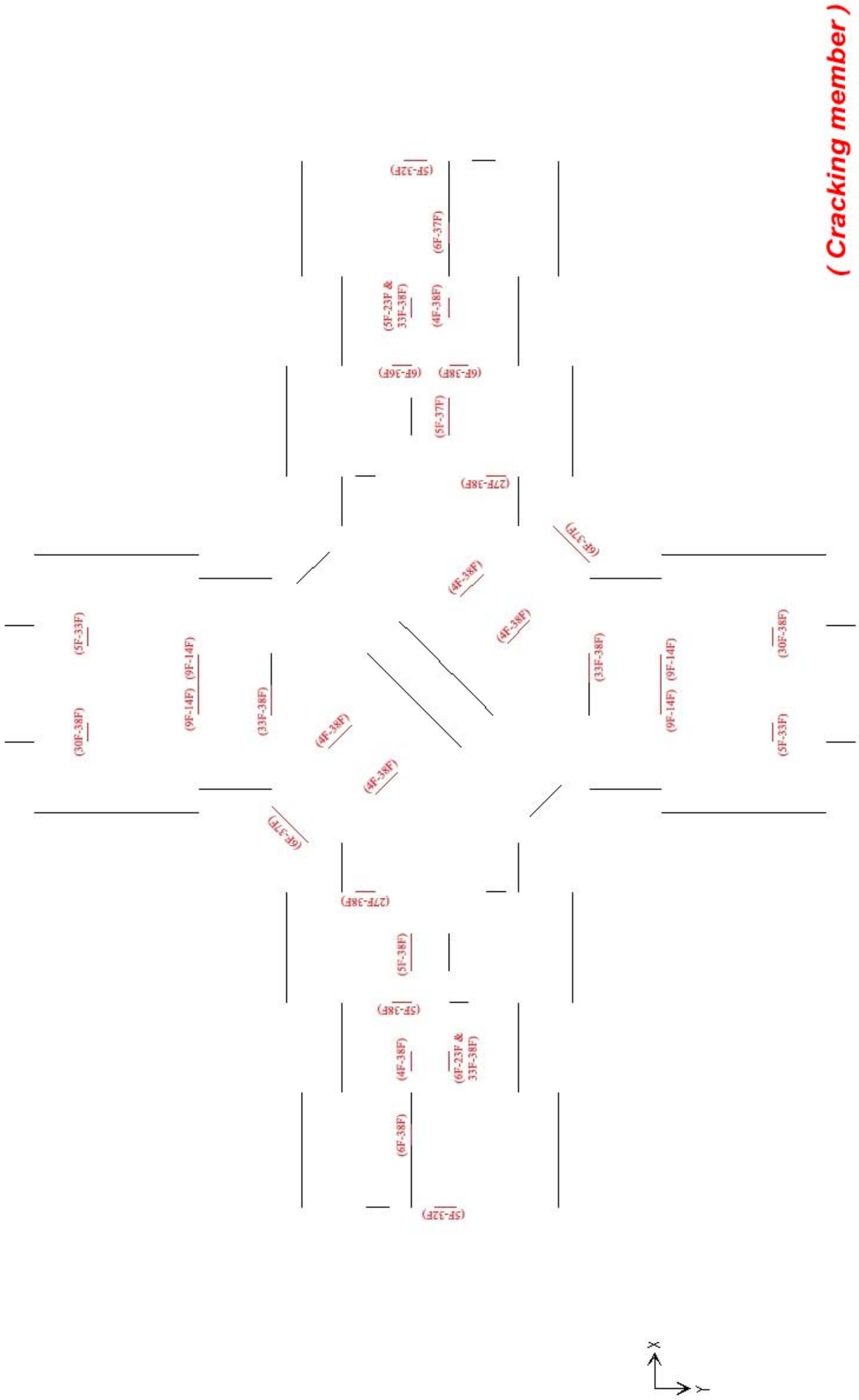

Figure 6.26 Location of cracking beams at the typical floor (4/F – 38/F) under super strong earthquake motion.

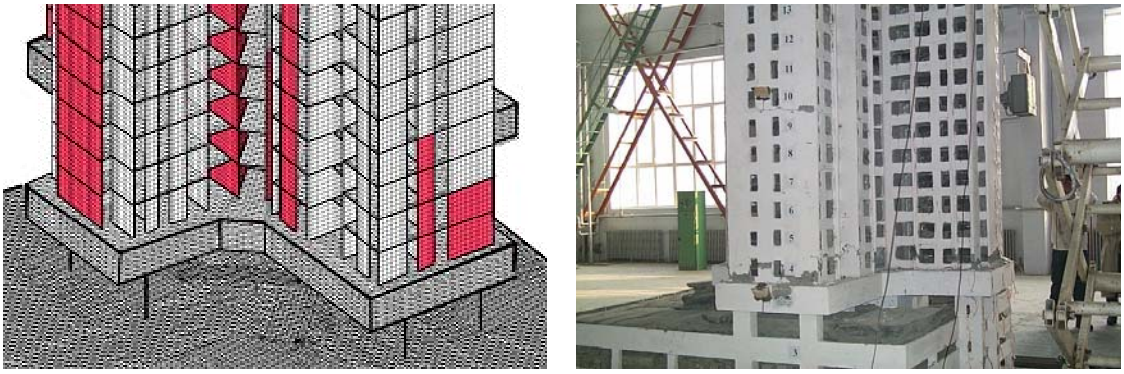

(a) Numerical predictions (b) Damage observed from tests

Figure 6.27 Comparison of damage predicted numerically (in red) with test results.

7 EFFECT OF SOFT SOTREY

In regions without seismic resistance provisions, it is common to use transfer plates as part of structural system. Based on the tests conducted in this study, damage and failure mechanism observed from the tests could be different from the traditional failure mechanism in the form of a “soft storey”. The failure mechanism for a high-rise building with a transfer plate is partially controlled by the bending stiffness of the transfer storey that provides a significant coupling effect with the columns and walls under the transfer plate. In this chapter, three cases studies were used to explore a method to estimate the flexural stiffness effect of the transfer storey. The evolution of the method is retraced in order to emphasize its unique reliance on experimental results and numerical analysis, which are needed to establish rules for the assignment of linear properties. Recent experimental results were used to initiate and to calibrate of the method. A critical review of the response of a soft storey during major earthquakes leads to be conclusion that any method based on the usual first theory of failure is not adequate and cannot predict the mode of failure in the high-rise building with a transfer plate.

In high-rise buildings, the disposition of columns and walls is dictated largely by functional, aesthetic and economic considerations. One of the main requirements is the need to provide column-free open space area on plan. This creates an interesting engineering problem that is uniquely solved with the use of transfer plates, as part of the structural system in a high-rise buildings.

Previous experiments to quantify the seismic performance of transfer plates include shaking table tests of a 1:20 scale reinforced concrete building. Detailed description of the shaking table test of a high-rise building with a transfer plate is given in Chapter 6. Based on the damage and failure mechanisms observed in the tests, it is concluded that the mode of failure in a high-rise building with a transfer plate is different to that for a low-rise building with a soft-storey. Notwithstanding the use of a transfer plate, the bending stiffness at the transfer plate is still significant due to the coupling with the columns by the relatively thick transfer plate. The ratio of deflection at the transfer plate level is proposed and used to indicate of the mode of failure in a high-rise building with a transfer plate.

7.1 SOFT STOREY

The main drawback in using the transfer plate system is that it leads to an abrupt change in the lateral stiffness at the transfer plate, e.g. from a stiffer shear wall system above the transfer plate to a relatively flexible column-girder system below it. This creates a soft (or weak) storey and violates the seismic design concept of “strong column weak beam” (Aoyama 2001) or alternatively the capacity design concept (Paulay & Priestley 1992). Therefore, a high-rise building with a transfer plate system could be vulnerable to possible earthquake attacks. Yoshimura (1997) conducted numerical studies to simulate the apartment house and concluded that “if first storey mechanism might occur, the collapse could be unavoidable even for buildings with base shear strength of as much as 60% of the total weight”. In particular, the so-called “piloti-type buildings” (in which strength and stiffness of the first storey are considerably smaller than the upper storeys) are extremely vulnerable to earthquakes (Sanada *et al* 2000).

7.1.1 TRADITIONAL APPROACH

To check the existence of a transfer or soft storey, design codes use the ratio of lateral stiffness at the transfer plate to lateral stiffness of the storey immediately above, e.g. in the United States seismic design codes - SEAOC (1999) and UBC (1997), Chinese seismic design code GB50011-2001, etc. In general, a soft storey can be defined as one in which the lateral stiffness is less than 70% of that of the storey immediately above or less than 40% of the combined stiffness of the three storeys above. Due to the irregularity in elevation, non-uniform and concentrated storey drift may occur at floors in the vicinity of the transfer plate. Design codes general require structural members at the transfer plate to be designed with enhanced ductility and strength. Other requirements include the need to carry out sophisticated analysis as well as experimental verifications.

Traditional (or Present) approach to earthquake resistant design, is regulated by building codes, focus a designer's attention on the provision of strength to a structure for resisting lateral loads. Consideration of lateral storey stiffness is reflected by a static lateral load method.

Figure 7.1 shows the traditional approach. The change in lateral stiffness is simply K_n/K_{n+1}.

The codified lateral stiffness R_s (Scarlat, 1997),

$$R_s = \frac{K_n}{K_{n+1}} \tag{7.1}$$

K_n and K_{n+1} are classified in the estimated lateral stiffness at the storey level “n” and that above at “n+1”. The method of estimated lateral stiffness at the level of “n” is presented as follows. Firstly, the translational and rotational degrees-of-freedom of all the vertical members are fixed at the level “n-1”. A horizontal force of magnitude “F” is then applied at the level “n”. If the corresponding lateral displacement is “δ”, the lateral stiffness at the level “n” will then be “F/δ”. This technique is very general and can be applied to estimate the respective lateral stiffness of the storey.

7.1.2 NEW APPROACH

For high-rise building structures subjected to lateral wind or earthquake motions, the lateral deflection of buildings are contributed to by both flexure and shear deflection actions. For example, the deflection at the top of a slender shear wall subjected to a lateral uniform distribution loads, representing the wind loadings applied at the horizontal direction along the height of a structure, is critically controlled by the bending moment, not the shear force. The shear deformation of the wall can be considerable. For typical walls with aspect ratios greater than about 2, the contribution of the flexural deformation to the top displacement is much greater than that of the shear deformation. In this study only the contribution of the flexural deformation to the wall displacement is considered. In this sense, the capacity and demand models, as well as the resulting fragility estimates, are appropriate for the coupled shear wall having a medium to large aspect ratio.

The new approach of approximating the storey stiffness not only includes the shear stiffness, but also includes the bending stiffness of the storey. In this method, a lateral uniform distribution load is applied the building for calculating bending and shear deflection. A “reference testing model” must be created to estimate the transfer plate effect in the soft storey by comparing with the results of the original testing model. Figure 7.2 shows the reference model is formed by erasing the transfer plate structure and changing the structural form below the transfer plate to the same size and structural form as that above the transfer plate.

The new approach uses a ratio of deflection at the transfer plate of the reference test model and the original building model to indicate the performance of the soft storey in the bending behaviour of the structure with a transfer plate. Two indications are considered, displacement ratio (R_u) and drift ratio ($R_{\Delta u}$), in the form of

$$R_u = \frac{u^*}{u} \tag{7.2}$$

$$R_{\Delta u} = \frac{\Delta u^*}{\Delta u} \tag{7.3}$$

where u is the displacement and Δu is the inter-storey drift. u^* and Δu^* are the respective reference displacement and reference inter-storey drift of a reference building. Values of R_u and $R_{\Delta u}$ at transfer are about 90%. Accordingly, it is suggested that the soft-storey may not occur.

7.2 NUMERICAL MODEL

Numerical models have been generated using the analysis program ETABS version 6.22. Three different types of high-rise building models have been developed, such as single shear wall structures, coupled shear wall structures and a typical residential building structure, as shown in Figure 7.3. All the numerical models are subject to a lateral uniform distribution load. In each case of high-rise structure, a reference model was provided for control purposes. The reference model allows all the shear walls above the transfer to continue down to the foundation, with the removal of all the columns below transfer and without the transfer plate. For the single shear walls and coupled shear wall structures, two different types of these numerical models were created. One type contains the transfer plate in the building structure and the other type contains no transfer plate element.

In each case of numerical high-rise structure models, the storey stiffness at the transfer storey in the original models in comparison with the "reference model" are reduced to "soft storey" type. Based on the comparisons of the numerical results between the "reference model" and the original models, the performance of the transfer plate in the high-rise building structure is classified and used to show the different between the new approach and the traditional approach for predicting the performance of the soft storey with a transfer plate.

A shaking table test of a 1/20 scaled high-rise building with a transfer plate model (Lam *et al.* 2002) has provided an extensive set of new data that is ideal for further investigation of damage systems under a series of earthquake motions. The results are considered ideal not only because they reflect the non-linear seismic performance and damage intensity of high-rise building with a transfer plate system. Based on the experimental results from the testing model, the building collapse mode can be classified. It is damaged by the flexural behaviour. The damage occurred in above the transfer plate. This result is used to motivate and extend significantly the calibration of method the new approach.

7.3 NUMERICAL RESULTS

7.3.1 SINGLE SHEAR WALL STRUCTURES

The problem being considered is an example of the static lateral load analysis of a single shear wall structure. The 40-storey single shear wall structures are used to resist the large bending moments caused by the applied lateral load. The soft storey is constructed at the below the transfer plate level. The stiffness of the soft storey is reduced to 30%, 50% and 70% with comparing that storey stiffness in the “reference model”.

Brief descriptions of the various models are as follows.

Model M-000 represents a 40-storey single shear wall structure with transfer structure and without a soft storey.

Model M-030 is similar to the model M-000, except that the stiffness of the soft storey is reduced to 30% of that storey stiffness in the “reference model”.

Model M-050 is similar to the model M-000, except that the stiffness of the soft storey is reduced to 50% of that storey stiffness in the “reference model”.

Model M-070 is similar to the model M-000, except that the stiffness of the soft storey is reduced to 70% of that storey stiffness in the “reference model”.

Figure 7.4(a) shows the deflected shape of a single shear wall with different stiffnesses in the weak storey. When a weak soft storey is provided in the single shear wall structure, the deflection at the top and at the transfer level of the structure are increased by reducing the storey stiffness in the soft storey. The increasing ratios of the deflection at top are 1.36, 1.16 and 1.07 when the stiffness of the soft storey is reduced to 30%, 50% and 70% of that storey stiffness in the “reference model”. The storey drift and its rotation at the transfer level are increasing rapidly when the stiffness of the weak storey reduces. The increasing ratios of the storey drift at the soft storey are 1.48, 1.21 and 1.09 when the stiffness of the soft storey is reduced to 30%, 50% and 70% of that storey stiffness in the “reference model”. The failure mode of the soft storey in a single shear wall structure is adopted by the failure mechanics of the soft storey.

Figure 7.5 shows how the different storey stiffness is estimated by the traditional approach and the new approach. For the traditional approach, the storey stiffness ratio in the soft storey is reduced by decreasing the width of a single shear wall. The soft storey will be damaged and failure is due to the large reduction of stiffness in the soft storey. However, in the cases of a single shear wall system used in this study, the deflection shapes of structures do not have significant change at the transfer plate level. Based on the numerical results as given in Table 7.1, the stiffness ratios estimated using the traditional approach are unreasonably small. The new approach indicates the stiffness of the soft storey is about 70% of the reference model. Therefore, flexural stiffness in the soft storey with a transfer plates is an important factor in estimating the storey stiffness in high-rise building structure.

7.3.2 COUPLED SHEAR WALL STRUCTURES

The problem is an example of a static lateral load analysis of a coupled shear wall structure. 40-storey coupled shear wall structures are used to resist the large bending moment caused by the applied lateral load. Three different numerical models are considered to explore the implications of the transfer effect on the structure. The various models have brief descriptions as follows.

Model MCT represents a 40-storey coupled shear wall structure with a transfer plate.

Model MCB represents the "reference model" of the 40-storey coupled shear wall structure with a transfer plate.

Model MC represents a 40-storey coupled shear wall structure without connecting beams. The purpose of the model is to estimate the increase in the stiffness due to the incorporation of the connecting beam and transfer plate effect by comparing with the analysis results of MCB and MCT.

Figure 7.4(b) shows the deflected shape of a two separated walls structure, a coupled shear wall structure (reference model) and a coupled shear wall structure with a transfer plate. In Figure 7.3, the coupling effect of the connecting beam in the coupled shear wall structures can be obtained by comparing the deflections at the top of the structures. When a connecting beam is provided between these two separated walls, the connecting beam ends are forced to rotate and displace vertically, the connecting beam is bent in double curvature and thus resists the free bending of the walls. Therefore, the top deflection of the coupled shear wall structure is much smaller than the structure with two separated walls.

The percentage stiffness contribution by walls/columns systems is defined as the roof displacement of the whole building model with coupling beams, divided by the roof displacement of the building with walls/columns elements only. The new approach factor for controlling the design of the transfer plate storey is determined by comparing the displacement at the transfer plate level with the standard testing model and the original structure model.

The comparison of the R_s, R_u and $R_{\Delta u}$ in coupled shear wall structures with transfer plates are shown in Figure 7.6. Table 7.2 shows the different storey stiffness is estimated by the traditional approach and the new approach. For the traditional approach, the storey stiffness ratio in the soft storey is reduced by increasing the percentage contribution of stiffness by walls/columns. The soft storey will be damaged and failure is due to the large reduction of stiffness in the soft storey. However, in the case of a high-rise building with a transfer plate, the transfer plate provides a large coupling effect on the structure. It reduces the magnitudes of the bending moment in the two walls by causing a proportion of the applied moment to be carried by axial forces. Therefore, the flexural stiffness in the soft storey with a transfer plates is an important factor in estimating the storey stiffness. The traditional approach cannot affect the transfer plate action on the soft storey in the structure as the stiffness ratio is very small. The new approach indicates the stiffness of the soft storey is about 60% of the reference model. Therefore the coupled shear wall with a transfer plate will failure in the zone above the transfer plate.

7.3.3 TYPICAL RESIDENTIAL BUILDING WITH A TRANSFER PLATE

For real case, a shaking table test of a 1/20 scaled high-rise building with a transfer plate model is demonstrated to explore the implications of the transfer effect on the structure and to make a calibration of the new approach. The various models are as follows.

Real Structural Model represents a high-rise building with a transfer plate model.

Standard Model represents the "reference model". In the standard model, the transfer plate structure is erased and the structural form below the transfer plate is the same as that above the transfer plate. This means all the vertical members above the transfer in the reference model will continue to the foundation.

Figure 7.7 shows the deflection behaviour of the high-rise building with a transfer plate and the standard model (reference model). The difference in the ratio of storey stiffness as estimated by the traditional approach and the new approach is shown in Figure 7.8. The lateral displacement at the transfer location of the reference model is greater than that of the building model with a transfer plate system. It means that the transfer plate in the soft storey provides a strong flexural stiffness and a large coupling effect between the core wall and column system. The estimated ratio of storey stiffness is given in Table 7.3. According to the traditional approach, stiffness of the soft storey in the x-direction is half of the value in the y-direction. It means the failure of the building will occur in the x-direction first. However, the experimental results showed that the building failed in the y-direction first and also above the transfer plate level. The traditional approach cannot reasonably predict the mode of failure.

Based on the new approaches, namely displacement ratio (R_u) and drift ratio ($R_{\Delta u}$), stiffness ratios in the y-direction are smaller than that in x-direction. If the stiffness ratios are greater than 1, failure will take place above the transfer plate level and the possibility of a softy storey type failure will be relatively remote.

7.4 CONCLUDING SUMMARY

The main objective of this study was to quantify, through a numerical analysis, the seismic performance of a high-rise building with a transfer plate. Based on the damage and failure mechanisms observed in the shaking table tests, it is concluded that the mode of failure in a high-rise building with a transfer plate is different from that in a low-rise building with a soft-storey. Notwithstanding the use of a transfer plate, the bending stiffness at the transfer plate level is still significant owing to the coupling of the columns by the relatively thick transfer plate. Using the new approach, namely displacement ratio (R_u) and drift ratio ($R_{\Delta u}$), at the transfer plate level to indicate the mode of failure in a high-rise building with a transfer plate, is recommended. If the displacement ratio (R_u) or drift ratio ($R_{\Delta u}$) below the transfer plate are smaller than 1, a softy storey may occur.

Table 7.1 Comparison of the storey stiffness in single shear wall structures by using different methods.

Mode type		Traditional approach (R_s)	New approach	
			R_u	$R_{\Delta u}$
M-030	without a transfer plate	0.05	0.78	0.68
	with a transfer plate	0.05	0.78	0.68
M-050	without a transfer plate	0.08	0.89	0.83
	with a transfer plate	0.08	0.89	0.83
M-070	without a transfer plate	0.12	0.95	0.92
	with a transfer plate	0.12	0.95	0.92
M-000	without a transfer plate	0.17	1.00	1.00
	with a transfer plate	0.17	1.00	1.00

Table 7.2 Comparison of the storey stiffness in coupled shear wall structures by using different methods.

Size of column (mm)	Mode type	% contribution of stiffness by columns	Traditional approach (R_s,)	New approach	
				R_u	$R_{\Delta u}$
1000 × 1000	without a transfer plate	0.061	0.05	0.96	0.91
	with a transfer plate	0.046	0.22	2.73	4.04
2000 × 2000	without a transfer plate	0.298	0.05	0.96	0.90
	with a transfer plate	0.219	0.12	2.76	3.02
3000 × 3000	without a transfer plate	0.492	0.05	0.94	0.87
	with a transfer plate	0.384	0.09	1.86	1.84

Table 7.3 Comparison of ratios of lateral stiffness of soft storey with a transfer plate by using different methods.

		In the x-direction	In the y-direction
Traditional approach	R_s	0.23	0.40
New approach	R_u	2.84	2.30
	$R_{\Delta u}$	3.15	2.75

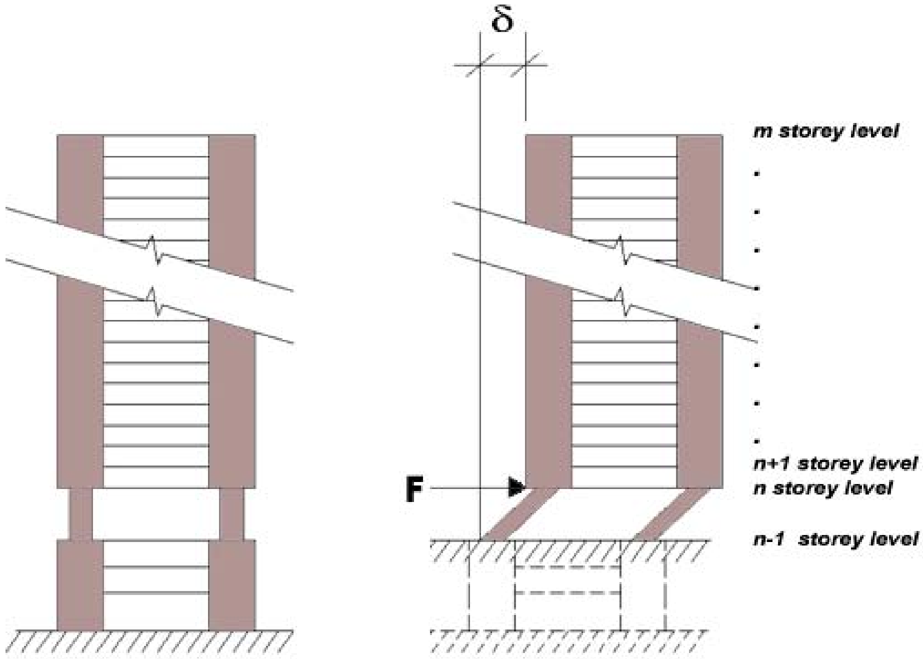

Figure 7.1 Determination of the storey stiffness by using traditional method.

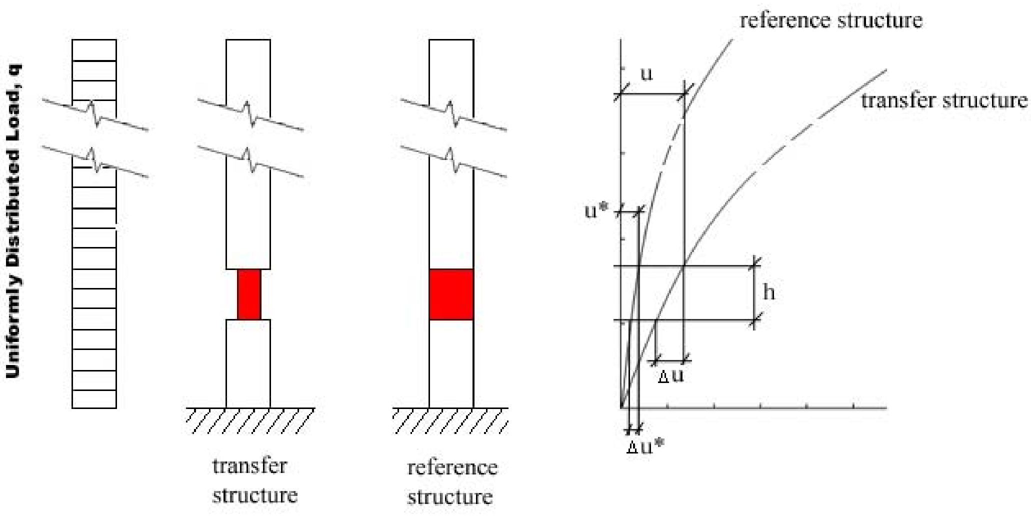

Figure 7.2 New approach of estimating the storey stiffness.

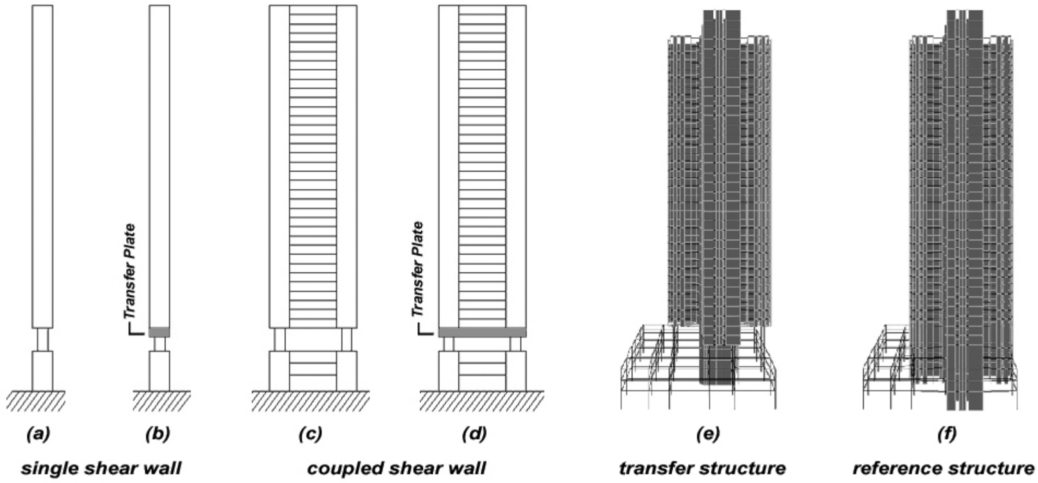

Figure 7.3 Numerical models.

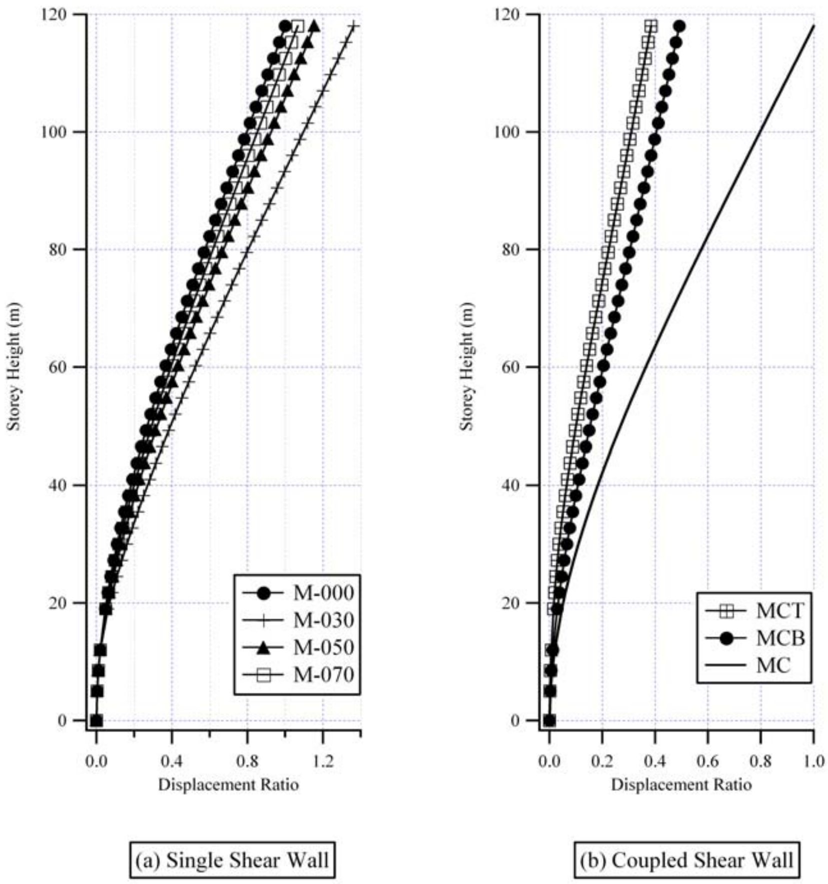

Figure 7.4 Deflection shape of the single shear wall and coupled shear wall structures.

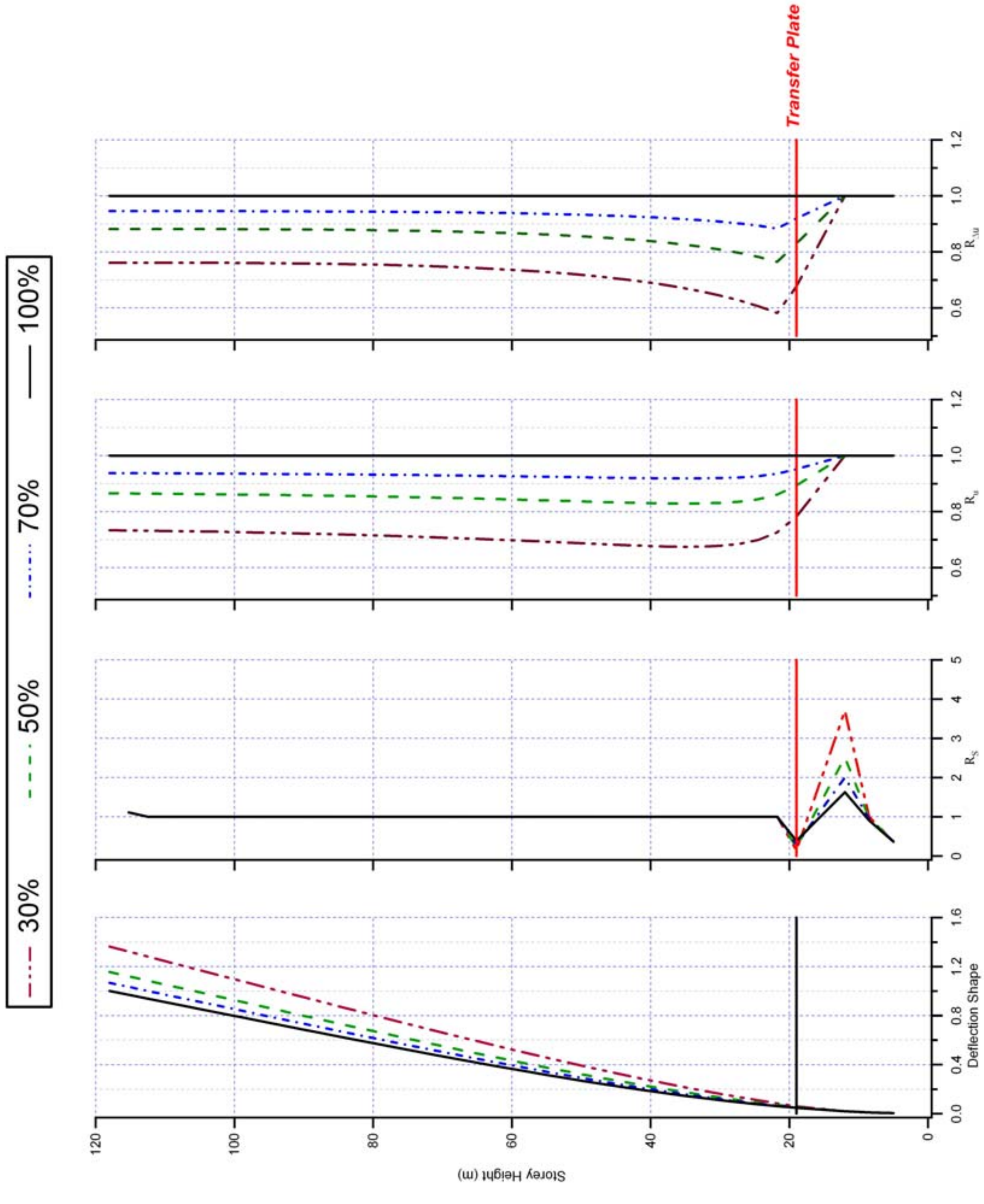

Figure 7.5 Comparison of the R_s, R_u and $R_{\Delta u}$ of single shear wall structures.

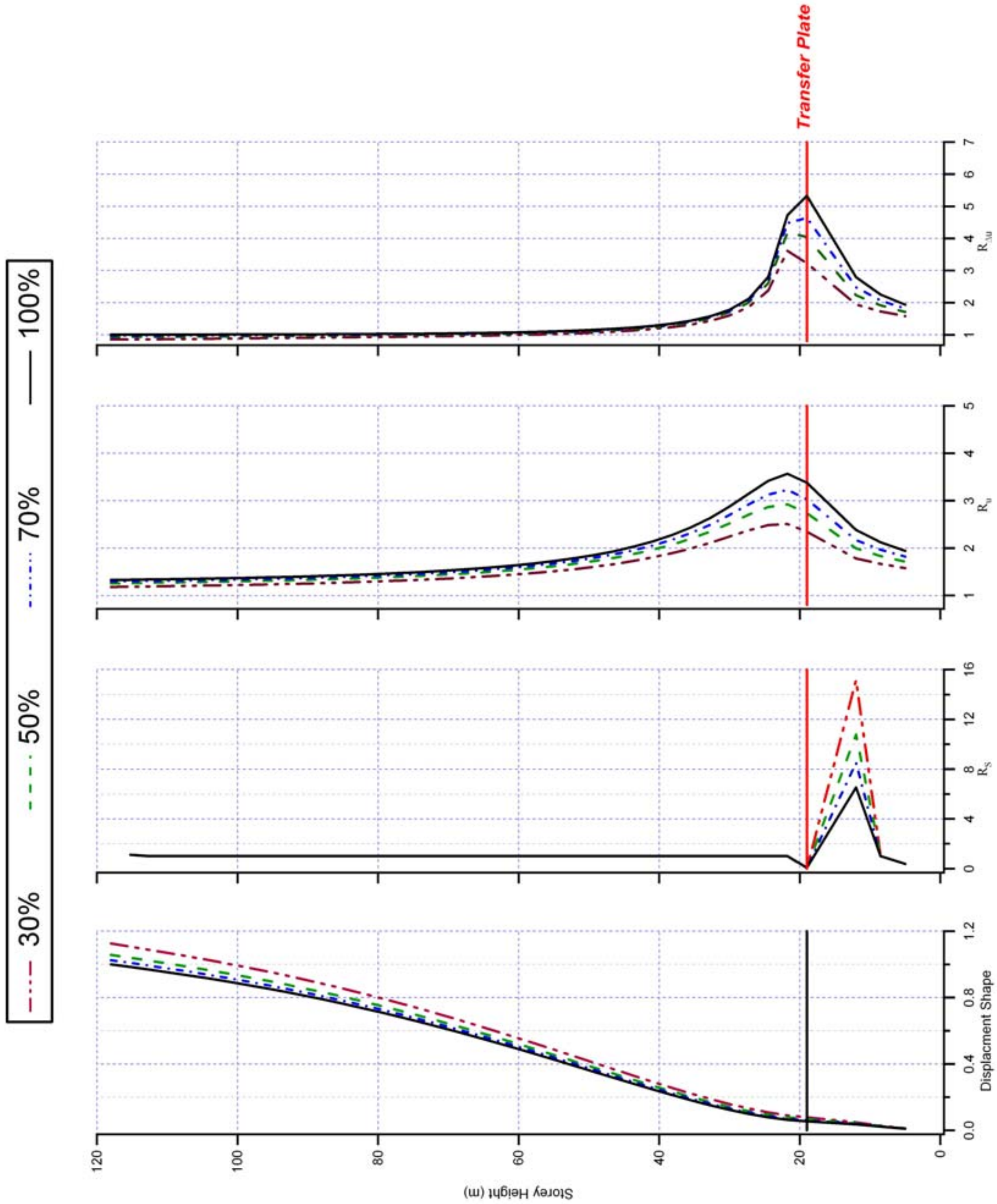

Figure 7.6 Comparison of the R_s, R_u and $R_{\Delta u}$ of coupled shear wall structures.

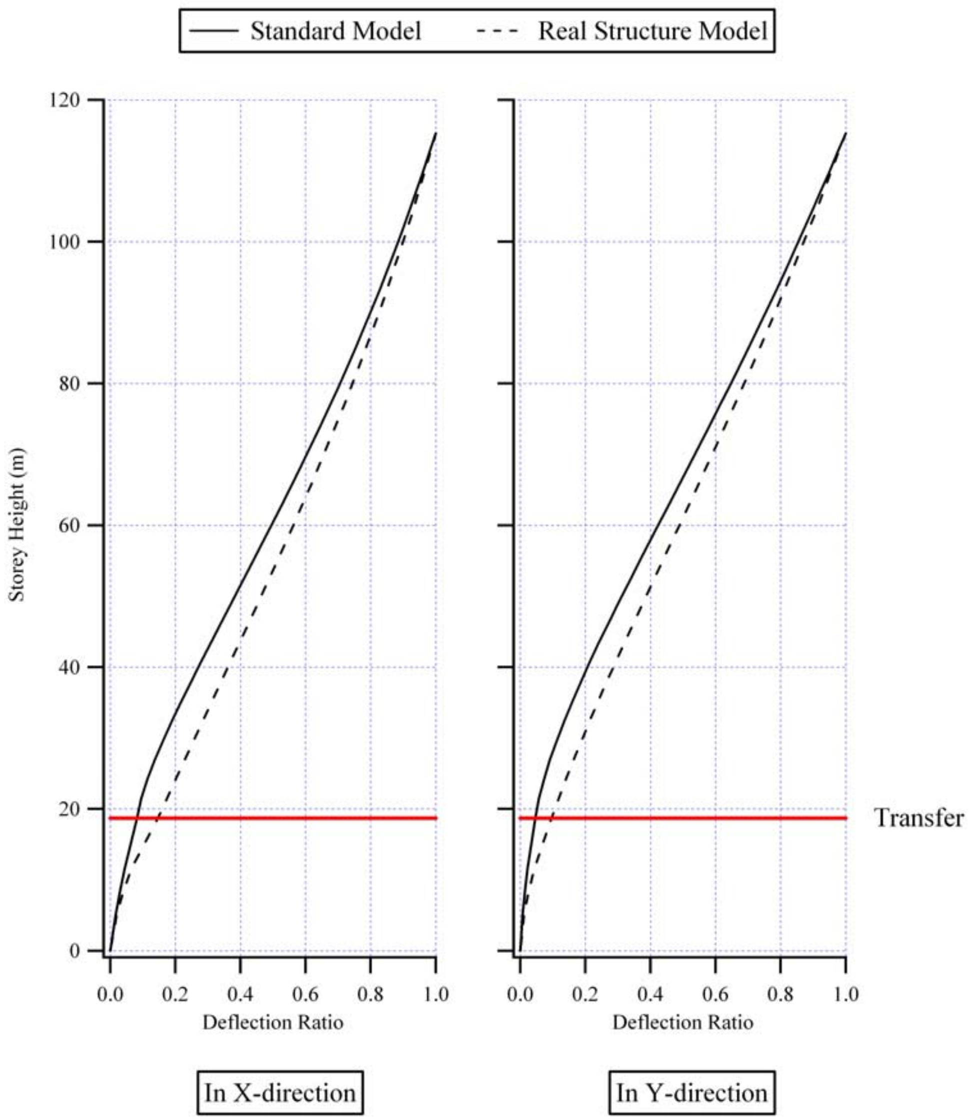

Figure 7.7 Deflection shape of typical residential high-rise building with a transfer plate.

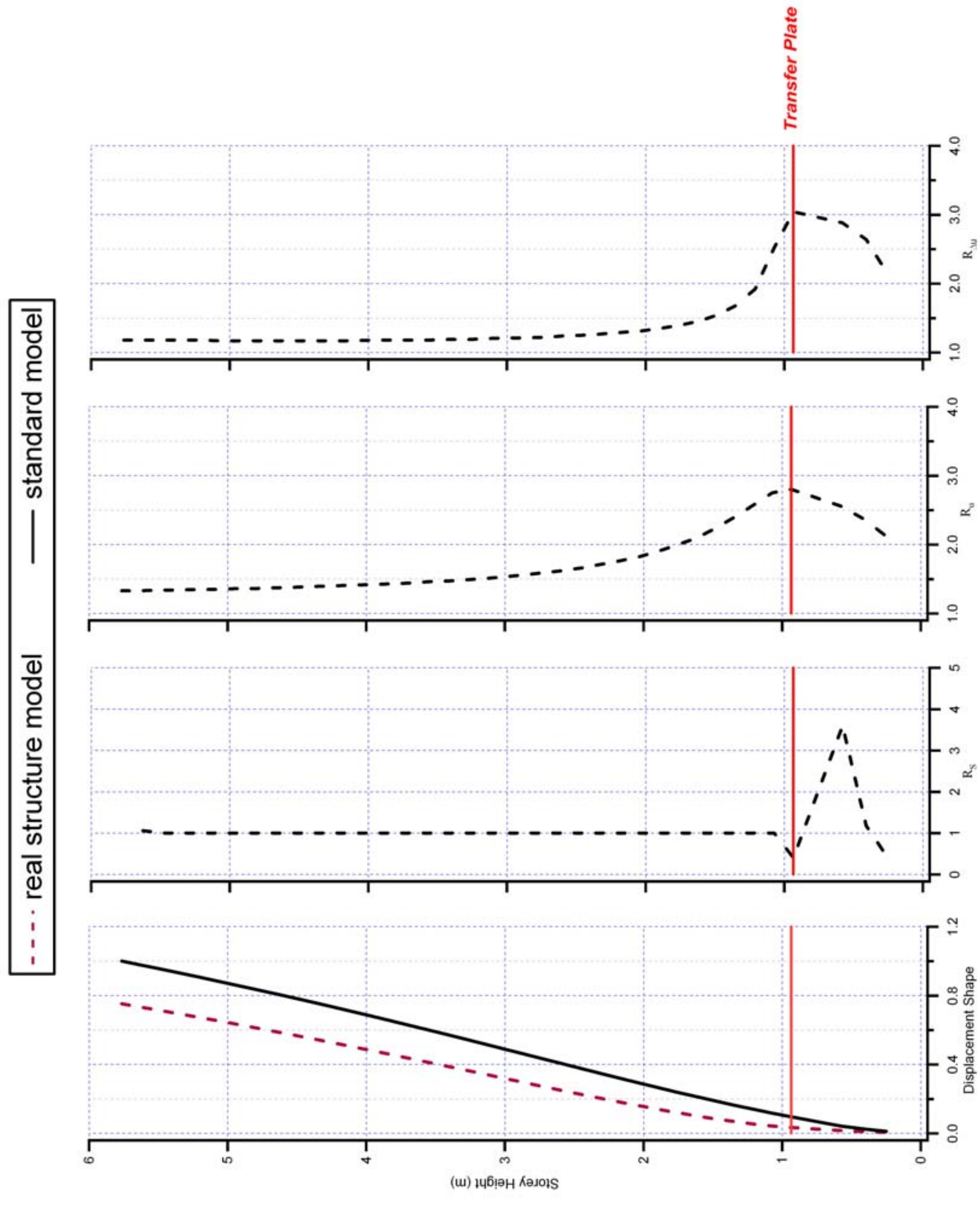

Figure 7.8 Comparison of the R_s, R_u and $R_{\Delta u}$ of a typical residential high-rise building with a transfer plate.

8 PSEUDO-DYNAMIC TEST OF HIGH-RISE BUILDING WITH A TRANSFER PLATE STRUCTURE

In regions without seismic resistance provisions, it is common to use a transfer plate as part of the structural system. In this study, pseudo-dynamic tests with sub-structure technique were conducted on a 1:4 scale test specimen representing the first two storeys of an 18-storey high-rise building with a transfer plate under earthquakes actions. Pseudo-dynamic tests were conducted in the Heavy Structural Laboratory of the Department of Civil & Structural Engineering of The Hong Kong Polytechnic University. Columns of the test specimen were strengthened to prevent them from failure under the pseudo-dynamic tests. Three types of time history records were applied, including triangular waves and a series of EI-Centro earthquake records. Based on the experimental results, it is predicted the bottom of the transfer plate will be severely damaged when subjected to an El-Centro earthquake record with maximum acceleration at 64%g.

The objective of this study was to assess the seismic performance of a transfer plate incorporated in an 18-storey high-rise building designed to non-seismic resistance requirements through a 1:4 scale test specimen. Pseudo-dynamic tests were implemented. It is a technique commonly used to predict and understand the response of structures when subjected to seismic attacks. Columns in the test specimen were strengthened to prevent them from failure under the pseudo-dynamic tests. Numerical models were developed using the commercial package, ABAQUS version 6.3.1. The purposes of the numerical studies are to verify the experimental results obtained from the pseudo-dynamic tests and to recommend practical means to represent possible damage.

In the last thirty years, pseudo-dynamic tests have been extensively developed for evaluating of the seismic performance of large scale structural models under earthquake actions. Development in recent years has already made the pseudo-dynamic testing method a reliable experimental tool. Among others, Shing and Mahin (1984) and Takanashi and Nakashima (1987) provided detailed description of the method. Nakashima *et al* (1992) developed a system capable of performing real-time pseudo-dynamic tests. Realistic dynamic response of the structural models are imposed by numerical computer simulation when performing the quasi-static test. Woo *et al* (1999) applied a pseudo-dynamic technique to evaluate the seismic performance of base-isolated structures with 1:4 scale. A full scale model of a four storey RC building was tested by Negro *et al* (1994). To facilitate the testing of a multi-degree-of-freedom system, a pseudo-dynamic testing system was developed and verified (Chen *et al* 2000). A substructure technique was used in this study to simply the test specimen.

8.1 THE PROTOTYPE BUILDING

The prototype building considered in this study is a reinforced concrete structure designed to non-seismic resistance requirement in accordance with BS8110:1985 and has 17 typical floors supported by a transfer plate and columns. A floor plan and elevation of the prototype building are shown in Figure 8.1 Loadings of the prototype building follow the Hong Kong Building (Construction) Regulations. The reinforced concrete transfer plate is 1.5 m thick with 0.7 % reinforcement. The typical floor plan consists of shear walls. The shear walls are 200 mm thick with 1.5 % reinforcement. Floor slabs at a typical floor are 160 mm thick with 1.55 % reinforcement. Below the transfer plate level, 900 × 900 mm square columns are used to support all the shear walls above the transfer plate level. The reinforcement ratio is 2.68 % for all columns.

The specified concrete grade for the transfer plate and columns is C40/20 concrete, i.e. having cube strength equals to 30 N/mm^2 and 20 mm maximum aggregate size. The specified concrete grade for shear walls and slabs is C30/20 concrete. The characteristic load at a typical floor is 6 kPa for dead load and 3 kPa for imposed load. The characteristic load for finishing and screeding at a typical floor is 5.4 kPa. The characteristic imposed load at the transfer plate is 15 kPa. The characteristic load for the waterproof system at the transfer plate is 5 kPa. Structural details and characteristic loads are given in Table 8.1.

8.2 TEST SPECIMEN

Using a substructure technique, the high-rise building was represented by a combination of numerical simulation and a test specimen as shown in Figure 8.2(a). The coupling effect of the floor slabs in storeys above the transfer plate is neglected in the test. Upper 16 storeys (3/F - 18/F) of the high-rise building are represented by numerical simulation using elastic beam elements. The test specimen included the ground floor, transfer (1/F) and one typical floor (2/F).

The size of the test specimen was limited by the capacity of the actuators and other factors, and it was designed to 1:4 scale, i.e. a length ratio (L_r) of 0.25. Plan and elevation of the 1:4 scale test specimen are shown in Figure 8.2. Strength of concrete specified in the test specimen was the same as in the prototype building. Using the similitude law, the frequency ratio of the model is 2 and the time ratio is 0.5. A half-model because of the symmetry of the prototype structure. Structural details of the test specimen are shown in Table 8.2. At the 2/F, a 40 mm thick slab is supported by a 100 mm thick shear wall, which combined the central 50 mm shear wall and two 25 mm half shear walls at the two sides. The shear walls in turn rest on the transfer plate. The transfer plate is 375 mm thick with 0.7 % main reinforcement. Below the transfer plate are evenly spaced columns of 225 × 225 mm square with 2.6 % reinforcement. The stirrup spacing is 75 mm. The reinforcement detail is shown in Figure 8.3.

The measured concrete cube strengths are listed in Table 8.2. Yield strengths of the high yield deformed bars and mild steel bars are 460 MPa and 250 MPa respectively. Two hydraulic actuators with different applied loading capacities were installed at the 1/F and 2/F floors as shown in Figure 8.2(c). Constant axial loads acting on the transfer plate and the columns were applied through two manually controlled hydraulic actuators. To restrain rotation of the transfer plate during application of the lateral displacements and to assess the axial load variation in the columns due to the coupling effect, four steel columns were used to act as roller supports as shown in Figure 8.2(b). These steel columns were installed after application of the axial loads. To prevent the columns from failure before the transfer plate, the columns were strengthened by epoxy-grouting.

Measurements included strains, displacements and reactions of the actuators. 37 strain gauges were installed to measure the strains in the reinforcement and concrete. 23 displacement transducers were installed to record the deformations.

8.3 TESTING PROCEDURE

Pseudo-dynamic tests were conducted using three types of loading histories as shown in Figure 8.4, namely triangular wave 1, triangular wave 2 and the NS component of the 1940 El Centro earthquake record. The similitude Law was used to scale the acceleration and time. Two triangular waves were used to check the response of the transfer plate and to verity the model. Finally, a series of El-Centro earthquake records with increasing magnitude of acceleration from 2%g to 64%g was applied. Peak accelerations of the earthquake excitations are listed in Table 8.3.

Sequence of the pseudo-dynamic tests is summarized in Table 8.4. Stage 0 is the control test with the objective of quantifying dynamic characteristic of the model. Stages 1 to 3 are the respective tests for three different sets of earthquake records including triangular wave 1, triangular wave 2 and EL-Centro records with different maximum values of acceleration.

8.4 CHARACTERISTICS OF THE TEST SPECIMEN

Before starting the pseudo-dynamic tests, a series of control tests was conducted to estimate the characteristic of the test specimen. The dynamic characteristic was quantified by using an impact load to evaluate the fundamental frequencies of the test specimen. Lateral stiffness of the 1/F and 2/F were determined by static loading tests.

The impact load was introduced by a hammer. The dynamic response of the structure is shown in Figure 8.5. A damping ratio ξ was also obtained from the free vibration curve,

$$\xi = \frac{1}{2\pi} \ln \frac{p_1}{p_2} \tag{8.1}$$

where p_1 and p_2 are the neighboring maximum responses.

The damping ratio of all the floors was estimated to be at 5%. Fast Fourier Transform (FFT) was carried out to determine the fundamental frequencies. The first mode of vibration of the test specimen is 10.89 Hz.

Two static loading tests were used to estimate the lateral load-displacement response of the test specimen at the 1/F and 2/F. During the tests, gravity load was applied and the lateral displacement at 1/F or 2/F was applied by the respective actuators. When lateral displacement was applied at the transfer plate level (1/F), the lateral displacement at the 2/F was fixed to zero. Vice versa, when lateral displacement was applied at the 2/F, the 1/F was fixed against any lateral movement by the actuator. All the upper floors were assumed to have the same stiffness as the 2/F, and were simulated numerically via the substructure technique.

8.5. EXPERIMENTAL RESULTS

8.5.1 OBSERVATIONS AFTER PSEUDO-DYNAMIC TESTS

After the application of the 700 kN vertical load at the top of the 2/F to simulate the gravity load, barely noticeable cracks were observed at the bottom of the transfer plate due to flexure. Figure 8.6 shows locations of the cracks at the bottom of transfer plate.

When the test specimen was subjected to the EI-Centro earthquake with maximum accelerations at 2%g and 4%g, there was no noticeable vibration. New cracks were not observed. When subjected to a maximum acceleration at 8%g, cracks which had previously appeared on the application of the applied load propagated with a slight increase in the crackwidths. Several new fine cracks were observed. A few diagonal cracks were observed on the transfer plate at the sides near the loading area due to the shear action. Under a maximum acceleration at 16%g, crackwidths increased and propagated. When subjected to a maximum acceleration at 32%g, the cracks cut through the transfer plate along the loading direction at the ends. This is probably due to the combined effects of shear and cyclic tension and compression of the shear wall on the top of transfer plate. Shear cracks were also observed at both ends of the transfer plate. The new cracks generated as a result of 32%g earthquake were easily noticeable with fully developed crackwidths. However, no cracks were observed in columns and walls. When the maximum acceleration was increased to 64%g, the test specimen was severely damaged and lost most of its load carrying capacity without collapse. Extensive increase in crackwidths and propagation of the cracks were found. New cracks were found on the bottom of the transfer plate near column heads. Table 8.5 and Figure 8.7 summarize the extent of damage at various levels of earthquake excitations.

8.5.2 SEISMIC RESPONSES OF TEST SPECIMEN

Figure 8.7 shows the seismic responses of the test specimen at the transfer (1/F) and 2/F. Displacement responses of the test specimen are virtually proportional to the maximum acceleration. When the high-rise building was attacked with the maximum acceleration equal to or less than 32%g EI-Centro earthquake, the time-history records of applied forces and lateral displacements at the 1/F and 2/F were in-phase with each other. Cracks at the bottom of the transfer plate increased. No damage to columns and shear walls were observed. There appeared to be no appreciable change in the lateral stiffness of the two floors. Under 64%g EI-Centro earthquake, the time-history records of applied forces and lateral displacements at the 1/F and 2/F are not in proportion to the responses at lower level accelerations and the lateral displacements at the 1/F and 2/F are out-of-phase as compared with the other EI-Centro earthquake records. Extensive structural damage was observed at the bottom side of the transfer plate.

Table 8.6 shows peak values of the lateral inter-storey displacement at the 1/F and 2/F when subjected to various maximum acceleration of the EI-Centro earthquake. The maximum inter-storey displacements at 1/F and 2/F are 0.24 mm and 0.18 mm respectively for the 2%g EI-Centro earthquake attacks. They increase to 12.15 mm and 7.88 mm respectively for the 64%g EI-Centro earthquake attacks. Inter-story drifts of the test specimen are virtually proportional to the maximum acceleration of the EI-Centro earthquake.

The correlations between the observed damage at the transfer plate and inter-storey drifts estimated from the displacement measurements are compiled in Table 8.7. There is a strong connection between the deformation in terms of inter-storey drift and the extent of structural damage, and the inter-storey drift is a useful indicator to provide some insight on the location of structural damage.

In considering the equation of motion of a simple single degree-of-freedom system in the form of

$$M\ddot{u} + Ku = 0 \tag{8.2}$$

The incremental form of equation (2) can be expressed as

$$M\Delta\ddot{u} + K\Delta u = 0 \tag{8.3}$$

or

$$K = \frac{M\Delta\ddot{u}}{\Delta u} = \frac{F}{\Delta u}, \quad \text{where} \quad F = M\Delta\ddot{u} \tag{8.4}$$

Therefore, plots of lateral loading “F” against displacement “Δu” provide a good indication on possible change in stiffness of the model and hence inelastic behaviour or damage. Figure 8.8 shows the load-displacement response at the 2/F. There is relatively no change in stiffness at the 2/F when subjected to the El-Centro earthquakes with maximum acceleration at 4%g, 8%g and 16%g. When the applied maximum acceleration of El-Centro earthquakes is greater than 32%g, there is considerable increase in the lateral displacement at the 2/F. From the observations, the shear wall was undamaged. The increase in the lateral displacement at the 2/F is due to the cracking of the transfer plate. The reduction in the flexural stiffness of the transfer plate increased the angle of rotation of the shear wall when seismic load was applied at the upper floors.

After the application of the 700 kN vertical load, the vertical displacement of the transfer plate at the centre of the wall was 2.19 mm. Figure 8.9 shows the increase in the vertical displacements at the centre of the transfer plate when subjected to the El-Centro earthquakes with maximum acceleration at 16%g, 32%g and 64%g. After 64%g, the vertical displacement of the transfer plate did not return to the initial configuration when unloaded. There was substantial structural damage at the transfer plate. The maximum increase in displacement of the transfer plate at the centre of wall is approximate 0.4 mm, leading to a maximum displacement at 2.59 mm.

Figure 8.10 shows variations of applied axial forces against the applied moments at the top of the columns. The variation in the axial force is due to the coupling effect between the transfer plate and the columns. This is simulated through the pseudo-dynamic procedure. Based on the experimental data and the numerical results, the columns collapsed when the building was attacked by a 32%g EI-Centro earthquake record. The solid lines indicated in figures represent the ultimate capacity of the column. As shown in dots are the estimated loading condition of the column based on the measurement at all the time intervals throughout the time history. As shown in the various interaction diagrams, failure of columns could have occurred at 32%g maximum acceleration if the columns had not been strengthened.

8.6 NUMERICAL MODELS

The various finite element models were constructed according to the 1:4 scale test specimen. Numerical models were developed and analysed using the commercial package, ABAQUS version 6.3.1. Figures 8.11 and 8.12 show two different types of model, namely "Model S" and "Model F", being used in the numerical analyses. Linear time history analyses were carried out under the EI-Centro ground acceleration earthquake records.

The test specimen was represented by "Model S" using three-dimensional finite elements. 5346 full integration 8-nodes brick elements were used to generate the columns, the transfer plate, the wall and the slab, as shown in Figure 8.11. Boundary conditions at the base were assumed to be in a fixed condition. Mass of the test specimen was incorporated in the form of self-weight.

Considering symmetry repeated geometry and loading patterns, "Model F" represents part of the prototype building in 1:4 scale. Figures 8.12 (a) and (b) show the elevation and 3D view of the numerical model which was generated using brick elements and shell elements. Floor to floor height at each typical floor is 715 mm. The thickness of the transfer plate is 375 mm and the size of each column is 225 x 225 mm. The thickness of the central wall, side walls and slab in each floor are 50, 25 and 40 mm respectively. Full integration 8-nodes brick elements were used to model the columns and transfer plate. The total number of brick elements used in columns and transfer plate were 1152 and 13728 respectively. All walls and slabs at typical floors (2/F-18/F) were modelled by full integration 4-nodes shell elements. At the typical floors, the dimensions were defined along the centrelines of the elements. The total number of shell elements used was 64260. Boundary conditions at the base were assumed to be fixed condition. Loadings were incorporated in the form of distributed mass acting on each floor.

8.7 ESTIMATION OF THE MODULUS OF ELASTICITY

“Model S” was used to estimate the Modulus of Elasticity of the test specimen. The measured concrete strengths of the test specimen are listed in Table 8.2. As an initial estimate, Modulus of Elasticity of concrete was determined by the BS 8110 short-term design stress-strain curve for normal-weight concrete and the poisson’s ratio of concrete is assumed to be 0.2. Minor adjustment of Modulus of Elasticity of concrete used in “Model S” are given in Table 8.8. Based on the numerical results, the first fundamental frequency of “Model S” was 10.80 Hz. This is close to the experimental result at 10.79 Hz. This was applied to “Model F” for subsequent time-history analysis.

8.8 NUMERICAL RESULTS

8.8.1 SEISMIC RESPONSE OF THE NUMERICAL MODEL

The finite element model “Model F” was used for linear analyses to estimate the deformation of the test specimen when subjected to various levels of El-Centro earthquake.

Time history analyses were conducted using the earthquake data used in the pseudo-dynamic test, see Figure 8.4. Simplified nonlinear analyses were conducted with the damage based on the observed damage of the test specimen in section 8.5. Based on the test data, the Modulus of Elasticity of the transfer plate was reduced to 0.3E for simulating the damage observed in the test. Figure 8.14 shows the seismic response at the 1/F and 2/F when the building was subjected to maximum accelerations of EI-Centro earthquake from 2%g to 64%g. Since the nonlinear behaviour of test specimen is simulated using linear elasticity time-history analysis, the displacement responses estimated from the numerical model are under-estimated when compared with the test data. The maximum displacement responses at the 1/F and 2/F estimated from the numerical analysis and test data were summarized in

Table 8.9 and Figure 8.15.

Better agreements are obtained at the transfer (1/F). Due to the inherited limitation of the simplified method of analysis, the analysis has neglected any plastic deformation cumulated during the hysteresis behaviour. As a result, the predicted values are smaller than the actual displacements. Modification factors are introduced to estimate the actual displacements in this type of structure. The structural system consists of reinforced concrete shear walls for the storeys above transfer plate and columns for the storey below transfer plate. Structural damage was observed at the transfer plate when the building was subjected to various level of EI-Centro earthquake excitations. The maximum displacement estimated using finite element approach through a linear elastic time-history analysis has to be increased by a factor of 2 for the 2nd floor and 1.2 for the storey below the transfer plate when the building was subjected to maximum accelerations of EI-Centro earthquake from 16%g to 64%g.

Table 8.10 and Figure 8.16 compare the inter-storey drifts estimated at the 1/F and 2/F from the numerical analysis with the test data. Due to the inherited limitation of the simplified method of analysis, the analysis has neglected any plastic deformation cumulated during the hysteresis behaviour. To estimate the maximum actual inter-storey drift by using the finite element model, the modification factors applied on the numerical results are 1.7 for the 2^{nd} floor and 1.2 for the storey at the transfer plate when maximum acceleration equal to or greater than 16%g of EI-Centro earthquake actions.

8.8.2 STOREY STIFFNESS

Two finite element models, namely “Model F” and “Model R”, have been used to estimate the change in storey stiffness due to the transfer plate (1/F). The finite element models are shown in Figures 8.12 and 8.13. “Model R” is a reference model. The reference model allows all the shear walls above the transfer to continue down to the foundation, with the removal of all the columns below transfer and without the transfer plate. Results of the lateral stiffness at the transfer plate (1/F) and the 2/F are shown in Table 8.11.

In this study, R_s is 14.1% and is significantly less than the code requirements, i.e. a minimum of 70%. Earlier studies have indicated that use of R_s may not be appropriate for high-rise building when flexural stiffness is also important (Li *et al*, 2003). As an alterative, two other indications are considered, displacement ratio (R_u) and drift ratio ($R_{\Delta u}$), values of R_u and $R_{\Delta u}$ at transfer are about 1.14. Accordingly, it is suggested that the soft-storey may not occur in the structural response.

8.9 CONCLUDING SUMMARY

The main objective of this study is to quantify the seismic performance of a transfer plate in a high-rise building through pseudo-dynamic tests. An 18-storey building has been designed with no seismic resistance provisions. A test specimen in ¼-scale was used to represent the lower storeys. Pseudo-dynamic tests using the substructure technique were conducted using three types of time-history records. The shear walls remained elastic throughout the loading histories, whereas the transfer plate was severely damaged when subjected to an El-Centro earthquake record with a maximum acceleration at 64%g. The main damage occurred at the transfer plate. Nevertheless, The transfer plate may have sufficient strength to resist any possible earthquake action that could be expected in a moderate seismic region, i.e. a 16%g EI-Centro earthquake. However, there is insufficient seismic resistance if the maximum acceleration of EI-Centro earthquake is greater than 32%g.

A test specimen in ¼-scale was used to represent the lower storeys. Pseudo-dynamic tests with substructure technique were conducted using three types of time-history records. This study reports the use of simplified numerical models to predict damage and seismic performance. Linear time-history analyses are used to approximate the non-linear response of the structure. It is possible to reasonably predict the extent and locations of damage through such a simple procedure. The estimated displacements and storey drifts are smaller than those obtained from the pseudo-dynamic tests. Maximum displacements estimated using the finite element approach has to be increased by a factor of 2 for the typical floor and 1.2 for the transfer plate when the building is subjected to the maximum accelerations of EI-Centro earthquake from 16%g to 64%g.

Table 8.1 Structural detail and characteristic loads of the prototype building.

Floor Level	Structural System	Structural Details	% Reinforcement	Specified Strength of Concrete (MPa)	Characteristic loads		
					Imposed Load (kPa)	Partition, Screeding and Ceiling (kPa)	Dead Load (kPa)
Typical Floor (2/F-18/F)	Shear wall	200 mm thick	1.50	30	3.00	5.40	6.00
	Slab	160 mm thick	1.55				
Transfer Plate (1/F)		1500 mm thick	0.70	40	15.0	5.00	-
Ground Floor (G/F)	Column	900 mm × 900 mm	2.68	40	4.00	6.00	12.00

Table 8.2 Structural details of the test specimen.

Floor Level	Structure Member	Elements Size	Measured concrete strength (N/mm^2)	Modulus of Elasticity ($x10^6$ kN/m^2) (*estimated by following BS8110: 1985)	Detail of Main Reinforcement
2/F	Shear Wall	100 mm	32.9	25.77	Y12@50+R6@50+ Y12@50 Each face
	Slab	40 mm	32.9	25.77	R6@100 - Top & Bottom
Transfer plate (1/F)		375 mm	41.1	28.77	Y10@60 - Top & Bottom
G/F	Column	2 @ 225 mm × 225 mm	42.9	29.39	12Y12

Table 8.3 Earthquake records.

Earthquake	Peak acceleration	Period
Triangular wave 1	1%g - 2%g	3s
Triangular wave 2	1%g - 2%g	1s
El-Centro Record	2%g - 64%g	random

Table 8.4 Sequences of the shaking table tests.

Type of tests	Test no	Detail
Stage 0 – Control tests		
Model tests	1	Frequencies measurement of the test specimen
Static tests	2-3	Stiffness of 1/F and 2/F floors measurement with applied axial load
Stage 1 – Triangular wave 1 records tests		
Model tests	4-6	Pseudo-dynamic tests with 2 sets of records
Stage 2 – Triangular wave 2 records tests		
Model tests	7-8	Pseudo-dynamic tests with 2 sets of records
Stage 3 – El-Centro records tests		
Model tests	9-14	Pseudo-dynamic tests with 6 sets of records

Table 8.5 Observed damage.

Maximum acceleration of EI-Centro Earthquake	Observations and types of damage	Transfer Plate Condition
2%g -4%g	New cracks were not observed in transfer plate and column	Serviceable condition
8%g -16%g	New cracks were observed at the bottom of transfer plate	Serviceable condition
32%g	New cracks cutting through the transfer plate	Moderately damaged, no collapse and requiring repair
64%g	Structure was severely damaged at the bottom of the transfer plate	Severely damaged and no collapse

Table 8.6 Summary of maximum inter-storey displacement and inter-story drift.

	maximum inter-storey displacement (mm)		maximum inter-storey drift	
Maximum acceleration of EI-Centro earthquake record	1/F	2/F	1/F	2/F
2%	0.24	0.18	1/5729	1/3972
4%	0.62	0.47	1/2218	1/1521
8%	1.15	0.95	1/1196	1/753
16%	2.49	1.98	1/552	1/361
32%	5.69	3.92	1/242	1/182
64%	12.15	7.88	1/113	1/91

Table 8.7 Relationship between structural damage and inter-storey drift.

Description of transfer plate damage on the transfer plate	Inter-storey drift at 2/F
No damage	1/1500
Slight damage	1/750
Moderately damage	1/360
Severely damage	≥ 1/180

Table 8.8 Material properties used in finite element models.

Floor Level	Structure Member	Density of Concrete (kg/m^3)	Modulus of Elasticity (x 10^6 kN/m^2)	
			BS8110: 1985	Numerical model
2/F-18/F	Shear Wall	2.334	25.77	24.60
	Slab	2.334	25.77	24.60
Transfer plate (1/F)		2.416	28.77	28.40
G/F	Column	2.334	29.39	28.40

Table 8.9 Summary of maximum displacement (mm) at 1/F and 2/F.

Maximum acceleration of EI-Centro earthquake	Numerical Model		Experiment Data	
	1/F	2/F	1/F	2/F
2%	0.15	0.30	0.24	0.36
4%	0.59	0.59	0.62	1.03
8%	1.18	1.18	1.15	2.02
16%	2.37	2.37	2.49	4.29
32%	4.73	4.73	5.69	9.31
64%	9.47	9.47	12.15	19.63

Table 8.10 Summary of maximum inter-storey drift (mm) at 1/F and 2/F.

Maximum acceleration of EI-Centro earthquake	Numerical Model		Experiment Data	
	1/F	2/F	1/F	2/F
2%	0.15	0.15	0.24	0.18
4%	0.59	0.29	0.62	0.47
8%	1.18	0.58	1.15	0.95
16%	2.37	1.16	2.49	1.98
32%	4.73	2.33	5.69	3.92
64%	9.47	4.66	12.15	7.88

Table 8.11 Comparisons of R_s , R_u and $R_{\Delta u}$.

	Stiffness of storey ($\times 10^6$ kN/m)	R_s	R_u	$R_{\Delta u}$
2/F	1.5601	-	-	-
Transfer (1/F)	0.2204	0.141	1.149	1.149

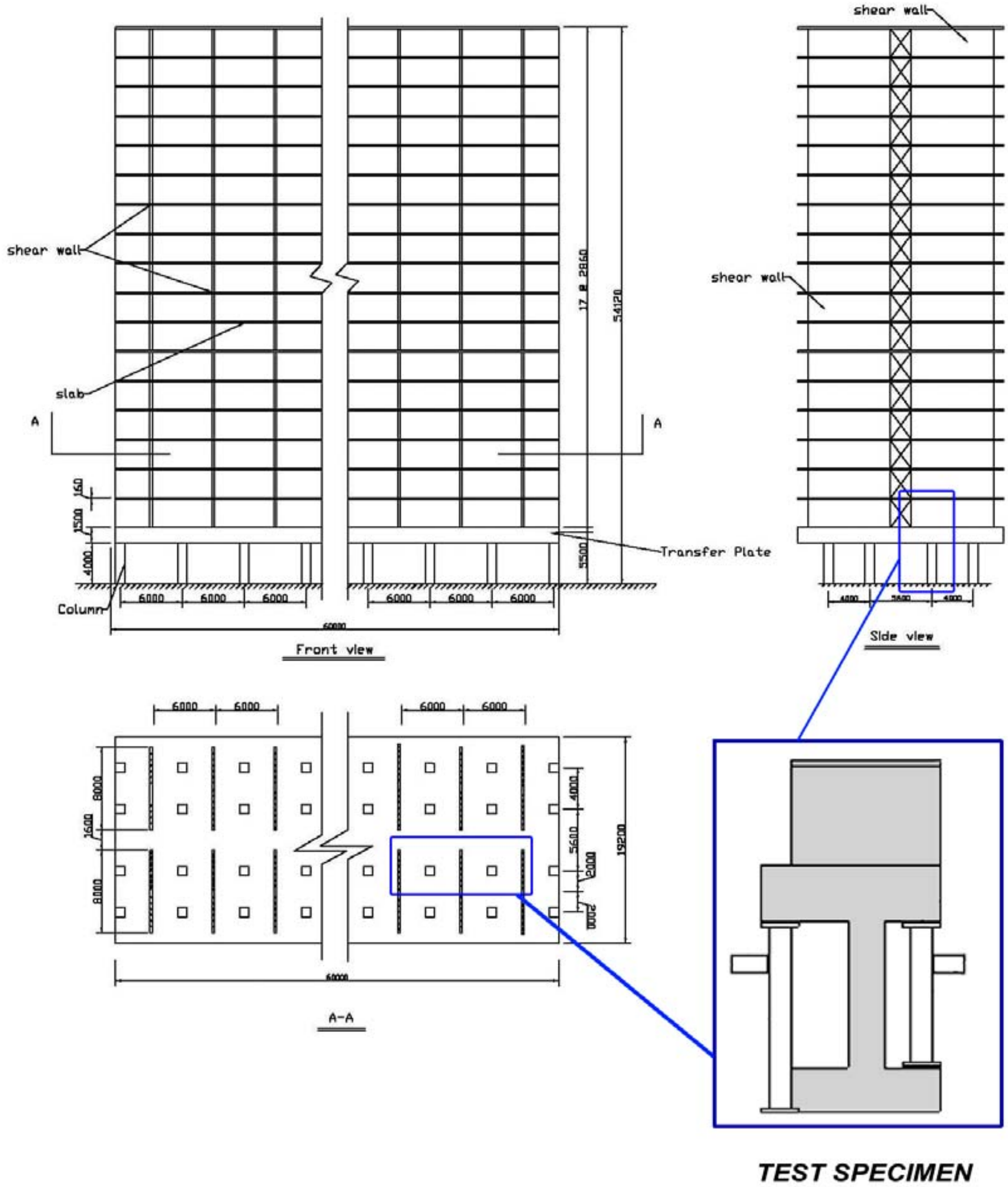

Figure 8.1 18-storey building with a transfer plate at the first floor.

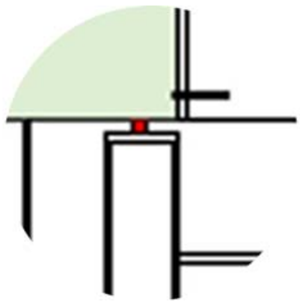

(b) Details of a roller at the corner of transfer plate.

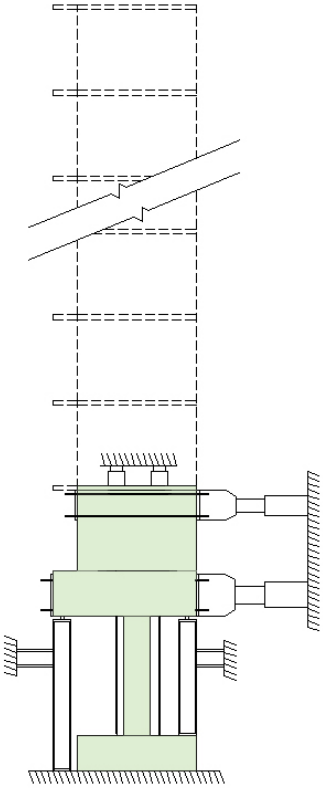

(a) Numerical simulation (in dotted line) and the test specimen.

(c) Test specimen.

Figure 8.2 Experimental set-up of the test specimen.

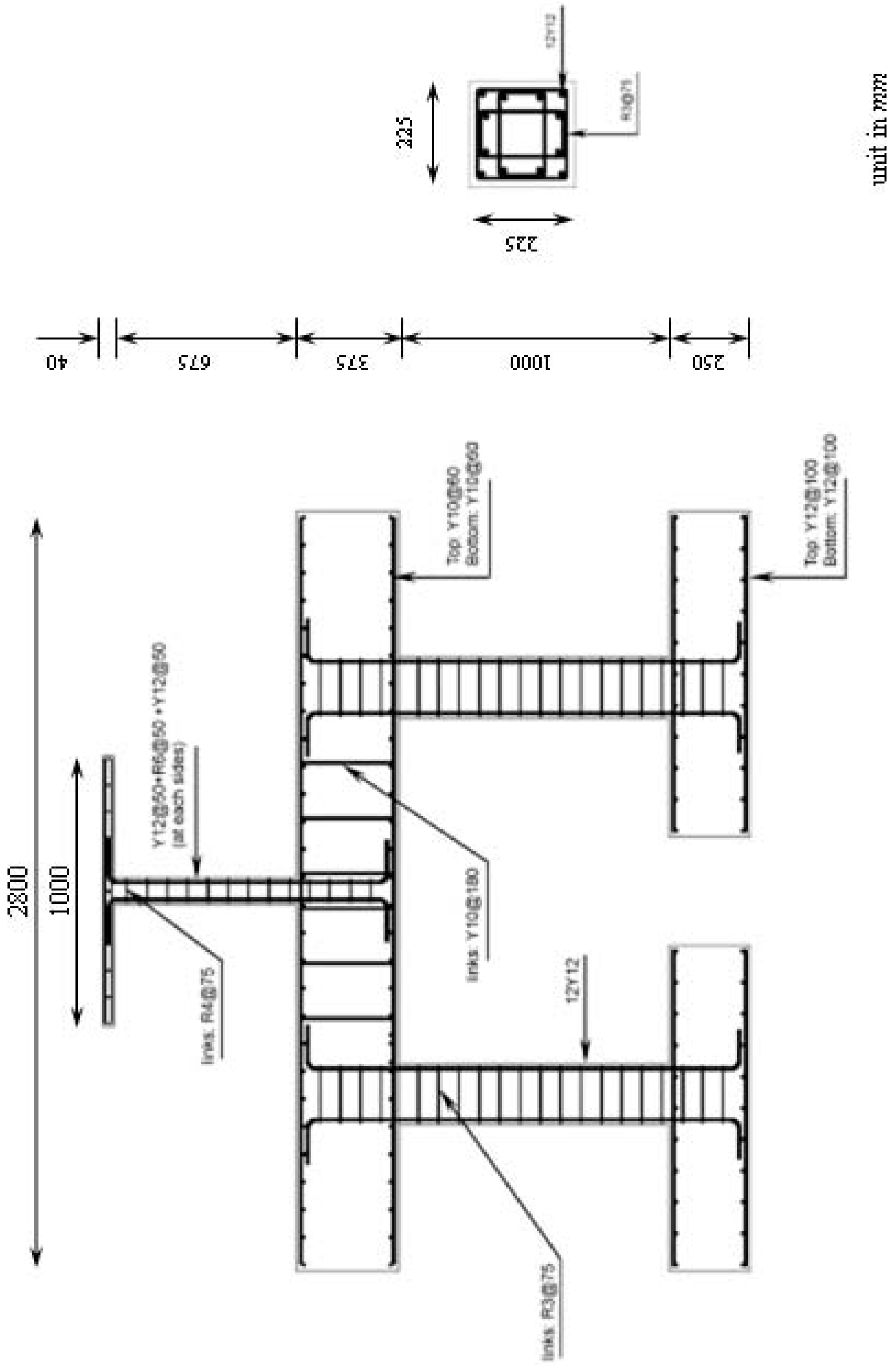

Figure 8.3 Reinforcement details of the test specimen.

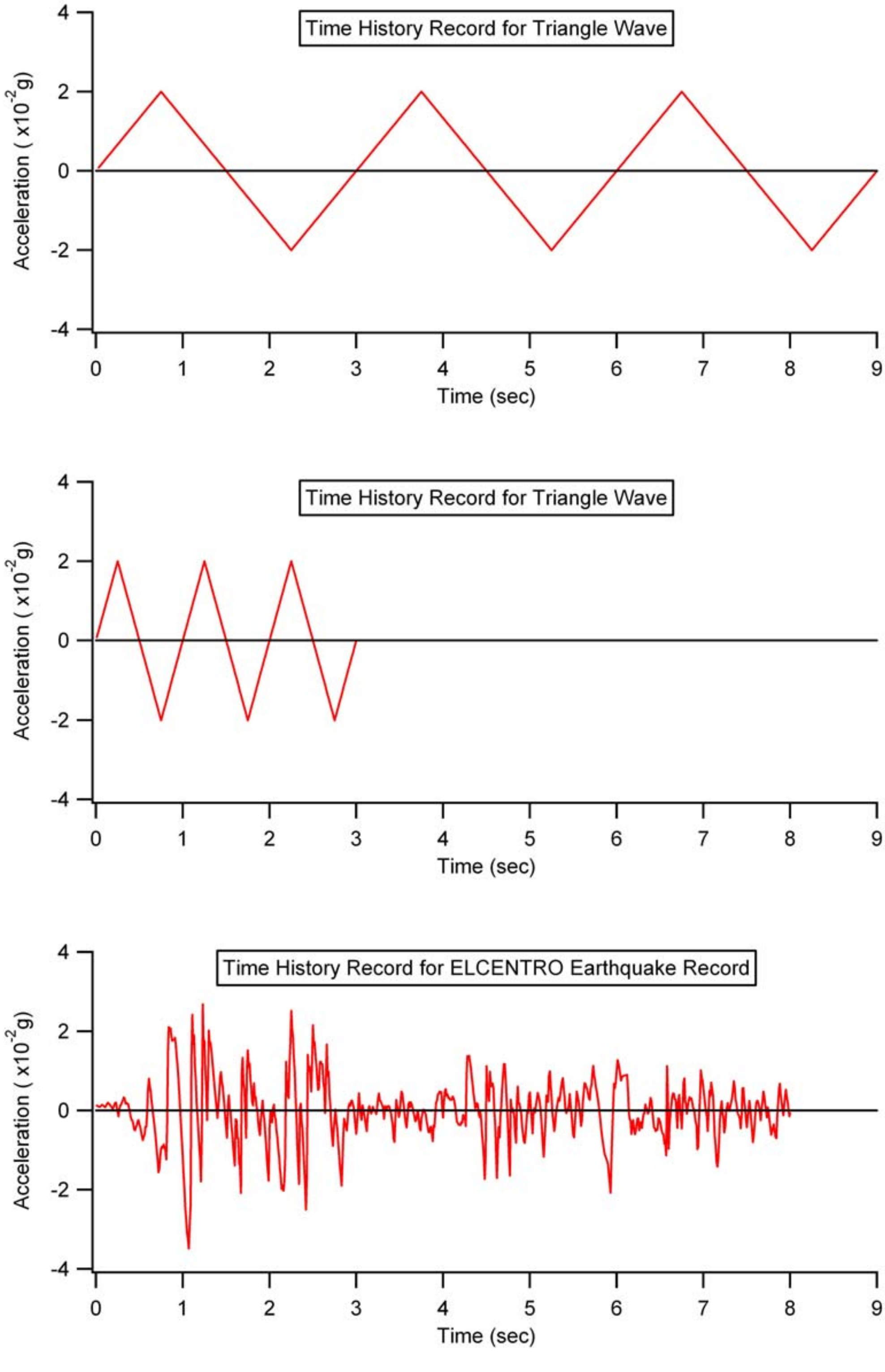

Figure 8.4 Time-history records.

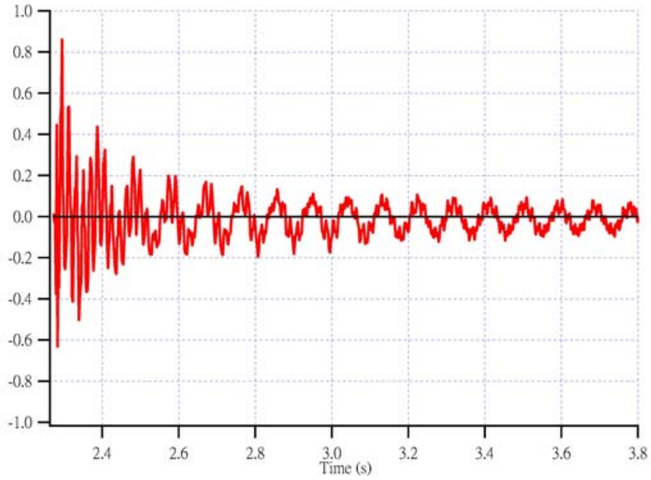

(a) Elastic dynamic response of the test specimen

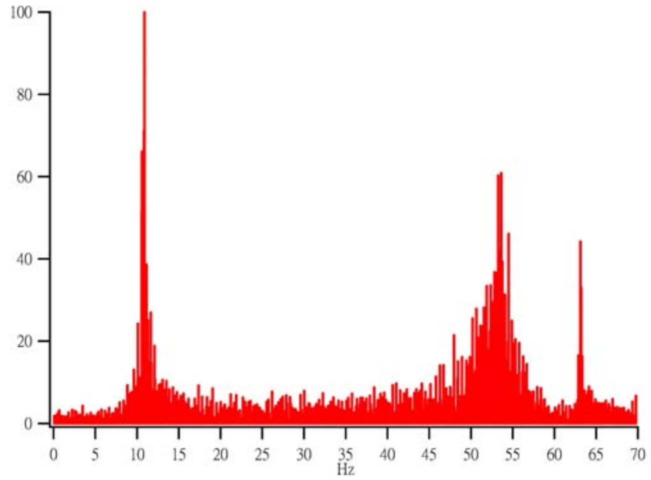

(b) FFT analysis result

Figure 8.5 Dynamic behaviour of the test specimen under impact load test.

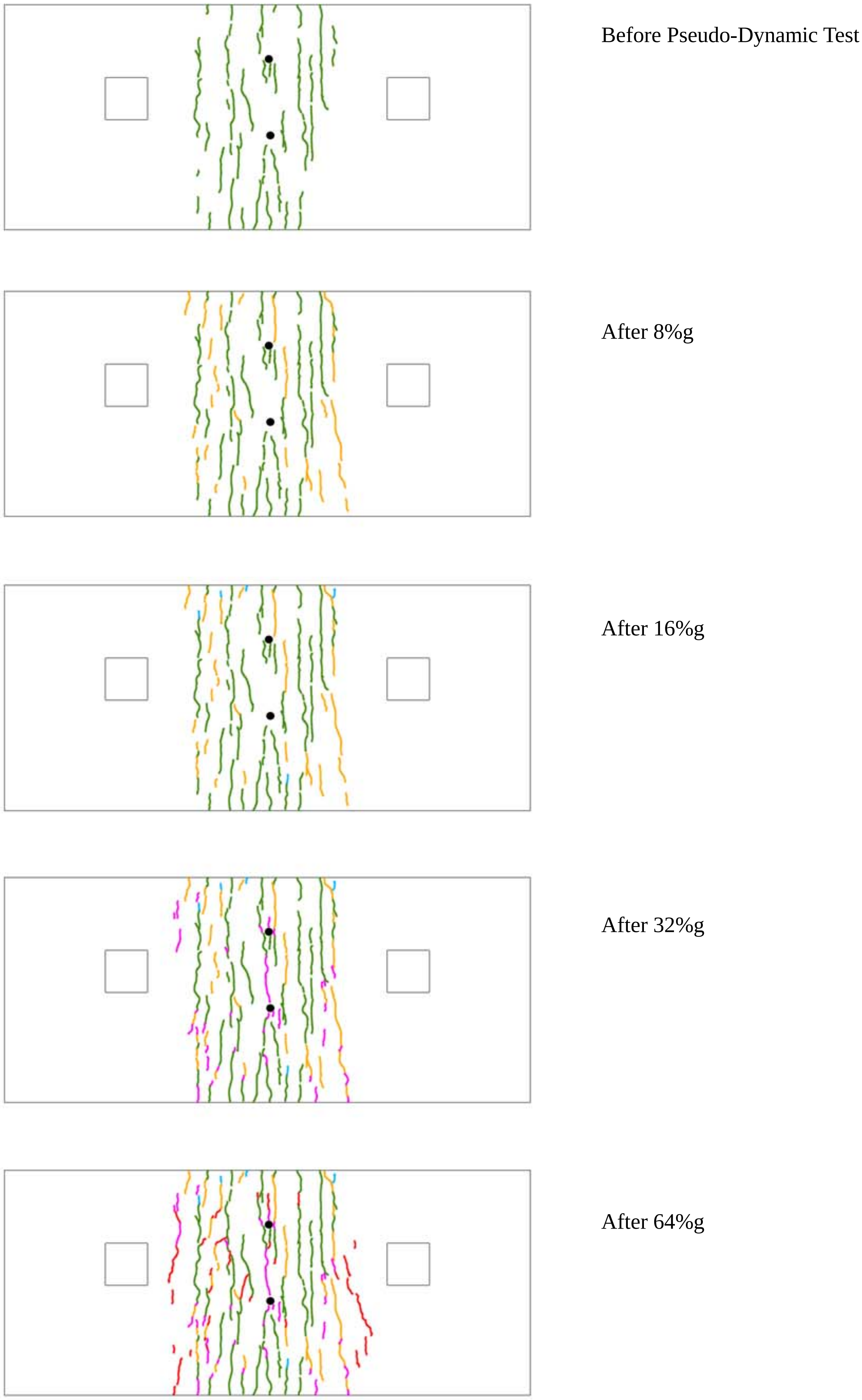

Figure 8.6 Cracking sequence at the bottom of transfer plate.

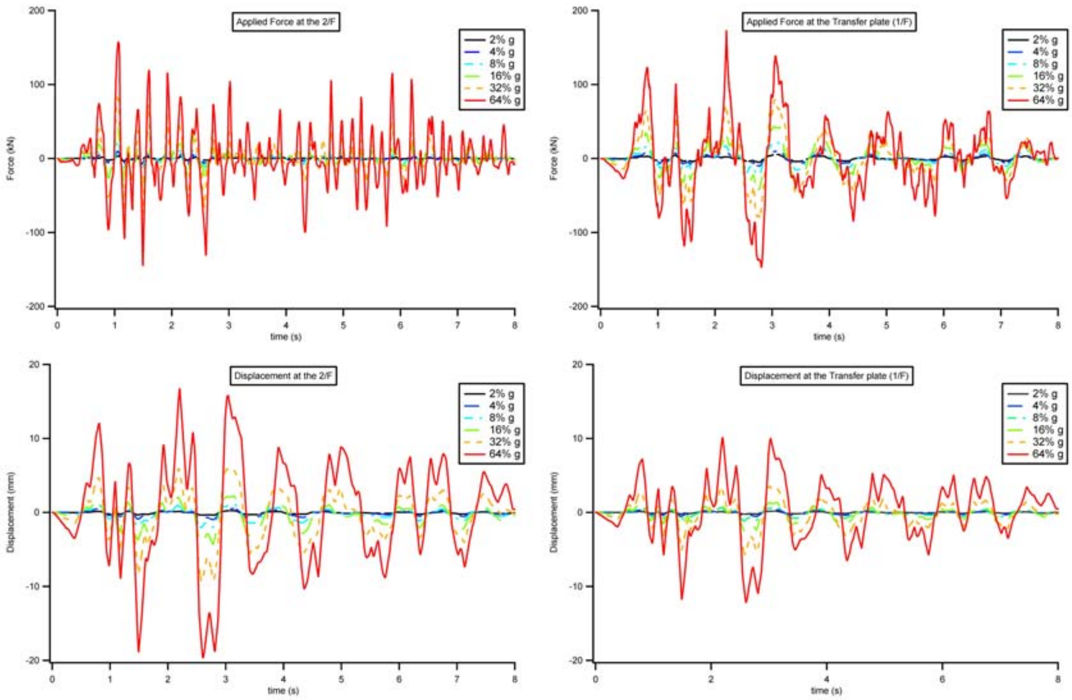

Figure 8.7 Applied force and lateral displacement at the 1/F and 2/F.

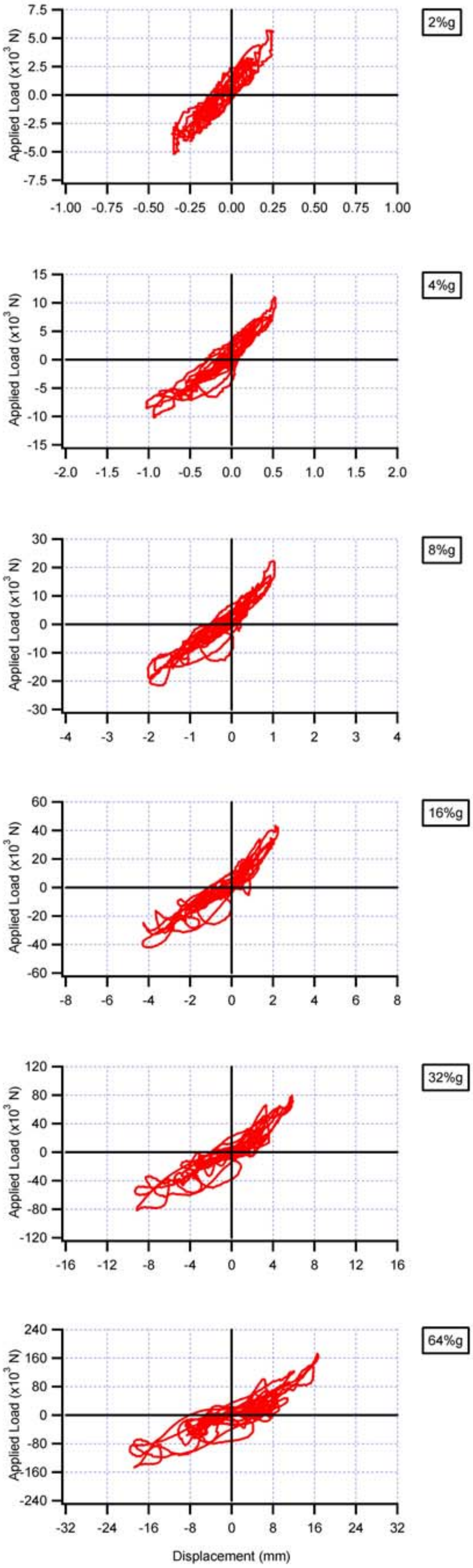

Figure 8.8 Hystereses of the 2/F when subjected to El-Centro earthquakes.

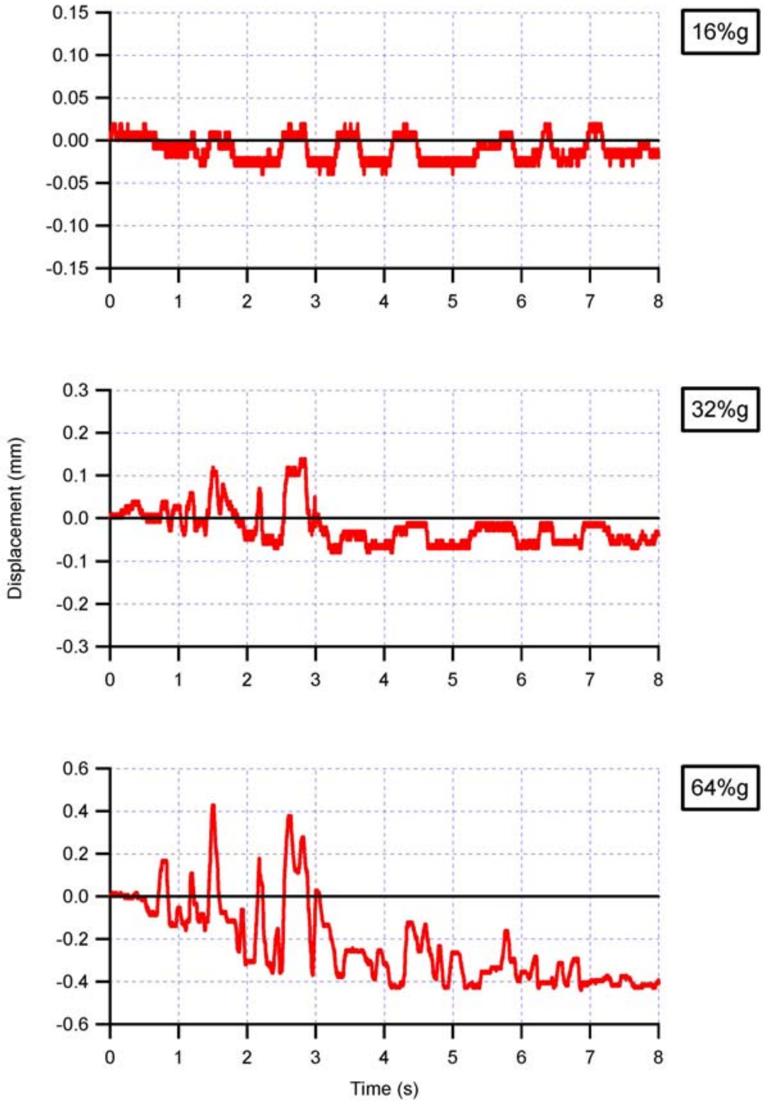

Figure 8.9 Additional vertical displacement at the transfer plate when subjected to El-Centro earthquakes.

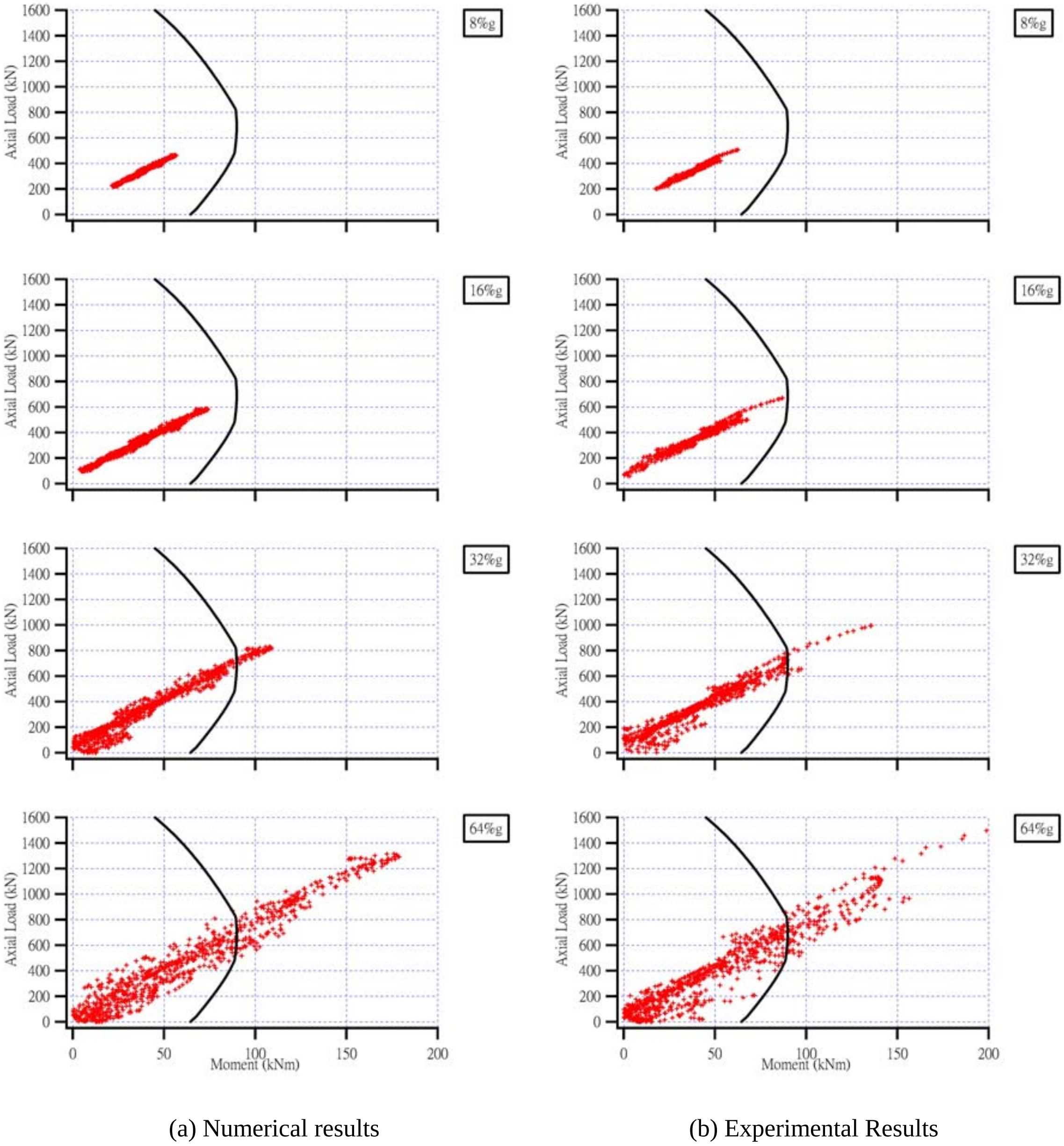

Figure 8.10 Axial force-moment plot at the top of column.

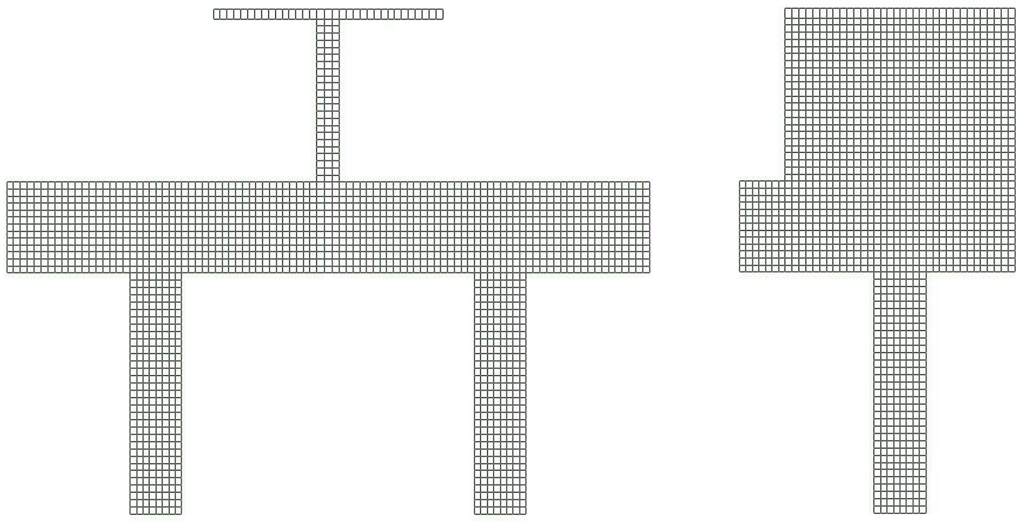

(a) Front View. (b) End View.

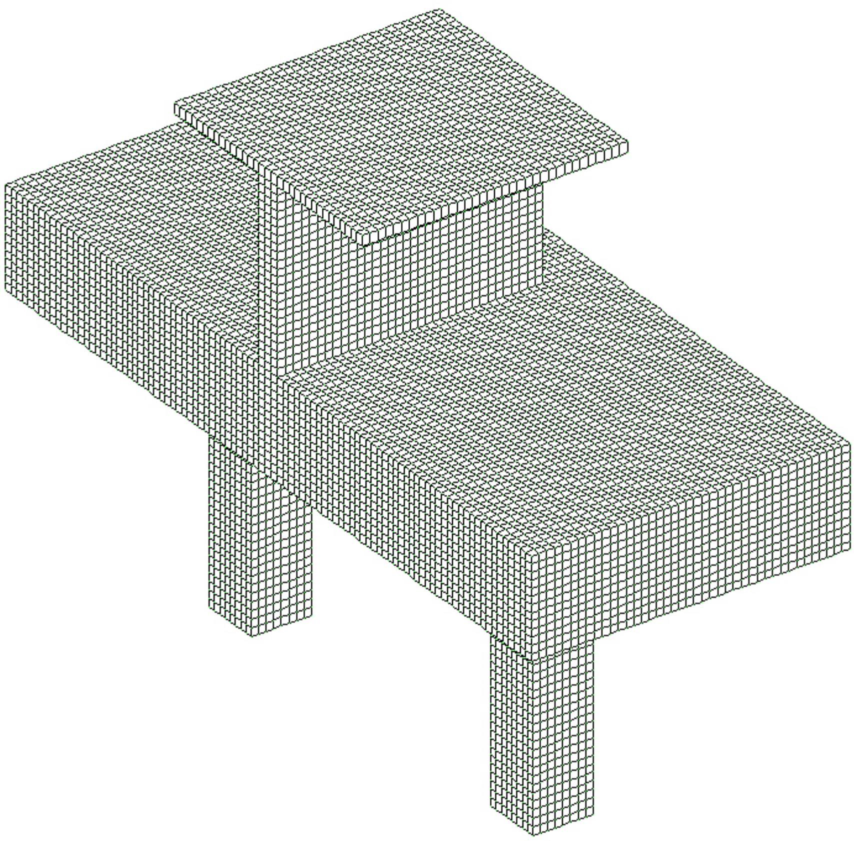

(c) 3D view of finite element model.

Figure 8.11 Finite element model – “Model S”.

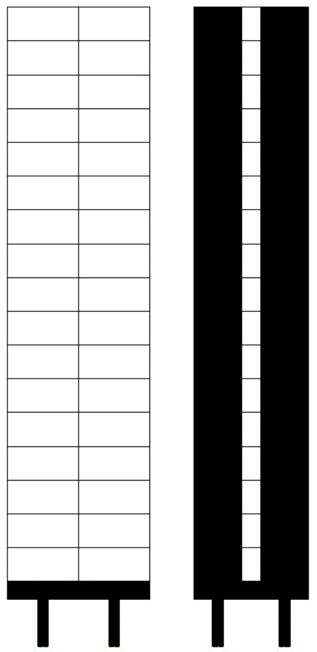

(a) End Views of Repeated Unit.

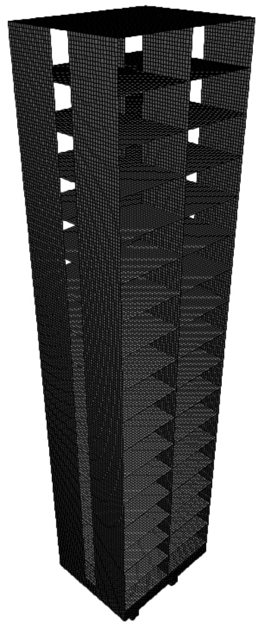

(b) 3D view of ABAQUS model.

Figure 8.12 Finite element model – “Model F”.

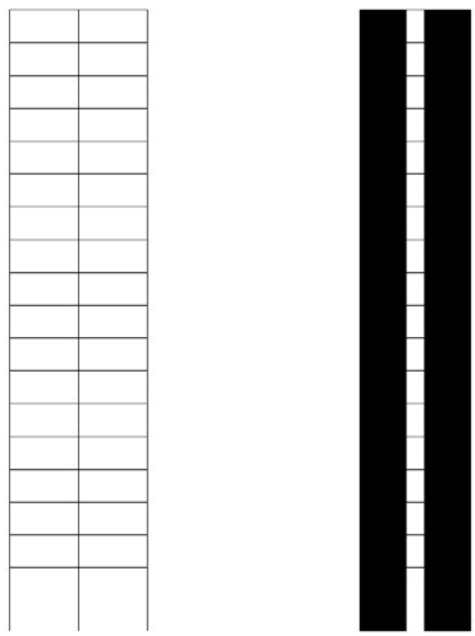

Figure 8.13 Finite element model – “Model R”.

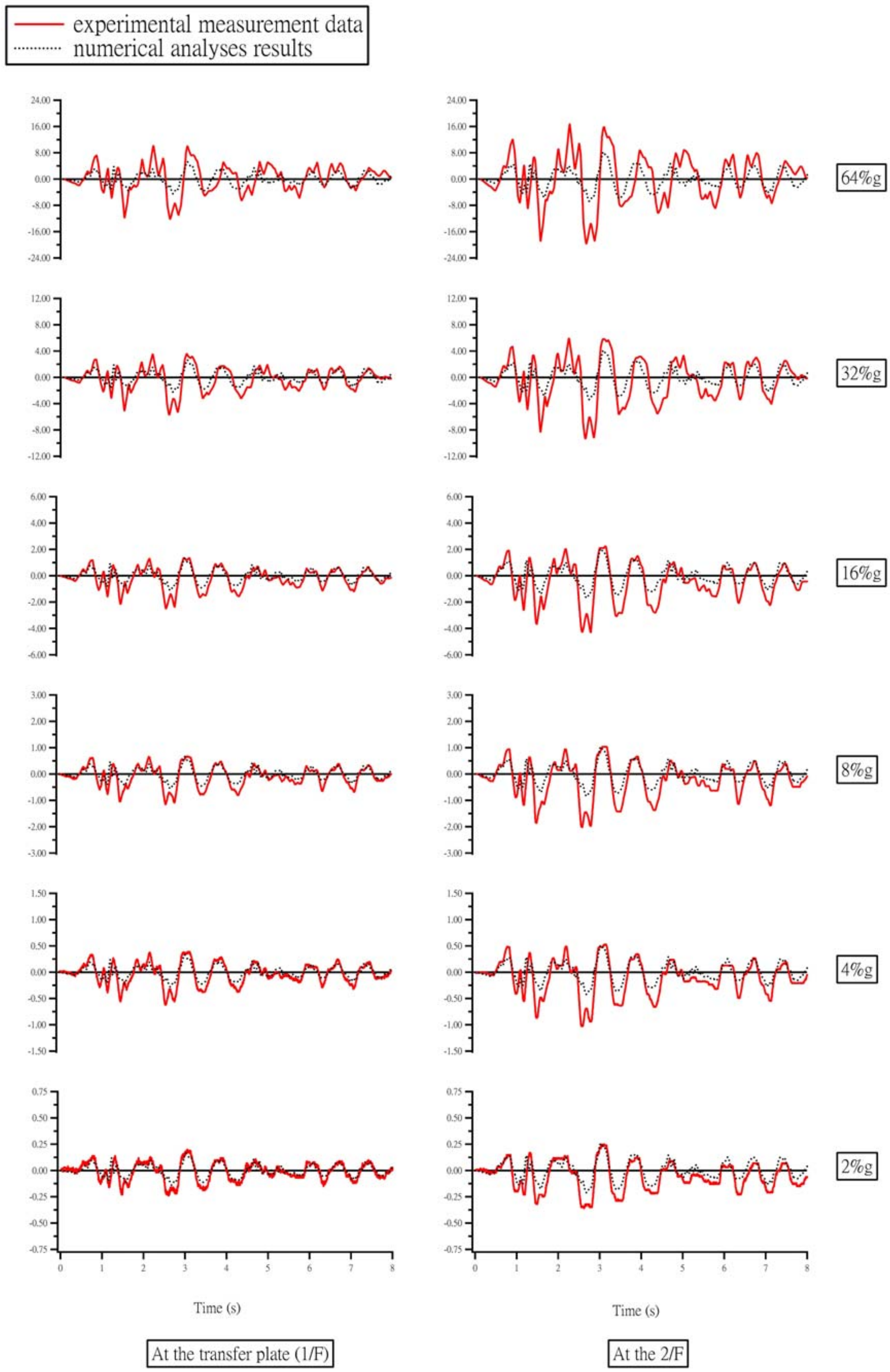

Figure 8.14 Comparison of the experimental and numerical results.

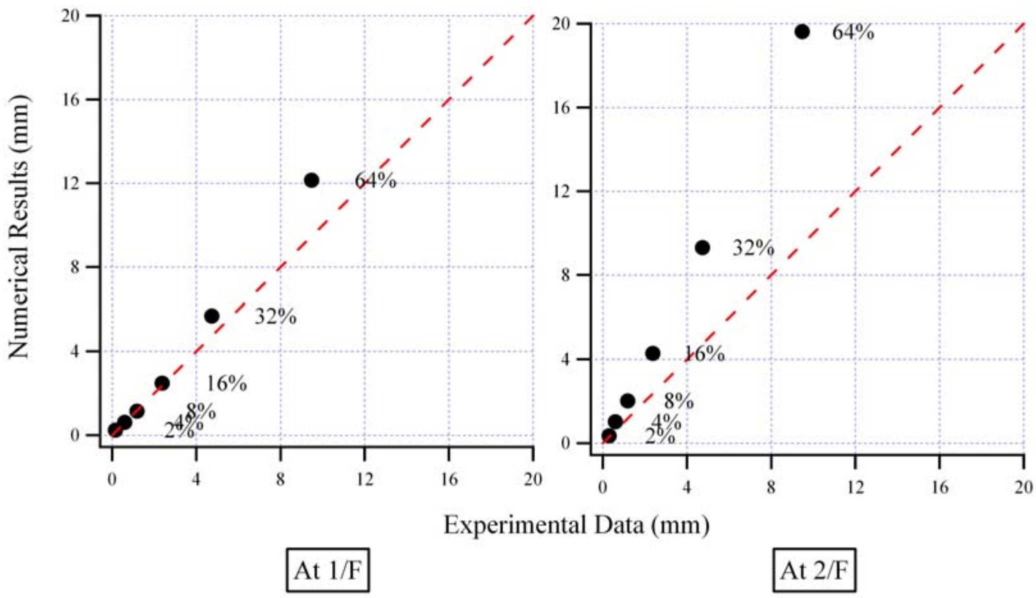

Figure 8.15 Comparison maximum displacements of the experimental and numerical results.

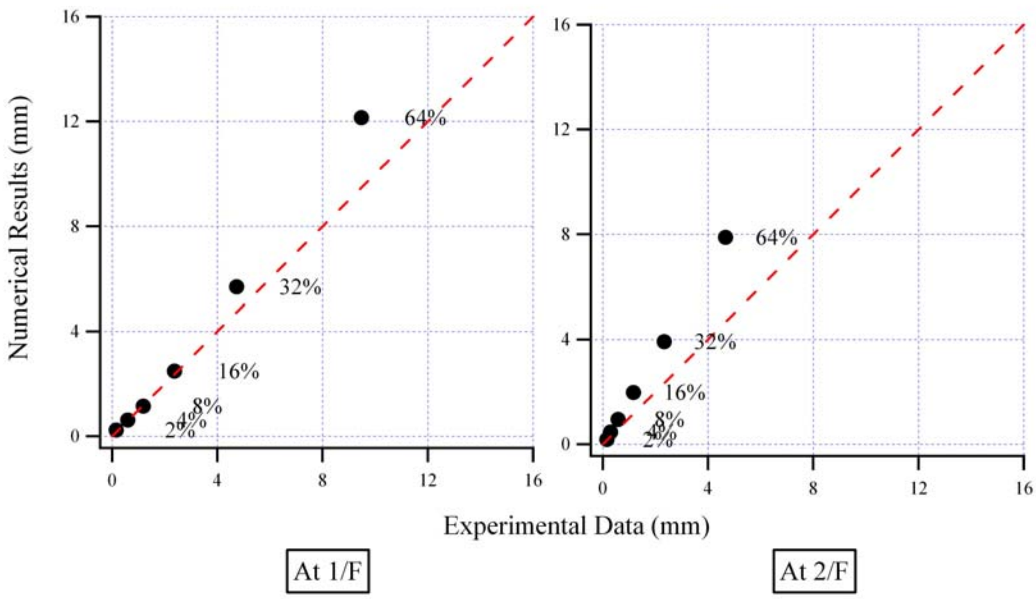

Figure 8.16 Comparison maximum inter-storey drift of the experimental and numerical results.

9 CONCLUSIONS AND FURTHER RESEARCH

This research study intended to quantify the seismic capacity of a typical residential high-rise building with a transfer plate using numerical analysis. The typical high-rise building is designed with no seismic resistance provision and has a transfer plate system. Based on this, numerical analysis and experimental studies were used to predict and understand the behaviour of structures. Furthermore, the interaction between the transfer plate system, upper floors and supporting structures has also been investigated. Several major findings have been made as described in next section.

9.1 SUMMARY OF CONCLUSIONS

In regions without seismic resistance provisions, it is common to use transfer plates as part of the structural system. The main objective of this study is to quantify the seismic capacity of a typical residential high-rise building with a transfer plate through numerical analysis. In all studies, the building structures were subjected to static lateral loads and subjected to earthquake attacks. Responses were estimated by using linear elastic analysis. The buildings were assumed to be located in a region with the basic seismic intensity categorized as VII degree.

Two experiments were undertaken in this study. The first was the testing of a 1:20 scale model that was conducted by the Laboratory of Earthquake and Engineering Vibration of the Institute of Engineering Mechanics, China Seismology Bureau in Harbin. It was fabricated and tested on a shaking table under various levels of earthquake excitations to indicate the dynamic characteristic of the high-rise building with a transfer plate structure. The other was conducted in this study and was pseudo-dynamic tests of 1:4 scale test specimen representing the first two storeys of an 18-storey high-rise building with transfer plate under earthquakes actions. The key findings of this study are described as follows:

1. In comparing the numerical analyses and the experimental results, the finite element approach is able to predict the deformation of structures accurately if the structures remain elastic. The estimated lateral responses of the structure using the finite element approach were different to those of the simplified un-coupled approach. Thus, the simplified un-coupled method of analysis

over-estimates the lateral response of the high-rise wall-frame structure.

1. In the finite element approach, the modelling of floor slabs are important to predict the lateral response of the high-rise wall-frame structures, because the slabs provide connection between the two separated side walls, and storey stiffness of the structure increases due to the coupling effect with the slabs.

2. A new analysis approach has been accordingly introduced to replace the simplified un-coupled approach. This is an advanced simplified un-coupled approach. The coupling effect of floor slabs in the buildings is considered based on increasing the modulus of elasticity of the material used in the numerical model. The general modification factors due to the coupling effect of floor slabs are 1.2 for the low-rise beam and column frame buildings, 2 for a low-rise core wall and column frame buildings and 1.7 for a high-rise wall-frame buildings. The transfer plate in the advanced simplified-coupled model is recommended located at the top level of the transfer plate.

3. From the shaking table tests, the high-rise building appears to have sufficient strength in resisting strong earthquake action at seismic intensity VII. However,

there is insufficient seismic resistance for super-strong earthquakes. Major damage and failure of the model occurred at the storey above the transfer plate. The central core is a key structural element in providing the seismic resistance. The connections between the central core and the periphery walls appear to be relatively weak and insufficient.

4. From the shaking table tests, the advanced simplified un-coupled models were also used to predict the damage and seismic performance. In this study, extent and location of damage observed in the numerical results was estimated using a simple non-linear analysis. Nonlinear behaviour was approximated through a series of linear time-history analyses. Inelastic behaviour was taken into account by reducing the stiffness of damaged members. Non-linear material behaviour must be incorporated in the analysis. In comparing the numerical analyses and experimental results, the numerical model using the simplified non-linear analysis can predict the first occurrence of damage on a high-rise building with a transfer plate. It is possible to reasonably predict the extent and locations of damage through such a simple procedure.

5. The estimated displacements and storey drifts were smaller than those obtained from the shaking table tests. For members that are severely damaged or in the vicinity of failure, actual storey drifts will be about 2 and 4 times the estimated values. Such modification factors should accordingly be applied to the estimated results.

6. Pseudo-dynamic tests using the substructure technique were conducted. A test specimen in ¼-scale was used to represent the lower two storeys. The upper storeys (3/F to 18/F) are assumed remain elasticity though the numerical simulations process. The transfer plate appears to have sufficient strength in resisting the maximum acceleration of EI-Centro earthquake action at 16%g.

7. From the pseudo-dynamic tests, the simplified numerical models using finite element approach were used to predict the damage and seismic performance. Nonlinear behaviour was approximated through a linear time-history analyses. It is possible to reasonably predict the locations of damage through such a simple procedure. The estimated displacements and storey drifts from the numerical model are smaller than those obtained from the pseudo-dynamic tests. Based on the structural system consists of columns at the storey below the

transfer plate and the structural damage with different seismic level of the EI-Centro earthquake records was observed in the transfer plate. The maximum displacement estimated using the finite element approach, has to be increased by a factor of 2 for the typical floor and 1.2 for the transfer plate when the building was subjected to the EI-Centro earthquake with the maximum acceleration at 16%g or greater. Such modifications should be accordingly applied to the estimated numerical results.

8. Based on the damage and failure mechanisms observed from the shaking table tests and pseudo-dynamic tests, it is concluded the mode of failure in high-rise building with transfer plate is different from that in a low-rise building with a soft-storey. The seismic performance of a high-rise building with a transfer plate can be estimated by numerical analysis. Bending stiffness at the transfer plate is still significant due to the coupling of the columns by the relatively thick transfer plate.

9. Based on the current methods used for the classification of a "soft-storey" are not appropriate for that storey just below the transfer plate in a high-rise building structure, a second new analytical approach is developed and used in

this study. It is recommended to use the displacement ratio (R_u) and storey drift ratio ($R_{\Delta u}$), to indicate the mode of failure. If the displacement ratio or storey drift ratio are smaller than 1, “softy storey” failure mechanism at storey below the transfer plate may occur.

10. Lastly, based on all finite element analysis results obtained in this study, it is well demonstrated that structural behaviour of the transfer plate itself can be classified as rigid. Therefore, a rigid floor assumption is recommended for use in the analysis of a high-rise building with a transfer plate.

9.2 LIMITATION OF THE PRESENT STUDY AND SUGGESTION FOR FURTHER RESEACH

The type of high-rise buildings involved in this study was limited to reinforced concrete residential buildings with the structural layout based on the “Harmony Block” shape. All the analyses conducted in this study were based on linear time-history analysis with limited number of earthquake records used in the study.

For further research study, other types of buildings with different structural layout should be investigated, e.g. commercial buildings and industrial buildings …etc. Different types of earthquake records should be considered in the linear time-history analysis. The non-linear material properties should be incorporated to predict the seismic response of a high-rise building with a transfer plate.

10 REFERENCES

Ahmed, Sk. Reaz., Idris, ABM. and Uddin, Md. W. (1995). "Numerical Solution of Both Ends Fixed Deep Beams." *Computers and Structures*, 61(1), 21-29.

Aoyama, H. (2001). "RC High-rise Buildings in Seismic Areas", Editor Aoyama, H., *Design of Modern High-rise Reinforced Concrete Structures*, Imperial College.

Archer, F. E. and Kitchen, E. M. (1960). "Stress Distributions in Deep Beams." *Civil Engineering and Public Works Review*, 55, 230-234.

ASCE-ACI Committee 445 (1998). "Recent Approaches to Shear Design of Structural Concrete." *Journal of Structural Engineerin*g, 124(5), 1375-1417.

Ashraf, A. F. (1997). "Test on Reinforced Concrete Continuous Deep Beams." *ACI Structural Journal*, 94(1), 3-12.

Averbuch, D. and Buhan P.d (1999). "Shear Design of Reinforced Concrete Deep Beams: A Numerical Approach." *Journal of Structural Engineering*, 125(3), 309-318.

Belarbi, A. and Hsu, T. T. C. (1994). “Constitutive Laws of Concrete in Tension and Reinforcing Bars Stiffened by Concrete.” *Structural Journal of the American Concrete Institute*, American Concrete Institute, 91(4), 465-474.

Belarbi, A. and Hsu, T. T. C. (1995). “Constitutive Laws of Softened Concrete in Biaxial Tension-compression.” *Structural Journal of the American Concrete Institute*, 92(5), 562-573.

Blondet, J. M., Clough R. W. and Maphin S. A. (1980). *Evaluation of Shaking Table Test Program on Response Behavior of a Two Story Reinforced Concrete Frame*, Report No. UCB/EERC-80/42, EERC, University of California, Berkeley, California.

BS8110:1985 (1985). *Structural Use of Concrete*, British Standards Institution, London, United Kingdom.

Carr, A. J. (1998). *RUAUMOKO – Inelastic Dynamic Analysis*, Department of Civil Engineering, University of Canterbury.

Chen, A., Lam, S. S. E. and Wong, Y. L. (2000). “Verification of a Pseudodynamic Testing System.” *Proceedings of the Int. Conf. on Advances in Structural Dynamics*, Hong Kong, 2, 851-858.

Code of Practice on Wind Effects Hong Kong (1983), Building Authority, HKSAR Government.

Code of Practice for the Structural Use of Concrete (1987), Building Authority, HKSAR Government.

Coull, A. (1966). “Stress Analysis of Deep Beams and Walls.” *The Engineer*, 22, 310-312.

Eurocode No. 2 (1991). *Design of Concrete Structures, Part 1: General rules and rules for building*, Thomas Telford, London.

Elwood, K. J. (2001). *Gravity Load Collapse of Reinforced Concrete Frames*, CE 229 Report, University of California Berkeley.

Foster, J. Stepthen and Malik, R. Andnan (2002). “Evaluation of Efficiency Factor Models Used in Struct-and-Tie Modeling of Nonflexural Members.” Journal of Structural Engineering, 128(5), 569-577.

Foster, J. Stepthen (1998). “Design of Nonflexural Members for Shear.” *Cement and Concrete Composites*, 20, 465-475.

Foster, J. Stepthen and Gilbert, R. Ian (1996). “The Design of Nonflexural Members with Normal and High-Strength Concretes.” *ACI Structural Journal*, 93(1), 3-10.

Foster, J. Stepthen and Gilber, R. Ian (1998). “Experimental Studies on High-Strength Concrete Deep Beams.” *ACI Structural Journal*, 95(4), 382-390.

GB50011-2001 (2001). *Code of Seismic Design of Buildings*, National Standard, Beijing, China.

GBJ11-89 (1989). *Code of Seismic Design of Buildings*, National Standard, Beijing, China.

Goh, T. C. A (1995). “Prediction of Ultimate Shear Strength of Deep Beams Using Neural Networks.” *ACI Structural Journal*, 92(1), 28-32.

Ho W. M. (1999). “62层高江长中心之设计与施工.” *第四届中日建筑结构技术交流会*,大连, 239-244.

Hong Kong Construction (Building) Regulations (1997). *The Laws of Hong Kong*, HKSAR Government.

Howard, O. J. Taylor (1972). "Shear Strength of Large Beams." *Journal of the Structural Division*, 98, 2473-2490.

Huang, X., Zhou, F., Xu, Z., Liu, W. and Luo, X. (2002). "Study on Seismic Simulator Experiment of Super High-rise Structure with High Transfer Story." *Proceedings of the International Conference on Advances and New Challenges in Earthquake Engineering Research*, Hong Kong Conference, 15-17 August 2002.

Hwang, S. K. and Yun, H. D. (2004). "Effects of Transverse Reinforcement on Flexural Behaviour of High-strength Concrete Columns." *Engineering Structures*, 26(1), 1-12.

Schlaich, J., Schäfer, K. and Jennewin, M. (1987). "Towards a Consistent Design of Structural Concrete." *PCI Journal*, 32(3), 72-150.

Kuang, J. S. and Puvvala Jawaharlal (1996). "*Continuous transfer beams supporting in-plane loaded shear walls in tall buildings*." *The Structural Design of High-rise buildings*, 5(4), 281-293.

Kuang, J. S. and Atanda, A. I. (1998). "*Interaction based analysis of continuous transfer girder system supporting in-plane loaded coupled shear walls*." *The Structural Design of High-rise buildings*, 7(4), 285-293.

Kuang, J. S. and Li, Shubin (2001). "*Interaction-based Design Tables for Transfer Beams Supporting In-plane Loaded Shear Walls*." The Structural Design of Tall Buildings, 10(2), 121–133.

Lam, S. S. E. (1997). "Inelastic Seismic Response of a Low-rise Building Designed by Chinese Code." *Proceedings of the International Conference on Structures in the New Millennium*, Hong Kong, 575-582.

Lam, S. S. E. (1999). "Analysis of a Reinforced Concrete Vierendeel Truss System." *第四届中日建筑结构技术交流会*, 大连, 504-512.

Lam, S. S. E., Li, C. S., Zhang, M. Z., Wong, Y. L. and Chau, K. T. (2002). *Shaking Table Tests of a Typical High-rise Building in Hong Kong*, Report, CIDARC April 2002, The Hong Kong Polytechnic University.

Lam, S. S. E., Wu, B., Wong, Y. L., Wang, Z. Y., Liu, Z. Q., and Li, C. S. (2003). “Drift Capacity of Rectangular Reinforced Concrete Columns with Low Lateral Confinement and High-Axial Load.” *Journal of Structural Engineering*, 129(6), 733-742.

Lee, C. F., Ding, Y. Z., Huang, R. H., Yu, Y. B., Guo, G. A., Chen, P. L. and Huang, X. H. (1996). *Seismic Hazard Analysis of the Hong Kong Region*, GEO Report No.65, Civil Engineering Services Department, Hong Kong Government.

Lee, H. S. and Woo, S. W. (2002). “Seismic Performance of a 3-story RC Frame in a Low-seismicity Region.” *Engineering Structures*, 24(6), 719-734.

Li, C. S., Lam, S. S. E., Wong, Y. L. (2003). “New Stiffness indicators for a High-rise Building with Transfer Plate.” *Proceedings of the Third Cross-strait Conference on Structural and Geotechnical Engineering*, 339-347.

Li, C. W., Harry, D. Conway, and George, Winter (1952). “Stresses in Deep Beam.” *Transactions of American Society of Civil Engineers*, 686-703.

Li, J. H., Su, R. K. L., Chandler A.M., and Lam, N. T .K (2002). “Seismic Assessment of Low-rise Building with Transfer Structure.” *Proceedings of the International Conference on Advances in Building Technology,* 1, 747-754.

Lin, Zhuhai (1995). “Application of Nonlinear Finite Strip Technique to Concrete Deep Beams.” *Engineering Structures*, 17(10), 725-736.

Lu, X. (1995). “Application of Identification Methodology to Shaking Table Tests on Reinforced Concrete Columns.” *Engineering Structures*, 17(7), 505-511.

Lu, X., Zhou, Q., Wu, X. and Zhang, W. (1998), “Shaking Table Testing on Model Building Constructed in Moderate Seismic Region.” *Proceedings of the International Workshop on Earthquake Engineering for Regions of Moderate Seismicity*, Hong Kong, 227-237.

Marti, P. (1985a). “Basic Tools of Reinforced Concrete Beam Design.” *ACI Structural Journal*, 82(1), 46-56.

Marti, P. (1985b). “Truss Models in Detailing.” *Concrete International*, 12, 66-79.

Marti, P. (1990). “Design of Concrete Slabs for Transverse Shear.” *ACI Structural Journal*, 87, 180-190.

Max, M. Frocht (1937). *A Photoelastic Investigation of Shear and Bending Stresses in Centrally Loaded Simple Beams,* Carnegie Institute of Technology, Pennsylvania.

Mirza, M. S., Harris., H. G., and Sabnis, G. M. (1979). “Structural Models in Earthquake Engineering.” *Proceedings of the Third 1Canadian Conference of Earthquake Engineering*, Montreal, Quebec, 1, 511-549.

Nakashima, M., Kato, H. and Takaoka, E. (1992). “Development of Real-time Pseudodynamic Testing.” *Earthquake Engineering and Structural Dynamics*, 21, 79-92.

Negro, P., Verzeletti, G., Magonette, G. E. and Pinto, A. V. (1994). *Tests on a Four Storey Full-Scale R/C Frame Designed According to Eurocodes 8 and 2: Preliminary Report*, EUR15879 EN, European Laboratory for Structural Assessment (ELSA), Joint Research Centre, Ispra, Italy.

Pang, X. B. and Hus, T. T. C. (1995), “Behavior of Reinforced Concrete Membrane Elements in Shear.” *Structural Journal of the American Concrete Institute*, 92(6), 665-679.

Pang, X. B. D. and Hus, T. T. C. (1996). “Fixed-angle Softened-truss Model for Reinforced Concrete.” *Structural Journal of the American Concrete Institute*, 93(2), 197-207.

Paulay, T. and Priestley, M. J. N. (1992). *Seismic Design of Reinforced Concrete and Masonry Buildings*, John Wiley & Sons.

Prakash, V. (1992). *Dynamic Response Analysis of Inelastic Building Structures: The DRAIN Series of Computer Programs,* Department of Civil Engineering, University of California, Berkeley, USA.

Pun, W. K., Lee, C. F. and Ding, T. Z. (1998). "Seismic Risk in Hong Kong." *Proceeding of the International Workshop on Earthquake Engineering for Regions of Moderate Seismicity*, Hong Kong, 19-29.

Ramirez, J. A. and Breen J. E. (1991). "Evaluation of a Modified Truss Model Approach for Beams in Shear." *Structural Journal of the American Concrete Institute*, 88(5), 562-571.

Reinhorn, A. M., Kunnath, S. K., and Panahshahi N. (1988). *Modeling of R/C Building Structures with Flexible Floor Diaphragms (IDARC2),* Technical Report NCEER-88-0035, Department of Civil Engineer, State University of New York at Buffalo, New York.

Robins O. J. (1973). “Modified Finite Element Method Applied to R.C. Deep Beams.” *Civil Engineering and Public Works Review*, 963-966.

Saad, S. and Hendry, A. W. (1961). “Stresses in a Deep Beams with a Central Concentrated Load.” *Experimental Mechanics*, 18(1), 192-198.

Sanada, Y., Kabeyasawa, Y. and Kuramoto, H. (2000). “Three-Dimensional Analysis of a Reinforced Concrete Frame-Wall Structure with Soft First Story.” *Transaction of the Japan Concrete Institute*, 22, 273-278.

Scarlat A.S. (1997). “Design of Soft Stories – A Simplified Energy Approach”, *Earthquake Spectra*, 13(2), 305-315.

SEAOC (1999). *Recommended Lateral Force Requirements and Commentary*, Seismology Committee, Structural Engineers Association of California.

Siao, W. B. (1993). “Strut and Tie Model for Shear Behaviour in Deep Beams and Pile Caps Failing in Diagonal Splitting.” *ACI Structural Journal*, 90(4), 356-363.

Siao, W. B. (1995). “Deep Beams Revisited.” *ACI Structural Journal*, 92(1), 95-102.

Shing, P. B. and Mahin, S. A. (1984). *Pseudodynamic Test Method for Seismic Performance Evaluation: Theory and Implementation*, UCB/EERC Report No. 84/01, University of California, Berkeley, California, USA.

Takanashi, K. and Nakashima, M. (1987). “Japanese Activities on On-line Testing.” *Journal of Engineering Mechanics*, 113(7), 1014-1032.

Tan, K. H., Kong, F.K., Teng, S. and Guan, L. (1995). “High-Strength Concrete Deep Beams with Effective Span and Shear Span Variations.” *ACI Structural Journal*, 92(4), 395-405.

Tan, K. H., Kong, F. K., Teng, S. and Weng, L.W. (1997a). “Effect of Web Reinforcement on High-Strength Concrete Deep Beams.” *ACI Structural Journal*, 94(5), 572-582.

Tan, K. H., Kong, F. K., Teng, S. and Lu, H.Y. (1997b). “Main Tension Steel in High-Strength Concrete Deep and Short Beams.” *ACI Structural Journal*, 94(6), 752-768.

Tan, K. H., Kong, F. K. and Weng, L. W. (1998). “High-Strength Concrete Deep and Short Beams: Shear Design Equations in North American and UK Practice.” *ACI Structural Journal*, 95(3), 318-329.

UBC (1997). *Uniform Building Code*, International Conference of Building Officials, U.S.A.

Vecchio, F. and Collins, M. P. (1981). "Stress-strain Characteristics of Reinforced Concrete in Pure Shear", Final Report, *IABSE Colloquium on Advanced Mechanics of Reinforced Concrete*, Delft, Netherland, 211-255.

Wong, Y. L., Zhao, J. X., Chau, K. T. and Lee, C. M. (1998a). "Assessment of Seismicity Model for Hong Kong Region." *HKIE Transaction*, 5(1), 50-62.

Wong, Y. L., Zhao, X., Lam, S. S. E. and Chau, K. T. (1998b). "Assessing Seismic Response of Soft Soil Sites in Hong Kong by Using Microtremor Records." *HKIE Transaction*, 5(3), 70-79.

Woo, J. C., Chung, B. Y., Nam, S. K. and Ju, W. S. (1999). "Shaking Table and Pseudodynamic Tests for the Evaluation of Seismic Performance of Base-isolated Structures." *Engineering Structures*, 21, 365-379.

Yoshimura, M. (1997). "Nonlinear Analysis of a Reinforced Concrete Building with a Soft First Story Collapsed by the 1995 Hyogoken-Nanbu Earthquake." *Cement and Concrete Composite*, 19(3), 213-221.

Zhang, L. X. and Hsu T. T. C. (1998). “Behavior and Analysis of 100MPa concrete membrane elements.” *Journal of Structural Engineering*, 124(1), 24-34.

Zhang, M. Z. (1997). “Some Opinion on The Application of Similitude Law in Earthquake Simulation Test.” *Earthquake Engineering and Engineering Vibration*, 17(2), (in Chinese).

Zhao, Z. Z., Kwan, A. K. H. and He, X. G. (2004). “Nonlinear Finite Element Analysis of Deep Reinforced Concrete Coupling Beams.” *Engineering Structures*, 26(1), 13-25.

Zunz, J. and Wise C. (1998). “Transfer Structures.” Editor Beedle, Lynn S. *Second Century of the Skyscraper,* Van Nostrand Reinhold, New York.